University of Montenegro
Biotechnical faculty

Univerzitet Crne Gore
Biotehnički fakultet

Agriculture and Forestry
Poljoprivreda i šumarstvo
2

Agriculture and Forestry, Vol.68. Issue 2: 1-248, Podgorica, 2022

ISSN 0554-5579; E-ISSN 1800-9492; DOI: 10.17707/AgricultForest
COBIS.CG-ID: 3758082
www.agricultforest.ac.me

Agriculture and Forestry - *Poljoprivreda i šumarstvo*
PUBLISHER - *IZDAVAČ*
University of Montenegro – Univerzitet Crne Gore
Biotechnical faculty (BTF), Podgorica - Biotehnički fakultet, Podgorica
Bul. M. Lalića 1, 81000 Podgorica, Crna Gora (Montenegro), P.Box 97,
Tel.: +382 20 268434; +382 20 268437; Fax: +382 20 268432
Web: www.agricultforest.ac.me; E-mail: agricultforest@ac.me

CIP – Каталогизација у публикацији
Централна народна библиотека Црне Горе, Цетиње
ISSN 0554-5579
COBIS.CG-ID 3758082

CONTENT

Rodrigues Neto, M.R.; Musselli, D.G.; Lense, G.H.E.; Servidoni, L.E.; Stefanidis, S.; Spalevic, V.; Mincato, R.L. (2022). Soil loss modelling by the IntErO model - Erosion Potential Method in the Machado River Watershed, Minas Gerais, Brazil. Agriculture and Forestry, 68 (2): 7-21. doi:10.17707/AgricultForest.68.2.01

DOI: 10.17707/AgricultForest.68.2.01

Manoel Ribeiro RODRIGUES NETO[1], Denis Giovanni MUSSELLI[1], Guilherme Henrique Expedito LENSE[1], Lucas Emanuel SERVIDONI[1], Stefanos STEFANIDIS[2], Velibor SPALEVIC[3] and Ronaldo Luiz MINCATO[1]

SOIL LOSS MODELLING BY THE IntErO MODEL - EROSION POTENTIAL METHOD IN THE MACHADO RIVER BASIN, MINAS GERAIS, BRAZIL

SUMMARY

Water erosion has radically affected the productive capacity of soils, especially in regions with a tropical climate, causing environmental and social damage, such as reduced agricultural productivity and siltation of water bodies. The objective of this research was to estimate soil losses with using the IntErO model - Erosion Potential Method in the River Machado Watershed (MRW), South Minas Gerais State (Brazil), with the idea to identify areas of increased soil losses due to water erosion, contributing with the research activities to the environmental planning in order to prevent land degradation. The Machado River basin was selected as study area because it is an important Sustainable Use Conservation Unit in Minas Gerais, which has abundant water resources, rich biodiversity, and intensive agricultural production. The estimated soil losses for the year 2020 were calculated, using the IntErO model - Erosion Potential Method, in a Geographic Information System (GIS) environment. The MRW presented an average soil loss of 18.2 Mg ha^{-1} yr^{-1}, and a total of about 2 million tons per year. In about 85% of the watershed, soil losses were greater than the tolerable limits, what leads to the conclusion that there is a need to adopt a comprehensive soil conservation management plan to reduce water erosion. The highest average soil losses occurred in areas of exposed soil as well as sporadic agricultural and pasture, and are concentrated in the southern sector of the studied area. The results obtained can support the environmental planning aimed at the conservationist use of the soil in the MRW.

Key words: Soil Conservation; Soil Erosion; IntErO model; EPM; Environmental Planning; GIS; Nature Conservation; Brazil.

---

[1] Manoel Ribeiro Rodrigues Neto, Denis Giovanni Musselli, Guilherme Henrique Expedito Lense, Lucas Emanuel Servidoni, Ronaldo Luiz Mincato (corresponding author: ronaldo.mincato@unifal-mg.edu.br), Federal University of Alfenas, UNIFAL-MG, Alfenas, Minas Gerais, BRAZIL;
[2] Stefanos Stefanidis, Laboratory of Mountainous Water Management and Control, Faculty of Forestry and Natural Environment, Aristotle University of Thessaloniki, Thessaloniki, GREECE;
[3] Velibor Spalevic, University of Montenegro, Biotechnical Faculty, Podgorica, MONTENEGRO;
Notes: The authors declare that they have no conflicts of interest. Authorship Form signed online.
Recieved:09/04/2022 *Accepted:12/06/2022*

INTRODUCTION

Soil erosion is one of the most widespread and a major environmental threat which decreases agricultural productivity and affects water quality (Artemyeva *et al*., 2021; Kavian *et al*., 2018; Kavian *et al*., 2017; Spalevic *et al*., 2017; Khaledi Darvishan *et al*., 2016; Mohammadi and Kavian, 2015; Spalevic *et al*., 2013; Nearing *et al*., 2005). Water erosion has drastically affected the productive capacity of soils, especially in tropical regions, due to the large volume of rainfall (Panachuki *et al*., 2006; Santos *et al*., 2010). The four basic factors that regulate water erosion rates are topography, climate, soil types and characteristics, and land cover (Panagos *et al.*, 2015). The erosion rates are generally higher on terrains with longer and steeper slopes due to increased runoff volume and velocity (Tavares *et al*., 2021).

Erosive processes accelerated or intensified by human activities (Bigarella, 2007) cause damage to the environment and society, both in places where they occur (in loco) and in nearby or distant areas, such as reduction or even closure of agricultural production, the loss of soil fertility and siltation of water bodies (Guerra and Mendonça, 2020).

Over the past 50 years, several water erosion estimation models have been developed and improved (Lovric and Tosic, 2018, Santana *et al.*, 2021). These models are based on mathematical equations that express the relationship between environmental parameters and allow the estimation of soil losses with an acceptable level of accuracy (Stefanidis and Stathis, 2018). In addition, the association of modelling with Geographic Information Systems allows the spatialization of results, facilitating the implementation of actions in the field of soil conservation management (Imamoglu and Dengiz, 2017).

The Erosion Potential Method (EPM) is a model for estimating water erosion, based on simple and low-cost obtaining parameters (Gavrilovic, 1962). EPM has been widely used in the South East European regions, Italy, the Middle East, and North Africa (El Mouatassime *et al.*, 2019; Stefanidis and Stathis, 2018; Nikolic *et al*., 2018; Darvishan *et al.*, 2017; Spalevic *et al*., 2017; Dragicevic *et al*., 2017; 2016;). It has also been recognized as the most quantitative of all the semi-quantitative models (De Vente *et al*., 2005). Noteworthy studies comparing EPM erosion model output with field measurements shows that give satisfactory results (Tazioli, 2009; Efthimiou *et al*., 2016). More recently, the IntErO model (www.geasci.org/IntErO) – EPM method have been applied to tropical conditions in Brazil, giving accurate results (Sakuno *et al*., 2020; Tavares *et al.*, 2019; Lense *et al.*, 2019; Silva *et al*., 2014).

In this scenario, the objective of the work was to estimate the soil loss rates by using the IntErO model - Erosion Potential Method in the Environmental Protection Area (APA) of the Rio Machado Watershed, southern of Minas Gerais State, to identify the areas with environmentally unsustainable soil loss due to water erosion and contribute to environmental planning and soil and water conservation policies. The Machado River Watershed was selected as the study area because it is an important Conservation Unit in the State of Minas Gerais, with abundant water resources and rich biodiversity, and, on the other hand, widely used by the agricultural sector.

MATERIAL AND METHODS

Study area. The Machado River Watershed (MRW) is a Conservation Unit (protected area) in the State of Minas Gerais, south-eastern Brazil. It has an area of 101,600 ha and covers eleven municipalities of southern of Minas Gerais State (Figure 1). The area is under the anthropogenic influence in certain degree, being endowed with abiotic, biotic, aesthetic, or cultural attributes. Its basic objectives are the protection of biodiversity and maintaining the sustainable use of natural resources (IEF, 2021).

The Machado River is the main watercourse of the watershed, having 112.2 km of extension and an expressive altimetric gradient between its high and medium course. Its main tributaries are the Machadinho do Campo and Machadinho streams, on the right bank, and, on the left bank, the Jacutinga and Conceição streams (Latuf *et al*., 2019). The Machado River watershed is part of the Rio Grande Watershed and has the Furnas Reservoir as its base level (Justino *et al*., 2019).

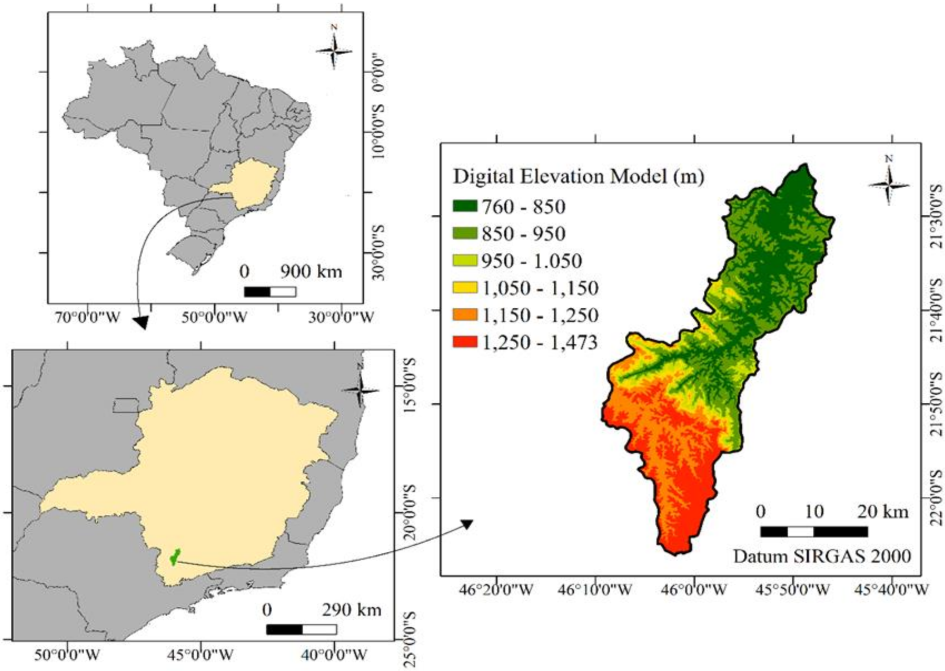

Figure 1. Study area of the Machado River Watershed, Minas Gerais, Brazil.

Climate. The Intergovernmental Panel on Climate Change (IPCC) special report on climate change and land underlines that the increase of the global mean surface temperature, relative to pre-industrial levels, may substantially affect processes involved in desertification (water scarcity), land degradation (soil erosion, vegetation loss, wildfire, permafrost thaw) and food security (Panagos *et al.*, 2021). Climate change and land use change are recognized as the main drivers of future soil erosion dynamics (Poesen, 2018).

The climate in the studied area is Tropical (Cwa), with a dry season between April and September, and a rainy season, between October and March, according to the Köppen-Geiger classification (Reboita *et al.*, 2015). The average annual precipitation and the average annual compensated temperature considering a historical series of 30 years, from 1981 to 2010, are 1,597 mm and 19.8° C, respectively (INMET, 2021).

Geology. The geological framework of the area consists of the following lithotypes: paragneisses, orthogneisses, quartzites, migmatites, biotite schist and associated granitoids (CPRM, 2014). The geological substrate has low permeability and high resistance to erosion, presenting rocky outcrops in the upper course of the Machado River and in steep areas (Servidoni *et al.*, 2019).

Soils. The pedological units, according to the Brazilian Soil Classification System (SiBCS) of EMBRAPA (2018) (Figure 2A), are the Haplic Cambisol, which predominates in the southern sector of the conservation unit, and the Red-yellow Latosol in the other sectors, with soils of the Red-yellow Argisol and Haplic Nitosol types in the northern sector (UFV *et al*., 2010). The soil map of the area was adapted from the "Soil Map of the State of Minas Gerais" in a scale of 1:650,000 (UFV *et al*., 2010). The relief of the area is predominantly smooth undulating, with an average slope between 3 and 8% (TOPODATA, 2008, EMBRAPA, 2013). The altitudes vary from 760 m, on the Machado River plain, to 1,470, mainly on the hills of the southern sector (Figure 1). The slope map (Figure 2B) was prepared with percentage values, from the Digital Elevation Model (DEM) covering the area, with a spatial resolution of 30 m (TOPODATA, 2008), using the ArcGis 10.5 Slope tool (ESRI, 2016).

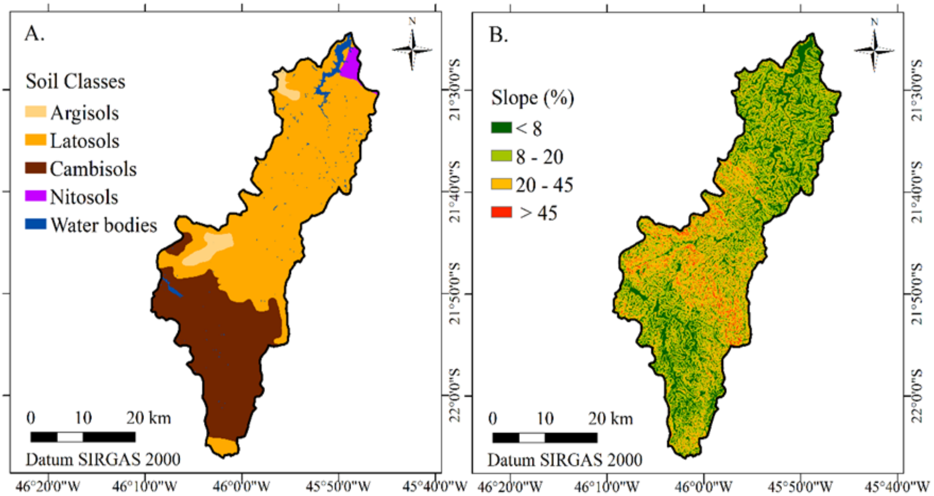

Figure 2. Soil classes (A) and slope (B) maps of the Machado River watershed, Minas Gerais, Brazil.

Land use. The study area has a predominance of the Atlantic Forest Biome, with transition to Cerrado (Savanna) to the north. In land use, temporary and permanent crops are highlighted, such as corn and coffee, respectively, in addition to forestry and pasture for cattle raising (Santos, 2019, MAPBIOMAS, 2020). The land use map considering the year 2020 (Figure 3) was obtained from the digital platform MapBiomas Project (2020), with a spatial resolution of 30 m.

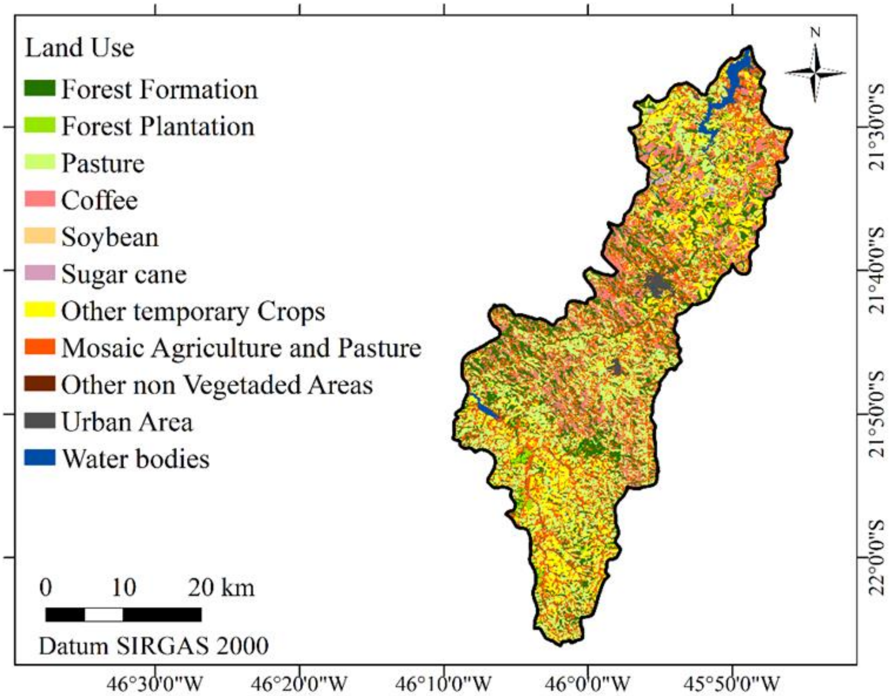

Figure 3. Land use map of the Machado River Watershed, Minas Gerais, Brazil. Adapted from the MapBiomas (2020).

The Erosion Potential Method (EPM). Soil erosion can present a major threat to agriculture due to loss of soil, nutrients, and organic carbon. Therefore, soil erosion modelling is one of the steps used to plan suitable soil protection measures and detect erosion hotspots (Bezak *et al*, 2021). For the modelling and analysis of soil erosion intensity in the Machado River Basin of the Minas Gerais, (Brazil), we used the IntErO model with the Erosion Potential Method in its algorithm background.

The EPM (Gavrilovic, 1972) considers factors dependent on climate, soil properties, topographic characteristics, land use and the degree of erosion of the watershed. Initially, the EPM estimates the susceptibility to the erosion process by calculating the erosion intensity coefficient (Z). Areas with a value of $Z > 1.00$ have high susceptibility to erosion, while areas with $Z < 0.19$ have a low tendency to the occurrence of the phenomenon (Gavrilovic, 1962). The Z parameter is calculated according to Equation 1:

$$Z = Y \cdot X_a \cdot \left(\varphi + \sqrt[2]{I_{sr}}\right) \qquad \text{Equation 1}$$

where: Y = soil resistance to water erosion, dimensionless; X_a = coefficient of land use and management, dimensionless; φ = coefficient of degree of erosive features, dimensionless and I_{sr} = mean slope of the area in %.

The Y parameter represents the soil resistance to water erosion and varies depending on the type of soil and its source material, having values between 0.20 and 2.00. The most resistant soils have values close to 0.20, while those more susceptible to erosion have values close to 2.00. The Y factor was determined for each soil class according to Sakuno *et al.* (2020), and its average value, considering the entire studied area, was 0.7.

Parameter X_a expresses the protection of the watershed against the erosive action of rain, considering the existing vegetation cover, and its values range from 0.05 (areas covered by dense vegetation) to 1.0 (areas with the presence of soil exposed). In the study area, the X_a parameter was determined for each land use class according to Sakuno *et al.* (2020), and its mean value for the entire study area was 0.54.

Factor φ represents the characteristics of erosive features observed in the field, ranging from 0.10, for areas without evidence of erosive processes, to 1.00, for areas affected by severe erosive processes, such as gullies. Through field surveys, it was verified that the occurrence of laminar erosion predominates in the watershed, thus the value of 0.5 was adopted for the parameter φ throughout of the MRW.

The I_{sr} factor (%) indicates the influence of relief on the erosive dynamics, and was obtained from the slope map, showing that the area has an average slope of 4.5%.

Using the Z coefficient, the EPM estimates the total soil loss (W_{yr}) in Mg ha^{-1} ano^{-1}, according to Equation 2:

$$W_{yr} = \left(\sqrt[2]{\frac{t_0}{10} + 0.1}\right) \cdot H_{yr} \cdot \pi \cdot \sqrt[2]{Z^3} \cdot Ds \qquad \text{Equation 2}$$

where: t_0 = average air temperature, in °C; H_{yr} = total annual precipitation, in mm; Ds = average soil density in kg dm^{-3}.

The parameters H_{yr} (mm) and t_0 (ºC) represent the influence of climatic factors on erosive dynamics and were obtained for the year 2020 based on a rainfall station located inside the watershed, at coordinates 45°53'35" W; 21°39'55" S, regulated by the National Institute of Meteorology (INMET, 2021). In the watershed, in the year 2020, the total annual precipitation was 1,534 mm and the average annual temperature was 20.5° C.

Finally, the Ds coefficient (kg dm^{-3}) demonstrates the average soil density, and its value was adopted for the study area according to Lense *et al.* (2019), being 1.21 kg dm$^{-3.}$

Obtaining the parameters as well as all the processing and modelling steps were developed with the aid of a Geographic Information System, using the ArcGis 10.5 software (ESRI, 2016).

The results estimated by using the IntErO model - EPM were compared with the soil loss tolerance limits (T). T can be defined as the maximum erosive intensity that still allows for sustainable agricultural production (Wischmeier and Smith, 1978). T values were obtained for each soil class based on the results of Lense *et al*. (2019), who calculated the T using the methodology of Bertol and Almeida (2000), which is the most recent and most used in Brazilian soils. The T values adopted were 7.40 Mg ha^{-1} yr^{-1} for Latosols, 4.75 Mg ha^{-1} yr^{-1} for Cambisols and 7.20 Mg ha^{-1} yr^{-1} for Argisols/Nitosols.

The IntErO model. The IntErO model uses the Erosion Potential Method in its algorithm background (Spalevic, 2011; Ouallali *et al*, 2020). The IntErO model is an upgrading of the River Basins (Spalevic, 1999; Spalevic *et al*., 2000) and the Surface and Distance Measuring (Spalevic, 1999) programs.

The model calculate a large number of data with the processing of 22 input parameters, returning, after the processing, 26 result parameters (Coefficient of the river basin form, *A*; Coefficient of the watershed development, *m*; Average river basin width, *B*; (A)symmetry of the river basin, *a*; Density of the river network of the basin, *G*; Coefficient of the river basin tortuousness, *K*; Average river basin altitude, *Hsr*; Average elevation difference of the river basin, *D*; Average river basin decline, *Isr*; The height of the local erosion base of the river basin, *Hleb*; Coefficient of the erosion energy of the river basin's relief, *Er*; Coefficient of the region's permeability, *S1*; Coefficient of the vegetation cover, *S2*; Analytical presentation of the water retention in inflow, *W*; Energetic potential of water flow during torrent rains, 2*gDF*½; Maximal outflow from the river basin, *Qmax*; Temperature coefficient of the region, *T*; Coefficient of the river basin erosion, Z; Production of erosion material in the river basin, *Wyear*; Coefficient of the deposit retention, *Ru*; Real soil losses, *Gsp*; Real soil losses per km^2. The model considers six factors related to lithology (rocks permeability in percent: *fp*, permeable; *fpp* semipermeable, *fo*, low permeability) and soil type (erodibility coefficient *Y*), topographic and relief data (*I* coefficient), monthly mean and annual precipitation (*P* coefficient), temperatures annual averages (*t* coefficient), land cover data (*X* coefficient) and the state of erosion patterns and development of the watercourse network (*Φ* coefficient).

The IntErO model can be characterized as semi-quantitative because it is based on a combination of descriptive and quantitative procedures. However, compared to other semi-quantitative methods, this is the most quantitative because it uses descriptive evaluation for three parameters only: soil erodibility, soil protection and extent of erosion in the catchment. All other parameters are quantitative catchment descriptors (Spalevic *et al*., 2020).

IntErO flowchart is presented in the Figure 4.

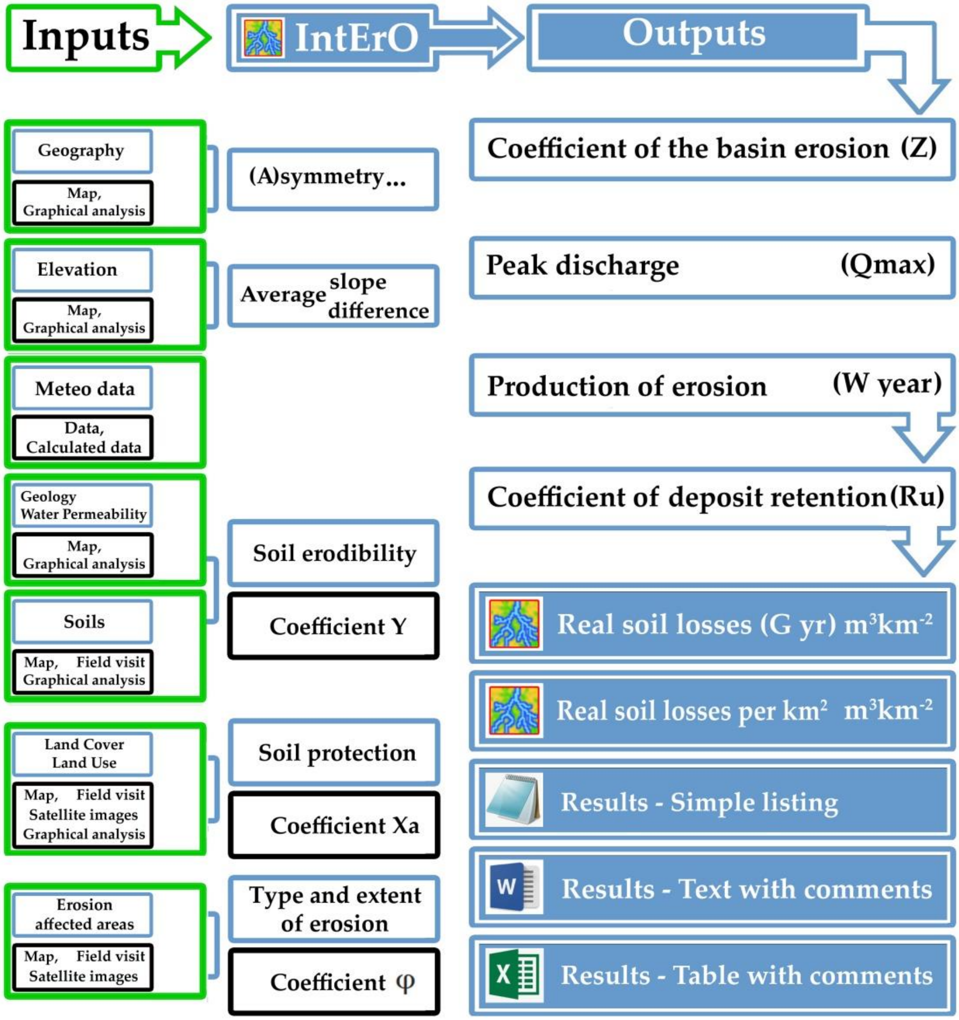

Figure 4. IntErO model Flow chart (based on Spalevic *et al*., 2020)

RESULTS AND DISCUSSION

The Machado River Watershed showed a total soil loss of about 2 million tons per year, and an average soil loss of 18.2 Mg ha^{-1} yr^{-1} (Figure 5).

The greatest soil losses per hectare (between 25 and 50 and > 50 Mg ha^{-1} yr^{-1}) are concentrated in the southern sector of the watershed, which is partly related to the fact that this sector presents the Haplic Cambisol (CXbd), as predominant soil class.

The haplic Cambisol has the lowest resistance to water erosion among the other classes of soil in the study area, with a value of 0.9 for the Y coefficient (Table 1). In this context, Silva *et al*. (2005), in their study on soil degradation by water erosion, found an average annual loss of soil about 14 times greater for the Haplic Cambisol compared to the Red Latosol.

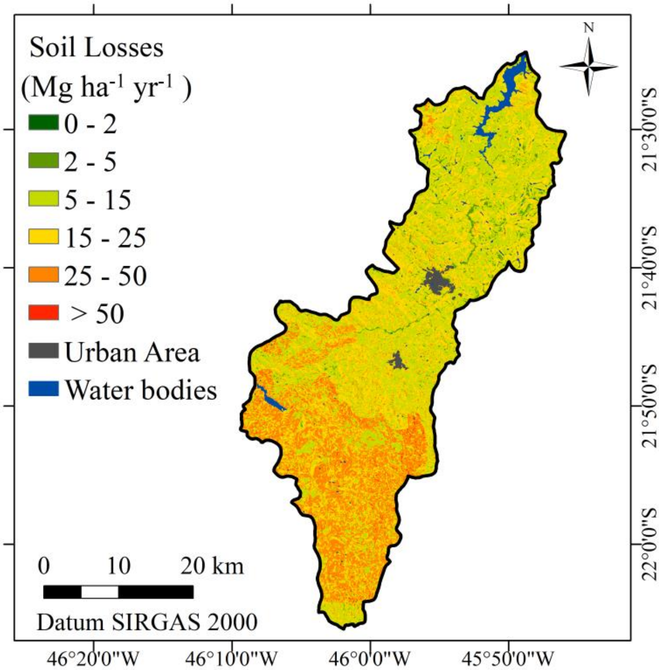

Figure 5. Map of spatial distribution of soil losses in the Machado River Watershed, Minas Gerais, Brazil.

It is noteworthy that the Haplic Cambisol is the second most abundant soil type in the watershed, occupying around 33% of its territory. Due to the low resistance to water erosion of Cambisols, it is necessary that the uses of this soil are subject to conservation measures, such as the implementation of agricultural management techniques and the mitigation of runoff and water erosion.

Table 1. Resistance to water erosion (Y) of soils in the Machado River Watershed, Minas Gerais, Brazil

Soil classes	**Area (%)**	**Y values**
Haplic Cambisol	33.48	0.9
Red-yellow Latosol	60.75	0.6
Haplic Nitosol	1.27	0.7
Red-yellow Argisol	3.00	0.8

Source: Adapted from Sakuno *et al*. (2020)

In addition, the southern sector of the area has a high Y coefficient, and the relief is soft, with a declivity of less than 8%, which favors the agro pastoral use of this area, which defines the predominant land cover and uses ("other temporary crops", with an X_a of 0.7; "pasture" with an X_a of 0.5; and "agricultural and grazing mosaic" with an X_a of 0.7) (Table 2). These uses offer low soil protection against water erosion. Furthermore, temporary crops and pastures are more susceptible to soil degradation due to the removal of the topsoil in agricultural areas (Mafra, 2020) and the soil compaction and runoff in preferential paths in pastures (Botelho and Silva, 2004).

It is noteworthy that despite the class "other non-vegetated areas" being the one with the highest average soil loss per hectare (31.4 Mg ha^{-1} yr^{-1}), its contribution to the total soil loss in the watershed it is very low (1,434.9 Mg yr^{-1}), due to its small area (0.04% of total area) (Table 2). On the other hand, the classes "other temporary crops", "pastures" and "agriculture and pasture mosaic" had the highest total soil losses in the watershed, losing together 1,723,350.9 Mg yr^{-1}, which is due to the large area occupied by them (67.2% of the MRW).

Table 2. Values of the X_a coefficient and soil losses in the land use classes of the Machado River Watershed, Minas Gerais, Brazil.

Land use classes	Area (%)	X_a	Soil loss (Mg ha^{-1} yr^{-1})	Soil loss (Mg yr^{-1})
Forest Formation	18.10	0.3	7.6	161,328.20
Forest Plantation	0.90	0.4	11.9	12,090.90
Pasture	26.90	0.5	16.7	528,541.60
Sugar cane	0.54	0.6	14.3	9,183.40
Mosaic Agriculture and Pasture	27.05	0.7	25.5	809,121.30
Urban Area*	0.78	-	-	-
Other non-Vegetated Areas	0.04	1.0	31.4	1,434.90
Water bodies*	1.50	-	-	-
Soybean	0.49	0.7	17.7	10,193.20
Other temporary Crops	13.30	0.7	24.7	385,688.03
Coffee	10.40	0.6	18.0	21,9263.40

Source: Adapted from Sakuno *et al*. (2020).
Notes: *Areas not considered in the calculation of soil loss.

On the other hand, the smallest soil losses (between 0 and 5 Mg ha^{-1} yr^{-1}) occurred mainly in the northeast and north sectors of the watershed. These areas have a gently undulating relief, with a slope ranging from 0 to 8%), covered by coffee plantations, pasture, temporary crops and forest fragments, with an X_a coefficient of 0.6; 0.5; 0.7 and 0.3, respectively (Table 2). Although clustered crops and pastures have potentially high susceptibility to water erosion, growing coffee and forest fragments are good protections for the soil against erosion, as vegetation with higher biomass control runoff more effectively (Bigarella, 2007).

In addition to the above factors, the areas that suffered the least loss of soil in the north and northeast sectors are Red-yellow Latosols, which have the highest erosion resistance among the watershed soils, with a Y of 0.6 (Table 1).

In general, the MRW is classified in category IV of erosion intensity, that is, in the watershed there is a predominance of low intensity erosion processes, with a Z coefficient of 0.34.

On the other hand, considering the values of T calculated by Lense *et al.* (2019) in about 85% of watershed, soil losses are above the limits of T. The high percentage of areas with losses above T is since the watershed has many mountainous areas with large slopes, which intensify soil losses. The results show the need to adopt soil conservation management plans to reduce water erosion. In addition, this result can help in the planning of land use and occupation policies in the watershed, respecting the agricultural suitability of each soil. It is noteworthy that the T is an index to assess soil losses in the short term, since in the long term the ideal is that water erosion rates are reduced to a minimum to promote the sustainability of agricultural systems.

MRW is part of southern Minas Gerais, an important Brazilian region for coffee production. The adoption of soil conservation practices in the region has the potential to reduce the loss of nutrients and organic matter in the soil due to water erosion and, thus, favour an increase in coffee production.

CONCLUSIONS

In 2020, the MRW presented an average soil loss of 18.2 Mg ha^{-1} yr^{-1}. The greatest soil losses per hectare occurred in non-vegetated areas and in agricultural and pasture mosaics, being 31.4 and 25.5 Mg ha^{-1} yr^{-1}, respectively. In about 85% of the MRW region, soil losses were greater than tolerable limits, which highlight the need to adopt a comprehensive soil conservation management plan to reduce soil losses from water erosion.

The results of estimating the intensity of erosion processes and potential soil losses by the IntErO – EPM method can serve as a support to the environmental planning and sustainable use of soils in the MRW, having the advantage of being an effective, simple, and low-cost method in application.

ACKNOWLEDGEMENTS

To the Coordenação de Aperfeiçoamento de Pessoal de Nível Superior (CAPES) for granting a scholarship to for the first and fourth authors. To the Fundação de Amparo à Pesquisa do Estado de Minas Gerais (FAPEMIG) for the scholarship offered to the third author.

Study was partially funded by the CAPES - Financial Code 001. The authors are grateful to the anonymous reviewers and the Editorial team for their insightful comments and suggestions.

REFERENCES

Artemyeva, Z.; Danchenko, N.; Kirillova, N.; Masyutenko, N.; Dubovik, E.; Kuznetsov, A. & Kogut, B. (2021). The Effect of Erosion Processes on the Content and Composition of Organic Matter in Macro-and Micro aggregates of Haplic Chernozem. Eurasian Soil Science. 54. 1659–1667. _

Bertol, I.& Almeida, J.A. (2000). Tolerância de perda de solo por erosão para os principais solos do Estado de Santa Catarina. Revista Brasileira de Ciência do Solo, 24(3): 657-668.

Bezak, N,; Mikoš, M.; Borrelli, P.; Alewell, C.; Alvarez, P.; Alexandre Ayach Anache, J.; Baartman, J.; Ballabio, C.; Biddoccu, M.; Cerdà, A.; Chalise, D.; Chen, S.; Chen, W.; De Girolamo, A.; Desta Gessesse, G.; Deumlich, D.; Diodato, N.; Efthimiou, N.; Erpul, G.; Fiener, P.; Freppaz, M.; Gentile, F.; Gericke, A.; Haregeweyn, N.; Hu, B.; Jeanneau, A.; Kaffas, K.; Kiani-Harchegani, M.; Lizaga Villuendas, I.; Li, C.; Lombardo, L.; López-Vicente, M.; Esteban Lucas-Borja, M.; Maerker, M.; Miao, C.; Modugno, S.; Möller, M.; Naipal, V.; Nearing, N.; Owusu, S.; Panday, D.; Patault, E.; Valeriu Patriche, C.; Poggio, L.; Portes, R.; Quijano, L.; Reza Rahdari, M.; Renima, M.; Francesco Ricci, G.; Rodrigo-Comino, J.; Saia, S.; Nazari Samani, A.; Schillaci, C.; Syrris, V.; Soo Kim, H.; Noses Spinola, D.; Tarso Oliveira, P.; Teng, H.; Thapa, R.; Vantas, K.; Vieira, D.; Yang, J.; Yin, S.; Antonio Zema, D.; Zhao, G. & Panagos, P. (2021). Soil erosion modelling: A bibliometric analysis. Environmental Research, 197, 111087.

Bigarella, J.J. (2007). Estrutura e origem das paisagens tropicais e subtropicais. 2. ed. Florianópolis, Ed. da UFSC. 1436 pp.

Botelho, R.G.M. & Silva, A.S. (2004). Bacia Hidrográfica e Qualidade Ambiental. In: Vitte, A.C. & Guerra, A.J.T., orgs. Reflexões sobre a Geografia Física no Brasil, pp. 153-188. Rio de Janeiro, RJ, Bertrand Brasil. 280 pp.

CPRM - Companhia de Pesquisa de Recursos Minerais. Mapa geológico no Estado de Minas Gerais. 2014. Available in: <http://www.portalgeologia.com.br/>. Access on: 03 Nov. 2021.

Darvishan, A.K.; Behzadfar, M.; Spalevic, V.; Kalonde, P.; Ouallali, A.; El Mouatassime, S. (2017). Calculation of sediment yield in the S2-1 watershed of the Shirindareh River Basin, Iran. Agriculture and Forestry, 63(3): 23-32.

Dragicevic, N.; Karleusa, B. & Ozanic, N. (2016). A review of the Gavrilovic method (Erosion Potential Method) application. Gradevinar, 9(68): 715-725.

Dragicevic, N.; Karleusa, B. & Ozanic, N. (2017). Erosion Potential Method (Gavrilovic method) sensitivity analysis. Soil and Water Research, 12(1): 51-59. doi:10.17221/27/2016-SWR

De Vente, J.& Poesen, J. (2005). Predicting soil erosion and sediment yield at the basin scale: Scale issue and semi-quantitative models. Earth Sciences Reviews. 71:95–125.

Efthimiou, N.; Lykoudi, E.; Panagoulia, D. & Karavitis, C. (2016). Assessment of soil susceptibility to erosion using the EPM and RUSLE models: The case of Venetikos River Catchment. Global NEST Journal., 18: 164–179.

El Mouatassime, S.; Boukdir, A.; Karaoui, I.; Skataric, G.; Nacka, M.; Darvishan, A.K.; Sestras, P. & Spalevic, V. (2019). Modelling of soil erosion processes and runoff for sustainable watershed management: Case study Oued El Abid Watershed, Morocco. Agriculture and Forestry, 65(4): 241-250.

EMBRAPA - Empresa Brasileira de Pesquisa Agropecuária. (2018). Sistema Brasileiro de Classificação de Solos. 9th ed. Rio de Janeiro: EMBRAPA Solos. 186 pp.

ESRI - Environmental Systems Research Institute (2016). ARCGIS Professional GIS for the desktop version 10.5. Redlands, Califórnia, Software. Retrieved from https://desktop.arcgis.com/en/arcmap/10.5/get-started/setup/arcgis-desktop-quick-start-guide.htm.

Gavrilovic S. (1972). Engineering of torrential flows and erosion. Izgradnja. Beograd p 272.

Gavrilovic, S. (1962). Method for estimating the average annual quantity of sediments according to the potency of erosion. Bulletin of the Faculty of Forestry, 26: 151-168.

Guerra, A.J.T. & Mendonça, J.K.S. Erosão dos Solos e a Questão Ambiental. In: Vitte, A.C. & Guerra, A.J.T., orgs. Reflexões sobre a Geografia Física no Brasil, p. 225-251. Rio de Janeiro, RJ, Bertrand Brasil. 280 pp.

IEF - Instituto Estadual de Florestas. Área de Proteção Ambiental - APA. Available in: <http://www.ief.mg.gov.br/component/content/article/3306-nova-categoria/117-area-de-protecao-ambiental-apa>. Access on: 15 July 2021.

Imamoglu, A. & Dengiz, O. (2017). Determination of soil erosion risk using RUSLE model and soil organic carbon loss in Alaca catchment (Central Black Sea region, Turkey). Rendiconti Lincei, 28: 11-23.

INMET - Instituto Nacional de Meteorologia. Banco de Dados Meteorológicos do INMET. Available in: <https://bdmep.inmet.gov.br/#>. Access on: 03 Aug. 2021.

INMET - Instituto Nacional de Meteorologia. Normais Climatológicas do Brasil: 1981 a 2010. Available: <https://portal.inmet.gov.br/normais>. Access on: 01 Aug. 2021.

Justino, R.C.; Mataveli, G.A.V.; Kawakubo, F.S.; Guerrero, J.V.R. & Chaves, M.E.D. (2019). Mapeamento do uso da terra e Áreas de Preservação Permanente (APP) nas bacias hidrográficas dos rios São Tomé e Machado, sul de Minas Gerais. Revista de Geografia, 9(1): 51-65.

Kavian, A.; Gholami, L.; Mohammadi, M.; Spalevic, V.; & Falah Soraki, M. (2018). Impact of Wheat Residue on Soil Erosion Processes. Notulae Botanicae Horti Agrobotanici Cluj-Napoca, 46(2), 553-562.

Kavian, A.; Hoseinpoor Sabet, S.; Solaimani, K. & Jafari, B. (2017). Simulating the effects of land use changes on soil erosion using RUSLE model. Geocarto International 3(1):97-111.

Khaledi Darvishan, A.; Homayounfar, V.; Sadeghi, SHR. (2016). The impact of standard preparation practice on the runoff and soil erosion rates under laboratory conditions. Solid Earth 7(5): 1293-1302.

Latuf, M.O.; Chinen, H.S.S.; Musselli, D.G. & Carvalho, P.H.S. (2019). Outorgas de uso dos recursos hídricos na Área de Proteção Ambiental do Rio Machado, sul de Minas Gerais. Caminhos de Geografia, 20(71): 311-327.

Lense, G.H.E.; Avanzi, J.C.; Parreiras, T.C. & Mincato, R.L. (2020). Effects of deforestation on water erosion rates in the Amazon region. Revista Brasileira de Ciências Agrárias, 15(4): e8500.

Lense, G.H.E.; Moreira, R.S.; Parreiras, T.C.; Silva, L.F.P.M.; Teodoro, A.E.M.; Santana, D.B.; Bolelli, T.M. & Mincato, R.L (2019). Assessment of Soil Loss Tolerance limit to Latosol, Argisol and Cambisol in the Southern Minas Gerais State. Caderno de Ciências Agrárias, 11:1–6.

Lense, G.H.E.; Parreiras, T.C.; Moreira, R.S.; Avanzi, J.C. & Mincato, R.L. (2019). Estimates of soil losses by the erosion potential method in tropical latosols. Ciência e Agrotecnologia, 43: e012719.

Lovric, N. & Tosic, R. (2018). Assessment of soil erosion and sediment yield using erosion potential method: Case study - Vrbas river basin (B&H). Bulletin of the Serbian Geographical Society, 98: 1-14.

Mafra, N.M.C. (2020). Erosão e planificação de uso do solo. In: Guerra, A.J.T.; Silva, A.S. & Botelho, R.G.M., orgs. Erosão e conservação dos solos, pp. 301-322. Rio de Janeiro, RJ, Bertrand Brasil. 339 pp.

MAPBIOMAS (2020). Coleção 6 da Série Anual de Mapas de Uso e Cobertura da Terra do Brasil, 2020. Available in: <https://mapbiomas.org/download>. Access on: 04 Oct. 2021.

Mohamadi, MA.& Kavian, A. (2015). Effects of rainfall patterns on runoff and soil erosion in field plots. International Soil and Water Conservation Research 3: 273-281.

Nearing, M.A.; Jetten, V.; Baffaut, C.; Cerdan, O.; Couturier.; A.; Hernandez, M.; Le Bissonnais, Y.; Nichols, M.H.; Nunes, J.P.; Renschler, C.S.; Souchere, V. & Van Oost, K. (2005). Modelling response of soil erosion and runoff to changes in precipitation and cover. Catena 61:131-154.

Nikolic, G.; Spalevic, V.; Curovic, M.; Darvishan, A.K.; Skataric, G.; Pajic, M.; Kavian, A. & Tanaskovik, V. (2018). Variability of Soil Erosion Intensity Due to Vegetation Cover Changes: Case Study of Orahovacka Rijeka, Montenegro. Notulae Botanicae Horti Agrobotanici Cluj-Napoca, 47(1): 237-248.

Ouallali, A.; Aassoumi, H.; Moukhchane, M.; Moumou, A.; Houssni, M.; Spalevic, V.; & Keesstra, S. (2020). Sediment mobilization study on Cretaceous, Tertiary and Quaternary lithological formations of an external Rif catchment, Morocco. Hydrological Sciences Journal, 65, 9: 1568-1582.

Panachuki, E.; Alves Sobrinho, T.; Vitorino, A.C.T.; Carvalho, D.F. & Urchei, M.A. (2006). Parâmetros físicos do solo e erosão hídrica sob chuva simulada, em área de integração agricultura-pecuária. Revista Brasileira de Engenharia Agrícola e Ambiental, 10(2): 261-268.

Panagos, P.; Ballabio, C.; Himics, M.; Scarpa, S.; Matthews, F.; Bogonos, M.; Poesen, J.; Borrelli, P. (2021). Projections of soil loss by water erosion in Europe by 2050. Environmental Science & Policy, 124, 380-392.

Panagos, P.; Borrelli, P.; Poesen, J.; Ballabio, C.; Lugato, E.; Meusburger, K.; Montanarella, L. & Alewell, C. (2015). The new assessment of soil loss by water erosion in Europe. Environmental Science & Policy, 54: 438-447.

Poesen, J. (2018). Soil erosion in the Anthropocene: research needs. Earth Surf. Process. Landf. 43, 64–84.

Reboita, M.S.; Rodrigues, M.; Silva, L.F. & Alves, M.A. (2015). Aspectos climáticos do estado de Minas Gerais. Revista Brasileira de Climatologia, 17(11): 206-226.

Sakuno, N.R.R.; Guiçardi, A.C.F.; Spalevic, V.; Avanzi, J.C.; Silva, M.L.N. & Mincato, R.L. (2020). Adaptation and application of the erosion potential method for tropical soils. Revista Ciência Agronômica, 51(1): e20186545.

Santana, D.B.; Bolleli, T.M.; Lense, G.H.E.; Silva, L.F.P.M.; Sestras, P.; Spalevic, V. & Mincato, R.L. (2021). Estimate of water erosion in coffee growing areas in Serra da Mantiqueira, Minas Gerais State, Brazil. Agriculture and Forestry, 67 (2): 75-88.

Santos, C.A. (2019). Diagnóstico e zoneamento geoambiental da APA da bacia hidrográfica do rio Machado-MG. Caderno de Geografia, 29(1): 144-163.

Santos, G.C.; Griebeler, N.P. & Oliveira, L.F.C. (2010). Chuvas intensas relacionadas à erosão hídrica. Revista Brasileira de Engenharia Agrícola e Ambiental, 14(2): 115-123.

Servidoni, L.E.; Teodoro, A.E.M.; Mincato, R L. & Santos, C.A. (2019). Avaliação de risco a enchentes e inundações por krigagem ordinária em sistemas de informação geográfica. Caderno de Geografia, 29(1): 126-143.

Silva, A.M.; Silva, M.L.N.; Curi, N.; Lima, J. M.; Avanzi, J.C. & Ferreira, M.M. (2005). Perdas de solo, água, nutrientes e carbono orgânico em Cambissolo e Latossolo sob chuva natural. Pesquisa Agropecuária Brasileira, 40(12): 1223-1230.

Silva, R.M.; Celso, A.G.S. & Silva, A.M. (2014). Predicting soil erosion and sediment yield in the Tapacurá Catchment, Brazil. Journal of Urban and Environmental Engineering, 8(1): 75-82.

Spalevic, V. (1999). Application of computer-graphic methods in the studies of draining out and intensities of ground erosion in the Berane valley. Master thesis, Faculty of Agriculture of the University of Belgrade, Serbia, 1999: 135p.

Spalevic, V. (2011). Impact of land use on runoff and soil erosion in Polimlje. Doctoral thesis, University of Belgrade, Faculty of Agriculture, Serbia, p 1-260.

Spalevic, V.; Barovic, G.; Vujacic, D.; Curovic, M.; Behzadfar, M.; Djurovic, N.; Dudic, B.; Billi, P. (2020). The Impact of Land Use Changes on Soil Erosion in the River Basin of Miocki Potok, Montenegro. Water 2020, 12, 2973-3000.

Spalevic, V.; Djurovic, N.; Mijovic, S.; Vukelic-Sutoska, M. &Curovic, M. (2013). Soil erosion intensity and runoff on the Djuricka River Basin (North of Montenegro). Malaysian Journal of Soil Science, 17(1):49-68.

Spalevic, V.; Dlabac, A.; Spalevic, B.; Fustic, B. & Popovic, V. (2000). Application of computer - graphic methods in the research of runoff and intensity of ground erosion - I program "River basins". Agriculture and Forestry 2000, 46, 1-2: 19-36.

Spalevic, V.; Lakicevic, M.; Radanovic, D.; Billi, P.; Barovic, G.; Vujacic, D.; Sestras, P. & Khaledi Darvishan, A. (2017). Ecological-Economic (Eco-Eco) modelling in the river basins of Mountainous regions: Impact of land cover changes on sediment yield in the Velicka Rijeka in Montenegro. Notulae Botanicae Horti Agrobotanici Cluj-Napoca, 45(2): 602-610.

Spalevic, V.; Radanovic, D.; Skataric, G.; Billi, P.; Barovic, G.; Curovic, M.; Sestras, P. & Darvishan, A.K. (2017). Ecological-Economic (Eco-Eco) modelling in the mountainous river basins: Impact of land cover changes on soil erosion. Agriculture and Forestry, 63(4): 9-25.

Stefanidis, S. & Stathis, D. (2018). Effect of Climate Change on Soil Erosion in a Mountainous Mediterranean Catchment (Central Pindus, Greece). Water, 10(10): 1-12.

Tavares, A.S.; Uagoda, R.E.S.; Spalevic, V. & Mincato, R.L. (2021). Analysis of the erosion potential and sediment yield using the IntErO model in an experimental watershed dominated by karst in Brazil. Agriculture and Forestry, 67 (2): 153-162.

TOPODATA: banco de dados geomorfométricos do Brasil. (2008). Acesso. Available in: <http://www.dsr.inpe.br/topodata/>. Access on: 25 Aug. 2021.

Tazioli, A. (2009). Evaluation of erosion in equipped basins: preliminary results of a comparison between the Gavrilovic model and direct measurements of sediment transport. *Environmental Geology*, 56(5): 825-831.

UFV; CETEC; UFLA & FEAM (2010). Mapa de Solos do Estado de Minas Gerais. Belo Horizonte, Fundação Estadual do Meio Ambiente. 49 pp. Available in: <http://www.feam.br/noticias/1/949-mapas-de-solo-do-estado-de-minas-gerais>. Access on: 10 Oct. 2021.

Wischmeier, W.H. & Smith, D.D. (1978). Predicting rainfall erosion losses. A guide to conservation planning. Supersedes Agriculture Handbook. Washington, United States Department of Agriculture. 67p.

Herbei, M.V., Bertici R., Sala F. (2022). The use of remote sensing images in order to characterize the soil agrochemical indexes in relation to the agricultural crops. Agriculture and Forestry, 68 (2): 23-33. doi:10.17707/AgricultForest.68.2.02

DOI: 10.17707/AgricultForest.68.2.02

Mihai Valentin HERBEI [1], Radu BERTICI [2], Florin SALA [3*]

THE USE OF REMOTE SENSING IMAGES IN ORDER TO CHARACTERIZE THE SOIL AGROCHEMICAL INDEXES IN RELATION TO THE AGRICULTURAL CROPS

SUMMARY

The present study evaluated the interdependence relationship between agrochemical soil indexes, agricultural crops, NDVI and SAVI indices, respectively Red Edge band, based on RapidEye remote sensing images. The NDVI, SAVI, and Red Edge were used to characterize the crops. Agrochemical indices of pH, humus (H), saturation in bases (V), nitrogen index (NI), phosphorus (P) and potassium (K) content, were used for the soil characterization. Kendall's correlation analysis revealed a very strong correlation between P and Red Edge (r = -0.905), moderate correlations between P and NDVI respectively SAVI (r = 0.619), and weak correlations between K and Red Edge (r = -0.524). The regression analysis facilitated the achievement of 2nd degree polynomial equations for the P prediction based on NDVI under the conditions of R^2= 0.724, p <0.01, the P prediction based on SAVI under conditions of R^2= 0.718, p <0.01, respectively P prediction based on Red Edge, under conditions of R^2= 0.985, p <<0.001. Prediction of K was possible based on NDVI, under the conditions of R^2= 0.774, based on SAVI under the conditions of R^2= 0.768, and respectively based on Red Edge under condition of R^2= 0.889. For the other agrochemical indices, the predictive relations in condition of low statistical safety were obtained (e.g. for pH based on Red Edge, R^2= 0.696; for H based on Red Edge, R^2= 0.538). For all agrochemicals, the safety predictions achieved through regression analysis were higher based on the Red Edge band compared to NDVI or SAVI indices.

Keywords: agrochemical indices, NDVI, prediction model, Red Edge, SAVI, soil

---

[1]Mihai Valentin Herbei: Banat University of Agricultural Sciences and Veterinary Medicine "King Michael I of Romania" from Timisoara, Timișoara, 300645, Romania, Remote Sensing and GIS

[2]Radu Bertici: Banat University of Agricultural Sciences and Veterinary Medicine "King Michael I of Romania" from Timisoara, Timișoara, 300645, Romania, Civil engineering

[3*]Florin Sala (Corresponding author: florin_sala@usab-tm.ro) Banat University of Agricultural Sciences and Veterinary Medicine "King Michael I of Romania" from Timisoara, Timișoara, 300645, Romania, Soil Science and Plant Nutrition

Notes: The authors declare that they have no conflicts of interest. Authorship Form signed online.

Recieved:22/01/2022 *Accepted:12/05/2022*

INTRODUCTION

Precision agriculture is growing ground due to the immense advantages it has in terms of practical, technically and economically, profitability at farm level, but also in terms of environmental protection and agricultural products (Wójtowicz *et al.*, 2016). The satellite techniques have already been used in the evaluation and characterization of the vegetal cover, the classification of the territory and the crops (Ustuner *et al.*, 2014; Gómez *et al.*, 2016; Dalmau *et al.*, 2017) on vegetative stages studies (Firoozi *et al.*, 2020), LAI and chlorophyll content evaluation (Delegido *et al.*, 2011; Frampton *et al.*, 2013), crop evapo-transpiration (Reyes-Gonźalez *et al.*, 2018), discrimination of subtle differences between C3 and C4 grasses (Shoko and Mutanga, 2017), estimation of grain and biomass production (Panda *et al.*, 2010; Prabhakara *et al.*, 2015; Kostić *et al.*, 2020).

The assessment of soil fertility by classical methods is no longer considered adequate due to the high workload, time consumed and lack of spatial exhaustiveness (Ge *et al.*, 2011). A very useful tool for precision farming is already remote sensing, which allows real-time, rapid, cost-effective information gathering and large spatial resolution to study and assess soil fertility (Kilic, 2021; Khaki *et al.*, 2017; Lense *et al.*, 2020). But this instrument, through the facilities they provide, can also be useful for farms that do not practice precision agriculture, for the more efficient management of soil and agricultural crops, sustainable agriculture (Popovici *et al.*, 2018). A wide range of soil-specific fertility properties and high agricultural importance such as moisture content, different textures, organic substances, carbon content, macro- and oligoelements, cation exchange capacity, pH, electrical conductivity and iron, can be successfully quantified with remote sensing (Kozar *et al.*, 2002; Wan *et al.*, 2004; Calina *et al.*, 2020). This already facilitates mapping of the soil in the field, with techniques based on satellite imagery and specific indices.

Techniques based on satellite imagery have been used to evaluate land with agricultural potential and to delimit land units and areas affected by certain limiting factors (Eldeiry and Garcia, 2010; Saleh *et al.*, 2015). Nutrient management also benefits from remote sensing and GIS facilities (Markoski *et al.*, 2015). Kim *et al.* (2014) conducted a survey of P and N soil based on remote sensing to characterize some water systems. Sharf *et al.* (2002) used remote sensing in nitrogen management studies, which have a very high impact on the increase in agricultural output but with high variability in the field. Similar studies have been conducted by Muñoz-Huerta *et al.* (2013).

The purpose of this study was to evaluate how certain agrochemical soil indices are reflected in the values of specific indices calculated on the basis of spectral information of agricultural crops based on satellite imagery.

MATERIAL AND METHODS

The purpose of the study was to evaluate the interdependence of the NDVI, SAVI and Red Edge indices based on spectral information from the satellite images and soil agrochemical indices, and to formulate remote sensing working models on the sustainable use of farmland.

The used satellite system. RapidEye is a satellite remote sensing system that allows you to have at any point on Terra, at least daily, a multispectral imaging capability. The Rapid Eye system consists of 5 spectral bands: Blue, Green, Red, Red Edge and NIR, with a 5-meter spatial resolution. The transition between Red Absorption and NIR (Near Infrared) reflecting the Red Edge band is able to provide additional information about the vegetation and its feature.

The studied area. The studied agricultural area is located within the Didactic and Experimental Resort of BUASVM Timisoara, Timis County, Romania. The study was conducted place during the agricultural year 2016 - 2017. In this study, a Rapid Eye satellite image was taken at the 5M resolution of 15.05.2017 from Planet portal (Planet Team, 2017) with the 3460215_2017-05-15_RE4_3A flag. The coordinate system of the Rapid Eye scene is the 34N UTM System, WGS 84. To view the studied area, two combinations of spectral bands were made, namely the RGB image combination 321 and the False Color image combination 532, Figure 1. The retrieved satellite data was processed with the ERDAS Image v. 11 and ArcGIS v. 10.5 software. Based on the satellite image, the Red Edge band numerical values were extracted and two vegetation indices, namely the NDVI (Normalized Difference Vegetation Index) introduced by Rouse *et al.* (1974), relationship (1) and SAVI (Soil Adjusted Vegetation Index), introduced by Huete (1988), relationship (2).

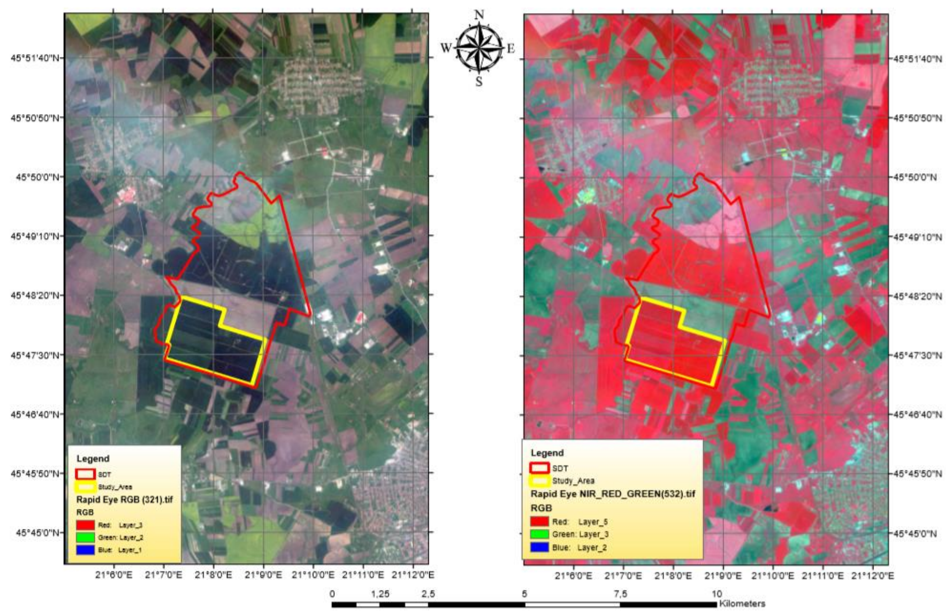

Figure 1. Studied area in Natural colors and False colors

$$NDVI = \frac{R_{800} - R_{670}}{R_{800} + R_{670}} = \frac{NIR - RED}{NIR + RED} = \frac{B5 - B3}{B5 + B3} \qquad (1)$$

$$NSAVI = \frac{(R_{800} - R_{670}) \times (1 + L)}{(R_{800} + R_{670} + L)} = \frac{(NIR - RED) \times (1 + L)}{(NIR + RED + L)} = \frac{(B5 - B3) \times (1 + L)}{(B5 + B3 + L)} \quad (2)$$

where: R_i is reflectance at the band centered at a given wavelength i (in nm); L= 0.5 – Vegetation cover correction factor.

Soil and agricultural crops. The soil in the studied area is cambic chernozem, the land being divided into 7 parcels with the area between 52.22 and 54.49 ha. There were wheat, oats and barley in culture. The agrochemical indices studied were the humus content (H), soil pH, phosphorus (P), potassium (K), the degree of saturation in bases (V) and Nitrogen Index (NI) (OSPA).

Processing of experimental data. The experimental data obtained were analyzed by the Kendall correlation analysis, descriptive statistics and regression analysis, using the EXCEL statistical calculation module, the OFFICE 2007 suite, the PAST 3 software (Rujescu *et al.*, 2014; Hammer *et al.* 2017).

RESULTS AND DISCUSSION

The values of the agrochemical indices on the land plots studied had variable values in relation to the specificity of the agrochemical index and the real situation in the field. The pH was between 6.27 and 7.35, the soil reaction being slightly acidic on 71.44% of the studied area (373.6 ha) and neutral on 28.56% of the area. Phosphorus supply is poor on 28.56% of the surface, average supply is 28.73% and very good supply is 42.71% of the area. Supply with K was good at 14.56% and very good on 85.44% of the surface. The supply of humus (H) was of medium level on the whole surface, the degree of saturation in bases (V) ranged from 84.0-94.5%, and the Nitrogen Index (NI) was the average level on the whole surface according to the standards in force (Sala, 2011), the values being presented in Table 1.

Cultures have expressed phenotypical the state of supply of land with nutrients. As a result, the agricultural images were compared with their real state at the time of the study, and the values of the NDVI, SAVI and Red Edge indices reflected crop information in close connection with the soil fertility status, agrochemical index values and of those calculated are shown in Table 1. Testing the level of correlation between the data series corresponding to the above indicators using the Kendall correlation coefficient, the data in Table 2 was obtained. A strong and statistically correlation was observed between P and Red Edge, correlated inversely ($r = -0.905$, $p = 0.004$). Direct intensity correlations between P and SAVI respectively between P and NDVI ($r = 0.619$ with p values close to 0.05) were observed. And the values of K correlate, but only slightly, $r = 0.429$ with NDVI and SAVI, respectively with Red Edge, $r = - 0.524$.

It is to be noticed that the NI and V values do not differ greatly from one plot to the other, with the differences between the minimum and maximum being low. Also, their series are homogeneous, with a low coefficient of variation, Table 3.

Table 1. Agrochemical index values and calculated indices for crop characterization

Parcel	Area (ha)	NDVI	SAVI	Red Edge	pH	P (ppm)	K (ppm)	H	V (%)	NI
1 / A84	52.22	0.677674	1.016389	6085.572	6.62	78.66	241.17	4.42	87	3.85
2 / A80	54.49	0.627742	0.941212	6111.502	6.74	69.59	234.4	4.05	88	3.56
3 / A75	52.32	0.661968	0.993197	6126.947	7.12	55.64	238.59	4.12	92	3.79
4 / A68	54.38	0.613137	0.920047	6242.421	7.35	19.94	178.41	3.71	94.5	3.51
5 / A77	52.85	0.62897	0.943328	6177.625	6.27	48.64	210.54	4.58	84	3.85
6 / A82	53.96	0.677191	1.015643	6034.912	6.30	97.53	298.7	3.66	84.5	3.09
7 / A86	53.38	0.681264	1.021864	5999.694	6.65	95.01	217.95	4.05	87	3.52

Table 2. Matrix correlation table (Kendall) between calculated indices and agrochemical indices

	NDVI	SAVI	Red Edge	pH	P	K	H	V	NI
NDVI		0.002	0.024	0.453	0.051	0.176	0.758	0.356	0.758
SAVI	1.000		0.024	0.453	0.051	0.176	0.758	0.356	0.758
Red Edge	-0.714	-0.714		0.293	0.004	0.099	0.538	0.218	0.538
pH	-0.238	-0.238	0.333		0.176	0.453	0.356	0.002	0.538
P	0.619	0.619	-0.905	-0.429		0.051	0.356	0.124	0.356
K	0.429	0.429	-0.524	-0.238	0.619		1.000	0.538	0.758
H	0.098	0.098	0.195	-0.293	-0.293	0.000		0.430	0.003
V	-0.293	-0.293	0.390	0.976	-0.488	-0.195	-0.250		0.636
NI	0.098	0.098	0.195	-0.195	-0.293	0.098	0.950	-0.150	

Table 3. Statistical parameters describing the values of agrochemical indices

	pH	P	K	H	V	NI
Min	6.271	19.940	178.410	3.660	84.000	3.090
Max	7.348	97.530	298.700	4.580	94.500	3.850
Sum	47.055	465.010	1619.760	28.590	617.000	25.170
Mean	6.722	66.430	231.394	4.084	88.143	3.596
Stand. Dev	0.398	27.501	36.764	0.337	3.837	0.270
Median	6.651	69.590	234.400	4.050	87.000	3.560
Coeff. Var	5.919	41.398	15.888	8.256	4.354	7.507

It is possible, therefore, that this aspect does not reveal a possible correlation between them and the calculated indices. Furthermore, low NI values of less than 4 for these parcels can make potassium inefficient, as only the presence of potassium under low nitrogen levels cannot effectively support plant growth.

The phenomenon identified and highlighted in this case, demonstrates the functionality of the minimum, maximum and optimum law.

Considering the complexity of the agrochemical mapping work in terms of the time of realization, the workload on the field and in the laboratory, the human resource involved and the costs, and starting from the correlation between the indices calculated on the basis of the spectral information in the satellite images and certain agrochemical indices, a regression analysis was performed to assess the possibility of soil situation prediction based on remote sensing.

In the case of phosphorus, the best correlated element in the studied conditions with NDVI, SAVI and Red Edge, regression analysis facilitated the obtaining of some 2nd degree polynomial equations for the prediction of P in relation to NDVI, the relation (3) under conditions of R^2= 0.724, $p < 0.01$, for P prediction in relation to SAVI, relation (4) under conditions of R^2= 0.718, $p < 0.01$ respectively P prediction in relation to Red Edge, relation (5) under conditions of R^2= 0.985, $p << 0.001$. The graphical distribution of real and predicted P values in relation to NDVI and Red Edge are shown in Figure 2, respectively Figure 3.

$$P_{NDVI} = -5307.2x^2 + 7702.3x - 2696.1 \qquad (3)$$

$$P_{SAVI} = -2257.6x^2 + 4936.6x - 2599.1 \qquad (4)$$

$$P_{REDEDGE} = -0.0005x^2 + 6.0476x - 17439 \qquad (5)$$

where: x – NDVI in relation (3); x – SAVI in relation (4); x – Red Edge in relation (5)

In the case of potassium, from correlation analysis resulted lower correlation coefficients with both NDVI and SAVI (r = 0.429), and as well as with Red Edge (r = 0.524). Regression analysis facilitated prediction K based on NDVI, under conditions of R^2= 0.774, relation (6), based on SAVI, under conditions of R^2= 0.768, relation (7) and based on Red Edge under condition of R^2= 0.889, the relation (8). The graphical distribution of real and predicted K values in relation to NDVI and Red Edge are presented in Figure 4, respectively Figure 5.

Different studies have approached fertilization models with mineral or foliar fertilizers to restore soil fertility, especially with P and K, and direct sustaining agricultural production (Rawashdeh and Sala, 2016).

$$K_{NDVI} = -12818x^2 + 7478x - 5706.6 \qquad (6)$$

$$K_{SAVI} = -5735.7x^2 + 11726x - 5742 \qquad (7)$$

$$K_{REDEDGE} = -0.0014x^2 + 17.178x - 51419 \qquad (8)$$

where: x – NDVI in relation (6); x – SAVI in relation (7); x – Red Edge in relation (8)

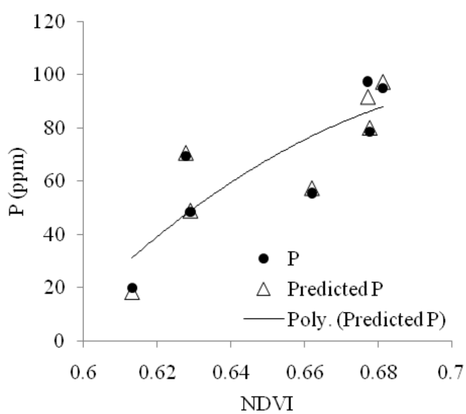

Figure 2. Graphical distribution of real and predicted P-values by NDVI

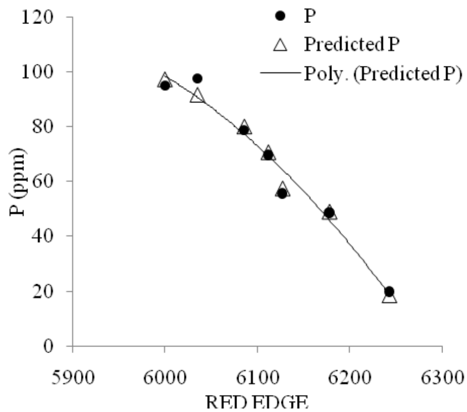

Figure 3. The graphical distribution of the real and predicted values of P by Red Edge

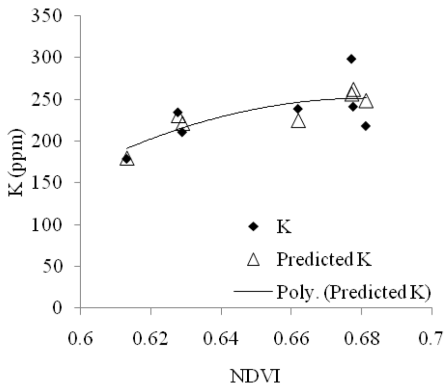

Figure 4. The graphical distribution of the real and predicted K values of the NDVI

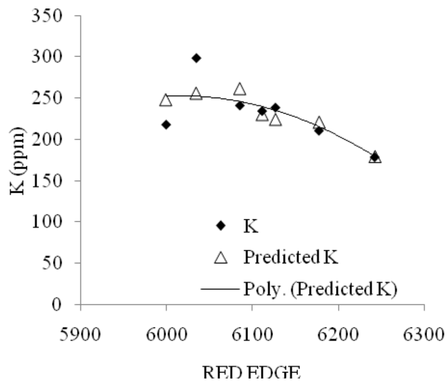

Figure 5. The graphical distribution of the real and predicted K by Red Edge

For the other agrochemical soil characterization indices, the correlation level was lower, according to the Kendall correlation analysis. As a result, regression analysis also facilitated the prediction of these indices with lower statistical safety. Thus, the soil pH was predicted by NDVI under condition of R^2= 0.324, depending on SAVI under conditions of R^2= 0.316, and depending on Red Edge under conditions of R^2= 0.696. The humus content (H) was predicted based on NDVI under conditions of R^2= 0.152, based on SAVI under conditions of R^2= 0.154, respectively based on Red Edge under conditions of R^2= 0.538. The degree of saturation in bases (V) was predicted based on NDVI under conditions of R^2= 0.325, under conditions of R^2= 0.317 based on SAVI, respectively under conditions of R^2= 0.703 based on Red Edge. The nitrogen index (NI) was predicted under conditions of R^2= 0.144 based on NDVI, under conditions of R^2=

0.147 based on SAVI, respectively under conditions of R^2= 0.623 based on Red Edge.

Red Edge band has proven to be particularly useful when studying crops health, nutrition and vegetation stress (Filella and Peñuelas, 1994; Li *et al.*, 2014), but it is also a tool for studies of astrobiology (Seager *et al.*, 2005). The Red Edge band is a unique feature that brings extra spectral information of RapidEye satellites to most multispectral satellites. The Red Edge band is located between the red band and the NIR band, without overlapping. The Red Edge band's sensitivity to the differences in leaf structure and chlorophyll content in relation to soil and nutrition factors, especially N, already has useful applications in the field of precision farming and resource monitoring and management (Clevers and Gitelson, 2013).

Vegetation indices are numerical indicators that reduce multispectral data (2 or more spectral bands) to a single variable for the prediction and evaluation of vegetation and vegetal carpet information.

The most widely used indicator of vegetation is the NDVI index, introduced in 1974 by Rouse and used to highlight vegetation health status, but also as an indicator of green biomass on the land surface or at the level farms, plots, agricultural crops. A series of scientific articles have been studied on the basis of remote sensing by means of dedicated indices of the state of the crops, the state of nutrition especially with nitrogen (Fitzgerald *et al.*, 2010). NDVI index values ranged from -1 to 1. In the case of normal and healthy vegetation, NDVI values are typically in the range of 0.1-0.75 and rarely reach 1, depending on its density, being one of the most use indices to characterize vegetation in relation to soil and growth conditions (Wu, 2014; Yang and Guo, 2014).

The SAVI index, introduced in 1988 by Huete, is a "hybrid" between the indices based on the ratio of spectral bands and perpendicular indices. The use of the SAVI index allows observation and monitoring of seasonal, annual and multi-annual vegetal cover, being used in various studies and underlying other vegetation indices, MSAVI, OSAVI (Hartfield and Prueger, 2010).

In the present study, for all soil agrochemical indices, the correlation coefficient with calculated indices (NDVI, SAVI and by Red Edge) and implicitly safety predictions made by regression analysis was higher based on the by Red Edge band compared to NDVI or SAVI indices.

CONCLUSIONS

Kendall's correlation analysis highlighted the high correlation between P and by Red Edge and weak average correlations between calculated indices and other agrochemical indices.

Regression analysis facilitated the acquisition of 2nd degree polynomial equations as predictive models of agrochemical indices based on NDVI, SAVI and by Red Edge, with high statistical safety for P and average statistical safety for K.

For all soil agrochemical indices considered, in the study agricultural area conditions (DER, BUASVM Timisoara, Timis County, Romania) the safety level of predictions made by regression analysis was higher based on the Red Edge band compared to NDVI or SAVI indices.

ACKNOWLEDGEMENTS

The authors thank to the staff of the Didactic and Experimental Resort of the Banat University of Agricultural Sciences and Veterinary Medicine "King Michael I of Romania" from Timisoara, Romania to facilitate this research.

Also, the authors thanks to the GEOMATICS Research Laboratory from BUASVM "King Michael I of Romania" Timisoara, for the facility to use the software for this research.

This paper is published from the own funds of the Banat`s University of Agricultural Sciences and Veterinary Medicine from Timisoara.

REFERENCES

Călina, J., Cãlina, A., Miluț, M., Croitoru, A., Stan, I., & Buzatu, C. (2020). Use of drones in cadastral works and precision works in silviculture and agriculture. *Romanian Agricultural Research*, 37: 273-284.

Clevers, J.G.P.W. & Gitelson, A.A. (2013). Remote estimation of crop and grass chlorophyll and nitrogen content using red-edge bands on Sentinel-2 and-3. *International Journal of Applied Earth Observation and Geoinformation* 23: 344-351.

Dalmau, O.S., Alarćon, T.E., & Oliva, F.E. (2017). Crop classification in satellite images through probabilistic segmentation based on multiple sources. *Sensors* 17(6): 1373.

Delegido, J., Verrelst, J., Alonso, L., & Moreno, J. (2011). Evaluation of Sentinel-2 Red-Edge bands for empirical estimation of green LAI and chlorophyll content. *Sensors* 11(7): 7063-7081.

Eldeiry, A.A. & Garcia, L.A. (2010). Comparison of regression kriging and cokriging techniques to estimate soil salinity using Landsat images. *Journal of Irrigation and Drainage Engineering* 136(6): 355-364.

Filella, I. & Peñuelas, J. (1994). The red edge position and shape as indicator of plant chlorophyll content, biomass and hydric status. *International Journal of Remote Sensing* 15(7): 1459-1470.

Firoozi, F., Mahmoudi, P., Amir Jahanshani, S.M., Tavousi, T., & Liu, Y. (2020). Evaluating various methods of vegetative cover change trend analysis using satellite remote sensing productions (Case study: Sistan Plain in Eastern Iran). *Carpathian Journal of Earth and Environmental Sciences*, 15(1): 211-222.

Fitzgerald, G.J., Rodriguez, D., & O'Leary, G. (2010). Measuring and predicting canopy nitrogen nutrition in wheat using a spectral index – the canopy chlorophyll content index (CCCI). *Field Crops Research* 116(3): 318-324.

Frampton, W.J., Dash, J., Watmough, G., & Milton, E.J. (2013). Evaluating the capabilities of Sentinel-2 for quantitative estimation of biophysical variables in vegetation. *ISPRS Journal of Photogrammetry and Remote Sensing* 82: 83-92.

Ge, Y., Thomasson, J.A., & Sui, R. (2011). Remote sensing of soil properties in precision agriculture: A review. *Frontiers of Earth Science* 5(3): 229-238.

Gómez, C., White, J.C., & Wulder, M.A. (2016). Optical remotely sensed time series data for land cover classification: A review. *ISPRS Journal of Photogrammetry and Remote Sensing* 116(2016): 55-72.

Hammer, Ø. Harper, D.A.T., & Ryan, P.D. (2017). PAST Paleontological Statistics Version 3.18 Reference manual, Natural History Museum University of Oslo. Available from: https://folk.uio.no/ohammer/past/past3 manual.pdf. Accessed: Nov. 12, 2017.

Hartfield, J.L. & Prueger, J.H. (2010). Value of using different vegetative indices to quantify agricultural crop characteristics at different growth stages under varying management practices. *Remote Sensing* 2(2): 562-578.

Huete, A.R. (1988). A soil-adjusted vegetation index (SAVI). *Remote Sensing of Environment* 25(3): 295-309.

Khaki, B.D., Honarjoo, N., Davatgar, N., Jalalian, A., & Golsefidi, H.T. (2017). Assessment of two soil fertility indexes to evaluate paddy fields for rice cultivation. *Sustainability* 9: 1299.

Kilic, O.M. (2021). Effects of land use and land cover changes on soil erosion in semi-arid regions of Turkey; a case study in Almus lake watershed. *Carpathian Journal of Earth and Environmental Sciences*, 16(1): 129-138.

Kim, J., Grunwald, S., Rivero, R.G. (2014). Soil phosphorus and nitrogen predictions across spatial escalating scales in an aquatic ecosystem using remote sensing images. *IEEE Transactions on Geoscience and Remote Sensing* 52(10): 6724-6737.

Kostić, M., Ljubičić, N., Ivošević, B., Popović, S., Radulović, M., Blagojević, D., & Popović, V. (2020). Spot-based proximal sensing for field-scale assessment of winter wheat yield and economical production. *Agriculture and Forestry* 67(1): 103-113.

Kozar, B., Lawrence, R., & Long, D.S. (2002). Soil phosphorus and potassium mapping using a spatial correlation model incorporating terrain slope gradient. *Precision Agriculture* 3(4): 407-417.

Lense, G.H.E., Moreira, R.S., Bócoli, F.A., Parreiras, T.C., Teodoro, A.E. de M., Spalević, V., & Mincato, R.L. (2020). Soil organic matter loss by water erosion in a coffee organic farm. *Agriculture and Forestry* 66(2): 45-50.

Li, F., Miao, Y., Feng, G., Yuan, F., Yue, S., Gao, X., Liu, Y., Liu, B., Ustin, S.L., & Chen, X. (2014). Improving estimation of summer maize nitrogen status with red edge-based spectral vegetation indices. *Field Crops Research* 157: 111-123.

Markoski, M., Arsov, S., Mitkova, T., & Janeska Stamenkovska, I. (2015). The benefit GIS technologies and precision agriculture principles in soil nutrient management for agricultural crop production. *Bulgarian Journal of Agricultural Science* 21(3): 554-559.

Muñoz-Huerta, R.F., Guevara-Gonzalez, R.G., Contreras-Medina, L.M., Torres-Pacheco, I., Prado-Olivarez, J., & Ocampo-Velazquez, R.V. (2013). A review of methods for sensing the nitrogen status in plants: Advantages, disadvantages and recent advances. *Sensors* 13(8): 10823-10843.

Oficiul de Studii Pedologice si Agrochimice Timis - OSPA (2010-2017).

Panda, S.S., Ames, D.P., & Panigrahi, S. (2010). Application of vegetation indices for agricultural crop yield prediction using neural network techniques. *Remote Sensing* 2(3): 673-696.

Planet, Team, (2017). Planet application program interface: In space for life on Earth. San Francisco, CA. https://api.planet.com.

Popovici, E.A., Kucsicsa, Gh., Bălteanu, D., Grigorescu, I., Mitrică, B., Dumitrașcu, M., & Damian, N. (2018). Past and future Land use/cover flows related to agricultural lands in Romania. An assessment using clue-s model and corine land cover database. *Carpathian Journal of Earth and Environmental Sciences*, 13(2): 613-628.

Prabhakara, K., Hively, W.D., & McCarty, G.W. (2015). Evaluating the relationship between biomass, percent groundcover and remote sensing indices across six winter cover crop fields in Maryland, United States. *International Journal of Applied Earth Observation and Geoinformation* 39: 88-102.

Reyes-Gonźalez, A., Kjaersgaard, J., Trooien, T., Hay, C., & Ahiablame, L. (2018). Estimation of crop evapotranspiration using satellite remote sensing-based vegetation index. *Advances in Meteorology* 2018: 4525021.

Rouse, J.W., Haas, R.H., Schell, J.A., & Deering, D.W. (1974). Monitoring vegetation systems in the great plains with ERTS. In: Proceedings third Earth resources technology satellite-1 symposium, Greenbelt, NASA SP– 351(1): 3010-3017.

Rujescu, C., Ciolac, R., Martin, S. C., & Butur, M. (2014). The use of a two-factor model for the fertilization of agricultural crops in order to determine the optimal production area. *Lucrări Științifice Management Agricol* 16(1): 9.

Sala, F. (2011). Agrochimie. Editura Eurobit, pp.187, 222, 287, 324.

Saleh, A.M., Belal, A.B., & Mohamed, E.S. (2015). Land resources assessment of El-Galaba basin, South Egypt for the potentiality of agriculture expansion using remote sensing and GIS techniques. *The Egyptian Journal of Remote Sensing and Space Sciences* 18(1): S19-S30.

Seager, S., Turner, E.L., Shafer, J., & Ford, E.B. (2005). Vegetation's red edge: a possible spectroscopic biosignature of extraterrestrial plants. *Astrobiology* 5(3): 372-390.

Sharf, P.C., Schmidt, J.P., Kitchen, N.R., Sudduth, K.A., Hong, S.Y., Lory, J.A., & Davis, J.G. (2002). Remote sensing for nitrogen management. *Journal of Soi land Water Conservation* N|D: 518-524.

Shoko, C. & Mutanga, O. (2017). Examining the strength of the newly-launched Sentinel 2 MSI sensor indetecting and discriminating subtle differences between C3 and C4 grass species. *ISPRS Journal of Photogrammetry and Remote Sensing* 129(2017): 32-40.

Ustuner, M., Sanli, F.B., Abdikan, S., Esetlili, M.T., & Kurucu, Y. (2014). Crop type classification using vegetation indices of Rapideye imagery. *The International Archives of the Photogrammetry. Remote Sensing and Spatial Information Sciences* XL-7: 195-198.

Wan, Z., Wang, P., & Li, X. (2004). Using MODIS land surface temperature and normalized difference vegetation index products for monitoring drought in the southern Great Plains, USA. *International Journal of Remote Sensing* 25(1): 61-72.

Wójtowicz, M., Wójtowicz, A., & Piekarczyk, J. (2016). Application of remote sensing methods in agriculture. *Communications in Biometry and Crop Science* 11(1): 31-50.

Wu, W. (2014). The Generalized Difference Vegetation Index (GDVI) for dryland characterization. *Remote Sensing* 6(2): 1211-1233.

Yang, X. & Guo, X. (2014). Quantifying responses of spectral vegetation indices to dead materials in mixed grasslands. *Remote Sensing* 6(5): 4289-4304.

Haji, K., Khaledi Darvishan, A., Mostafazadeh, R. (2022). Identification of erosion critical areas based on soil erodibility and terrain influence factors in the Iranian part of the Caspian Sea Basin. Agriculture and Forestry, 68 (2): 35-47. doi:10.17707/AgricultForest.68.2.03

DOI: 10.17707/AgricultForest.68.2.03

Khadijeh HAJI[1], Abdulvahed KHALEDI DARVISHAN[*2], Raoof MOSTAFAZADEH[3]

IDENTIFICATION OF EROSION CRITICAL AREAS BASED ON SOIL ERODIBILITY AND TERRAIN INFLUENCE FACTORS IN THE IRANIAN PART OF THE CASPIAN SEA BASIN

SUMMARY

Understanding the contribution of different land uses in soil erosion leads to optimal management and conservation practices to reduce the severity of erosion and consequently, the sustainable management. Changeability of the most effective factors on soil erosion especially soil erodibility and topography in different land uses is a first step to have a general view of soil erosion in the watersheds. Therefore, the present research was carried out to study the soil erodibility (S) and terrain influence (T) factors in different land uses in the Iranian part of the Caspian Sea Basin and identification of erosion critical areas based on topography and soil erodibility factors. In order to prepare land use, S and T maps for the study area, were prepared by using satellite data of moderate resolution imaging spectroradiometer (MODIS), shuttle radar topography mission (SRTM 90m) and harmonized world soil database (HWSD) and the use of geographic information system (GIS) and remote sensing (RS), respectively. The results showed that the mean soil erodibility in the Iranian part of the Caspian Sea Basin varied from zero (soilless areas) to 0.044 (t ha hr ha^{-1} MJ^{-1} mm^{-1}). While, among eight studied land use, the highest and lowest mean values of soil erodibility were obtained in the rangeland and permanent snow-water body equal to 0.040 and zero (t ha hr ha^{-1} MJ^{-1} mm^{-1}), respectively. Also, the mean terrain influence (T) factor varied from 0.01 to 35.83 and shows more changeability in the study basin. As a result, by considering the high soil erodibility and terrain influence, the maximum erosion potential in the study area are located in the middle parts of the basin, where the highest slope gradients have high soil erodibility values. These areas are mainly located in the south slopes of the Alborz mountains. In this regard, defined critical regions based on topography and soil erodibility factors along with natural and anthropogenic factors can be considered in the planning of soil erosion control in watersheds and soil and water conservation programs.

Keywords: Land use, Management practices, Satellite data, Soil erodibility, Topography.

[1]Khadijeh Haji, Abdulvahed Khaledi Darvishan (corresponding author: a.khaledi@modares.ac.ir), Department of Watershed Management Engineering, Faculty of Natural Resources, Tarbiat Modares University, Noor, IRAN; Raoof Mostafazadeh, Department of Watershed Management and Member of Water Management Research Institute, University of Mohaghegh Ardabili, IRAN..
Received: 27/02/2022 Accepted:23/05/2022

INTRODUCTION

Soil erosion is one of the most significant forms of land (soil truncation, loss of fertility, slope instability) and is greatly influenced by biodiversity, land use and management (Solaimani *et al*., 2009; Spalevic *et al*., 2013; Behzadfar *et al*., 2014; Chalise *et al*., 2018; Lense *et al*., 2020; Spalevic *et al*., 2020; Spalevic *et al*., 2021; Stefanidis *et al*., 2022). It is likely to be exacerbated by extensive human activities and global warming (Rosas and Gutierrez, 2019), and is a serious problem in developing countries (Chalise *et al*., 2019; Khaledi Darvishan *et al*., 2019). Soil erodibility (S) can be viewed as the integral result of the processes determining the infiltration of rain into the soil and of the processes determining the soil's resistance to the detachment of its particles and their subsequent transport (Renschler *et al*., 1999; Karami *et al*., 2018). It is generally considered as an inherent soil property with a constant value for a given soil type and widely adopted as an important factor in soil erosion prediction models (Kulikov *et al*., 2017; Dutal and Reis, 2020). It is closely related to the basic physico-chemical characteristics of soils. Soil erosion is not only different for various types of soils, but also it is different for the same type of soil under different climate conditions or land use management. Different land use systems might alter several soil properties and processes (Karami *et al*., 2018; Tavares *et al*., 2019; Ouallali *et al*., 2020; Lense *et al*., 2021; Costea *et al*., 2022). The most important driving forces for soil erosion in Iran include soil vulnerability, land use change, unnecessary and improper development of infrastructures and illegal exploitation of natural resources (Sadeghi, 2009).

Both topographic factors, such as slope gradient and altitude, and anthropogenic factors, such as land use change, poor plant coverage, and inadequate erosion control measures, are primary reasons for soil erosion (Reis *et al*., 2017; Billi & Spalevic, 2022). The annual soil loss amounting from arable lands is 75 billion tons and costs approximately $400 billion each year in agricultural production worldwide (Wang and Zhang, 2021). To carry out a suitable plan for the management of degraded slope lands to control erosion rates and loss of productivity, it would require first a realistic assessment of soil degradation by assessing the risk of erosion in the target area. This is the main objective that can be achieved according to many previous studies by direct field and laboratory measurements of soil erodibility (Aburas *et al*., 2020). Therefore, information about soil erodibility is the main necessity for an assessment of the soil degradation process and conservation techniques in a watershed (Vaezi *et al*., 2016) and also preventing reservoir siltation (Stefanidis and Stefanidis, 2012). Identification of critical area is an important procedure to control runoff and erosion phenomenon and considered as effective way in management of watersheds and achieving sustainable development (Mostafazadeh *et al*., 2017). Hence, studies on soil erodibility have been conducted by many researchers in the world. Therefore, the always growing availability of earth observation (EO) data and technological advancement lead to the development of automated geospatial workflows in order to fasten soil loss estimation (Stefanidis *et al*., 2021).

The effects of land management on soil erodibility in a part of Zayandeh-Rood watershed showed the average soil erodibility of 0.05 (ton h MJ-1 mm-1) in good pasture and 0.09 (t h MJ^{-1} mm^{-1}) in pasture land use and 0.09 (t h MJ^{-1} mm^{-1}) in degraded pastures (Karami *et al*., 2018). They found that the low soil organic matter content in the degraded pastures land is probably caused by livestock overgrazing and ultimately grazing. Evaluation of the soil erodibility of unpaved road slopes at the Bom Jardim city in the mountain region of the state of Rio de Janeiro showed the highest erodibility of the C horizons in relation to the other horizons of the Oxisol and Ultisol studied (Lima Soares *et al*., 2018). This fact explains the main process of observed instability, erosion at the toe of the slope and fall of the upper horizons. These results highlighted the anthropogenic effects and land use changes on soil erosion.

The effects of land use on soil erodibility in the Mediterranean highland regions of Turkey were determined by Dutal and Reis (2020). The results showed that the average erodibility (USLE-K) value was 0.09 for forest, while it was 0.12 and 0.22 for pasture and agriculture, respectively. The difference between agriculture with forest and pasture was statistically significant, while no statistically significant difference was found between forest and pasture in the study area. Parmar and Sharma (2020) calculated soil loss and soil erodibility for different crops, nutrient managements, soil series and four different slope gradients (0.5, 1≤ to <3, 1≤ to <3 and >5 %) and showed that soil loss decreased with decreasing slope gradient. The soybean cropping found more vulnerable to the soil loss whereas the orchard system found safest for soil erosion.

Soil legislation is of great importance around the globe to limit the amount of soil loss. Although there are many studies on the relationships between land use and soil erodibility, but no study has been reported yet regarding the effects of land use change on soil erodibility in Caspian Sea Basin. Therefore, the objective of this study was identification of erosion critical areas based on soil erodibility and terrain influence factors in the Iranian part of the Caspian Sea Basin.

MATERIAL AND METHODS

Study area

The Iranian part of the Caspian Sea Basin with an area of 176393.9 km^2, covers about 10% of the total area of the country and lies between 35º-39º 45′ N-latitude and 44º-59º 05′ E-longitude (Figure 1). Compared to the other parts of the country, this region has relatively more hydrometric stations and larger recorded rainfall and runoff data. With a permanent river network as well as productive farmlands, rangelands and forests, this region is of a major interest. The study basin has a complex topography with a diversity of slopes and average slope gradient of 26 %. The altitude ranges between -28 (Caspian coast) to 5671 m (Mount Damavand) and the average altitude of the study area is 1195 m. A total of 54 synoptic weather stations are operated in the study area (Chavoshi *et al*., 2013). Figure 1 shows the location of the Caspian Sea Basin among all mega-basins of Iran. The land use of the study area and also, S and T raster maps were prepared. Then, the distribution of S and T values for each land use were calculated.

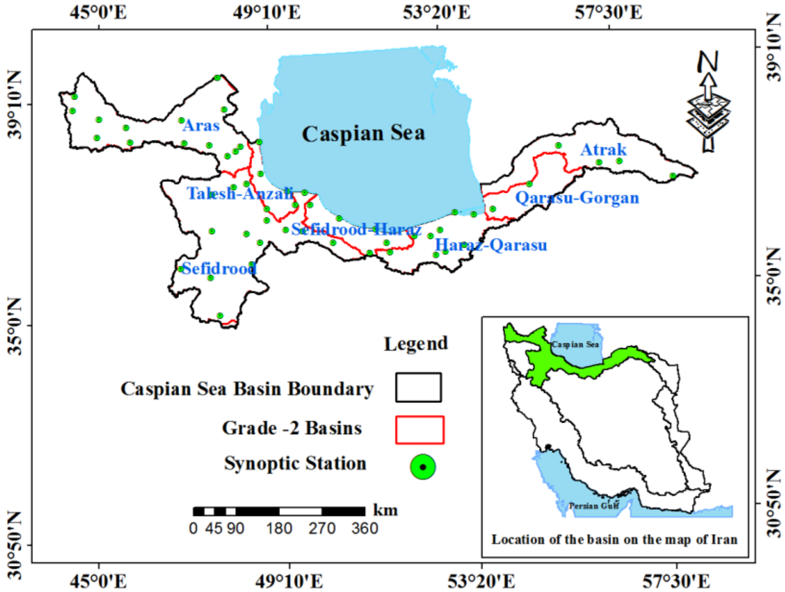

Figure 1. The location of the Caspian Sea Basin among all mega-basins of Iran

Land use map

Land use plays a critical role in soil sensitivity analysis. As a result, land should be properly used in terms of its ability and limitations, otherwise it will cause severe soil erosion (Mostafazadeh *et al*., 2017). The availability of land use information permits decision-makers to develop plans in short to long-term period for the conservation, sustainable use and development of natural resources and watersheds (Talebikhiavi *et al*., 2017; Kuriqi and Hysa, 2021). In this study, image interpretation from moderate resolution imaging spectroradiometer (MODIS) data was used to prepare land use map of the Iranian part of the Caspian Sea Basin for the year 2018. The MODIS land cover type product (MCD12Q1) supplies global maps of land cover at annual time steps and 500m spatial resolution (Sulla-Menashe and Friedl, 2018). The MCD12Q1 product is created using supervised classification of MODIS reflectance data (Friedl *et al*., 2010). Also, modifications and updates in Google Earth software used and classified to land use eight studied. Finally, ArcGIS 10.5 software were used for land use mapping (Figure 2).

Soil erodibility (S) map

Soil erodibility (denoted as the K-factor in the USLE and the S-factor in the G2 model) is best estimated from direct measurements of natural plots (Panagos *et al*., 2014). As this is not financially sustainable at the regional/national level, the S-factor Equation (1) relates to soil properties as proposed for the USLE model by Renard *et al*. (1997):

$$S = \left[\frac{2.1 * 10^{-4} * M^{1.14} * (12 - OM) + 3.25 * (s - 2) + 2.5 * (p - 3)}{100}\right] * 0.1317 \quad (1)$$

where, K: soil erodibility (t ha hr ha^{-1} MJ^{-1} mm^{-1}); M: textural factor defined as percentage of silt plus very fine sand fraction content (0.002-0.1 mm) multiplied by the factor: 100 - clay fraction; OM: organic matter content in percent (%); s: soil structure class (s = 1: very fine granular, s = 2: fine granular, s = 3: medium or coarse granular, s= 4: blocky, platy or massive); and p permeability class (p = 1: very rapid, …, p = 6: very slow) (Panagos *et al*., 2012). In the present study, the soil data of the study area was extracted from the Harmonized World Soil Database (HWSD).

Terrain influence (T) map

To estimate the influence of topography on erosion risk (T-factor, or terrain influence, or LS as denoted by the USLE), the G2 model uses an equation developed and proposed by Desmet and Govers (1996):

$$T = \left(\frac{A_S}{22.13}\right)^{0.6} * \left(\frac{\sin b}{0.0896}\right)^{1.3} \quad (2)$$

where, T: terrain influence (dimensionless, ≥0); As: unit contributing area, or flow accumulation (the numbers of upstream cells flowing into a specific cell, in m^2/m); and b: slope gradient (rad). Equation (2) is an adaptation of the Moore and Burch (1986) algorithm for spatially distributed USLE applications to grid systems. The method estimates T values equivalent to length and steepness (LS) values resulting from the original USLE formulas. The flow accumulation layers for every basin were computed from a Shuttle Radar Topography Mission (SRTM 90m) digital elevation model (DEM).

Two factors (L and T) were extracted from satellite image data and S-factor was extracted from HWSD using the ArcGIS10.5 software (Table 1).

Table 1. Summary of the input data for final mapping (Karydas & Panagos, 2018)

Factor type	Input data	Scale	Range	Dimensionality*	Source
Dynamic	Land use derived from MODIS satellite data (L)	Pixel size 1 km	[1,+∞]	0	http://earthexplorer.usgs.gov
Static	Soil Parameters (S)	Cell size 1 km	[0, 0.1]	[M] [L^{-1}] [P^{-1}]	http://www.fao.org/soils-portal/data-hub/soil-maps-and-databases/harmonized-world-soil-database-v12/en/
	DEM extracted from SRTM satellite (T)	Pixel size 90 m	[0, 200]	0	http://earthexplorer.usgs.gov

*P: Power; L: Length; M: Mass

Erosion potential map

After preparing and classification of each layer according to the conditions of the region and the range of numbers obtained, the final map of erosion potential by overlaying the layers (T and S factors) was prepared and classified into different classes of erosion potential based on multiplying soil erodibility and terrain influence factors. The values of K-RUSLE or S-G2 (soil erodibility) and LS-RUSLE or T-G2 (topography) factors in a given area do not change in the short term. Therefore, based on the conditions of the study area as well as land use status, it is necessary to identify the critical areas in order to implement of the control and protection operations in these areas (Fagbohun *et al*., 2016).

RESULTS AND DISCUSSION

The present study was performed to assess soil erosion potential based on soil erodibility (S) and terrain influence (T) factors for each individual land use in the Iranian part of the Caspian Sea Basin. Figure (2) shows the land use map of the study area. The lower soil erosion rates in the forests, is because of increasing the vegetation retention value which prevents of soil loss in this land use. But it is very important to note that without vegetation cover, the soil erosions rates even in the forests may be very high potentially specially where the soil erodibility and slope gradient is high enough to increase soil erosion.

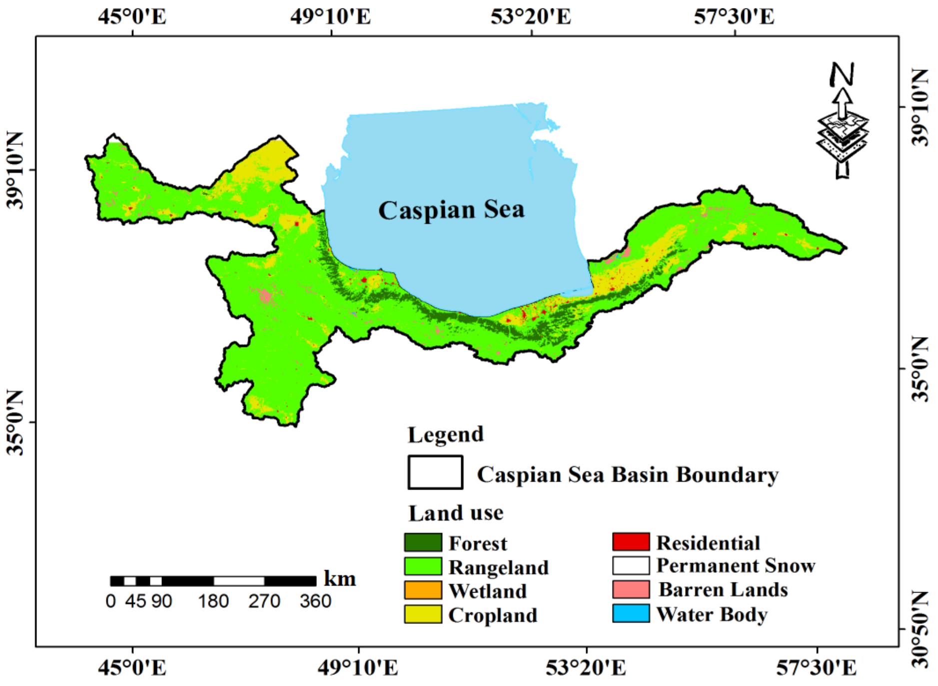

Figure 2. Land use map in the Iranian part of the Caspian Sea Basin

The terrain influence factor (T) of the Iranian part of the Caspian Sea Basin is shown in Figure (3). The mean value of terrain influence factor varies from 0.01 to 35.83 in various land uses. The lowest values of terrain influence factor are related to the flat regions (Alamdari *et al*., 2013), while the highest values of terrain influence factor (T) are related to the steep and long slope regions (Alborz mountains). In other words, in flat regions the effect of terrain influence on soil erosion value may less than the effects of rainfall intensity, soil type and vegetation. The effect of topography factors on soil loss were mentioned by other researchers (Biswas and Pani, 2015; Chalise & Kumar, 2020; Parmar and Sharma, 2020).

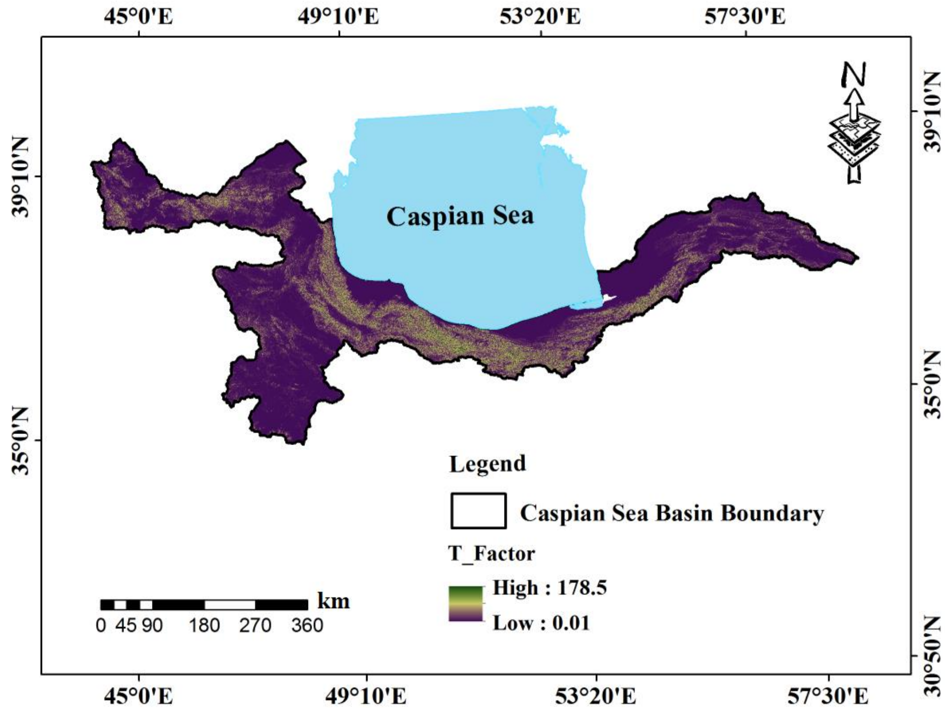

Figure 3. Terrain influence factor map (Iranian part of the Caspian Sea Basin)

Figure 4 shows soil erodibility factor (S) map in the Iranian part of the Caspian Sea Basin. Most of the dominant soils in Iran territory have less than 2% organic matter. Therefore, these soils have relatively weak soil structure and high erodibility and are sensitive to erosion. The results of the present study show that the soil erodibility value in the Iranian part of the Caspian Sea Basin ranged from zero (no soil regions) to 0.044 (t ha hr ha^{-1} MJ^{-1} mm^{-1}).

The mean values of soil erodibility (S) and terrain influence (T) factors in different land uses in the Iranian part of the Caspian Sea Basin are shown in Table 2. Among eight studied land uses, the rangeland has the highest area in the study basin (about 77 %). Also, the highest and lowest mean values of soil erodibility factor were obtained in the rangeland (0.040 t ha hr ha^{-1} MJ^{-1} mm^{-1}) and permanent snow - water bodies (zero t ha hr ha^{-1} MJ^{-1} mm^{-1}), respectively. These results confirmed the findings reported by Taleshian Jeloudar *et al*. (2018). While the highest and lowest mean values of terrain influence factor (35.83) were obtained in the permanent snow areas (peak and steep slopes of the mountains) and water bodies (0.01), respectively.

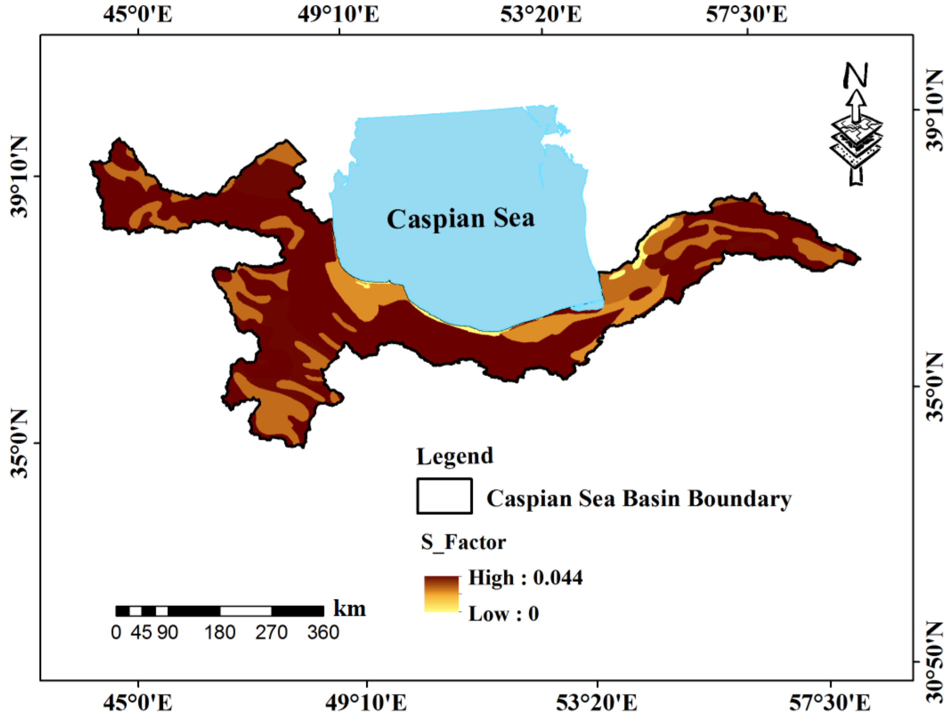

Figure 4. Soil erodibility factor (S) (Iranian part of the Caspian Sea Basin)

Whereas, with increasing terrain influence factor, runoff and soil erosion are increased too, but due to freezing soil and very low soil erodibility, the areas with permanent snow in mountain regions are not considered as critical area. The mean values of soil erodibility (S) and terrain influence (T) factors in different land uses in the Iranian part of the Caspian Sea Basin are shown in Table 2. The erosion potential map of the study area based on multiplying the soil erodibility (S) and terrain influence (T) factors is shown in Figure 5. Erosion critical areas (%) for T×S > 1.34 in different land uses of the Iranian part of the Caspian Sea Basin are shown in Figure 6.

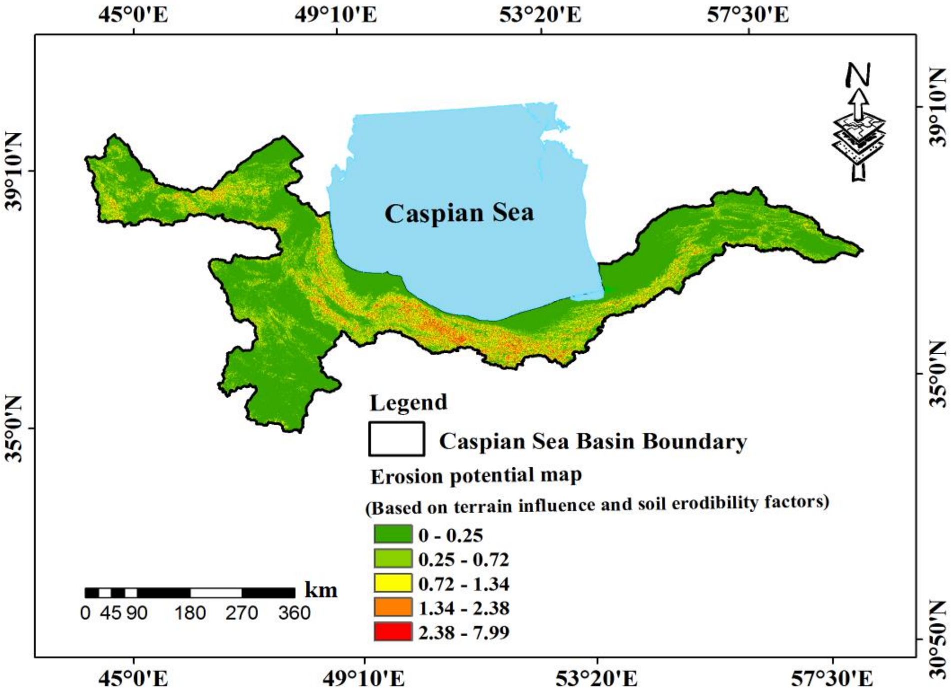

Figure 5. The erosion potential map (based on multiplying soil erodibility and terrain influence factors) in the Iranian part of the Caspian Sea Basin

Table 2. The mean values of soil erodibility (S) and terrain influence (T) factors in different land uses in the Iranian part of the Caspian Sea Basin

Land use/Land cover	Area (Km^2)	Soil erodibility (S) (t ha hr ha^{-1} MJ^{-1} mm^{-1})	Terrain influence (T)
Forest	10632.1	0.038	19.28
Rangeland	135543.7	0.040	7.72
Wetland	271.8	0.020	0.09
Cropland	25624.1	0.037	3.35
Residential	1353.8	0.028	0.50
Permanent snow	1.81	0.000	35.83
Barren lands	2695.1	0.036	6.74
Water body	271.5	0.000	0.01

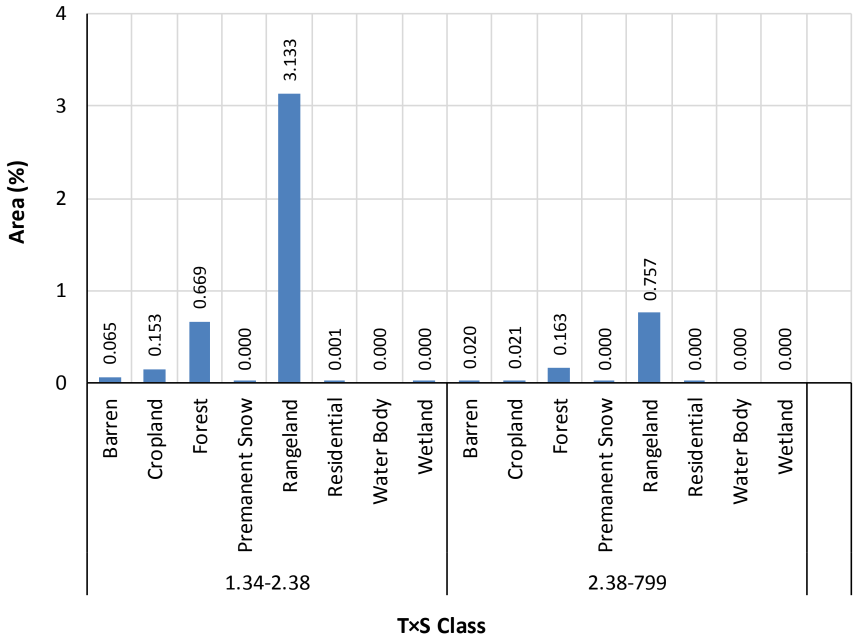

Figure 6. Erosion critical areas (%) for T×S > 1.34 in different land uses of the Iranian part of the Caspian Sea Basin

According to Figure 6, rangeland has the highest values of terrain influence multiplied by soil erodibility in the study watershed. In other words, 3.89 % of the rangelands can be considered as erosion critical areas and therefore, any vegetation removal and land use change especially to agricultural lands in these areas can lead to accelerated soil erosion rates.

The results showed that by considering the high soil erodibility and terrain influence factors, the highest erosion potential value as 7.99 located in the middle parts of the basin, where the highest slope gradients have relatively high soil erodibility values too. These areas are mainly located in the south slopes of the Alborz mountains. These results confirmed the findings reported by Mohammadi *et al*. (2021). As a result, the lack of vegetation cover as well as heavy rainfalls will cause more severe erosion in these areas, compared to the other parts of the basin. It is highly recommended to study the vegetation cover in the study area and also to compare soil erosion observations and estimations using other soil erosion models to increase the accuracy of the results. Confirming the findings reported by Mostafazadeh *et al*. (2017) and Belayneh *et al*. (2019), this conclusion most be used by natural resources managers and design-makers to avoid any land use change specially from rangeland to cultivation in the erosion critical areas.

CONCLUSION

According to the study results, the mean values of soil erodibility (S) and terrain influence (T) in the Iranian part of the Caspian Sea Basin were 0.039 (t ha hr ha^{-1} MJ^{-1} mm^{-1}) and 7.68, respectively. Soil erodibility was found to be moderate and high in most parts of the study area, (especially in rangelands, forests and croplands). Soil erosion potential map based on multiplying two main factors of soil erodibility and terrain showed the critical areas. It is highly recommended to study and focus more on these critical areas to locate urgent crop and grazing management programs and soil conservation measures. In other word, the critical areas should have more vegetation cover especially during seasons with erosive and high intensity rainfalls.

ACKNOWLEDGMENTS

This research was conducted as a part of doctoral dissertation of Khadijeh Haji and with the financial support of Tarbiat Modares University, Iran. Authors would like to thank Shahin Mohammadi for his great helps in preparing land use map of the study area.

REFERENCES

Aburas, M.M., Habel, A.Y., Alferjani, A.S., Yous, M.S. (2020). Assessment of soil erodibility and erosion risk of some semiarid slopes of Libya. Quality Assurance Center of Eastern Province Quality Assurance Journal for Academic Researches: 1-13.

Alamdari, P., Nematollahi, O., Alemrajabi, A.A. (2013). Solar energy potentials in Iran: A review. Renewable and Sustainable Energy Reviews 21: 778-788.

Behzadfar, M., Djurovic, N., Simunic, I., Filipovic, M. and Spalevic, V. (2014). Calculation of soil erosion intensity in the S1-6 Watershed of the Shirindareh River Basin, Iran; p. 207-213. Conference: Challenges in Modern Agricultural Production, Dec 2014, Skopje, N.Macedonia. Book of Proceedings, p. 273.

Belayneh, M., Yirgu, T., Tsegaye, D. (2019). Potential soil erosion estimation and area prioritization for better conservation planning in Gumara watershed using RUSLE and GIS techniques. Environmental Systems Research 8(20): 1-17.

Billi, P., Spalevic, V. (2022). Suspended sediment yield in Italian rivers. Catena 212(2022):106119. Doi: 10.1016/j.catena.2022.106119

Biswas, S.S., Pani, P. (2015). Estimation of soil erosion using RUSLE and GIS techniques: a case study of Barakar River basin, Jharkhand, India. Model. Earth Systems and Environment 1-42.

Chalise, D., Kumar, L., Shriwastav, C.P., Lamichhane, S. (2018). Spatial assessment of soil erosion in a hilly watershed of Western Nepal. Environmental Earth Sciences 77 (19): 685.

Chalise, D., Kumar, L., Spalevic, V., Skataric, G. (2019). Estimation of Sediment Yield and Maximum Outflow Using the IntErO model in the Sarada River Basin of Nepal. Water 11: 952, https://doi.org/10.3390/w11050952.

Chalise, D., Lumar, L. (2020). Land use change affects water erosion in the Nepal Himalayas. PLoS ONE 15(4).

Chavoshi, S., Sulaiman, W.N.A., Saghafian, B., Sulaiman, M.N.B., Abd Mana, L. (2013). Flood prediction in southern strip of Caspian Sea Watershed. Water Resources and The Regime of Water Bodies 40(6): 593-605.

Costea, A., Bilasco, S., Irimus, I.-A., Rosca, S., Vescan, I., Fodorean, I., Sestras, P. (2022). Evaluation of the Risk Induced by Soil Erosion on Land Use. Case Study: Guruslau Depression. Sustainability 2022, 14, 652.

Desmet, P.J.J., Govers, G. (1996). A GIS procedure for automatically calculating the USLE LS factor on topographically complex landscape units. Journal of Soil and Water Conservation, 51(5): 427-433.

Dutal, H., Reis, M. (2020). Determining the effects of land use on soil erodibility in the Mediterranean highland regions of Turkey: a case study of the Korsulu stream watershed. Environmental Monitoring and Assessment 192 (192): 1-15.

Fagbohun, B.J., Anifowose, A.Y.B., Odeyemi, C., Aladejana, O.O., Aladeboyeje, A.I. (2016). GIS-based estimation of soil erosion rates and identification of critical areas in Anambra sub-basin, Nigeria. Modeling Earth Systems and Environment 2(159): 1-10.

Friedl, MA., Sulla-Menashe, D., Tan, B., Schneider, A., Ramankutty, N. *et al*. (2010). MODIS Collection 5 global land cover: Algorithm refinements and characterization of new datasets. Remote Sens Environ, 114(1): 168-182.

Karami, E., Ghorbani Dashtaki, S., Khalilimoghadam, B. (2018). Effects of land management on soil erodibility-A case study in part of Zayandeh-Rood watershed. Journal of Agricultural Engineering, 40(2): 105-119.

Karydas, C.G., Panagos, P. (2018). The G2 erosion model: An algorithm for month-time step assessments. Environmental Research 161: 256-267.

Khaledi Darvishan, A., Mohammadi, M., Skataric, G., Popovic, S., Behzadfar, M., Rodolfo Ribeiro Sakuno, N., Luiz Mincato, R., Spalevic, V. (2019). Assessment of soil erosion, sediment yield and maximum outflow, using IntErO model (Case study: S8-Inta Shirindarreh watershed, Iran). Agriculture and Forestry, 65 (4), 203-210

Kulikov, M., Schickhoff, U., Gröngröft, A., Borchardt, P. (2017). Modelling soil erodibility in mountain rangelands of South-Western Kyrgyzstan. Pedosphere, https://doi. org/10.1016/S1002-0160(17)60402-8.

Kuriqi, A., Hysa, A. (2021). Multidimensional Aspects of Floods: Nature-Based Mitigation Measures from Basin to River Reach Scale. In: The Handbook of Environmental Chemistry. Springer, Berlin, Heidelberg. https://doi.org/10.1007/698_2021_773

Lense, G.H.E., Moreira, R.S., Parreiras, T.C., Silva, L.F.P, M., Teodoro, A.E.M., Mincato, R.L. (2020). Simulating the effect of permanent preservation areas on soil erosion rates. Cerne, 26 (2), 193-201.

Lense, G.H.E., Parreiras, T.C., Spalevic, V., Avanzi, J.C., & Mincato, R.L. (2021). Soil losses in the State of Rondônia, Brazil. Ciência Rural, 51(5), 1-10. e20200460. Epub March 08, 2021. https://doi.org/10.1590/0103-8478cr20200460

Lima Soares, D., Polivanov, H., Velloso Barroso, E., Goretti da Motta, L.M., Camacho de Souza, C. (2018). Soil erodibility on cutting slopes of Unpaved roads. Anuario do Instituto de Geociencias 41(1): 179-193.

Mohammadi, S., Balouei, F., Haji, Kh., Khaledi Darvishan, A., Karydas, C.G. (2021). Country-scale spatio-temporal monitoring of soil erosion in Iran using the G2 model. International Journal of Digital Earth, 14(8): 1019-1039.

Moore, I.D., Burch, G.J. (1986). Physical basis of the length-slope factor in the Universal Soil Loss Equation. Soil Science Society of America Journal 50: 1294-1298.

Mostafazadeh, R., Haji, Kh., Esmali-Ouri, A., Nazarnejad, H. (2017). Prioritization the critical sub-watersheds based on soil erosion and sediment using watershed erosion response model (WERM) and Morphometric Analysis (Case study: Rozechai Watershed, West Azerbaijan Province). Journal of Watershed Management Research 8(16): 142-156 (in Persian).

Ouallali, A,, Aassoumi, H., Moukhchane, M., Moumou, A., Houssni, M., Spalevic, V., Keesstra, S. (2020). Sediment mobilization study on Cretaceous, Tertiary and Quaternary lithological formations of an external Rif catchment, Morocco, Hydrological Sciences Journal, 65(9), 1568-1582.

Panagos, P., Meusburger, K., Alewell, C., Montanarella, L. (2012). Soil erodibility estimation using LUCAS point survey data of Europe. Environmental Modelling Software 30: 143-145.

Panagos, P., Meusburger, K., Ballabio, C., Borrelli, P., Alewell, C. (2014). Soil erodibility in Europe: a high- resolution dataset based on LUCAS. Science of the Total Environment 479: 189-200.

Parmar, S., Sharma, S.K. (2020). Estimation of soil loss and soil erodibility for different crops, nutrient managements and soil series. International Journal of Pure Applied Bioscience 8(1): 204-212. doi: http://dx.doi.org/10.18782/2582-2845.7984

Reis, M., Aladag, I.A., Bolat, N., Dutal, H. (2017). Using Geoweep model to determine sediment yield and runoff in the Keklik watershed in Kahramanmaras Turkey. Sumar. List 141: 563-569.

Renard, K.G., Foster, G.R., Weesies, G.A., McCool, D.K., Yoder, D.C. (1997). Predicting soil erosion by water: a guide to conservation planning with the revised universal soil loss equation (RUSLE). In: Agriculture Handbook, U.S. Department of Agriculture, 703: 404 p.

Renschler, C.S., Mannaerts, C., Diekkrüger, B. (1999). Evaluating spatial and temporal variability in soil erosion risk-rainfall erosivity and soil loss ratios in Andalusia, Spain. Catena 34: 209-225.

Rosas, M.A., Gutierrez, R.R. (2019). Assessing soil erosion risk at national scale in developing countries: The technical challenges, a proposed methodology, and a case history. Science of the Total Environment 703: 135474.

Sadeghi, S.H.R. (2009). An overview on sediment problems and management in Iran. Sediment Problems and Sediment Management in Asian River Basins, In: Proceedings of the ICCE Workshop, Hyderabad, India, Sep. IAHS Pub 349:14-20.

Solaimani, K., Modallaldoust, S., Lotfi, S. (2009). Investigation of land use changes on soil erosion process using geographical information system. International Journal of Environmental Science and Technology, 6(3): 415-424.

Spalevic, V., Barovic, G., Vujacic, D., Curovic, M. Behzadfar, M., Djurovic, N., Dudic, B., Billi, P. (2020). The Impact of Land Use Changes on Soil Erosion in the River Basin of Miocki Potok, Montenegro. Water, 2020, 12, 2973.

Spalevic, V., Djurovic, N., Mijovic, S., Vukelic-Sutoska, M., Curovic, M. (2013). Soil Erosion Intensity and Runoff on the Djuricka River Basin (North of Montenegro). Malaysian Journal of Soil Science. 17, 49-68.

Spalevic, V., Zejak, D., Curovic, M., Glisic, I., Radovic, A. (2021): Analysis of the impact of fruit growing development on the intensity of soil erosion and runoff: Case study of Krusevo, Bijelo Polje, Montenegro. Agriculture and Forestry, 67 (2): 37-51

Stefanidis, P., & Stefanidis, S. (2012). Reservoir sedimentation and mitigation measures. Lakes & Reservoirs: Research & Management, 17(2): 113-117.

Stefanidis, S., Alexandridis, V., Ghosal, K. (2022). Assessment of Water-Induced Soil Erosion as a Threat to Natura 2000 Protected Areas in Crete Island, Greece. Sustainability 14(5): 2738.

Stefanidis, S., Chatzichristaki, C., Stefanidis, P. (2021). An ArcGIS toolbox for estimation and mapping soil erosion. J. Environ. Prot. Ecol, 22, 689-696.

Sulla-Menashe D, Friedl MA (2018). User guide to collection 6 MODIS land cover (MCD12Q1 and MCD12C1) Product. 1-18.

Talebikhiavi, H., Zabihi, M., Mostafazadeh, R. (2017). Effects of land-use management scenarios on soil erosion rate using GIS and USLE model in Yamchi dam watershed, Ardabil. Journal of Water and Soil Science (Science and Technology of Agriculture and Natural Resources), 21(2): 221-234 (in Persian).

Taleshian Jeloudar, F., Ghajar Sepanlou, M., Emad, S.M. (2018). Impact of land use change on soil erodibility. Global Journal of Environmental Science and Management, 4(1): 59-70.

Tavares, A.S., Spalevic, V., Avanzi, J.C., Nogueira, D.A., Silva, M.L.N., Mincato,R.L. (2019). Modeling of water erosion by the erosion potential method in a pilot subbasin in southern Minas Gerais. Semina: Ciencias Agrarias, 40(2), 555-572.

Vaezi, A.R., Hasanzadeh, H., Cerda, A, (2016). Developing an erodibility triangle for soil textures in semi-arid regions, NW Iran. Catena, 142: 221-232.

Wang, H., Zhang, G. (2021). Temporal variation in soil erodibility indices for five typical land use types on the Loess Plateau of China. Geoderma 381: 114695.

Stefanidis, S., Alexandridis, V., Spalevic, V., Mincato, R.L. (2022). Wildfire Effects on Soil Erosion Dynamics: The Case of 2021 Megafires in Greece. Agriculture and Forestry, 68 (2): 49-63. doi:10.17707/AgricultForest.68.2.04

DOI: 10.17707/AgricultForest.68.2.04

Stefanos STEFANIDIS[1*], Vasileios ALEXANDRIDIS[2], Velibor SPALEVIC[3] and Ronaldo Luiz MINCATO[4]

WILDFIRE EFFECTS ON SOIL EROSION DYNAMICS: THE CASE OF 2021 MEGAFIRES IN GREECE

SUMMARY

In recent decades, the frequency and severity of wildfires have increased, especially in the Mediterranean Basin. Aside from their direct effects, accelerated soil erosion is observed in fire-affected areas due to the destruction of vegetation. The 2021 Greece megafires were one of the country's major ecological disasters, destroying over 125,000 hectares of forest and agricultural land. The present study aims to quantify the effects of selected wildfire events on erosion dynamics over the 2021 fire season. To accomplish the goals of the current research the RUSLE erosion prediction model was implemented using readily available earth observation (EO) data. The results demonstrated a shift to the erosion hazard from very low and low (pre-fire) to severe and very severe (post-fire), in all cases. In particular, the increase in potential erosion, expressed in t ha^{-1} y^{-1}, was found to be equal to 98.5, 65.9, 57.0, 56.3, 51.6 and 35.6 for the Gytheio (Laconia), Schinos (Corinthia – West Attica), Northern Evia, Ancient Olympia – Gortynia (Ilia), Vilia (Western Attica) and Varympompi (Attica) regions, respectively. Moreover, the spatial distribution of post-fire soil erosion rates provides sufficient information for the identification of the erosion prone-areas and the corresponding emergency rehabilitation treatments.

Keywords: Megafires, Soil erosion, RUSLE, Earth Observation, Mediterranean Basin.

INTRODUCTION

The prevention of soil erosion and reduction of its damage requires reliable knowledge of the whole processes and effective factors (Bilasco *et al*., 2021; Dragicevic *et al*., 2017; Katebikord *et al*., 2017; Vujacic *et al*., 2017) including many natural and human-induced environmental factors. Fire is one of the

[1]Stefanos Stefanidis [*](corresponding author: ststefanid@gmail.com), Laboratory of Mountainous Water Management and Control, Faculty of Forestry and Natural Environment, Aristotle University of Thessaloniki, 54124 Thessaloniki, GREECE; Vasileios Alexandridis, Independent Researcher, 54621 Thessaloniki, GREECE; Velibor Spalevic, Biotechnical faculty, University of Montenegro, 81000 Podgorica, MONTENEGRO; Ronaldo Luiz Mincato, Federal University of Alfenas, UNIFAL-MG, Alfenas, Minas Gerais, BRAZIL.
Received: 11/03/2022 Accepted:28/05/2022

effective factors on soil characteristics such as organic content, structure and infiltration which can change the runoff and erosion conditions on the soil surface. Climate change has the potential to influence many aspects of wildfire behaviour and risk. Wildfires constitute the most severe abiotic disturbance in the Mediterranean forest ecosystems. Although fire is an integral part of these ecosystems (Pausas *et al*., 2006), its frequency, duration and severity have significantly increased during the last decades (Fernandez-Anez *et al*., 2021). The prevailing burning conditions (fuel, weather, topography) under which a wildfire occurs synthesize the pyric environment that influences fire behaviour and suppression tactics (Dimitrakopoulos *et al*., 2011).

In Southern Europe, the Mediterranean-type climate with the prolonged dry and warm summer period, the flammable vegetation, the complex topography, as well as human activities, favors both the ignition and the spread of wildfires. Furthermore, warmer and drier conditions in the Euro-Mediterranean region are expected over the next decades under future climate projections (Cos *et al*., 2022; Hysa *et al*., 2021; Hysa & Spalevic, 2020; Zittis *et al*., 2019; Nemeth, 2015). Hence, there will be increases in fire extent, intensity and duration of the fire season (Amatulli *et al*., 2013; Mitsopoulos *et al*., 2016; Kotroni *et al*., 2020) leading to an increased likelihood of large wildfires, known as megafires.

Megafire is called an extraordinary fire that devastates a large area. They are notable for their physical characteristics including intensity, size, duration, and uncontrollable dimension, as well as their social characteristics, including suppression cost, damages and fatalities (Buckland, 2019). Megafires are not always a single wildfire, but sometimes a grouping or “complex” of inter-acting multiple fires across a large geographic area (Williams *et al*., 2011). However, there is no single, consistent, quantitative definition of a megafire. In Europe, they are characterized as beginning at 1,000 hectares (ha), in size, while in the United States beginning at 10,000 ha. Disastrous megafires events have been reported in the recent history of Greece. The fire of August 2007 in Peloponnese (South Greece) resulted in a loss of 84 human lives and 177,000 ha of burned area (Gitas *et al*., 2008), the biggest number of burned area among European countries (San-Miguel-Ayanz *et al*., 2013). Additionally, in July 2018 (Eastern Attica), Greece experienced the deadliest event ever (102 casualties) which burned approximately 1250 ha (Lagouvardos *et al*., 2019). Another ecological disaster was the megafires that occurred in Greece during the 2021 summer period, where multiple fire events burned a total area of almost 100.000 hectares, setting a new tragic record in the country’s history (Papadopoulos *et al*., 2021).

It is well known fact that the land use change leads to changes in hydrologic response, soil erosion, and sediment dynamics characteristics (Spalevic *et al.*, 2021; Kuriqi & Hysa, 2021; Spalevic *et al.*, 2020; Spalevic *et al.*, 2013). Wildfires are taking significant part in this. In the aftermath of wildfires, significant changes occur on hydrological and erosion regimes (Shakesby 2011; Efthimiou *et al*., 2020; Curovic *et al*., 2021; Lecina-Diaz *et al*., 2021; Soulis *et al*., 2021). This is mainly due to the complete or partial loss of vegetation that decreases water infiltration rate and water storage capacity while surface runoff increases. Except for the damages to plant communities, fire affects the texture and the physico-chemical properties of the surface soil layer, turning it into a hydrophobic layer and thereby leading to higher soil erosion rates (Kokaly *et al*., 2007; McGuire and Youberg, 2021).

Quantitative soil erosion assessment in fire-affected areas is a crucial tool for policymakers to evaluate the magnitude of post-fire erosion risk and implement mitigation measures, such as emergency hillslope rehabilitation treatments and watershed stabilization measures (Myronidis and Arabatzis, 2009; Robichaud and Ashmun, 2012). The ever-growing availability of high-resolution earth observation data and the well-established use of geospatial technologies facilitate the large-scale quantitative analysis of soil erosion, in a short period.

During the last decade, Greece has experienced large-scale wildfire phenomena with unprecedented fire behaviour and impacts (Kalabokidis *et al*., 2015). The present study aims to quantify the erosion dynamics changes immediately after the megafires in 2021 over Greece. The analysis was not limited to a single event, but multiple destructive wildfires were studied. To that end, pre-fire and post-fire erosion dynamics were assessed, exploiting the combined use of freely EO data and the RUSLE model.

MATERIAL AND METHODS

The study was conducted in selected fire-affected areas of Greece territory from the destructive megafires in 2021. The analysis included the areas that suffered the greatest ecological disaster with burned areas of more than 5.000 ha. The location map of the selected megafires and the associated burned areas are given in the following figure (Figure 1).

Figure 1. The location map of the selected megafires over Greece in 2021: i) Northern Evia, ii) Varympompi (Attica), iii) Vilia (Western Attica), iv) Schinos (Corinthia – West Attica), v) Ancient Olympia - Gortynia (Ilia) and vi) Gytheio (Laconia).

The spatial extent of the burned areas was retrieved from the Copernicus Emergency Management Service (EMS)[2]. This service consists of the on-demand and fast provision (hours-days) of geospatial information in support of emergency management activities immediately following a disaster. The service is based on the acquisition, processing and analysis, in rapid mode, of satellite imagery and other geospatial raster and vector data sources. Analytical details of the start date and the burned area (ha) for the selected wildfire events based on the EMS data are given in the table (Table 1).

Table 1. Characteristics of the wildfire event based on EMS rapid mapping activations

A/A	Location	Start Date	EMS (Act. Code)	Burned Area (ha)
i	Northern Evia	03/08/2021	EMSR527	51245
ii	Varympompi (Attica)	03/08/2021	EMSR527	8454
iii	Vilia (Western Attica)	16/08/2021	EMSR540	10175
iv	Schinos (Corinthia – West Attica)	19/05/2021	EMSR510	7005
v	Ancient Olympia - Gortynia (Ilia)	04/08/2021	EMSR528	18400
vi	Gytheio (Laconia)	03/08/2021	EMSR531	11209

RUSLE Model

According to the various reports of the European Soil Bureau Institute for Environment and Sustainability and the European Environment Agency, the Universal Soil Loss Equation model (USLE) is extensively used in the following European countries: Austria, Bosnia, and Herzegovina (including the Republic of Srpska), Bulgaria, Greece, Italy, Hungary, Norway, Romania, Slovakia, Finland, Czech Republic, Spain, and Switzerland. The Revised Universal Soil Loss Equation (RUSLE) is used in Belgium; the UK, Germany, and France are using their domestic/national models (Spalevic *et al.*, 2019). In the countries of Balkan Peninsula, the Erosion Potential Method (EPM) for mapping the intensity of water erosion is the preferred model (Volk *et al.*, 2009; Spalevic, 2011; Kostadinov *et al.*, 2018; Gocic *et al.*, 2020; Tosic *et al.*, 2019; Nikolic *et al.*, 2021), and recently Globally the IntErO model, based on the EPM (Sabri *et al.*, 2019; Chalise *et al.*, 2019; Sakuno *et al*., 2020; Ouallali *et al.*, 2020; Mohammadi *et al.*, 2021).

In this research we used the revised (R) Universal Soil Loss Equations (USLE), known as RUSLE, is an empirical model that computes mean annual soil loss by sheet and rill water erosion (Renard *et al.*, 1991). The mathematical description of the model is expressed as a linear combination of five factors, related to climate, topography, vegetation cover, pedology and land management (Lense *et al.*, 2021).

The equation is presented as following:

[2] https://emergency.copernicus.eu/mapping/list-of-activations-rapid

$$A = R \times K \times LS \times C \times P \tag{1}$$

where A is the computed annual soil loss (t ha^{-1} y^{-1}), R is the rainfall erosivity factor (MJ mm ha h^{-1} y^{-1}), K is the soil erodibility (t ha h ha^{-1} MJ^{-1} mm^{-1}), LS is the combined effect of slope length (L) and slope steepness factor (S) (dimensionless), C is the cover management factor (dimensionless) and P is the conservation practice factor (dimensionless).

In the current approach, the RUSLE model was implemented in a GIS framework using open available geospatial data. These datasets include gridded precipitation, satellite imagery, and digital elevation model (DEM) and soil properties. The data were organized in GIS thematic layers. Subsequently, the determination of each factor during the implementation of the soil loss model is described in the following sub-sections. The conservation practice factor was not considered in this study and a constant value equal to 1 was assigned to each case study. This was done for two reasons. Firstly, there were no reliable available data to define its values. Secondly, the conservation practices (P-factor), including contour farming, stone walls and grass margins has profound effects on cropland and rangeland. However, these types of practices are generally limited in forest ecosystems, as the examined burned areas.

The footprint of megafires on erosion dynamics was achieved by comparing the RUSLE values before and after the vegetation destruction from the fire events.

Rainfall Erosivity Factor (R)

The rainfall erosivity factor (R) is the model's climate component, accounting for the effect of rainfall amount and intensity on soil loss. It is defined as the average annual sum of the kinetic energy of storm events having a maximum rainfall intensity of 30 minutes. However, sub-hourly rainfall rate records from ground-based meteorological stations are rarely available in Greek territory. Therefore, in the present study average monthly precipitation data from the CHELSA (v2.1) dataset (Karger *et al.*, 2017) for the period 1979-2018 were used. CHELSA (Climatology at high resolution for the earth's land surface areas) is a very high resolution (30 arcsec, ~1km) global downscaled climate data set currently hosted by the Swiss Federal Institute for Forest, Snow and Landscape Research WSL. It is built to provide free access to high-resolution climate data for research and application, and is constantly updated and refined.

To calculate the annual R-factor, a simplified mathematical equation developed by Arnoldus (1980) was applied. The mathematical description of the formula is given below:

$$R = \sum_{i=1}^{12} 1.735 \times 10^{\left(\left(1.5 \log\left(\frac{P_i^2}{P}\right) - 0.08188\right)\right)} \tag{2}$$

where R is the rainfall erosivity factor (MJ mm ha h^{-1} y^{-1}), P_i is the monthly rainfall (mm) and P is the annual rainfall (mm).

Soil Erodibility Factor (K)

The soil erodibility factor describes the susceptibility of soil types to detachment and transport as a result of the raindrop and runoff process. It depends on physical and chemical soil properties such as soil texture (contents of silt, sand, clay, and organic carbon), permeability, shear strength, organic matter and chemical composition. The K factor is rated on a scale from 0 to 1, where lower values indicate soils less prone to erosion.

Herein, the K-factor was estimated according to the Renard *et al* (1997) approach based on the soil's sand, silt and clay contents. The necessary data were retrieved in raster format from ISRIC-World Soil Information SoilGrids250m dataset (Hengl *et al* 2017) with a spatial resolution of 250m. Soil grids is a system for digital soil mapping based on a global compilation of soil profile data (WoSIS) and environmental layers using machine learning techniques. Afterward, the following mathematical equations were used to estimate K-factor in each grid cell:

$$K = 7.594 \left\{0.0034 + 0.0405 \times \exp\left[-0.5\left(\frac{\log D_g + 1.659^2}{0.7101}\right)\right]\right\} \quad (3)$$

$$D_g = \exp\left(0.01 \sum f_i \ln m_i\right) \quad (4)$$

where K is the soil erodibility factor (t ha h ha^{-1} MJ^{-1} mm^{-1}), D_g is the geometric mean particle diameter (mm), for each size class (clay, silt, sand), f_i is the primary particle size fraction in percent and m_i is the arithmetic mean of the diameter limits for each particle size class (mm) based on the USDA classification.

Topographic factor (LS)

The combination of slope length (L) and slope steepness (S) individual factors describe the effect of topography on the erosion process. The slope length is the distance from the origin of overland flow along its flow path to the location of either concentrated flow or deposition, while slope steepness is the segment or site gradient slope, expressed as a percentage. The higher values of LS-factor represent steeper relief, where erosion and sediment yield increase due to an increase in the runoff.

The LS-factor was calculated in the System for Automated Geoscientific Analyses (SAGA) GIS software package which incorporates the multiple flow algorithm (Pilesjö and Hasan, 2014). In this module, a digital elevation model (DEM) is required as an input parameter for the calculation of the LS-factor. The FABDEM (Forest and Buildings removed Copernicus DEM) was selected for this analysis. This is a global DEM at 30 m grid-spacing, with artefacts from forests and buildings removed (FABDEM). FABDEM has notable benefits compared to existing global DEMs, resulting from the use of the new Copernicus GLO-30 DEM and a machine learning correction of forests and buildings. This makes it preferable for many purposes where a bare-earth representation of terrain is needed (Hawker *et al*., 2022).

The S-factor is calculated, considering the slope gradient, in degrees (ϑ) based on the mathematical equation provided by McCool *et al.* (1989)

$$S = \begin{cases} 10.8 \times sin\vartheta + 0.03, \vartheta < 0.09 \\ 16.8 \times sin\vartheta - 0.5, \vartheta > 0.09 \end{cases} \quad (5)$$

Regarding the L-factor, it is calculated using the proposed equation by Desmet and Govers (1996). This approach takes into account that the slope steepness is not uniform for the whole area and introduces the concept of the unit-contributing area. The mathematical formula given below:

$$L = \frac{(A_{i,j-in} + D^2)^{m+1} - A_{i,j-in}^{m+1}}{D^{m+2} \times x_{i,j}^{m} \times 22.13^{m}} \quad (6)$$

where $A_{i,j,-in}$ is the contributing area (m^2) at the inlet of grid pixel (*i,j*), D is the grid pixel size (m), $x_{i,j}$ is the summation of the sine and cosine of aspect direction ($\alpha_{i,j}$) of grid pixel ($x_{i,j} = \sin \alpha_{i,j} + \cos \alpha_{i,j}$), and *m* is a coefficient related to the ratio β of the rill to inter-rill erosion. The *m* values range between 0 and 1 and ϑ is the angle of slope in degrees. The equation for the *m* coefficient is:

$$m = \frac{\beta}{\beta + 1} \quad (7)$$

$$\beta = \frac{\frac{sin\vartheta}{0.0896}}{[0.56 + 3 \times sin\vartheta^{0.8}]} \quad (8)$$

Cover Management Factor (C)

The C-factor reflects the effect of surface cover and cover management practices on erosion rates. It is defined as the ratio of soil loss from a certain area with specific vegetation coverage to a constantly barren region. The C-factor ranges between 0 and 1, while the lowest values indicate the well-protected land.

There are several methods in the literature for calculating the C-factor using vegetation indices derived from satellite images (Phinzi and Ngetar, 2019). The most well-known approaches analyzed the linear correlation between C-factor and NDVI (Van der Knijff *et al*., 2000; Durigon *et al*., 2014). Also, the NDVI is sufficient for change detection (Polykretis *et al*., 2020; Tariq *et al*., 2021). The NDVI was calculated considering the near-infrared (NIR) and red (RED) spectrums of a multispectral satellite image using the following mathematical formula:

$$NDVI = \frac{NIR - Red}{NIR + Red} \quad (9)$$

Subsequently, the following equations were used to calculate the C-factor based on NDVI vegetation index.

$$C = \exp\left[-\alpha\left(\frac{NDVI}{\beta - NDVI}\right)\right] \tag{10}$$

where a and b are unitless parameters and equal to 2 and 1, respectively. The C-factor ranges from 0 to 1, with closeness to 0 indicating well-protected land.

NDVI index derived from Sentinel-2A imageries, which provides optical data with atmospheric and radiometric corrections. The spatial resolution on the red (RED) and near-infrared (NIR) spectral bands that are required for the NDVI calculation has a spatial resolution of 10 m. In the current approach, pre-fire and post-fire Sentinel-2A images (single-date) were obtained for each fire event. The images were acquired from the European Space Agency (ESA) Copernicus Access Hub (https://scihub.copernicus.eu) and a universal cloud coverage threshold <10% for all the images was used. Dates of the selected images per fire event can be seen in the next table (Table 2).

Table 2. Dates of the Sentinel 2-2A imageries per fire event.

Fire event	**Sentinel-2 image pre-fire**	**Sentinel-2 image post-fire**
Northern Evia	1/8/2021	18/8/2021
Varympompi (Attica)	3/8/2021	8/8/2021
Vilia (Western Attica)	28/7/2021	26/8/2021
Schinos (Corinthia - West Attica)	13/5/2021	23/5/2021
Ancient Olympia - Gortynia	2/8/2021	17/8/2021
Gytheio (Laconia)	1/8/2021	11/8/2021

RESULTS AND DISCUSSION

The erosion prediction model of RUSLE was implemented in a GIS environment under pre-fire and post-fire conditions for the selected natural ecosystems. Unfortunately, no actual measurements are available to validate the model’s accuracy. However, the performance of RUSLE in quantifying soil loss rate has been found to be satisfactory in the neighbouring Mediterranean basin (Efthimiou, 2016; Napoli *et al*., 2016; Porto *et al*., 2022). Significant changes in erosion dynamics were found in the fire-affected areas (Figure 2). It is worth noting that the soil loss rate in the most pre-fire case was quite low. On the contrary, the megafires increased potential erosion by nearby 10 times compared to the pre-fire conditions. Particularly, the magnitude of the erosion dynamic changes, expressed in t ha^{-1} y^{-1}, was equal to +98.5, +65.9, +57.0, +56.3, +51.6 and +35.6 for the Gytheio, Schinos, Northern Evia, Ancient Olympia – Gortynia, Vilia and Varympompi region respectively. Similar increases in the post-fire erosion potential have been documented in Mediterranean ecosystems (Mallinis *et al*., 2009; Myronidis *et al*., 2010).

Subsequently, the obtained values of soil loss were grouped into six classes according to the Reneuve and Galevsky (1955) classification scheme. This classification approach is effective for the identification of areas threaten by accelerated erosion (Myronidis *et al*., 2010).

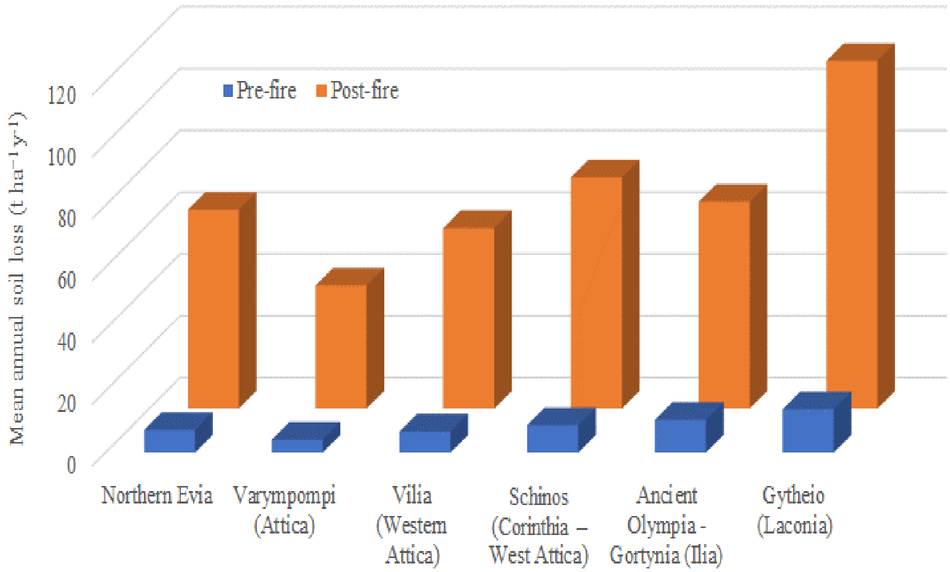

Figure 2. Soil loss rate in the study areas under each condition

The erosion hazard classes and their corresponding break values (t ha^{-1} y^{-1}) are as follow: Very Low (<5), Low (5-12), Moderate (12-50), Severe (50-100), Very Severe (100-200) and Extreme (>200). In the pre-fire scenario, all the examined areas had very low and low erosion hazard for more than 70% of their entire area. On the contrary, severe, very severe and extreme hazard classes are negligible except in Laconia, where they account for around 6.5% of the total area. The coverage distribution of the erosion hazard classes is directly affected by the megafires. In general, there was a transition from very low and low hazard (pre-fire) to severe and very severe (post-fire). Additionally, a remarkable rise in the moderate and extreme hazard classes has been noted. Detailed results on the coverage rates for each erosion hazard class category, between the pre-fire and post-fire conditions, are presented in the next figure (Figure 3).

The analysis highlighted the footprint of the 2021 megafires on erosion regulation ecosystem service. Beyond the numerical statistics concerning soil loss rate, the spatial mapping of erosion dynamics provides critical information to policymakers. These maps could be a useful tool for selecting the appropriate erosion mitigation strategy. The emergency hillslope rehabilitation treatments and watershed stabilization measures could be determined in a cost-effective way based on the identified erosion prone areas, proximity to the stream network and settlements, and geomorphological conditions. The spatial distribution of erosion hazard after the megafires events were given in the following figure (Figure 4).

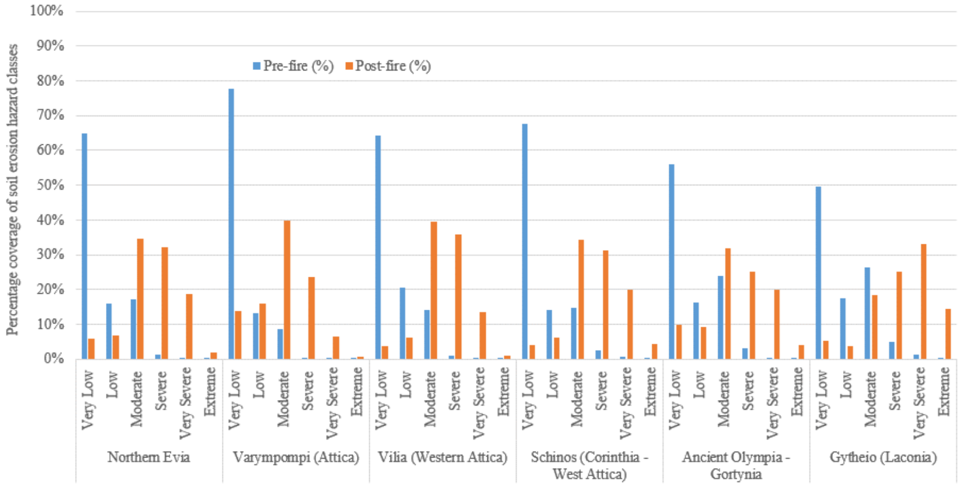

Figure 3. Erosion hazard classes coverage rate in the examined areas

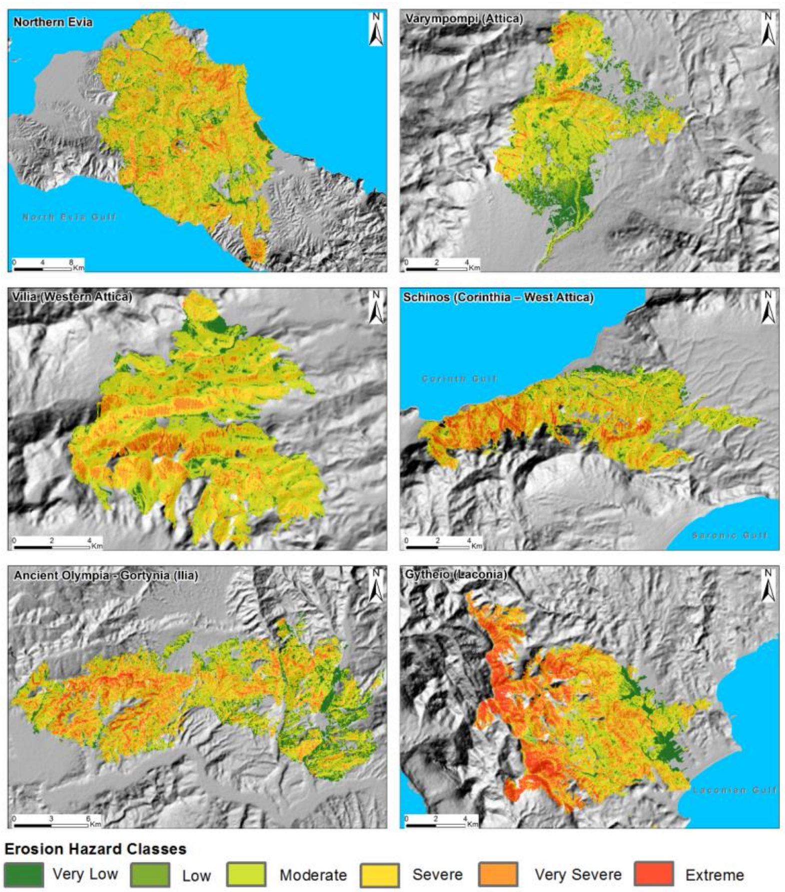

Figure 4. Post-fire erosion hazard mapping in the fire-affected ecosystems

CONCLUSION

This paper quantifies the spatiotemporal changes in soil erosion dynamics driven by Greece's megafires in 2021. Our approach integrates freely accessible EO data and the empirical RUSLE model for the estimation of the potential soil loss. Aside from its practical usefulness, the proposed methodology is simple, easy to use, has minimal input data requirements and low computational demands. To that end, quantitative and spatial distribution of erosion hazard was achieved at high spatial resolution. The developed methodology can easily transfer to any region and scaled at national or even Pan-European level.

Significant increases in soil loss rates have been reported in fire-affected regions, based on a comparison of pre-fire and post-fire RUSLE model outputs in each case. The investigation also highlighted the footprint of multiple destructive fire occurrences on natural ecosystems' erosion regulation services. Furthermore, the produced erosion hazard maps provide helpful information for identifying the erosion prone areas. It may also be employed by policymakers for targeted management and planning of post-fire erosion mitigation strategy. Controlling accelerated erosion following wildfires is a primary concern for stabilizing soils and enhancing natural regeneration in Mediterranean pinewoods. Future research could focus on the development of an automated workflow for the spatial determination of emergency erosion control works based on the previously described erosion hazard maps.

REFERENCES

Amatulli, G., Camia, A., & San-Miguel-Ayanz, J. (2013). Estimating future burned areas under changing climate in the EU-Mediterranean countries. Science of the Total Environment, 450, 209-222.

Arnoldus, H.M.J. (1980). An Approximation of the Rainfall Factor in the Universal Soil Loss Equation. In: De Boodt, M. and Gabriels, D., Eds., Assessment of Erosion, John Wiley and Sons, New York, 127-132.

Bilasco, S.; Rosca, S.; Vescan, I.; Fodorean, I.; Dohotar, V.; Sestras, P. (2021). A GIS-Based Spatial Analysis Model Approach for Identification of Optimal Hydrotechnical Solutions for Gully Erosion Stabilization. Case Study. Appl. Sci. 2021, 11, 4847. https://doi.org/10.3390/app11114847

Buckland, M. K. (2019). What is a megafire? Defining the social and physical dimensions of extreme US wildfires (1988-2014). Doctoral dissertation, University of Colorado at Boulder, pp. 47.

Chalise, D., Kumar, L., Spalevic, V., Skataric, G. (2019). Estimation of Sediment Yield and Maximum Outflow Using the IntErO Model in the Sarada River Basin of Nepal. Water, 11, 952. https://www.mdpi.com/2073-4441/11/5/952.

Cos, J., Doblas-Reyes, F., Jury, M., Marcos, R., Bretonnière, P. A., & Samsó, M. (2022). The Mediterranean climate change hotspot in the CMIP5 and CMIP6 projections. Earth System Dynamics, 13(1), 321-340.

Curovic, M., Spalevic, V., Stijovic, A., Curovic, Z., Buskovic, V. (2021). Forests of the Coast of Montenegro. In: Joksimović, D., Đurović, M., Zonn, I.S., Kostianoy, A.G., Semenov, A.V. (eds) The Montenegrin Adriatic Coast. The Handbook of Environmental Chemistry, vol.110. Springer, Cham. 51- 67

Desmet, P. J. J. and Govers, G. (1996). A GIS procedure for automatically calculating the USLE LS factor on topographically complex landscape units. Journal of Soil and Water Conservation, 51(5), 427-433.

Dimitrakopoulos, A., Gogi, C., Stamatelos, G., & Mitsopoulos, I. (2011). Statistical analysis of the fire environment of large forest fires (> 1000 ha) in Greece. Polish Journal of Environmental Studies, 20(2), 327-332.

Dragicevic, N., Karleusa, B., Ozanic, N. (2017). Erosion Potential Method (Gavrilovic method) sensitivity analysis. Soil & Water Res., 12: 51-59.

Durigon, V. L., Carvalho, D. F., Antunes, M. A. H., Oliveira, P. T. S., & Fernandes, M. M. (2014). NDVI time series for monitoring RUSLE cover management factor in a tropical watershed. International Journal of Remote Sensing, 35(2), 441-453.

Efthimiou, N. (2016). Performance of the RUSLE in Mediterranean mountainous catchments. Environmental Processes, 3(4), 1001-1019.

Efthimiou, N., Psomiadis, E., & Panagos, P. (2020). Fire severity and soil erosion susceptibility mapping using multi-temporal Earth Observation data: The case of Mati fatal wildfire in Eastern Attica, Greece. Catena, 187, 104320.

Fernandez-Anez N, Krasovskiy A, Müller M, Vacik H, Baetens J, Hukic E, Solomun MK. *et al* (2021). Current wildland fire patterns and challenges in Europe: a synthesis of national perspectives. Air, Soil Water Res 14(SAGE Publications Ltd STM).11786221211028184. https://doi.org/10.1177/11786221211028185

Gitas, I. Z., Polychronaki, A., Katagis, T., & Mallinis, G. (2008). Contribution of remote sensing to disaster management activities: A case study of the large fires in the Peloponnese, Greece. International journal of remote sensing, 29(6), 1847-1853.

Gocic, M., Dragicevic, S., Radivojevic, A., Martic Bursac, N., Stricevic, L. & Djordjevic, M. (2020). Changes in Soil Erosion Intensity Caused by Land Use and Demographic Changes in the Jablanica River Basin, Serbia. Agriculture, 10, 345.

Hawker, L., Uhe, P., Paulo, L., Sosa, J., Savage, J., Sampson, C., & Neal, J. (2022). A 30m global map of elevation with forests and buildings removed. Environmental Research Letters.

Hengl, T., Mendes de Jesus, J., Heuvelink, G. B. M., Ruiperez Gonzalez, M., Kilibarda, M., Blagotic, A, *et al.* (2017). SoilGrids250m: Global gridded soil information based on machine learning. PLoS ONE 12(2). e0169748. https://doi.org/10.1371

Hysa, A., Spalevic, V., Dudic, B., Rosca, S., Kuriqi, A., Bilasco, S., Sestras, P. (2021). Utilizing the Available Open-Source Remotely Sensed Data in Assessing the Wildfire Ignition and Spread Capacities of Vegetated Surfaces in Romania. Remote Sensing, 13(14), 2737. doi:10.3390/rs13142737

Hysa, A., Spalevic, V. (2020). Testing NDVI, Tree Cover Density and Land Cover Type as Fuel Indicators in the Wildfire Spread Capacity Index (WSCI). Case of Montenegro. Notulae Botanicae Horti Agrobotanici Cluj-Napoca, 48(4), 2368–2384, DOI: 10.15835/NBHA48411993.

Kalabokidis, K., Palaiologou, P., Gerasopoulos, E., Giannakopoulos, C., Kostopoulou, E. & Zerefos, C. (2015). Effect of Climate Change Projections on Forest Fire Behavior and Values-at-Risk in Southwestern Greece. Forests, 6, 2214-2240.

Karger, D.N., Conrad, O., Böhner, J., Kawohl, T., Kreft, H., Soria-Auza, R.W., Zimmermann, N.E., Linder, P., Kessler, M. (2017). Climatologies at high resolution for the Earth land surface areas. Scientific Data. 4, 170122.

Katebikord, A., Khaledi Darvishan, A., & Alavi, S.J. (2017). Changeability of soil erosion variables in small field plots from different rainfall durations with constant intensity. Journal of African Earth Sciences, 129, 751-758.

Kokaly, R. F., Rockwell, B. W., Haire, S. L., & King, T. V. (2007). Characterization of post-fire surface cover, soils, and burn severity at the Cerro Grande Fire, New Mexico, using hyperspectral and multispectral remote sensing. Remote Sensing of Environment, 106(3), 305-325.

Kostadinov, S., Braunovic, S., Dragicevic, S., Zlatic, M., Dragovic, N. & Rakonjac, N. (2018). Effects of Erosion Control Works: Case Study—Grdelica Gorge, the South Morava River (Serbia). Water, 10, 1094.

Kotroni, V., Cartalis, C., Michaelides, S., Stoyanova, J., Tymvios, F., Bezes, A. *et al*. (2020). DISARM early warning system for wildfires in the eastern Mediterranean. Sustainability, 12(16), 6670.

Kuriqi A., Hysa A. (2021). Multidimensional Aspects of Floods: Nature-Based Mitigation Measures from Basin to River Reach Scale. In: The Handbook of Environmental Chemistry. Springer, Berlin, Heidelberg. https://doi.org/10.1007/698_2021_773

Lagouvardos, K., Kotroni, V., Giannaros, T. M., & Dafis, S. (2019). Meteorological conditions conducive to the rapid spread of the deadly wildfire in eastern Attica, Greece. Bulletin of the American Meteorological Society, 100(11), 2137-2145.

Lecina-Diaz, J., Martínez-Vilalta, J., Alvarez, A., Vayreda, J., & Retana, J. (2021). Assessing the Risk of Losing Forest Ecosystem Services Due to Wildfires. Ecosystems, 24(7), 1687-1701.

McCool, D. K., Foster, G. R., Mutchler, C. K., & Meyer, L. D. (1989). Revised slope length factor for the Universal Soil Loss Equation. Transactions of the ASAE, 32(5), 1571-1576.

McGuire, L. A., & Youberg, A. M. (2019). Impacts of successive wildfire on soil hydraulic properties: Implications for debris flow hazards and system resilience. Earth Surface Processes and Landforms, 44(11), 2236-2250.

Mitsopoulos, I., Mallinis, G., Karali, A., Giannakopoulos, C., & Arianoutsou, M. (2016). Mapping fire behaviour under changing climate in a Mediterranean landscape in Greece. Regional Environmental Change, 16(7), 1929-1940.

Myronidis, D., & Arabatzis, G. (2009). Evaluation of Greek post-fire erosion mitigation policy through spatial analysis. Polish Journal of Environmental Studies, 18(5), 865-872

Napoli, M., Cecchi, S., Orlandini, S., Mugnai, G., & Zanchi, C. A. (2016). Simulation of field-measured soil loss in Mediterranean hilly areas (Chianti, Italy) with RUSLE. Catena, 145, 246-256.

Nemeth, A. (2015). Forest Fires in South Eastern Europe. Regional Environmental Center for Central and Eastern Europe. Retrieved 2020 April 30 from http://www.rec.org/publication.php?id=505

Nikolic, M., Dragicevic, S., Zivanovic, S., Ivanovic, R., Martic Bursac, N., Stricevic, Lj., Radivojevic, A. & Zivkovic, J. (2021). Assessment of soil erosion intensity in the Kutinska river basin in the period 1971-2016, Fresenius Environmental Bulletin, 30(9).10890-10898

Ouallali, A., Aassoumi, H., Moukhchane, M., Moumou, A., Houssni, M., Spalevic, V., Keesstra, S. (2020). Sediment mobilization study on Cretaceous, Tertiary and Quaternary lithological formations of an external Rif catchment, Morocco, Hydrological Sciences Journal, 65:9, 1568-1582.

Papadopoulos, I., Falaras, T., Petani, A., Krassakis, P., Karavias, A., Bafi, D., Tselka, I., Gkougkoustamos I., Nikolidaki, M., Parcharidis, I. Greece (2021). Wildfires: Operational Mapping Using Geospatial Intelligence and Restoration-needed Knowledge Dissemination Through a Cloud-based Platform. In Proceedings of the 8th International Conference on Civil Protection and New Technologies “SafeGreece 2021”, 24-26 November 2021; pp. 61-64.

Pausas, J. G., Llovet, J., Rodrigo, A., & Vallejo, R. (2008). Are wildfires a disaster in the Mediterranean basin? – A review. International Journal of wildland fire, 17(6), 713-723.

Phinzi, K., & Ngetar, N. S. (2019). The assessment of water-borne erosion at catchment level using GIS-based RUSLE and remote sensing: A review. International Soil and Water Conservation Research, 7(1), 27-46.

Pilesjö, P. & Hasan, A. (2014). A triangular form-based multiple flow algorithm to estimate overland flow distribution and accumulation on a digital elevation model. Transactions in GIS, 18(1), 108-124.

Polykretis, C., Grillakis, M. G. & Alexakis, D. D. (2020). Exploring the impact of various spectral indices on land cover change detection using change vector analysis: A case study of Crete Island, Greece. Remote Sensing, 12(2), 319.

Porto, P., Bacchi, M., Preiti, G., Romeo, M., & Monti, M. (2022). Combining plot measurements and a calibrated RUSLE model to investigate recent changes in soil erosion in upland areas in Southern Italy. Journal of Soils and Sediments, 1-13.

Renard, K. G., Foster, G. R., Weesies, G. A., McCool, D. K. & Yoder, D. C. (1997). Predicting Soil Erosion by Water: A Guide to Conservation Planning with the Revised Universal Soil Loss Equation. USDA Agric. HB No. 703, Washington DC.

Renard, K.G., Foster, G.R., Weesies, G.A. & Porter, J.P. (1991). RUSLE: Revised universal soil loss equation. Journal of Soil and Water Conservation, 46, 30–33.

Reneuve, P., & Galevski, M. (1955). La corrélation entre les pluies torrentielles et l'intensité de l'érosion (d'après les observations faites dans un périmètre torrentiel)-Avant-propos. Annales de l'Ecole Nationale des Eaux et Forêts et de la Station de Recherches et Expériences Forestières, 14(2), 379-428.

Robichaud, P. R., & Ashmun, L. E. (2012). Tools to aid post-wildfire assessment and erosion-mitigation treatment decisions. International Journal of Wildland Fire, 22(1), 95-105.

Sabri, E.M., Boukdir, A., Karaoui, I., Skataric, G., Nacka, M., Khaledi Darvishan, A., Sestras, P. & Spalevic, V. (2019). Modelling of soil erosion processes and runoff for sustainable watershed management: Case study Oued el Abid Watershed, Morocco. Agriculture and Forestry, 65 (4), 241-250

Sakuno, N. R. R., Guicardi, A. C. F., Spalevic, V., Avanzi, J. C., Silva, M. L. N., & Mincato, R. L. (2020). Adaptacao e aplicacao do metodo de erosao potencial para solos tropicais. Revista Ciencia Agronomica, 51(1), 1-10, e20186545. https://doi.org/DOI: 10.5935/1806-6690.20200004.

San-Miguel-Ayanz, J., Moreno, J. M., & Camia, A. (2013). Analysis of large fires in European Mediterranean landscapes: lessons learned and perspectives. Forest Ecology and Management, 294, 11-22.

Shakesby, R. A. (2011). Post-wildfire soil erosion in the Mediterranean: review and future research directions. Earth-Science Reviews, 105(3-4), 71-100.

Soulis, K. X., Generali, K. A., Papadaki, C., Theodoropoulos, C., & Psomiadis, E. (2021). Hydrological response of natural mediterranean watersheds to forest fires. Hydrology, 8(1), 15.

Spalevic, V. Impact of Land Use on Runoff and Soil Erosion in Polimlje. Ph.D. Thesis, Faculty of Agriculture, University of Belgrade, Belgrade, Serbia, 2011; pp. 1–260.

Spalevic, V., Djurovic, N., Mijovic, S., Vukelic-Sutoska, M., & Curovic, M. (2013). Soil Erosion Intensity and Runoff on the Djuricka River Basin (North of Montenegro). Malaysian Journal of Soil Science. 17, 49-68.

Spalevic, V., Zejak, D., Curovic, M., Glisic, I., & Radovic, A. (2021). Analysis of the impact of fruit growing development on the intensity of soil erosion and runoff: Case study of Krusevo, Bijelo Polje, Montenegro. Agriculture and Forestry, 67 (2). 37-51.

Spalevic, V., Barovic, G., Vujacic, D., Curovic, M., Behzadfar, M., Djurovic, N., Dudic, B., & Billi, P. (2020). The Impact of Land Use Changes on Soil Erosion in the River Basin of Miocki Potok, Montenegro. Water, 12, 2973.

Tariq, A., Shu, H., Gagnon, A.S., Li, Q., Mumtaz, F., Hysa, A., Siddique, M.A., Munir, I. (2021). Assessing Burned Areas in Wildfires and Prescribed Fires with Spectral Indices and SAR Images in the Margalla Hills of Pakistan. Forests, 12(10):1371. https://doi.org/10.3390/f12101371

Tosic, R., Lovric, N., & Dragicevic, S. (2019). Assessment of the impact of depopulation on soil erosion: Case study – Republika Srpska (Bosnia and Herzegovina). Carpathian Journal of Earth and Environmental Sciences, 14(2), 505-518,

Van der Knijff, J.M, Jones, R.J.A, Montanarella, L. (2000). Soil erosion risk assessment in Europe. Luxembourg (Europe). Office for Official Publications of the European Communities. EUR 19044 EN

Volk, M., Liersch, S., & Schmidt, G. (2009). Towards the implementation of the European Water Framework Directive? Lessons learned from water quality simulations in an agricultural watershed. Land Use Policy, 26, 580–588.

Vujacic, D., Barovic, G., Djekovic, V., Andjelkovic, A., Khaledi Darvishan, A., Gholami, L., Jovanovic, M. & Spalevic, V. (2017). Calculation of Sediment Yield Using the River Basin and Surface and Distance Models A Case Study of the Sheremetski Potok Watershed Montenegro. Journal of Environmental Protection and Ecology, 18(3), 1193-1201.

Williams, J.T., Albright, D., Hoffmann, A.A., Eritsov, A., Moore, P.F., Mendes de Morais, J.C., Lionard, M., San-Miguel-Ayanz, J., Xanthopoulos, G., & van Lierop, P. (2011). Findings and implications from a coarse-scale global assessment of recent selected mega-fires. In Proceedings of the 5th International Wildland Fire Conference, Sun City, South Africa, 9-13, May 2011; pp. 27-40.

Zittis, G., Hadjinicolaou, P., Klangidou, M., Proestos, Y., & Lelieveld, J. (2019). A multi-model, multi-scenario, and multi-domain analysis of regional climate projections for the Mediterranean. Regional Environmental Change, 19(8), 2621-2635.

Božović, D., Knežević, M., Aleksić, M., Iker, O., Gostimirović, L. (2022). Forest fire risk management information systems. Agriculture and Forestry, 68 (2): 65-81. doi: 10.17707/AgricultForest.68.2.05

DOI: 10.17707/AgricultForest.68.2.05

Dražen BOŽOVIĆ[1], Mirko KNEŽEVIĆ*[2], Marinko ALEKSIĆ[3], Oto IKER[4], Ladin GOSTIMIROVIĆ[5]

FOREST FIRE RISK MANAGEMENT INFORMATION SYSTEMS IN MONTENEGRO

SUMMARY

In times of increasingly pronounced climate change, wildfires are among the key threats to forest ecosystems and pose a global environmental and economic problem. Montenegro's forests are particularly endangered due to its geographical position and the increasingly adverse climate effects. Wildfires occur as a causal link between climatic and meteorological conditions, humidity of forest cover, and plant vegetation with social activities in the area concerned (revised Forestry Development Strategy, 2018). Increasing attention is being paid to improving risk assessment and early warning using modern information systems to mitigate the wildfire risk preventively. Research on the capability and capacity of responsible institutions in Montenegro for establishing an information system is particularly important for wildfire risk management. The research showed that Montenegro's capabilities and capacities for risk assessment and early warning of wildfires are limited. The research showed that the system could be improved by establishing a single national wildfire information system. Various forms of early warning and wildfire risk management systems applied, including the Macedonian Forest Fire Information System (MKFFIS), Croatian's Integral Forest Fire Monitoring System (in Croatian IPNAS), and others, have already shown a high level of efficiency. Through a systemic approach, a large part of the tools used by these systems could be realistically developed and subsequently upgraded, taking into account their modularity in terms of software and hardware.

Keywords: forest fires, risk, early warning, information system

[1] Dražen Božović, Faculty for the Mediterranean Business Studies, Adriatic University, Tivat, MONTENEGRO

[2] Mirko Knežević* (corresponding author: mirkok@ucg.ac.me), University of Montenegro - Biotechnical Faculty, Podgorica, MONTENEGRO

[3] Marinko Aleksić, Maritime and Tourism Faculty, Adriatic University, Bar, Montenegro

[4] Oto Iker, Faculty for the Mediterranean Business Studies, Adriatic University, Tivat, MONTENEGRO

[5] Ladin Gostimirović, College of Business and Technology, Doboj, Republic of Srpska, BOSNIA AND HERZEGOVINA

Notes: The authors declare that they have no conflicts of interest. Authorship Form signed online.

Recieved:25/03/2022 *Accepted:17/06/2022*

INTRODUCTION

The forests are among the most important natural ecosystems and components on which Montenegro's sustainable development is based. In times of global climate change, wildfires pose one of the key threats to forest ecosystems (Bowman *et al*., 2009), causing economic losses (Bowman *et al*., 2009; Westerling *et al*., 2006; Lohman *et al*., 2007). Only 5% of fires are attributed to natural causes, while 95% are caused by human activities such as negligence (Miguel, 2003). However, investigations of frequent wildfires in unpopulated areas of Canada showed that from 1991 to 2000, there were about 8 000 wildfires per year, of which 48% were started by lightning (Wotton *et al*., 2005). Where there are no people, wildfires have to be caused primarily by natural causes. Furthermore, the role of vegetation is significant, so wildfires link climate characteristics, human activity, and the type of vegetation (Ichoku *et al*., 2003). According to the definition of natural disasters and classification set out in the Annual Disaster Statistical Review of the Centre for Research on the Epidemiology of Disasters (CRED) (Debarati *et al*., 2016:50), wildfires are classified as a group of climatological natural disasters.

Wildfires that burn 200-500 million hectares of land over the year cause damage to larger areas and destroy biomass worldwide more than any other factor (Lavorel *et al*., 2007; Ichoku *et al*., 2008). Thus, the awareness of the damaging effects of wildfire on biodiversity, human health, and the economy is increasing (Lohman *et al.,* 2007). Particular importance is attached to the rising air temperature and relative humidity. Flaming (Flamming *et al*., 2009) claims that wildfires during 2003 were a transient occurrence of what the future will look like and that we can expect more intensive wildfire seasons in the future. Continuous warming will produce greater seasonal contrast, which combined with expected increases of 44% in lightning strikes, will increase burnt areas by 78% over the next 50 years".

Due to the geographical position in the Mediterranean and the increasing adverse climate impacts, Montenegro's forests are particularly vulnerable (Disaster Risk Reduction Strategy, 2017). Wildfires occur as a causal link between climatic and meteorological conditions, relative humidity of forest cover, and plant vegetation with social activities in the area concerned (revised Forestry Development Strategy, 2018).

Montenegro supported United Nations Convention to Combat Desertification (UNCCD) initiative Land Degradation Neutrality Target Setting Process (LDN TSP) in 2016, as a platform for promotion of sustainable land management. LDN TSP resulted in national report containing identification of 15 hotspots and 25 measures with an aim to achieve LDN in Montenegro up to 2030. According to the LDN Report (Land Degradation Neutrality, 2018), main threats and pressures on soil in Montenegro, are urbanization and wildfires.

Even though fires are a highly stochastic phenomenon, Gonzalez *et al*. (2006) have set up a model that can be used in practice. Brown *et al*. (2004) made long-term forecast models for periods (2010-2029, 2030-2049, 2050-2069, 2070-

2089) for the Western United States. International strategies for disaster reduction (ISDR), the Hyogo Framework for Action (2005-2015), as well as the Sendai Framework for Disaster Risk Reduction (2015-2030), highlighted the need for a more comprehensive approach, where efforts would be made to avoid or mitigate the risk before the disaster begins, and today, this proactive concept is recognised and established as a risk management process.

A stable and sustainable risk management system is based on widely-accepted results and proven standards, such as ISO Guide 73:2009 and ISO 31000:2009, which establishes the principles, generic guidelines, and a logical risk management process. It includes five activities: 1) communication and consultation, 2) establishing a context, 3) risk assessment, 4) risk treatment, and 5) monitoring and reviewing activities, which was accepted in Montenegro.

Some common objectives and tasks for carrying out risk assessments, which may be relevant to many, include:

-Develop a risk profile that provides a quantitative analysis of the types of threats the organisation is facing;

-Develop an accurate inventory of available data sets and data resources;

-Provide a rationale for the cost of security measures to mitigate risks and vulnerabilities;

-Development of accurate IT support (software, hardware) and networking;

-Identify, prioritise and document risks, threats, and known vulnerabilities to a related organisation or sector;

-Determining the budget for reduction or mitigation of the risks, exposures and vulnerabilities identified;

-Understanding the return on investment, if the funds are invested in infrastructure or other assets to compensate for potential risks.

Numerous studies describe the risk of wildfire/forest fire as a result of the interaction between the two components - wildfire hazard and vulnerability. Among others, the risks of wildfires are addressed by the European Commission Expert Group on Forest Fires (EC EGFF) in the publication "Basic criteria to assess wildfire risk at the pan-European level" (JRC Technical Report, 2018). The basic wildfire risk components can be illustrated in a simplified manner, as shown in Figure 1. In this context, the wildfire risk components (hazards) concern the likelihood of ignition and spread of wildfire, while vulnerability concerns the susceptibility to damage. The wildfire risk assessment should take into account the most relevant components associated with the wildfire occurrence. To assess when and where the wildfire will cause undesired effects, it is necessary to model also (1) the fire ignition and propagation potential and (2) fire vulnerability (E. Chuvieco *et al*. 2010). Fire risk varies with environmental conditions and characteristics of vegetation types (Servodoni *et al*. 2021). Generally, the factors (triggers) that cause fires can be characterised as external and internal (forest-related). External factors are associated with increased temperatures and droughts, as they predispose fuel to ignition. The internal or forest-related drivers are linked to the forest and vegetation composition and structure, including the topography of the forest location as well as activities affecting the composition of forest trees. The relationship between internal and external factors, which may be significant triggers of wildfires, is illustrated in Figure 2.

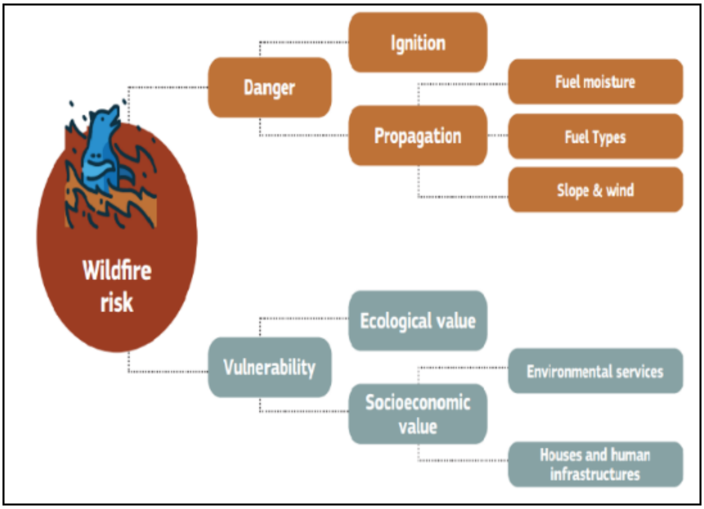

Figure 1. Basic forest risk assessment components (Source: JRC Technical Report, 2018)

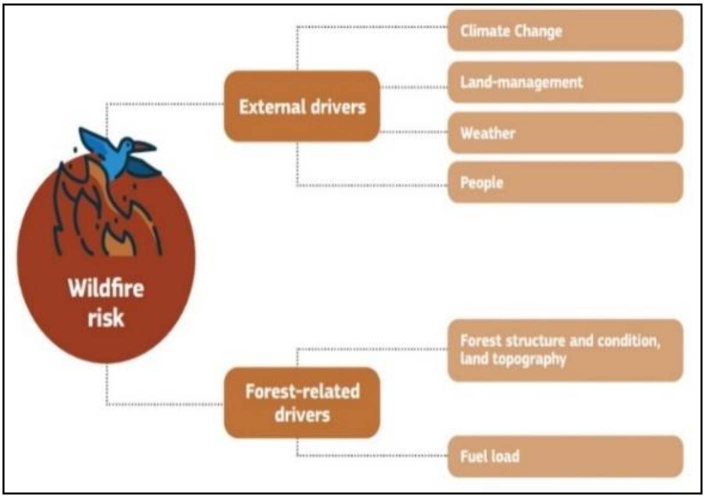

Figure 2. Wildfire risk drivers (Source: JRC Technical Report, 2018)

The development of advanced technologies and programs has enabled the modern methods for wildfire risk component analysis and wildfire effects assessment to find their place in wildfire prevention (Birkmann, 2006; Cardon *et al*.,2012; Kaplan and Garrick, 1981). Accordingly**,** wildfire/forest fire information systems often include dynamic fire risk assessment modules and frequent updates of fire risk components such as fuel distribution, vegetation structure, and moisture content. Furthermore, satellite technology and geographic information systems allow the integration of spatial data layers for the analysis of spatial patterns of wildfire occurrence and the wildfire risk at different scales. Dynamic digital maps have become an important tool to present risks, vulnerability, exposure, and risks. The maps greatly help all participants involved in the assessment work, facilitate the presentation of results, assist in understanding the risks, and visualise risk levels (Servidoni, *et al*. 2021). The following maps can be made to assess the risk of wildfires: 1. Hazard maps, 2. Maps of exposure of the population, critical infrastructure, facilities, etc.; 3. Capacity and capability maps (resources, equipment, roads, etc.); 4. Other information, such as administrative borders, roads, settlements, railways, bridges, other critical infrastructure, etc.; 5. Forest vegetation, protected areas, hydrographic network, basins, topsoil, etc. According to Watts (2002), decisions concerning wildfire risk not only require challenging technical steps to assess the risk of wildfire but, at the same time, require identification of an acceptable risk level, which is more of a task for society than for an engineer.

The wildfire risk assessment is based on the scenario when the wildfire is started, where it will occur, and how it will propagate. The assessment system consists of indices describing the state of the basic hazard components. Since 1947, when the Angstrom Index was established in Sweden, several fire hazard indices have been developed worldwide. Comparison of characteristics of 11 indices (Hahamed *et al*., 2017): Angstrom, Nesterov (N), M-Nesterov (M-N), Keetch-Byram Drought Index (KBDI), modified KBDI, Baumgartner, Canadian Fire Weather Index (FWI), Simple Fire Danger (F), Czech Fire Danger Index (FD), Lebanese Fire Danger (L), shows that the most widely used index is FWI, also used in the Western Balkan region. Furthermore, the modified Angstrom Index is in use in Serbia (Ratknić Tatjana, 2017). In 2004 and 2008, the Institute of Hydrometeorology and Seismology of Montenegro (IHSM), in cooperation with the Sector for Emergency Management and Civil Protection Montenegro, applied the FWI (Fire Weather Index). This method is based on the assessment of the forest fuel flammability index depending on past and current weather conditions. The meteorological elements that affect the hazard are: air temperature, relative air humidity, wind speed, and precipitation in the previous 24 hours. The forecast results were extremely good; however, further work on the forecast was suspended due to a lack of funds.

Such monitoring, risk assessment, and early warning from the meteorological viewpoint are already widely used in practice. At the global level, it is the World Meteorological Organization (WMO), through the World Weather Watch Programme - WWWP and the World Weather Research Programme WWRP, and others. The European Organisation for the Exploitation of Meteorological Satellites - EUMETSAT is an intergovernmental organisation providing its users with weather and climate-related satellite data, images, and products 24 hours a day, 365 days a year. From the aspect of wildfires, the European Commission's (EC) Joint Research Center (JRC), while working to develop and implement advanced methods for assessing wildfire hazards and mapping the burnt areas at the European level, developed the European Forest Fire Information System (EFFIS), which is part of the EU Copernicus programme, under the Emergency Management Service (EMS). EFFIS publishes two indicators providing information on the FWI local/time variability compared to the historical series of approximately 30 years. The EFFIS fire hazard forecast module currently provides access to fire hazard indices using numerical weather forecasts from two deterministic models, i.e. km spatial resolution. EFFIS generally serves the needs of the EU Member States, but non-EU countries can also obtain certain information and services. There is also an initiative to establish a Global Wildfire Information System (GWIS).

In almost all European countries, there are national wildfire information systems. With support from the Japan International Cooperation Agency (JICA), RN Macedonia developed the MKFFIS, which has been functioning successfully for years. Furthermore, most countries have established fire surveillance systems, which include different types of fire detection sensors, CCD smoke detection cameras, infrared (IR) radiometers that detect heat radiating from the fire, IR spectrometers for identification of the spectral characteristics of smoke gases, as well as laser detection systems (LIDAR) that determine the three-dimensional position of the smoke particles with a laser beam, etc.

Numerous analyses and reports (*Izvještaj DRI o reviziji, 2019*) on wildfires in Montenegro show insufficient efficiency of the system and limited capacity in terms of lack of coordination, lack of knowledge of probability assessment, and consequences of the potential hazard, with the emphasis on the fact that the system is not supported by an appropriate information service and database, for the necessary risk assessments, mapping and hazard mapping, and the absence of supervision of the execution of tasks. Accordingly, the DRI's assessment is that Montenegro does not have in place a sufficiently efficient system of protection against wildfires (*Izvještaj DRI o reviziji, 2019*). In this regard, the Government of Montenegro and JICA launched in 2021 the NFFIS project for Montenegro, modelled after the MKFFIS.

The aim of this paper is to explore the existing national information capacities for wildfire risk management, databases, information capacities, coordination, risk assessment procedures, and early warning for wildfire risks in Montenegro.

MATERIAL AND METHODS

Since "MKFFIS is intended as a possible prototype or model for the system whose functions should be achieved by establishing an NFFIS in Montenegro" for this purpose, the research started with the analysis of the content of the online materials available for the MKFFIS (http://mkffis.cuk.gov.mk/broshura/MKFFIS-en.pdf). Since the MKFFIS is a prevention and early warning system for wildfires, it integrates 4 (four) basic modules: (1) assessment of forest fire hazards; (2) assessment of exposure; (3) assessment of vulnerability and losses;

and, (4) assessment of capacity/inventory. In order to gain an understanding of the methodological basis of the MKNFFIS basic modules, a detailed analysis of the material referred to in Chapter 5 was performed, notably item 5.1 "The Methodological setting of the Integrated System for Prevention and Early Warning –of Forest Fires - MKFFIS, Table A) Forest fire risk elements and risk assessment tools and Table C) Data necessary for the creation of tools for the forest fires risk assessment. The results and features of the MKFFIS are presented in Chapter 6 of the MKFFIS brochure. As regards the research of the forest fire surveillance system and early warning system, research and practices in the application of these systems were considered with a focus on the development project, analyses (Stipaničev *et al.*, 2010), and reports on the application of the Integral Forest fire Monitoring System – (in Croatian IPNAS) in the Republic of Croatia.

In order to look at the possibilities for establishing an NFFIS in Montenegro, an analysis of the situation related to forest fire was carried out in three key sectors involved in the NFFIS establishment, which are the Rescue and Protection Directorate as the leading organisation in the disaster risk reduction, forestry institutions responsible for forest management and the IHSM in terms of early warning for potential hazards, as well as an appropriate general analysis of the situation regarding forest fires in Montenegro, including causes, hot spots, damage, history, monitoring, and imaging, etc.

The following methods were used in the research: content analysis, statistical method, and the comparative method. The content analysis method was applied during the analysis of national *(Izvještaj o realizaciji programa gazdovanja šumama, 2011,…; Izvještaj o stanju sistema zaštite, 2010,...)* and international reports (JRC Forest Fires, annual reports) on Forest Fires, climate change, conceptual-normative and other documents (Strategija DRR, 2017). The statistical method was applied to explore the trends of individual risk elements, such as climate change (Pavićević, 2012). The comparative method was applied primarily for the comparison of data obtained by content analysis and statistical method on the forest fire risk elements and the features of the risk assessment and early warning system.

The data sources were publicly available legal normative documents and annual reports of the institutions mentioned above; some data were obtained through a questionnaire - survey in these institutions. In preparing this paper, analysis was carried out with respect to each wildfire risk element and the possibilities of developing appropriate risk assessment tools for the purpose of setting up an NFFIS in Montenegro.

RESULTS AND DISCUSSION

The research showed that the MKFFIS functions as an integrated web platform for communication and information exchange among all relevant actors involved in wildfire prevention and early warning of wildfire hazards. Guided by the risk concept, the methodological setting of the integrated wildfire prevention and early warning system – MKFFIS - provides the designed wildfire risk elements and risk assessment tools, as follows:

1) Wildfires hazard: hot spots map and wildfire history map;

2) Exposure: forest vegetation map and map of forest damage values;

3) Vulnerability: vegetation map and a wildfire weather index map;

4) Capacity: all necessary topographic and other basic maps and data on the resources for the control.

In view of the tools and risk assessment function of the MKFFIS and the data necessary for their creation, the following requirements may be listed for the NFFIS of Montenegro:

1) For the creation of the Hot Spot Map and the Vegetation Dryness Map data from the publicly available or licensed sources through the providers mentioned above, such as EUMESAT with additional engagement or NASA's Fire Information for Rescue Management System (FIRMS) indicating global hot spots in easy-to-use formats;

2) Establish a Fire Weather Index Map; a precondition is a sufficiently dense automated weather stations (AWS) network managed by the IHSM, which will be able to automatically (at certain time intervals) send data on key weather parameters measured (temperature, humidity, wind speed and direction, precipitation) to the central NFFIS (RPD) unit;

3) For the Forest Vegetation Map, the key data supplier should be the forest sector entities, mainly the Forest Administration of Montenegro (FA) and others, as necessary. A precondition for providing quality data on forest vegetation (species, age, diameter, wood volume, slope, etc.) is the existence of a quality National Forest Inventory (NFI), i.e. digitized forestry data, in a specific format and standards;

4) In order to introduce a Fire History Map in the NFFIS Montenegro, there is a need for a consistent process and procedures for preparing fire reports by the Forestry Sector and RPD, and accordingly, this needs to be developed during the NFFIS development process;

5) The existence of a Topographic Map and other basic maps in the appropriate format and quality is also a precondition from a technical point of view, given that NFFIS should be established as an integrated GIS platform. In terms of providing continuous services to the NFFIS in relation to basic maps and other digital base layers, the main source of data should be the Cadastre and State Property Administration (CaSPA) of Montenegro. The CaSPA has recently worked on the development of a digital topographic map at a 1:25 000 scale in collaboration with JICA. Based on this project, a digital topographic map at a 1:25 000 scale was prepared for 70% of the territory of Montenegro, after which the CSPA completed the rest on its own. The following data are maintained on the CaSPA website: Orthophoto for the entire territory of Montenegro (imaging date 2007. pixel size 0.5 m), digital map of Montenegro at a 1:25 000 scale for the entire territory, thematic data including road network, railway network,

watercourses, settlements, facilities, digital terrain model, relief, administrative boundaries, cadastral unit boundaries. The CaSPA Geoportal (www.geoportaluzn.me) was implemented with the following services - view, download, transformation, and invoke;

6) A Map of Forest fire control resources can be a very useful tool to support Montenegro's national forest fire management system. If providers under the MKFFIS are taken as a starting point contributing to the establishment of this tool, it can be concluded that it is a complex function that depends on several factors, highlighting the need for the establishment of resources databases from several national institutions. This model should be a challenge for the RPD and a roadmap for the establishment of a similar system during the NFFIS implementation project in Montenegro.

7) The implementation of the damaged forests value table depends mostly on the available data of the Forest Administration of Montenegro. In other words, the basic precondition for this tool is established procedures and a price list set for all parameters in accordance with the forestry legislation.

Some key findings of the research, which are essential for the establishment of basic NFFIS functions and products in Montenegro, are as follows:

1) Forestry Sector, from a strategic point of view, is governed by the Law on Forests (Zakon o šumama, 2010), the National Forest and Forestland Management Policy *(Nacionalna šumska politika, 2008; Godišnji program gazdovanja šumama, 2013)*, and the Strategy with the Forestry Development Plan for the period 2014-2023 *(Nacionalna šumska strategija, 2014)*, on the basis of which the legal framework and forestry policies were implemented by the competent institutions in this period. The First National Forest Inventory (NFI) was completed in 2011 *(Prva nacionalna inventura šuma Crne Gore, 2013)*, and as regards the methodology, the NFI complies with the EU standards (European glossary for Wildfires, 2012; Council Directive (ECC) no. 2158/92; Risk Assessment and Mapping Guidelines, 2010,) and is compatible with national inventories implemented in Europe. It uses the elements of the systematic sample in cluster form. The distribution of clusters and sample plots is based on a rectangular grid 2 km x 2 km (basic grid), determined by Gauss-Kruger coordinate system, zone 6. For data processing within the FA, an "NFI Analysis Software" was put in place. The NFI program was developed according to the NFI assessment methodology; the program can be used as a standalone application to work with the MS database access platform or to work with the central database and the MS SQL server database. The program also allows connection to GIS platforms to link the NFI data to digital maps. A more detailed technical analysis of this software script should be considered in order to determine the possibility of connecting to the NFFIS as such (source) or with some adaptation/adjustment;

The research has shown differences in the various data records, such as the percentage of forest and forestland using different criteria (Figure 3). As regards the "Forest fire damage and historical records", the FA has so far used a classic method of assessing burnt areas - in field visits, using GPS, it followed the boundaries of the burnt area, and eventually, a model was created where the burnt area in hectares is automatically calculated and shown on the map. Discrepancies are evident in the information from the annual reports of the FA and EFFIS (Table 1).

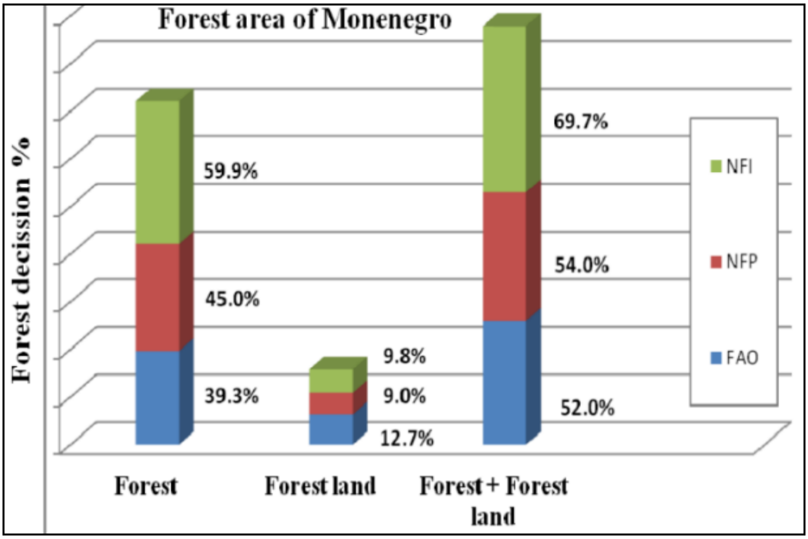

Figure 3. Montenegro's forest cover according to the NFI, NFP and FAO sources

Table 1. Comparative overview of forest fires (2010-2020)

Year	Surface/ha		Difference
	Source EFFIS	Source MFA	
2010	No data	695	/
2011	10 798	49 009	38 211
2012	23 872	11 858	12 287
2013	1 043	171	872
2014	No data	62	/
2015	7 388	3 124	4 264
2016	3 238	1 099	2 139
2017	35 969	21 215	14 754
2018	2 339	3 416	1 077
2019	9 284	1 170	4 641
2020	25 812	4 643	21 169

Source: The authors' own calculations based on the data from the reports of the organisations mentioned above

Despite the significant steps forward it has made thus far, Montenegro lacks a single and well-organised system to monitor and prevent the wildfire risk.

It is necessary to establish a more efficient system of fire protection, monitoring, as well as efficient remediation (Curovic *et al*. 2021).

Setting up the NFFIS would be a great opportunity to increase the overall capacity of relevant stakeholders to effectively manage the wildfire risk, and the NFI provides an excellent basis for this. Further analysis of the FA capacities is needed in terms of their readiness to achieve the necessary preconditions for establishing the process of assessing forest fire damage and losses (clarification of the price list, forest fire recording procedures, method for assessing damage and losses from forest fires, burnt areas, wood volume, etc.).

2) The Institute of Hydrometeorology and Seismology of Montenegro (IHSM), in order to provide the metrological data for the NFFIS functions, currently disposes of 55 meteorological stations, of which 33 automated (AMSs), transmitting the measured data automatically from the field to the central server and 22 classical meteorological stations (CMSs). The automated and classical meteorological stations, operated by the IHSM, measure the meteorological parameters, such as: air temperature, relative humidity, wind (direction and speed), and precipitation, and can be used to create FWI, etc.

Table 2. Overview of the numerical models used by IHMS

	Model 1	**Model 2**	**Model 3**	**Model 4**
Model	Oper 1 WRF-NMM Input data from ECMWF Oper11 WRF-NMM Downscale from oper 1	Oper0, oper2, Oper 22, drownscale from oper 2.	WRFChem v4.1.2 Input data from WCMWF.	NMME-DREAM1 Input data from ECMWF NMME-DREAM11 Downscale from NMME-DREAM1
Resolution (km)	3km; 1km; 0,5km	12km; 9km; 3km	6km; 2km	5km; 2km
Results availability time	00 UTC initialization 8:00UTC, 13:00 UTC 12 UTC initialization 20:00 UTC, 24:00 UTC	00 UTC initialization 5:44 UTC, 4:57 UTC 6:48 UTC, 12 UTC initialization 17:45 UTC, 16:58 UTC, 18:53 UTC	Initialization 00 UTC available: 10:40 initialization 12 UTC, 22:40	NMME-DREAM1 – 10:42 UTC NMME-DREAM11- 15:40 UTC
Max. Forecasted Period (days)	5 days	5 days	3 days	3 days

Source: The authors' own creation based on the data from the reports of the IHMS

The IHSM applies the computer-based forecast and the corresponding numerical models. The computer-based forecast is a direct result of numerical modelling, and forecasters have no subjective influence on it. There are two models of computer-based forecasts in use; input data for Model 1 originate from the NCEP/USA global model, and for Model 2 from the ECMVF global model, as follows: model1 WRF NMM v3.9.1 and model2 WRF NMM v3.9.1. Whereas numerical modelling, or numerical weather forecast, starts from the viewpoint that, knowing the current weather situation, the development of the process can be presented through mathematical formulas and the logical laws of physics. For 20 years, the IHSM has been continuously using the latest numerical models for the weather forecast, the NCEP/USA by Prof. Zaviša Janjić and Prof. Slobodan Ničković, (Eta, NMM-E, VRFNMM, NMMB, EtaDREAM, NMME-DREAM). The characteristics of these "numerical modelling" models can be seen in the Table 2.

The IHSM, in accordance with the Law on Hydro meteorological Affairs in the process of daily (24.7.365) data dissemination from global world meteorological centres, has taken the following:

-6.5 GB k 2 (00.12) + 1.2 GBk2 (06.18) = 15.2 GB data grib1 from ECMVF Reading

-3.2 GB k (00,06,12,18) = 15.2 GB data grib2 from NCEP / USA Washington

-7 GB k 4 (00,06,12,18) = 24 GB grib2 data with ICON DVD Offenbach

These data are extracted from global forecasting models on a daily basis and are used to launch the high-resolution model. High-resolution models WRF NMM a9km, WRF NMM a3km, WRF NMM e3km, WRF NMM e3km, WRF NMM e1km, WAM, Eta-DREAM are being launched daily (24/7/365). The products of these models were available on the IHMS web servers on a daily basis.

At present, the IHMS does not use satellite data to produce products similar to those produced by the MKFFIS. Regarding the NFFIS establishment objectives in Montenegro and the need to access certain products serviced by the EUMETSAT, it is important to note that Montenegro is not yet a full or associated EUMETSAT member. Therefore, Montenegro has only limited access to the EUMESAT products and services based on the DAWBEE project. The research showed that for some time, the IHMS was calculating FWI, but not currently, which is why it is necessary to take measures to establish this function.

3) Rescue and Protection Directorate (RPD), as the main pillar of the national disaster risk mitigation system, should have a central position within the NFFIS Montenegro, which means that the PRD would be the location of the NFISS central server unit and the institution that will assume responsibility for the administration and maintenance of the entire system. The research on the RPD organisation and capacity showed that in its current organisational structure, the RPD has a 112 Unit or an Operational Communication Centre (OCC) within which there are certain capacities in terms of server installations and other IT equipment, but of course, the NFFIS' needs have to be assessed in a comprehensive manner, as well as human resources and technical strengthening.

Therefore, as regards the introduction of some functions in the NFFIS, from a technical point of view, it is recommended that for some products, it would be best to take the same approach/concept used in the MKFFIS, such as the technology of publishing the hot spots map and the vegetation dryness map, using the channels of the EUMETSAT network and other satellite channels. To establish a sustainable and operational NFFIS, it is essential that this system is included in the appropriate regulatory framework of the institutions, which are the key JICA project partners (RPD, IHSM, and FA).

Over the past few years, the early warning systems for forest fires in the Mediterranean region, but also further, have been increasingly relying on technical and electronic surveillance from the ground, which is already showing a significant improvement in the early warning system. In the forest fire seasons in 1999 and 2000, Germany tested the “Autonomous Early Warning System For Forest Fires” (AVFS). In a test area of about 800 km^2, 45 forest and field fires occurred, all detected and identified by the AVFS within the prescribed deadline, even earlier than by experienced observation staff, and the software false alarm rate was below 1%, the operator can deal with easily (Kührt E., Knollenberg J., Mertens V., 2001). Croatia has developed its own Integral Forest fire Monitoring System – the IPNAS, which is an integrated and intelligent forest fire monitoring and observation system based on video cameras in the visible and/or infra-red part of the spectrum. The IPNAS is a modular system in terms of both hardware and software. Hardware modularity allows it to easily add new camera observation locations. Software modularity allows it to easily add completely new functionalities. The IPNAS is not only a fire detector but an advanced, integrated and intelligent fire monitoring and observation system that can be used as a fire detector system but also as an advanced system for remote video presence. It is an integrated system because it is based on the fusion of different data types (video signals, weather data, and GIS information), and intelligent because it is designed on the knowledge of artificial and computer intelligence.

Table 3. Overview of wildfire damage for the period 2016-2020

	Burnt area (ha)	Number of wildfires	Wood volume burnt (m3)	Crops burnt (plantings)	Damage (€)	Fire extinguishing costs (€)
2016	1 100	73	24 334	/	66 834	1 560
2017	21 216	154	142 629	/	1 794 553	3 440
2018	3 417	18	132	6 200	3 660	760
2019	1 170	82	26 738	68 260	329 307	8 920
2020	4 644	220	39 013	0	1 434 870	1 220
TOTAL	31 547	547	232 846	74 460	3 629 224	15 900

Source: The authors' calculations based on annual reports from the Forest Directorate

The financial aspect is also important for the establishment of such systems. The cost of the entire system of 56 observation stations and 10 operating centres, which are being implemented in several stages throughout the Split Dalmatia County, amounts to around €2.1 million, which is only 2.5% of the officially estimated damage from wildfires in 2003 in this County (about €66 million), so investing in such systems, though they cannot reduce the number of fires, but can significantly reduce the fire damage, is justified and useful (Stipaničev, D. *et al*., 2010).

The French project PRODALIS (Motorola Case Study, 2008), implemented in 2008 on the Atlantic coast of France, showed that a system of 14 firefighting video observation units weekly detected more than 90 burn-offs that were illegal in the fire season, so in this way, the firefighting video surveillance system provides a direct weekly income of more than €8 000. (Motorola Case Study, 2008). The official data from the Forest Directorate of Montenegro show that direct damage from wildfires for the period 2016 to 2020 was €3 629 224 (Table 1), while the damage for 2012 alone on 11 858 hectares of burnt area was €4 268 099, and in 2011, as many as 49 009 hectares of burnt areas, but financial indicators were not available. There are also the costs for the engagement of observers of EUR 18 000 only for August each year (annual management programme of the FA).

CONCLUSIONS

The practice and numerous analyses after the fire seasons have shown that Montenegro still lacks an efficient system of protection against wildfires, which primarily relies on its fire response ability. The research has shown that the development of information technologies has significantly improved the capabilities of the early warning system and efficient wildfire risk management. The efficiency of numerous national and global systems has already been confirmed, which imposes the need to pay particular attention to this issue in Montenegro.

The research showed very high possibilities for software solutions for numerical and mapped MKFFIS products for efficient wildfire risk management. The analysis of the capabilities and capacities in three key institutions in Montenegro for the NFFIS establishment showed that certain information segments for automated risk assessment were developed but were not systematised or sufficiently supported by IT, and the capabilities and capacities could be considered underdeveloped. With a systematic approach, most of the tools could be developed realistically and other MKFFIS tools could be developed under additional projects, which would significantly improve the system of protection against wildfires. The cost-effectiveness and efficiency of the systems for the early detection of wildfires, such as the IPNAS, are realistically applicable in Montenegro, considering its geographical and climatic characteristics. As these systems are modular in terms of software and hardware, they can be combined and complemented. Montenegro's accession to the European Union and other forms of cooperation also impose the compliance of this system, so the pilot projects implemented should not be in collision with the NFFIS but complementary to it. The cost analysis showed that for some years (2012), direct financial damages were higher than the price of such systems for the whole of Montenegro.

With the current issues of unsystematised data, procedures, risk assessments, and early warning, it is unlikely to expect more effective prevention of wildfires. On the contrary, they will become increasingly frequent due to current climate trends and cause more damage, especially in marginalised and inaccessible areas. Without a decisive policy shift and clearly defined objectives to improve the risk management system and its use, significant progress in preventing forest fires can hardly be expected. The establishment of NFFIS, whose significance is becoming increasingly apparent, could provide a solution to many problems in mitigating the risk of disasters in the forest sector, i.e. in the protection against wildfires in Montenegro.

ACKNOWLEDGEMENT

This study mainly relies on the research conducted under the Project on Capacity Building for Disaster Risk Reduction through National Wildfire Information System (NFFIS) and Eco-DRR, supported by the Japan International Cooperation Agency (JICA).

REFERENCES

Birkmann, J. (2006). Measuring vulnerability to promote disaster-resilient societies: Conceptual frameworks and definitions.

Blount, T. (1661). London, Glossographia, or, a dictionary interpreting all such hard words of whatsoever language now used in refined English tongue;

Bowman, M. J. S. D., Balch, H. J., Artaxo, P., Bond, J. W., Carlson, M. J., Cochrane, A. M., D, Antonio, M. C., DeFries, S. R., Doyle, C. J., Harrison, P. S., Johnston, H. F., Keeley, E.J., Krawchuk, A.M., Kull, A. C., Marston, B., Moritz, A.M., Prentice, C., Roos, I.C., Scott, C. A., Swetnam, W.T., van der Werf, R. G., Pyne, J.S. (2009). Fire in the Earth System, SCIENCE, Vol. 324, No. 5926, pp. 481-484.

Cardona, O.D., M.K. van Aalst, J. Birkmann, M. Fordham, G. McGregor, R. Perez, R.S. Pulwarty, E.L.F. Schipper, and B.T. Sinh, (2012). Determinants of risk: exposure and vulnerability. In: Managing the Risks (https://www.ipcc.ch/site/assets/uploads/2018/03/SREX-Chap2_FINAL-1.pdf);

Council Directive (ECC) no. 2158/92 on protection of EU forests against fire (1992)

Chuvieco, E., *et Al*. 2010, "Integrating geospatial information into fire risk assessment": https://www.publish.csiro.au/wf/WF12052.

Curovic, M., Spalevic, V., Stijovic, A., Curovic, Z., Buskovic, V. (2021). Forests of the Coast of Montenegro. In: Joksimović, D., Đurović, M., Zonn, I.S., Kostianoy, A.G., Semenov, A.V. (eds) The Montenegrin Adriatic Coast. The Handbook of Environmental Chemistry, vol 110. Springer, Cham. p.51-67 https://doi.org/10.1007/698_2020_711

Debarati, G. S., Hoyois, P., Below, R., (2016). Annual Disaster Statistical Review 2015 The numbers and trends, Centre for Research on the Epidemiology of Disasters (CRED), p. 50.

European glossary for Wildfires and Forest Fires, European Forest Fire Networks (2012)

Risk Assessment and Mapping Guidelines for Disaster Management, EU Commission. Brussels, 2010.

Godišnji program gazdovanja šumama za 2013. godinu, Ministarstvo poljoprivrede i ruralnog razvoja, Uprava za šume, 2013. godina

Hamadeh, N., Karaouni, A., Daya, B., Chauvet, P. (2017). Using correlative data analysis to develop weather index that estimates the risk of wildfires in Lebanon: assessment versus prevalent meteorological indices, European Journal of Agriculture and Forestry Research, Vol.5, No.1, pp. 9-34.

Flannigan, M., Stocks, B., Turetsky M., Wotton, M. (2009). Impacts of climate change on fire activity and fire management in the circumboreal forest, Global Change Biology, Vol. 15, pp.549-560.

Ichoku, C.,Remer, L. A., Kaufman, Y. J., Levy, R., Chu, D. A., Tanré, D., Holben, B. N. (2003). MODIS observation of aerosols and estimation of aerosol radiative forcing over southern Africa during SAFARI 2000, Journal of Geophysical Research, Vol. 108, No. D13, doi:10.1029/2002JD002366

Ichoku, C., Giglio, L., Wooster, M.J., Remer, L.A. (2008). Global characterization of biomass-burning patterns using satellite measurements of Fire Radiative Energy, Remote Sensing of Environment, Vol.112, pp. 2950–2962.

Miguel, J.S., coordinator EFFIS za Inter Press Service 16.08.2003.

Motorola Case Study, Fire-Fighting in France Goes Hihg-Tech with Video Surveillance, Motorola Inc. 2008.

ISO Guide 73:2009, Risk management — Vocabulary.

ISO 31000:2009, Risk management — Principles and guidelines;

Izvještaj DRI o reviziji o uspješnosti sprovođenja politike zaštite životne sredine u Crnoj Gori – zaštita od šumskih požara, Podgorica, 2019.

Izvještaj o stanju sistema zaštite i spašavanja u Crnoj Gori za 2010, 2011, 2012, 2013, 2014, 2015, 2016, 2017, 2018, 2019, 2020. godinu, Ministarstvo unutrašnjih poslova;

Izvještaj o realizaciji programa gazdovanja šumama za 2011, 2012, 2013, 2014, 2015, 2016, 2017, 2018, 2019, 2020. godinu, Uprava za šume,

JRC Tehnical Report, Forest Fires in Europe, Middle East and North Africa – Annual Report (*2011, 2012, 2013, 2014, 2015, 2016, 2017, 2018, 2019, 2020.)*

JRC Technical Report: Basic criteria to assess wildfire risk at the pan-European level, 2018, https://effis.jrc.ec.europa.eu/reports-and-publications/effis-related-publications;

Kaplan, S., Garrick, B.J. (1981). "On the Quantitative Definition of Risk". Risk Analysis.

Land Degradation Neutrality Target Setting Process, Montenegro National Report, Podgorica, June, 2018.

Lavorel, S., Flannigan, M.D., Lambin, E.F., Scholes, M.C. (2007). Vulnerability of land systems to fire: interactions among humans, climate, the atmosphere, and ecosystems, Mitigation and Adaptation Strategies for Global Change, Vol. 12, pp. 33–53.

Lohman, J. D., Bickford, D., Sodhi, S. N. (2007). Enviroment. The burning issue, Science, Vol. 316, pp. 376.

Nacionalna šumska strategija sa planom razvoja šuma i šumarstva 2014–2023. godine, Ministarstvo poljoprivrede i ruralnog razvoja, 2014. godina;

Nacionalna šumska politika,Crne Gore, Vlada Crne Gore, Podgorica, 2008.

Strategy with the plan of forest and forestry development 2014 - 2023, Ministry of Agriculture and Rural Development.

Pavićević, S. (2012). *Studija o ugroženosti od klimatskih promjena*, Crna Gora, SEEFCCA.

Prva nacionalna inventura šuma Crne Gore – Završni izvještaj, Ministarstvo poljoprivrede i ruralnog razvoja, Podgorica, 2013.

Servidoni, L.E., Silva, L.F.P., Santana, D.B., Rodrigues Neto, M.R., Lense, G.H.E., Ayer, J.E.B., Spalevic, V., Mincato, R.L. (2021). Monitoring of regeneration of native forest fragment impacted by fire. Agriculture and Forestry, 67 (4): 71-80. doi:10.17707/AgricultForest.67.4.07

Strategija (DRR) za smanjenje rizika od katastrofa sa dinamičkim planom aktivnosti za sprovođenje Strategije za period 2018-2023. godina, Podgorica 2017.

Stipaničev, D., Štula, M., Krstinić, D., Šerić, Lj., (2010). Suvremeni sustavi za rano otkrivanje i praćenje požara raslinja mrežom naprednih video motrilačkih jedinica, Centar za istraživanje požara otvorenog prostora i Katedra za modeliranje i inteligentne računalne sustave Sveučilište u Splitu Fakultet elektrotehnike, strojarstva i brodogradnje

Stipaničev, D., Vuko, T., Krstinić, D,. Štula, M., Bodrožić, Lj. (2006). Forest fire Protection by Advanced Video Detection System - Croatian Experiences. Tiems Workshop Croatia, 26th – 27th Sept. 2006, Trogir, Croatia

Suzuki,D., http://www.davidsuzuki.org/Forests/Forests_101/FIRE/Climate_Change.asp

Zakon o šumama („Službeni list Crne Gore, br.74/10“)

Watts, J.M. (2002). The SFPE Handbook, Fire Protection Enginering, section five, chapter 10, 3rd edition.

Westerling, L.A., Hidalgo, G.H., Cayan, R.D., Swetnam, W.T. (2006). Warming and Earlier Spring Increase Western U.S. Forest Wildfire Activity, SCIENCE, Vol.313, pp. 940-943.

Wotton *et al*, 2005. prema Canadian Concil of Forest Ministers, 2003.

Ozbey, A.A., Bilir, N. (2022). Variation in growth among provenances of Pinus brutia in a 32-year-old experiment from southern Turkey. Agriculture and Forestry, 68 (2): 83-91. doi:10.17707/AgricultForest.68.2.06

DOI: 10.17707/AgricultForest.68.2.06

Alper Ahmet OZBEY[1], Nebi BILIR[2*]

VARIATION IN GROWTH AMONG PROVENANCES OF *PINUS BRUTIA* IN A 32-YEAR-OLD EXPERIMENT FROM SOUTHERN TURKEY

SUMMARY

The provenance trial established by seedlings of 46 seed sources of Turkish red pine (*Pinus brutia* Ten.) was investigated based on 32-year-old tree height and diameter at breast height in this study.

Averages of tree height, and diameter at breast height were 9.32 m, 17.9 cm, respectively, while there were large differences among provenances and within provenance for the characters. Tree height varied between 7.04 m and 10.62 m, and diameter at breast height ranged from 14.48 cm to 21.46 cm in the provenances.

Results of analysis of variance showed significant ($p \leq 0.05$) differences among provenances for the characters. Block, and block x provenance interaction were also significant ($p \leq 0.05$) for the characters. Provenances were more homogenous for diameter at breast height than tree height based on results of Duncan's multiple range tests. There was positive and significant (r=0.74, $p<0.05$) relations between height and diameter at breast height.

The results showed importance of the provenance and local forestry practices in the species.

Keywords: Adaptation, Afforestation, Origin, *Pinus brutia*, Variance

INTRODUCTION

Turkish red pine (*Pinus brutia* Ten.) is classified as one of the most economically important tree species for Turkish forestry and the "National Tree Breeding and Seed Production Programme" (Koski and Antola, 1993) because of its commercial wood product and the largest natural distribution by 5.2 million ha which of %26 of total forest area of Turkey (Anonymous, 2020). The species has high adaptation ability to different environmental conditions (Ortel *et al*., 2010) such as annual rainfall varies between 400 mm and 2000 mm (Atalay *et al*., 1998). It is getting importance of the species and its provenances based on climate change. Provenance or also called origin can be defined shortly the place

[1]Alper Ahmet Ozbey, South-Western Anatolia Forest Research Institute, Antalya, TURKEY
[2]Nebi Bilir, (corresponding author: nebibilir@isparta.edu.tr), Faculty of Forestry, Isparta University of Applied Sciences, Isparta, TURKEY
Notes: The authors declare that they have no conflicts of interest. Authorship Form signed online.
Recieved:11/04/2022 *Accepted:20/06/2022*

that vegetative or generative material collected. Provenance trial is one of the main stages of tree breeding programmes to estimate variations, seed transfer regions (e.g., White *et al*., 2007) and adaptation ability, and to establishment and selection of seed sources for future plantations, and for other purposes such as resistance to biotic and a-biotic damages (e.g., Hattamer and König, 1975; Falkenhagen, 1991), and also to determine better seed source to afforestation area to obtain higher quality and quantity forest products. For instance, it was estimated that, by selecting suitable provenances, 30% to 50% gain could be realized in the species (Isik *et al*., 2002). Reflection of provenances of a species can vary to the ability and damages according to different environmental conditions.

For the purposes, national provenance trials were established by 50 provenances in Turkish red pine in 1987 (Cengiz *et al*., 1999). However, performances of provenances can change because of many biological and environmental factors such as edaphic, climatic, species, especially provenance and years (e.g., Cengiz *et al*., 1999; Ortel *et al*., 2010; Calikoglu *et al*., 2011; Calikoglu *et al*., 2020), and also their interactions.

Future studies are suggested based on different growth performances reported in provenances of the species in early studies by Ortel *et al*. (2010), Isik *et al*. (2002), and Calikoglu *et al*. (2020).

It is suggested that provenance trial should be surveyed by rotation age which is 60 years in the species (Eler, 1992) or by half of rotation age which is 30^{th} years (Isik *et al*., 2002) for accurate estimations. Rotation age is also related to selection age (Ozbey *et al*., 2020) as known. They emphasize importance of new studies on future years of provenance trials. While, 10^{th} and 20^{th} years of the trial were examined by Isik *et al*. (2002) and Ortel *et al*. (2010), 32^{nd} year result has not been investigated in the trial, yet.

The present study is including new results by 32^{nd} year collected data.

In this study, growth performances of provenances, and their variations were compared in a 32-year-old trial of Turkish red pine to estimate whether significant differences among provenances for height and diameter or not to contribute present and future practices in the species.

MATERIAL AND METHODS

The provenance trial was established by one-year containerized seedlings grown 30 seed trees selected phenotypic from each 46 seed sources (mostly seed stands, P2-P50) (Table 1).

The seedlings were planted by 3x1.5 m spacing by three replicates also called block at experiment site from southern part of Turkey (37°02'02" N latitude, 30°10'49" E longitude, 1045 m altitude) in 1998 (Figure 1). Tree height (**H**), and diameter at breast height ($\mathbf{D_{1.30}}$) were measured at end of growth period of 2020.

Table 1. Geographic details of the provenances

No	Latitude (N)	Longitude (E)	Altitude (m)	No	Latitude (N)	Longitude (E)	Altitude (m)
P2	35°17'	33°24'	500	**P25**	39°12'	28°08'	400
P3	35°18'	33°32	320	**P26**	39°36'	26°34'	550
P4	37°05'	34°33'	1000	**P28**	39°50'	25°55'	400
P5	36°11'	32°45'	600	**P29**	39°24'	28°22'	350
P6	36°05'	32°41'	650	**P30**	39°58'	28°40'	450
P7	36°14'	33°15'	650	**P31**	40°00'	28°55'	600
P8	37°07'	34°31'	800	**P32**	37°04'	30°32'	1100
P9	36°55'	34°26'	750	**P33**	37°30'	30°51'	650
P10	36°13'	33°43'	100	**P34**	37°21'	30°54'	400
P11	36°45'	34°10'	1150	**P35**	36°21'	35°57'	385
P12	36°57'	34°24'	1150	**P36**	37°46'	36°42'	800
P13	36°17'	32°48'	1000	**P37**	35°54'	36°01'	480
P14	37°24'	30°37'	800	**P38**	37°00'	28°19'	60
P15	37°30'	30°41'	800	**P39**	37°06'	28°32'	750
P16	36°59'	30°33'	275	**P40**	37°17'	28°34	750
P17	36°45'	31°58'	650	**P41**	38°50'	28°04'	350
P18	36°42'	32°10'	1000	**P42**	39°42'	28°37'	600
P19	36°24'	29°30	720	**P43**	40°11'	30°49'	600
P20	36°24'	29°32	830	**P44**	41°39'	35°27'	100
P21	37°17'	30°58'	750	**P45**	40°38'	36°43'	250
P22	36°36'	31°57'	350	**P46**	41°05'	32°41'	450
P23	36°26'	30°15'	250	**P47**	37°29'	42°00'	700
P24	36°35'	30°28'	350	**P50**	35°18'	33°03'	200

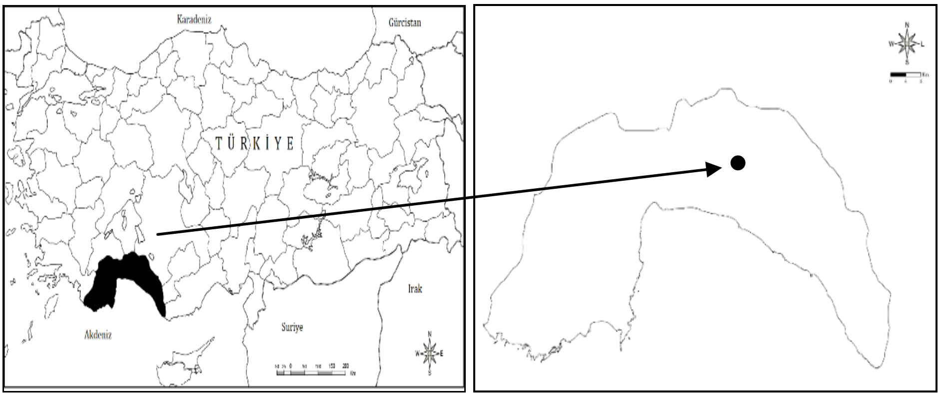

Figure 1. Location of the experiment site

The provenances were compared by following model of multiple analyses of variance (MANOVA) using SAS (2004). Provenances were grouped by Duncan’s multiple range test (Duncan, 1955) based on results of analyses of variance.

$$Y_{ijk} = \mu + P_i + S_j + P(S)_{i(j)} + e_{ijk} \qquad (1)$$

Where Y_{ijk} is the observation from the k^{th} tree of i^{th} block/replicate of j^{th} provenance, μ is overall mean, P_i is the effect of the i^{th} block, S_j is the effect of j^{th} provenance (j= 1, 2….46), $P(S)_{i(j)}$ is the effect of interaction between block and provenance, e_{ijk} is random error.

Phenotypic Pearson' correlation (r_p) between tree height and diameter at breast height were estimated by Rohlf and Sokal (1995):

$$r_P = \frac{\sum xy}{\sqrt{\sum x^2 \sum y^2}} \qquad (2)$$

Where $\sum xy$ is the sum of the factors of the characters x and y, $\sum x^2$ and $\sum y^2$ are phenotypic variances the characters x and y, respectively.

RESULTS AND DISCUSSION

Averages of tree height (**H**), and diameter at breast height (**$D_{1.30}$**) were 9.32 m, 17.9 cm, respectively, while there were large differences among provenances and within provenance for the characters (Table 2).

Average of tree height was 61 cm at 5^{th} year (Cengiz *et al*., 1999), while averages of tree height and diameter at breast height were 2.38 m and 2.3 cm at at provenance trial of the species at 10^{th} year (Isik *et al*., 2002), respectively. They were 6.3 m and 11.9 cm at 20^{th} year (Ortel *et al*., 2010).

The results showed that growth increments were lower in early years. It emphasized importance of years for accurate estimations in provenance trials. Tree height and diameter at breast height were ranged from 7.04 m (P47) to 10.62 m (P33) for H, and between 14.48 (P47) cm and 21.46 cm (P6) for $D_{1.30}$ (Table 2).

Large differences among provenances were also reported in early studies in the species (Cengiz *et al*., 1999; Isik *et al*., 2002; Ortel *et al*., 2010; Calikoglu *et al*., 2011; Calikoglu *et al*., 2020).

Marginal provenances (P45, P46 and P47) of the species showed lower growth performances than other provenances in the site (Table 2). The result was well accordance with early result in provenance trial of the species (Isik *et al*., 2002).

However, many environmental and biological factors together with provenance could be effective on growth performance such as climatic, edaphic or site (e.g., Isik *et al*., 2002; Yazici and Turan, 2016; Calikoglu *et al*., 2020), species (e.g., Yazici, 2018). It showed importance of local seed sources.

Table 2. Averages and results of Duncan's multiple range test for height (**H**) and diameter at breast height (**$D_{1.30}$**) of the provenances

Provenance no	**H** Number of individuals	Average (m)*	Provenance no	**$D_{1.30}$** Number of individuals	Average (cm)
P33	24	10.62^{a}	P6	22	21.46^{a}
P7	24	10.34^{ab}	P35	23	20.75^{ab}
P6	22	10.32^{ab}	P10	20	20.19^{abc}
P15	22	10.29^{ab}	P16	21	20.14^{abc}
P10	20	10.23^{abc}	P9	23	20.01^{abcd}
P5	23	10.21^{abc}	P11	22	20.00^{abcd}
P11	22	10.11^{abcd}	P39	19	19.92^{abcd}
P9	23	10.02^{abcde}	P33	24	19.73^{abcd}
P40	23	9.97^{abcdef}	P7	24	19.61^{abcde}
P39	19	$9.95^{abcdefg}$	P15	22	19.52^{abcde}
P24	22	$9.94^{abcdefg}$	P37	19	18.81^{abcdef}
P3	24	$9.88^{abcdefg}$	P8	21	$18.72^{abcdefg}$
P35	23	$9.85^{abcdefg}$	P40	23	$18.63^{abcdefg}$
P19	20	$9.73^{abcdefgh}$	P5	23	$18.47^{abcdefgh}$
P16	21	$9.65^{abcdefgh}$	P29	22	$18.45^{abcdefgh}$
P2	21	$9.65^{abcdefgh}$	P42	23	$18.42^{abcdefgh}$
P29	22	$9.64^{abcdefgh}$	P24	22	$18.28^{abcdefgh}$
P18	22	$9.60^{abcdefgh}$	P23	18	$18.27^{abcdefgh}$
P38	17	$9.56^{abcdefgh}$	P3	24	$18.10^{abcdefgh}$
P21	23	$9.54^{abcdefgh}$	P21	23	$18.10^{abcdefgh}$
P8	21	$9.50^{abcdefgh}$	P38	17	$18.10^{abcdefgh}$
P44	24	$9.50^{abcdefgh}$	P19	20	$18.04^{abcdefghi}$
P37	19	$9.42^{abcdefgh}$	P36	24	$17.71^{bcdefghi}$
P13	24	$9.34^{abcdefgh}$	P12	21	$17.69^{bcdefghi}$
P30	23	$9.29^{abcdefghi}$	P34	24	$17.65^{bcdefghi}$
P14	21	$9.25^{abcdefghi}$	P26	18	$17.61^{bcdefghi}$
P25	22	$9.23^{abcdefghi}$	P22	23	$17.54^{bcdefghi}$
P17	23	$9.19^{bcdefghi}$	P4	23	$17.50^{bcdefghi}$
P23	18	$9.18^{bcdefghi}$	P13	24	$17.38^{bcdefghi}$
P42	23	$9.18^{bcdefghi}$	P18	22	$17.33^{bcdefghi}$
P22	23	$9.09^{bcdefghi}$	P14	21	$17.26^{bcdefghi}$
P34	24	$8.97^{bcdefghi}$	P28	21	$17.19^{bcdefghi}$
P20	21	$8.83^{cdefghi}$	P32	24	$17.18^{bcdefghi}$
P41	20	$8.80^{defghij}$	P20	21	$17.11^{cdefghi}$
P50	23	$8.78^{defghij}$	P25	22	$17.06^{cdefghi}$
P36	24	$8.73^{defghij}$	P41	21	$16.90^{cdefghi}$
P4	23	$8.70^{defghij}$	P17	23	$16.79^{cdefghi}$
P12	21	8.66^{efghij}	P44	24	$16.79^{cdefghi}$
P32	24	8.63^{efghij}	P50	23	16.47^{defghi}
P43	21	8.58^{fghij}	P31	21	16.39^{defghi}
P31	21	8.54^{ghij}	P2	21	16.21^{efghi}
P26	18	8.54^{ghij}	P30	23	16.17^{efghi}
P28	21	8.38^{hij}	P43	21	15.91^{fghi}
P46	20	7.91^{ijk}	P45	21	15.38^{ghi}
P45	21	7.47^{jk}	P46	20	15.04^{hi}
P47	17	7.04^{k}	P47	17	14.48^{i}
General	**997**	**9.32**		**997**	**38.5**

*; Same letters show similar groups.

Order of provenances changed for the characters (Table 2). For instance, provenances 33 (10.62 m), 7 (10.34 m), 6 (10.32 m), 15 (10.29 m),and 10 (10.23 m) showed highest performance for height as the first five provenances, while they were 6 (21.46 cm), 35 (20.75 cm), 10 (20.19 cm), 16 (20.14 cm) and 9 (20.01 cm) for diameter at breast height (Table 2, Figure 2). They also changed in provenance trials of the species at different ages (Isik *et al*., 1987; Gurses, 1993; Cengiz *et al*., 1999; Isik *et al*., 2002; Ortel *et al*., 2010). Coefficient of variation of diameter at breast height (23.11%) was higher than that of height (17.45%) in total provenances. However, provenances were more homogenous for diameter at breast height than tree height based on number of homogenous groups of results of Duncan's multiple range test (Table 2).

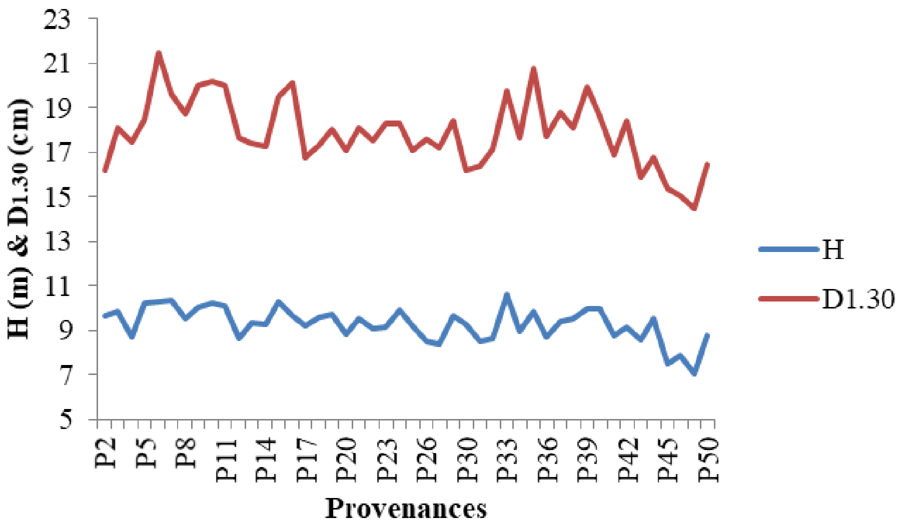

Figure 2. Averages of the provenances for the characters

The differences among provenances (Table 2) were also well accordance with results of analysis of variance. Results of ANOVA showed significant ($p \leq 0.05$) differences among provenances for the characters (Table 3). It was also reported early results of the provenance trial (Cengiz *et al*., 1999; Isik *et al*., 2002; Ortel *et al*., 2010; Calikoglu *et al*., 2020). The results of ANOVA also showed that block and block x provenance interaction were also significant ($p \leq 0.05$) effective on the characters (Table 3). It could be related to numbers of provenance and planted seedlings from each provenance. The interaction could change for the years (Cengiz *et al*., 1999; Isik *et al*., 2002; Ortel *et al*., 2010; Calikoglu *et al*., 2020). It was also found that the results could vary by type of statistical models used in estimations in provenance trials (Magnussen, 1993; Hamann *et al*., 2002; Joyce *et al*., 2002; Dutkowski *et al*., 2006; Funda *et al*., 2007; Ye and Jayawickrama, 2008; Calikoglu and Ozbey, 2017; Ozbey, 2022).

Environmental variance had higher in the variance component for the both characteristics (66.25% for H and 84.42% for $D_{1.30}$) (Table 4). The results (Tables 3 and 4) showed that importance of the provenance and local forestry practices. Similar result was also found by Isik *et al*. (2002). It was clear that it could be getting importance by climate change as also emphasized by Calikoglu *et al.* (2020). It could be said that mass selection among provenances and individual selection within provenance would play important roles in forestry practices based on higher variation.

Table 3. Results of analysis of variance

Characters	Source of variation	Degrees of freedom	Sum of squares	Averages of squares	F value	P value
H	Block (B)	2	2146532	1073266	31.5	<.0001
	Provenance (P)	45	5120382	113786	3.32	<.0001
	BxP	90	3095261	34392	1.88	<.0001
	Error	859	15737175	18320.34		
$D_{1.30}$	Block (B)	2	33551	16775	7.47	<.001
	Provenance (P)	45	217429	4831.76	2.14	<.001
	BxP	90	203577	2261.96	1.54	<.002
	Error	859	1260753.07	1465.99		

Table 4. Variance components of the characters

Characters	σ_B^2	σ_P^2	σ_{BxP}^2	σ_e^2
H	3137 (11.34%)	3927.1 (14.19%)	2269.1 (8.20%)	18324 (66.25%)
$D_{1.30}$	39.20 (2.25%)	123.43 (7.09%)	108.31 (6.22%)	1468.5 (84.42%)

$\sigma^2_{\mathbf{B}}$ is the variances among blocks, $\sigma^2_{\mathbf{P}}$ is the is the variances among provenances, $\sigma^2_{\mathbf{BxP}}$ is the variances of interaction between block and provenance, $\sigma^2_{\mathbf{e}}$ is the environmental variances.

Positive and significant (*r=0.74*, *p<0.05*) relations were found between the pairs of height and diameter at breast height. It was also reported by Cengiz *et al*. (1999), Isik *et al*. (2002), Ortel *et al.* (2010), Calikoglu *et al.* (2020), and Ozbey (2022) in early results of provenance trials of the species. The result could be used for forestry practices of the species such as selection and tending.

CONCLUSIONS

Variation for growth among provenances and with provenance emphasized importance of local seed sources and individual selection within provenance instead of mass selection. P6 and P10 provenances had higher growth performances for both characteristics. They could be used in forest establishment of the trial site.

Tree height and diameter at breast height were examined in present study. Quality characters such as stem form should be also added to future studies to obtain higher quality wood product in the trial.

ACKNOWLEDGEMENTS

Authors thank to local forestry managers for their administrative support and help during data collection. This study was a part of Ph.D. thesis, prepared under supervision of Professor Nebi Bilir. Author thanks to the scientific committee members for their valuable contributions during the study.

REFERENCES

Anonymous. (2020). Forest inventory of Turkey. General Directorate of Forestry of Turkey, Ankara.

Atalay, I., Sezer, I., Cukur, H. (1998). Ecological Characteristics of Forests and Seed Transfer Regions in *Pinus brutia* Ten. The Research Directorate of Forest Tree Seeds and Tree Breeding, Ankara.

Calikoglu, M., Sabuncu, R., Alan, M., Çoşgun, S., Yolcu, H.I. (2011). Genetic Gain in Seed Orchards of Turkish Red Pine (*Pinus brutia* Ten.). South-Western Anatolia Forest Research Institute, Technical Bullettin, 41, Antalya.

Calikoglu, M., Ozbey, A.A., Ortel, E., Altun, Z.G., Atmaca, C., Tastan, Y., Arslan, M., Yurdabak, U., Akbin, G., Karatay, H., Yirik, A., Yildizbakan, A., Tasdemir, C., Boza, A. (2020). Provenance Trials of *Pinus brutia* Ten. Final Project Report of South-Western Anatolia Forest Research Institute, Antalya.

Calikoglu, M., Ozbey, A.A. (2017). Decreasing possibility of altitude, provenance x block variance of a provenance trial established by error in *Pinus brutia* Ten. Inter Project Report of South-Western Anatolia Forest Research Institute, Antalya.

Cengiz, Y., Isik, F., Keskin, S., Genc, A., Dogan, B., Tosun, S., Ozpay, Z., Aksoy, C., Ortel, E., Gurgen, D., Dagdas, S., Ugurlu, S. (1999). Provenance Trials of *Pinus brutia* Ten. South-Western Anatolia Forest Research Institute, Antalya.

Duncan, D.B. (1955). Multiple range and multiple F-test. Biometrics, 11:1-5.

Dutkowski, G.W., Costa e Silva, J., Gilmour, A.R., Wellendorf, H., Aguiar, A. (2006). Spatial analysis enhances modelling of a wide variety of traits in forest genetic trials. Canadian Journal of Forest Research, 36(7):1851-1870.

Eler, U. (1992). Researches on the yield of *Pinus brutia*. Journal of Forestry Faculty of Istanbul University, 42:176-187.

Falkenhagen, E.R. (1991). Provenance variation in *Pinus radiata* at six sites in South Africa. Silvae Genetica, 40: 41-50.

Funda, T., Lstibůrek, M., Klápště, J., Permedlová, I., Kobliha, J. (2007). Addressing spatial variability in provenance experiments exemplified in two trials with black spruce. Journal of forest science, 53(2):47-56.

Gurses, K. (1993). Provenance trials of *Pinus brutia* at Eastern Mediteranian region. Brutian Pine Symposium, 12-23 October, Antalya, Book of proceedings, 314-323.

Hamann, A., Namkoong, G., Koshy, M.P. (2002). Improving precision of breeding values by removing spatially autocorrelated variation in forestry field experiments. Silvae Genetica, 51:210-215.

Hattamer, H.H. König, A. (1975). Geographic Variation of early growth and frost resistance in Douglas-fir. Silvae Genetica, 24(4): 97-106.

Isik, F., Cengiz, Y., Genc, A., Dogan, B., Tosun, S., Ozpay, Z., Ugurlu, S., Ortel. E., Dagdas, S., Karatay, H., Yoldag, G. (2002). 10^{th} Results of Provenance Trials of *Pinus brutia* Ten. Technical Bulletin of South-Western Anatolia Forest Research Institute, Antalya.

Isik, K., Topak, M., Keskin, A.C. (1987). 10^{th} Growth Results of Provenance Trials of *Pinus brutia* Ten.: Six Populations at Five. The Research Directorate of Forest Tree Seeds and Tree Breeding, Ankara.

Joyce, D., Ford, R., Fu, Y.B. (2002). Spatial patterns of tree height variations in a black spruce farm-field progeny test and neighbors-adjusted estimations of genetic parameters. Silvae Genetica, 51(1):13-18.

Koski, V., Antola, J. (1993). National Tree Breeding and Seed Production Programme for Turkey 1994-2003. The Research Directorate of Forest Tree Seeds and Tree Breeding, Ankara.

Magnussen, S. (1993). Bias in genetic variance estimates due to spatial autocorrelation. Theoretical and Applied Genetics, 86(2):349-355.

Ortel, E., Çalikoglu, M., Cetinay, S., Altun, Z.G., Cengiz, Y., Boza, A., Turker, H.A., Kahraman, T., Gokdemir, S., Tosun, S., Arslan, M., Ozpay, Z., Karatay, H., Karzaoğlu, C. (2010). 20^{th} Results of Provenance Trials of *Pinus brutia* Ten. Technical Bulletin of South-Western Anatolia Forest Research Institute, Antalya.

Ozbey, A.A. (2022). Investigation on Plot Error in Provenance and Progeny Trials of Turkish Red Pine. Graduate School, Isparta Universityof Applied Sciences, PhD. Thesis, Isparta.

Ozbey, A.A,, Çalikoglu, M., Cobanoglu, A., Erpulat, M. (2020). Determination of Selection Ages and Plus Families in Provenance and Progeny Trials of *Pinus brutia* Ten. Final Project Report of South-Western Anatolia Forest Research Institute, Antalya.

Rohlf, F.J., Sokal, R.R. (1995). Statistical Tables. Macmillan.

SAS. (2004). Statistical Analysis System, SAS Institute, Inc. Cary., N.C., USA.

White, T.L., Adams, W.T., Neale, D.B. (2007). Forest Genetics. Cabi.

Yazici, N, Turan, A. (2016). Effect of forestry afforestation on some soil properties: A case study from Turkey. Fresenius Environmental Bulletin, 25:2509-2513.

Yazici, N. (2018). Effect of species and environmental factors on growth performances in afforesration of *Cedrus libani* and *Pinus brutia*. Fresenius Environmental Bulletin, 27:6913-6917.

Ye, T., Jayawickrama, K.J. (2008). Efficiency of using spatial analysis in first-generation coastal Douglas-fir progeny tests in the US Pacific Northwest. Tree Genetics & Genomes, 4(4):677-692.

Čadro, S., Bećirović, E., Makaš, M., Omerović, Z., Zahirović, Ć., Crljenković B. (2022). Geothermal energy for sustainable agriculture: a case study Sarajevo, Bosnia and Herzegovina. Agriculture and Forestry, 68 (2): 93-108. doi: 10.17707/AgricultForest.68.2.07

DOI: 10.17707/AgricultForest.68.2.07

Sabrija ČADRO*[1], Emir BEĆIROVIĆ[1], Merima MAKAŠ[1], Zuhdija OMEROVIĆ[1], Ćerima ZAHIROVIĆ[1], Benjamin CRLJENKOVIĆ[1]

GEOTHERMAL ENERGY FOR SUSTAINABLE AGRICULTURE: A CASE STUDY SARAJEVO, BOSNIA AND HERZEGOVINA

SUMMARY

Bosnia and Herzegovina is strategically committed to agriculture. Although it has adequate natural resources to engage in modern agriculture, it is also an area that faces a number of problems, such as small landholdings, low technological level of production, abandonment of rural areas, low yields, high exposure and poor adaptability to climate change. Given these conditions, the main goal of this paper was to determine the possibility for the stallholder farmer in Bosnia and Herzegovina to increase its sustainability using geothermal heating system to heat the greenhouse during the winter and achieve safer production with higher yields. Lettuce (*Lactuca sativa*) was chosen as the test crop. By heating, a higher air temperature was achieved in the greenhouse (2.20 - 3.82 ^{o}C), a higher growth intensity was also achieved, as well as much shorter lettuce vegetation, which was only 67 days. However, the economic aspects of sustainability have not been realized, these higher yields are not enough to cover costs. Fixed cost value, was covered with gross margin five times (502%) in the control greenhouse, while achieved gross margin is not sufficient to cover fixed costs in the heated greenhouse, shown by the calculated value of 60%.

Keywords: geothermal heating system, greenhouse, sustainability, gross margin, lettuce

INTRODUCTION

Most of the area of Bosnia and Herzegovina (BiH) belongs to humid climate region (S. Čadro *et al.*, 2017) and same situation is within the area around capital city of Sarajevo (Drešković & Mirić, 2013). As a result of climate change, the air temperature in BiH has risen in all regions and for all sessions (Popov *et al.*, 2018), this is also true for Sarajevo area where this increase is about 0.37 ^{o}C per decade (Čadro, Uzunovic, *et al.*, 2019; Trbic *et al.*, 2017).

[1]Sabrija Čadro (corresponding author: s.cadro@ppf.unsa.ba), Bećirović Emir, Makaš Merima, Omerović Zuhdija, Zahirović Ćerima, Crljenković Benjamin. University of Sarajevo, Sarajevo, BOSNIA AND HERZEGOVINA

Notes: The authors declare that they have no conflicts of interest. Authorship Form signed online.

Recieved:09/02/2022 *Accepted:01/06/2022*

Along with the increase in temperature, the frequency of occurrence of extremely low and extremely high temperatures has also increased (Čadro, Uzunovic, *et al*., 2019; Trbic *et al*., 2017).

In addition, the area is increasingly exposed to droughts, late spring frosts and floods (Čadro *et al*., 2018; Sabrija Čadro *et al*., 2017; Zurovec *et al*., 2017; Žurovec *et al*., 2011). It is interesting that during 2021, a drought was recorded at this location in the period from June to September, and abundant rainfall in November, when the deviation of the monthly rainfall from the climatological standard normal (1961-1990) was 259.4% (FHMZ, 2021).

Such climate trends make agricultural production very difficult, especially for smallholder farmers which are most numerous in this location and generally in Bosnia and Herzegovina (Žurovec *et al*., 2015). The solution, both for reducing the contribution to climate change and increasing the security of agricultural production, can be the application of modern technologies, smart agriculture and use green energy sources. The application of modern technologies and smart agriculture certainly has advantages on both large and small-scale farms in BiH (Čadro, 2019; Čadro, Škaljić, *et al*., 2019).

Since the use of on-farm management software's, digital sensors to monitor plant growth and conditions, UAVs or green energy solutions is a relatively new practice in agriculture and it requires both financial resources and certain skills, further research into the justification of using this technology by the farmers is needed. For this reason, it is important to analyze the affordability and acceptance of these approaches among smallholder farmers in BiH, as well as to undertake focused training aimed at raising the knowledge and awareness of the benefits by application of this technology (Čadro, Škaljić, *et al*., 2019).

BiH is a significant agricultural region, with about one-third of its land under cultivation or pastures. There are excellent conditions for greenhouse vegetables production that is performed in all types of greenhouses (temporary and permanent protected areas). According to research by (Karić *et al*., 2016) many small farmer producers in BiH are choosing production in greenhouses, because this is for them economically most profitable production.

The key to making a profit in greenhouses is to ensure the continuity of production throughout the year. Lettuce (*Lectuca sativa*) is one of the most often cultivated vegetable in BiH, that can successfully be grown in almost all seasons, especially in the greenhouse with heating system (Čivić *et al*., 2017). Taking into consideration the fact that lettuce production in the last decade is showing significant expansion in BiH and that introduction of new varieties is frequent, improvement of technical production level in greenhouses is very important. The correct choice of technical equipment often resulted in higher yields or a shortening of the growth period even at low temperatures and less light intensity periods such is winter.

Producing vegetables in greenhouses during the winter period is a big challenge for many farmers. From the energy point of view, greenhouse farming requires high energy use, which results in one of the most energy consuming sectors in industry (Canakci & Akinci, 2006; Hedau *et al*., 2013).

The heating costs represent almost 30% of the operational cost of a greenhouse (Aramyan *et al*., 2007; Heidari & Omid, 2011). Since the energy costs are high, the use of renewable and affordable heating systems would be of primary importance to achieve significant energy savings (Aramyan *et al*., 2007). According to the new Europe 2020 Strategy and it`s main goals, that are to evenly decrease greenhouse gases emissions by 30% and reach a 20% share of total energy consumption from renewable energy (European Commission, 2020), heat pump systems are more acceptable for many farmers for heating greenhouses. For these reasons, many countries have started to use ground-source heat pumps to heat greenhouses. Leaders in annual geothermal energy use for greenhouse heating are Turkey, Russia, Hungary, China and Italy (Lund & Falls, 2012). Generally, different types of heat pump are used in agriculture, such as: air source-air supply, water source-air supply and water source-water supply heat pumps. However, the ground water heat sources have been demonstrated to have higher performance than air heat sources (Furuno & Sugawara, 2012). Ground-source heat pump systems are able to extract the low temperature energy content of a shallow geothermal resource and make it available for practical uses for greenhouse heating or cooling (Wu, 2009). According to (Harjunowibowo *et al*., 2021) using ground-source heat systems in the greenhouse reached from 2 to 7 degrees higher soil temperature then greenhouses without a heat system. Mentioned differences in soil temperature affect the faster and better plant`s root system growth. A lot of authors were researching using ground-source heat pumps for heating greenhouses but most of these works are based on calculations of energy efficiency coefficients of those systems but there wasn`t any mention of their effect on the yield and growth of cultivated plants.

The aim of this research is to determine the possibility for the stallholder urban farmer in Sarajevo to increase its sustainability using renewable energy sources and achieve economic justification in the production of vegetables in a greenhouse with an installed geothermal heating system.

MATERIAL AND METHODS

In order to conduct research and respond to the set goal, two identical greenhouses with an area of 100 m^2 each (6.3 m x 16 m) were set up next to each other in May 2020 at the experimental site of the Faculty of Agriculture and Food Science, University of Sarajevo located in Butmir near Sarajevo.

The basic geographical characteristics of this location are given in Table 1.

Table 1. Basic geographical characteristic of research location

Location	Longitude	Latitude	Altitude (m)	Slope (%)
Sarajevo, Butmir	18.3216	43.8259	503.32	> 0

Butmir is considered an urban zone and part of the city and Canton Sarajevo, so the agricultural production in this area can be considered us urban (El Bilali *et al*., 2013).

The greenhouse type and construction elements do not deviate from the greenhouses used by farmers locally. However, one greenhouse was equipped with geothermal heating system and other one was a control without heating.

The installed heat pump (Ecoterm, Type 263, max power 3.2 kW) has soil-heat collectors made of plastic pipes, laid down in trenches 120 cm deep and 60 cm wide. For satisfying the heating needs of 100 m^2 of greenhouse (12kW) an earth collector at in three trenches, 50 meters long, were installed.

After the soli-heat collector pipes were installed, the top soil layer was removed. Then, thin 40 cm high metal plates were installed around the edge of the area of the greenhouse, secured by wooden pegs. Their purpose is to physically separate the heated soil from the non-heated surrounding. After that, a layer of PVC foil was laid on the ground, followed by a layer of EPS (50 mm styrofoam) which is used as a thermal insulation, then PVC foil again. The heating pipes were installed at least 5 cm above the mentioned thermal insulation. Soil earlier set aside, was then put back to the area of greenhouse and flattened.

Heat pumps are installed in metal housing alongside the greenhouses, to be protected from physical damage. Two pipes, containing glycol solution, are connecting the heat pumps with the collecting shaft, which is connected directly to earth-heat collectors. One pipe is feeding pre-heated liquid to the heat pumps while the other is feeding cooled down liquid to the earth collectors to be pre-heated again. In addition, heat pumps are connected to the fancoil instilled inside of the greenhouse for purpose of air heating.

After conducting an analysis of the heating power of installed geothermal pump, as well as the resulting soil and air temperatures, it was decided to use the pump as follows:

-Output temperature at the heat pump: 25°C

-Simultaneous operation of the geothermal pump and air fan

-Powering the pump when the air temperature in the greenhouse drops below 10 °C

-Switching off the pump when the temperature in the greenhouse rises above 10°C

Therefore, the heating system is manually switched on and off depending on the air temperature inside the greenhouse. The date and time of the start and end of the operation of the heating system was recorded, as well as the consumption of electricity during its operation.

To measure climate conditions inside and outside greenhouses, *Spectrum Technlogies, Inc.* WatchDog Micro Stations, equipped with sensors for soil temperature and humidity (SMEC300), leaf wetness and air temperature and humidity were used. All the date were recorded in 30-minute time interval.

Lettuce (NEIL F1) was chosen as the vegetable crop to be tested, as an important winter crop that is intensively cultivated in BiH. Exactly the same methodology from the use of the same planting material, soil preparation and fertilization, the same protective equipment, agricultural techniques and all actions was carried out in booth greenhouses. The total observation period lasted 116 days, ie from October 12, 2020 to February 5, 2021.

During the vegetation period of lettuce, the initial height of plants (seedlings) and plant growth were measured every 7 days. At the end of the vegetation, during the harvest, the number of harvested plants was determined, as well as the width, height, number of leaves and weight of the plant. Based on these data, the intensity of growth and development of lettuce was calculated, as well as the realized yields, depending on the method of production.

Before the beginning of vegetation, the opening of the pedological profile and the analysis of the basic physical and chemical characteristics of the soil in the heated and control greenhouse were performed. Soil in each profile was divided into two separate layers: anthropogenic surface layer depth from 0 - 25 cm and subsurface layer depth from 25 – 40 cm. The following analyzes had been carried out: Soil physical characteristics through analysis of soil texture (international pipette B method) and bulk density (gravimetric method in Kopecky cylinders); Soil water characteristics through soil water retention (Θv) at a given matric potentials using a pressure-membrane extraction apparatus. Following negative potentials (Ψ) were used: -0.33 bar (pF 2.54: field water capacity), and -15.5 bar (pF 4.2: permanent wilting point). Maximum water capacity (MWC) was divided from bulk and absolute density while totally (TAW) available water capacity of soil was calculated from relation TAW = FWC – WP (Čustović & Tvica, 2003).

Analyzed soil chemical characteristics were active (H_2O) and substitution (KCl) pH reaction (electrometrically in suspension 1:2.5 - pH meter) humus content, using colorimetric method (spectrophotometry) and content of easily accessible forms of phosphorus (P_2O_5) and potassium (K_2O) in the soil with AL-method (Hanić *et al*., 2008).

IBM SPSS Statistics software will be used for statistical data processing. To examine the influence of the heating system on the morphological and productive parameters of the lettuce, the parametric independent t-test will be used. Conclusions will be made with a significance level of 0.05.

To analyze the economic aspects of sustainability, the gross margin (GM) was calculated as a basis for further analysis and recommendations. It represents the difference between revenue (R) and variable costs (VC) of all individual productions realized on the farm. Therefore, it can be shown as GM = R – VC. Gross margin serves to cover fixed costs, own labor, and invested capital as opportunity costs (Kay & Edwards, 1999). This paper analyzes how many times the fixed cost can be covered with realized GM.

Calculations are based on the achieved yields and used inputs at the experimental site of the Faculty of Agriculture and Food Science in Sarajevo

(Butmir) during the 2020/2021 winter season. The inputs prices are taken from the paid invoices. Average prices on the Sarajevo market during the harvesting period are taken as the assumed sales prices. Only the production of lettuce as a winter crop in the greenhouse was the subject of this study and other crops grown during the warmer part of the year were not taken into account. The reason is that in the area of Sarajevo, only winter production requires heating and heat pump is not used for the rest of the year.

RESULTS AND DISCUSSION

Research conditions

Based on the time period 1967 – 2016 the average amount of annual precipitation in Sarajevo is found to be 938 mm, average air temperature 10.01 °C, relative humidity 71%, wind speed 1.63 m/s and insolation 4.96 h (Čadro, Uzunovic, *et al*., 2019). The following graph (Graph 1) shows the difference between air temperatures outside and inside the greenhouse, as well as the difference between the temperatures in lettuce vegetation period in 2020/21 and climatological normal for Butmir, Sarajevo.

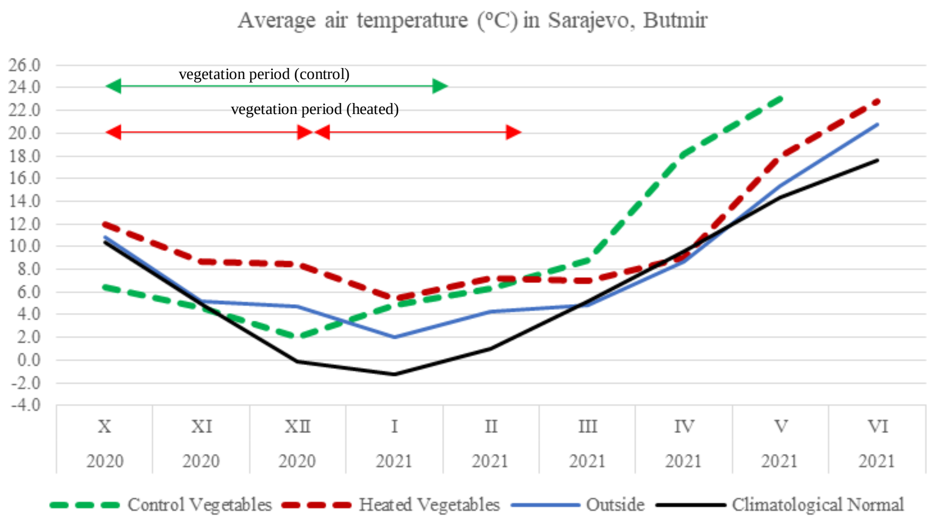

Graph 1. Average air temperature (°C) in Butmir - Sarajevo for control, heated and area outside greenhouse

Compared to the climatic normal, the vegetation period of lettuce, i.e. the period from October 2021 to the end of February 2021, was 2.45 °C warmer. The biggest difference was recorded in December (4.84 °C), then January (3.36 °C) and February (3.31 °C), when the temperatures are the lowest.

Also, comparing to outside or control greenhouse, as the result of soil and air heating higher air temperatures were recorded in the heated greenhouse. The difference in temperature ranges from 2.20 to 3.82 °C, with biggest difference in December. The lowest recorded temperature -9.9 °C was in the control greenhouse on 19.01.2021 at 7:00h while lowest air temperature in heated greenhouse was -2.6 °C, and it was recorded on 01.12.2020. This is a big difference, which can prevent crops from freezing, especially in conditions when such low temperatures persist. In heated greenhouse, air temperature never dropped below its biological minimum (Kurtović, 2008; Maksimović, 2011), which means that lettuce in heated greenhouse had better-growing conditions.

Pedological analysis found that alluvial soil is located at the research site and based on its physical characteristics we can conclude that is a clay loam with approximately equal ratio of clay, silt and sand (Table 2).

Table 2. Soil physical characteristics

	Depth cm	Clay %	Silt %	Send %	BD g/cm^3	WP %	MWC %	FC %	TAW %	RAW %	AC %
C	0 - 25	32.9	33.5	33.6	1.3	20.5	45.0	36.7	16.2	8.1	8.3
	25 - 40				1.6	23.5	43.0	38.4	14.9	7.4	4.6
H	0 - 25	33.1	35.0	31.9	1.3	23.9	45.0	36.7	12.8	6.4	8.3
	25 - 40				1.6	28.6	43.0	38.4	9.8	4.9	4.6

Note: C - control greenhouse; H – heated greenhouse; BD – Bulk density; WP – Wilting point; MWC – maximum water capacity; FC – Filed capacity; TAW – Totally available water; RAW - Readily Available Water; AC – Air capacity

We can also notice a very dense second layer of soil where the bulk density is 1.6 g/cm^3. The surface layer of soil up to 25 cm deep has much better water-physical characteristics than the subsurface. Low values (4.9 – 8.1 %) of readily available water (RAW) show the small plant accessible water capacity and the need for frequent irrigation with smaller amounts of water. It is interesting that, the soil in heated greenhouse, as a result of the installation of the heating system and the disturbance of the natural state of the soil in Sarajevo has a slightly lower water capacity than the soil in control greenhouse.

Soil chemical characteristics were analyzed twice. The results are shown in Table 3. For the analysis of chemical characteristics, the surface layer of the soil was observed.

Table 3. Soil chemical characteristics

	Date	pH in H_2O	pH in KCl	Humus %	P_2O_5 mg/100g soil	K_2O mg/100g soil
Control	5.6.2020	7.45	6.40	3.00	40.00	60.00
Heated		7.45	6.40	3.15	45.00	64.50
Control	5.1.2021	7.50	6.40	2.70	34.00	48.00
Heated		7.40	6.50	2.50	36.00	41.00

According to the chemical characteristics, the soil in the heated and control greenhouse at location of Sarajevo do not differ. Soil has a neutral pH reaction (7.4 – 7.5), while the humus content is at a medium level. The content of easily accessible forms of phosphorus (P_2O_5) and potassium (K_2O) in the soil is very high. Soil fertility was improved by adding organic and mineral fertilizer. Organic manure was added, 100kg/100 m^2, as well as mineral fertilizer NPK 7:20:30 given in the amount of 7 kg/100 m^2 of greenhouse area.

Crop production

Duration of the vegetation period for lettuce was calculated based on the date of planting and harvesting. The obtained length of vegetation between the heated and control greenhouses shows certain differences. In the heated greenhouse vegetation period of lettuce was 67 days. Longer period of time, 49 days more, was needed to achieve a similar yield in the control greenhouse. Based on the results we can claim that heating had a great influence on shortening the vegetation period.

During vegetation period irrigation requirements were based on data from soil moisture sensors placed inside the greenhouse. The drip irrigation system was used, and the source of water is a well located near the greenhouse. In the winter period, that is from the beginning of December 2020 until the end of February 2021, due to very low temperatures, the water was given by manual watering. The total water used, as well as the used water in liters per square meter of production area, is shown in Table 4.

Table 4. Applied irrigation water for lettuce production in Sarajevo, Butmir

Greenhouse	**Total area under curtain crop (m^2)**	**Water used (m^3) per greenhouse**		**Total water used (m^3)**	**Total water used (l/m^2)**
		Drip irrigation	**Manual irrigation**		
Control	100	8.228	0.400	8.628	86
Heated	100	9.076	0.264	9.340	93

The total water used for irrigation of the lettuce in the heated greenhouse is 9.340 m^3 and the control slightly less 8.628 m^3. As can be seen there were no substantial differences in water consumption between two methods of production.

Eclectic energy is used to operate the heat pump. To calculate total electricity cost in Euro per 100 m^2 of production of a tested plant species in a greenhouse average electricity price 0.057 Euro/kWh (FERK, 2020) was used (Table 5).

In order to grow lettuce in the first round, in the period from 12.10.2020 to 18.12.2020 or during 67 days of vegetation, a total of 950 kWh of electricity was consumed (54.49 Euro).

During October (19 days), there was no need for heating because the temperatures in the greenhouse were always above 10 ^{o}C, in November (30 days) we had reheating, while in December (18 days) the heating system worked every day. Usually between 3pm and 11am the next morning, but sometimes constantly.

During the vegetation period, the heating system worked for 27 days, i.e. 40.3% of the total vegetation time. The November consumption is 32.66 kWh for each day of heating, or if we consider 30 days of November 13.1 kWh/day (0.75 Euro/daily). December consumption is much higher and amounts to 37.2 kwh for each day of heating, i.e., for 18 days of vegetation in December 31.0 kwh/day (1.78 Euro/daily).

Table 5. Electricity consumption in kWh

Greenhouse	**Total area under curtain crop (m^2)**	**Monthly electricity consumption in kWh per 100 m^2 greenhouse**		**Total electricity consumption kWh/100 m^2**	**Total electricity cost in Euro/100 m^2**
		November	**December**		
Heated	100	392	558	950	54.49

Measurement of growth intensity was based on the percentage of soil cover with lettuce leaves, since this value depends on a specific heat sum as stated by Bierhuizen *et al.* (1973). Observations calculated in percentage values of soil coverage for control and heated greenhouse are given in Graph 1.

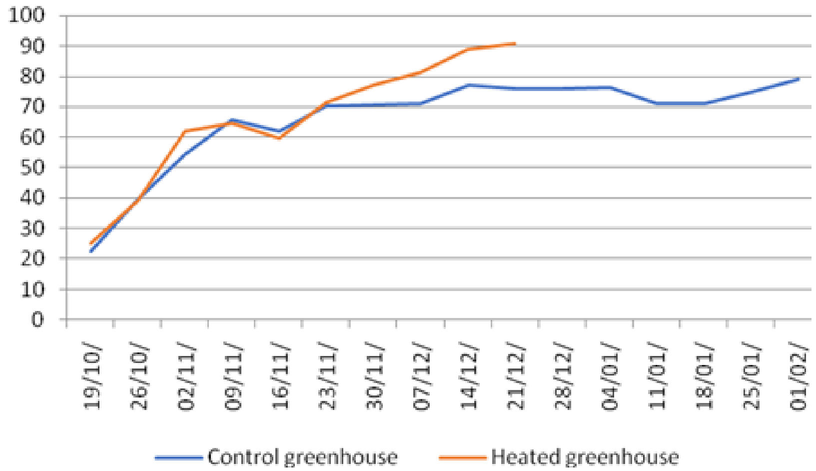

Graph 1. Average soil coverage by lettuce plants (%) for control and heated greenhouse

It is noticeable that the plants in heated conditions reached a soil coverage of over 90% in just under 70 days.

The average, minimum, maximum values and standard deviations for general indicators of some morphological and productive parameters of lettuce depending on the experimental heating are given in Table 6.

Table 6. Diameter, height, mass, number of leaves and yield per m^2 of lettuce

Parameters	Type	Average	St. dev.	Min.	Max.	t-test
Diameter (cm)	Control	24.85	1.73	22.00	28.00	**P<0.001**
	Heated	26.90	1.25	25.00	29.00	
Height (cm)	Control	13.00	1.72	10.00	16.00	**P<0.001**
	Heated	15.65	1.27	13.00	18.00	
Weight (g/plant)	Control	209.00	52.33	125.00	310.00	P=0.723
	Heated	204.00	33.82	155.00	285.00	
Yield (kg/m^2)	Control	3.34	0.84	2.00	4.96	P=0.722
	Heated	3.26	0.54	2.48	4.56	
Number of leaves	Control	40.15	5.76	33.00	56.00	P=0.449
	Heated	41.15	4.65	35.00	51.00	

Independent t-test was performed in order to determine whether there was a statistically significant difference between production of lettuce in heated and control greenhouses. Based on the results, it can be concluded that there are significant differences between the diameter and height of lettuce in heated and control greenhouses. In the heated greenhouse lettuce diameter and height were about 2 cm higher than in the control.

On the other side, there are no significant differences in the weight per plant and yield which means that the weight of lettuce head in control and heated greenhouses is similar. Lettuce weight (g/plant) in heated greenhouse was in range from 155 to 285 which coincides with the results achieved in similar studies (Koudela & Petříková, 2008; Todorović *et al.*, 2012, Barbosa *et al.*, 2015). It can be concluded that the length of vegetation did not affect the yield of lettuce as much as did the heating, which is a consequence of relatively low air temperatures in the control greenhouse during the winter months when lettuce stopped its growth. The factors such as cultivation season and weather conditions influenced the formation of phytomass of leaf rosette, which affected its total weight (Karić *et al.*, 2018).

Furthermore, there are also no significant differences between the numbers of leaves. While lettuce in heated greenhouse have a slightly more leaves (41.15±4.65) than in the control (40.15±5.67).

As a result of the higher growth intensity, in the heated greenhouse, the total length of vegetation was 67 days, while in the control it took additional 49 days (116 in total) to achieve similar yields. We can claim that heating had a great influence on shortening the vegetation period. It can be concluded that the length of vegetation did not affect the yield of lettuce as much as did the heating, which is a consequence of relatively low air temperatures in the control greenhouse during the winter months when lettuce stopped its growth. Therefore, in heating conditions, it is possible to achieve two cycles of lettuce production during the winter months (October – February), while in control conditions, only one is possible.

Economic justification

A calculation was made to show the economic aspect of greenhouse lettuce production while using renewable energy sources, implying investments in greenhouses equipment with and without a geothermal pump.

Expected investments in a greenhouse production without a geothermal pump in BiH are 1,348.94 Euro. Considering the 15 years of depreciation, the amount of annual depreciation, in that case, would be 89.96 Euro. However, if the farmer decides on greenhouses with geothermal pump, depreciation would be higher by eight times, and the total amount of investment would be 10,845.68 Euro. As a result, the amount of annual amortization would be 723.28 Euro. So, with a heated greenhouse, it is necessary to have higher GM for 633.32 Euro in one season to justify additional investment in the pump (Table 7).

Table 7. Total investment in the greenhouses with and without heating (in Euro)

Describe	Greenhouse	
	Control	**Heated**
Greenhouse with standard equipment	1,349	1,349
Installation of geothermal heating systems		9,497
Investments	**1,349**	**10,846**
Years of depreciation	15	15
Amount of annual depreciation	**90**	**723**

Lettuce was grown on 100 m^2 of the control greenhouse, opposite to 200 m^2 in the heated greenhouse (two production cycles in one season). The total yield of 336.8 kg was achieved in the control greenhouse, while a total of 652.0 kg was produced in heated one. Thus, heating the greenhouse in the experiment did not increase the average lettuce yield (326 kg/100 m^2). Both of these results are similar to previous research. According to Bećirović (2015) expected yield of lettuce in continental climate type of BiH in the greenhouse is 329 kg/100m^2, while in Canton Sarajevo expected yield is 371 kg/100m^2 (Stojanović, 2016). Also, no significant differences in the price of lettuce were found on the market in the time interval between picking lettuce in the control and the heated greenhouse. Therefore, this expected competitive advantage was not achieved either. The average price of lettuce was 2 Euro/kg.

The revenues are also similar (Table 8), amounting to 689 Euro (on 100 m^2) for the control, i.e., 1,333 Euro (on 200 m^2) for the heated greenhouse. Thanks to the higher selling price, revenues per 100 m^2 have a higher value compared to previous research 289 Euro (Becirovic, 2015) and 367 Euro (Stojanovic, 2015). There was no significant difference in the cost for seeds, fertilizers, and pesticides between those greenhouses. The average price per production unit (100 m^2) is almost identical. There is an expected difference due to the different production amounts, so the total costs are twice as high in a heated greenhouse. However, a significant difference occurs in heating costs, which amount to 436 Euro. These costs represent an additional burden in the cost section for the heated greenhouse, while outputs are similar (per 100 m^2). The variable costs for the control greenhouse are 237 Euro and 900 Euro for the heated greenhouse. GM in the control greenhouse is 452 Euro, while in the heated greenhouse it is 433 Euro. So we can see that Lettuce production in both greenhouses has similar achieved GM. However, we needed 3.7 times more working capital in the heated greenhouse for these results. Therefore, we can say that from the economic aspect, the production in the control greenhouse was more successful because we engaged fewer funds for a similar result.

Table 8. Gross margin for *Lettuce* in control (100 m^2) and heated greenhouse (200 m^2) (in Euro)

Description	**Greenhouse**	
	Control	**Heated**
REVENUES VARIABLE COST	689.04	1,333.09
Seedlings	61.34	112.68
Fertilizer	12.78	25.56
Pesticide	6.65	28.62
Mechanization	10.22	20.45
Labor	111.43	178.39
Geothermal pump	0.00	436.01
Irrigation	10.22	20.45
Supporting material	12.27	24.54
Other costs	12.27	42.94
TOTAL VARIABLE COST	237.18	899.63
GM	**451.86**	**433.46**
Depreciation coverage with GM (%)	**502**	**60**

This is especially noticeable if we look at the coverage of annual depreciation with realized GM. The depreciated value, i.e., fixed cost value, was covered with GM five times (502%) in the control greenhouse. On the other hand, the achieved GM is not sufficient to cover fixed costs in the heated greenhouse, shown by the calculated value of 60%. Thus, observing the relative indicators, we can say significantly better financial results were achieved in the control greenhouse. Therefore, preference is given to increasing the volume of greenhouse production, ie to possible investment in this type of heating. According to this analysis, in current conditions it is better to expand production capacity instead of investing in a geothermal pump. These results should be taken with caution, above all, these are preliminary results done for just one vegetation period, also, due to COVID-19 crisis the agricultural products market was partially disrupted, and when sales and input prices were volatile and unreliable.

CONCLUSIONS

Since the aim of this research was to analyse the possibility for smallholder urban farmers to increase their sustainability using renewable energy sources all relevant environmental and economic aspects of this production were analysed.

During the winter period in Sarajevo (October – December), by using a heating pump in the greenhouse, compared to control the air temperature increased from 2.20 to 3.82 ^{o}C depending on the month. By this, it was achieved that lettuce grown in the heated greenhouse had better-growing conditions and air temperature never dropped below its biological minimum

As a result, lettuce in the heated greenhouse had a larger diameter and height and grew faster, which shortened the vegetation, which lasted only 67 days, and ensured the possibility of producing two cycles. This was not possible in a greenhouse without heating, where 116 days of vegetation were needed to achieve the same yields.

However, financial results in this study show that there is no economically justified investment in the heat pump. Based on economic analysis we can conclude that in Sarajevo instead of investing in a geothermal pump for lettuce production, it is better to focus on expanding production capacity, i.e., in a larger number of greenhouses. Namely, for the price of one geothermal pump, it is possible to equip seven more greenhouses, leaving a surplus of investment funds. If a particular farm had a sufficient volume of labor, especially its own, the benefit of additional greenhouse areas would be more significant than the investment in a single greenhouse with a geothermal pump. However, future research should consider combining different types of renewable energy sources (solar, wind, biomass, etc.) in order to try to achieve more efficient production results.

Also, we believe that crop selection is very important. Lettuce has not proved to be a good choice, however, such analyzes need to be done on the production of peppers and cucumbers. The first reason is that both crops are expected in greenhouse production in BiH. The second reason is related to the cucumber because it is the only fruitful crop that in spring sowing/planting yields after only a month.

ACKNOWLEDGEMENTS

The authors would like to thank Caritas Switzerland in Bosnia and Herzegovina for financing the field part of this research, which includes the procurement and installation of a geothermal heat pump, greenhouses, measuring sensors, and the procurement of other agricultural inputs and planting material.

REFERENCES

Aramyan, L. H., Lansink, A. G. J. M. O., & Verstegen, J. A. A. M. (2007). Factors underlying the investment decision in energy-saving systems in Dutch horticulture. *Agricultural Systems,* 94(2), 520–527. DOI: 10.1016/j.agsy.2007.01.005

Baćirović, E. (2015). Komparativna analiza proizvodno-ekonomskih rezultata plasteničkog uzgoja povrća u uslovima mediteranske i kontinentalne klime Bosne i Hercegovine, *Master thesis, Poljoprivredno-prehrambeni fakultet Univerziteta u Sarajevu,* Sarajevo, BiH.

Barbosa, G. L., Gadelha, F. D. A., Kublik, N., Proctor, A., Reichelm, L., Weissinger, E., Wohlleb, G. M., & Halden R. U. (2015). Comparison of land, water, and energy requirements of lettuce grown using hydroponic vs. conventional agricultural methods. International journal of environmental research and public health, 12, 6879-6891. DOI:10.3390/ijerph120606879.

Canakci, R., & Akinci, I. (2006). Energy use pattern analyses of greenhouse vegetable production. *Energy, 31*(8-9), 1243-1256. doi:10.1016/j.energy.2005.05.021

Čadro, S., Uzunovic, M., Zurovec, J., & Zurovec, O. (2017). Validation and calibration of various reference evapotranspiration alternative methods under the climate conditions of Bosnia and Herzegovina. *International Soil and Water Conservation Research, 5*(4), 309-324. doi:10.1016/j.iswcr.2017.07.002

Čadro, S., Žurovec, J., & Cherni-Čadro, S. (2017). Severity, Magnitude and Duration of Droughts in Bosnia and Herzegovina Using Standardized Precipitation Evapotranspiration Index (SPEI). *Agriculture & Forestry, 63*(3), 199-206. doi:DOI:10.17707/AgricultForest.63.3.20.

Čadro, S., Miseckaite, O., Gavrić, T., Baublys, R., & Žurovec, J. (2018). *Impact of Climate Change on the Annual Water Balance in a Humid Climate*. Retrieved from Podgorica:

Čadro, S. (2019). *Razvoj i primjena softvreskih modela u cilju održivog upravljanja vodom i povečanja produktivnosti poljoprivrednih kultura u BiH.* (PhD), University of Sarajevo, Sarajevo.

Čadro, S., Škaljić, S., Rakita, N., & Žurovec, J. (2019). *A Modern Hardware and Software Solutions for Corn Irrigation*. Paper presented at the 4th International Symposium Agricultural Engineering ISAE 2019, Belgrade.

Čadro, S., Uzunovic, M., Cherni-Čadro, S., & Žurovec, J. (2019). Changes in the Water Balance of Bosnia and Herzegovina as a Result of Climate Change. *Agriculture and Forestry, 65*(3).

Čivić, H., Muminović, Š., Karić, L., Drkenda, P., Ĉorbo, S., Avdić, J., & Škaljić, S. (2017). Osnove biljne proizvodnje.

Čustović, H., & Tvica, M. (2003). *Praktikum za pedološka istraživanja* (Vol. I). Sarajevo: Poljoprivredno-prehrambeni fakultet, Univerziteta u Sarajevu.

Drešković, N., & Mirić, R. (2013). Klimatski tipovi u Bosni i Hercegovini. *Zbornik radova trećeg kongresa geografa Bosne i Hercegovine*(Geografsko društvo u Federaciji BiH).

El Bilali, H., Berjan, S., Simić, J., Despotović, A., Čadro, S., & Kulina, M. (2013). Urban and peri-urban agriculture in Sarajevo region: an exploratory study. *Journal of Central European Agriculture, 14*(4), 1585-1601. doi:10.5513/JCEA01/14.4.1401

European Commission. (2020). Europe 2020 – a strategy for smart, sustainable and inclusive growth. COM. p. 35.

FERK. (2020). Odluka o referentnoj cijeni električne energije, 07-02-1-783/20 C.F.R.

FHMZ. (2021). *Klimatološka analiza mjeseca Novembar - Studeni 2021.* Retrieved from Sarajevo:

Furuno, S., & Sugawara, K. (2012). Heat pump characteristics and application to flower production - The application of water source heat pump systems in greenhouse horticulture. *NIRE*, 13-24.

Harjunowibowo, D., Siddig, O., Saffa, R. (2021). Experimental investigation of a ground-source heat pump system for greenhouse heating-cooling. International Journal of Low-Carbon Technologies 2021, 16, 1529-1541, Oxford Uiversity. doi: 10.1093/ijlct/ctab052

Hanić, E. E., Čivić, H., & Murtić, S. (2008). *Osnovi ishrane biljaka sa praktikumom*. Mostar: Agromediteranski fakultet Mostar, Poljoprivredno-prehrambeni fakultet Sarajevo.

Hedau, N. K., Tuti, M. D., Stanley, J., Mina, B. L., Agrawal, P. K., Bisht, J. K., & Bhatt, J. C. (2013). Energy-use efficiency and economic analysis of vegetable cropping sequences under greenhouse condition. *Energy Efficiency, 7*(3), 507–515. doi:10.1007/s12053-013-9239-1

Heidari, M. D., & Omid, M. (2011). Energy use patterns and econometric models of major greenhouse vegetable productions in Iran. *Energy, 36*(1), 220-225. doi:10.1016/j.energy. 2010.10.048

Karić, L., Rakita, N., & Marušić, D. (2016). Potential of protected vegetable production in Bosnia and Herzegovina and future perspectives. *Acta Hortic. 1142*, 475-482. doi:doi.org/10.17660/ActaHortic.2016.1142.72

Karić, L., Zahirović, Ć., Žnidarčič, D., Jurković., J., Muminović, Š., Hadžiasimbeg, A., & Sefo, E. (2018). *Influence of the selected varieties of lettuce (Lactuca sativa L.) on yield and nitrate concentrations.* Paper presented at the Proceedings of the IX International Agricultural Symposium "Agrosym 2018", Jahorina, Bosniand Herzegovina.

Kay, D. R., & Edwards, W. M. (1999). *Farm management* (Vol. Fourth edition). Boston, USA: WCB/MCGRAW-Hill.

Koudela, M., & Petříková, K. (2008). Nutrients content and yield in selected cultivars of leaf lettuce (Lactuca sativa L. var. crispa). *Hort. Sci. (Prague), 35*(3), 99-106. doi:doi.org/10.17221/3/2008-HORTSCI

Kurtović, O. (2008). *Proizvodnja u plastenicima*. Sarajevo: Begen d.o.o.

Lund, J. W., & Falls, K. (2012). Direct heat utilization of geothermal energy. *Renewable Energy, 7*, 171–188. doi:10.1016/B978-0-08-087872- 0.00707-1

Maksimović, P. (2011). *Proizvodnja povrća u zaštićenom prostoru*: Partenon.

Popov, T., Gnjato, S., Trbic, G., & Ivanisevic, M. (2018). Recent Trends in Extreme Temperature Indices in Bosnia and Herzegovina. *Carpathian Journal of Earth and Environmental Sciences, 13*(1), 211-224. doi:10.26471/cjees/2018/013/019

Regulatorna komisija za energiju Federacije Bosne i Hercegovine - FERK (2020). Odluka o referentnoj cijeni električne energije, 07-02-1-783/20 C.F.R.

Stojanović, A. (2016). Ekonomika plasteničke proizvodnje na području Kantona Sarajevo, *Master thesis, Poljoprivredno-prehrambeni fakultet Univerziteta u Sarajevu*, Sarajevo, BiH.

Todorović, V., A., G. R., Markvić, S., Đurovka, M., & Vasić, M. (2012). Influence of temperature on yield and earliness of lettuce grown in the winter period. *Agroznanje, 13*(3), 475-481.

Trbic, G., Popov, T., & Gnjato, S. (2017). Analysis of air temperature trends in Bosnia and Herzegovina. *Geographica Pannonica, 21*(2), 68-84. doi:10.18421/Gp21.02-01

Wu, R. (2009). Energy efficiency technologies—air source heat pump vs ground source heat pump. *Journal of Sustainable Development, 2*, 14-23.

Zurovec, O., Cadro, S., & Sitaula, B. K. (2017). Quantitative Assessment of Vulnerability to Climate Change in Rural Municipalities of Bosnia and Herzegovina. *Sustainability, 9*(7). doi:10.3390/Su9071208

Žurovec, J., Čadro, S., & Murtić, S. (2011). *Drought Analysis in Sarajevo Using Standardized Precipitation Index (SPI)*. Paper presented at the 22nd International Scientific expert Conference in Agriculture and Food Industry, Sarajevo.

Žurovec, O., Vedeld, P. O., & Sitaula, B. K. (2015). Agricultural Sector of Bosnia and Herzegovina and Climate Change—Challenges and Opportunities. *Agriculture, 5*(2), 245-266. doi:10.3390/agriculture5020245

Kolev, V. (2022). Growth rate of Squalius orpheus (Kottelat and Economidis 2007) in the rivers Chepinska and Vacha. Agriculture and Forestry, 68 (2): 109-120. doi:10.17707/AgricultForest.68.2.08

DOI: 10.17707/AgricultForest.68.2.08

Vasil KOLEV*[1]

GROWTH RATE OF *SQUALIUS ORPHEUS* (KOTTELAT AND ECONOMIDIS 2007) IN THE RIVERS CHEPINSKA AND VACHA

SUMMARY

This paper presents a study of Orpheus dace (*Squalius orpheus*) populations from the rivers Chepinska and Vacha, right tributaries from the middle zone of the Bulgarian part of the Maritsa River's watershed. The research was conducted in the summer and autumn months of 2006–2011. A total of 470 specimens of Orpheus dace from the Chepinska River were caught. The study material from the Vacha River is relatively small. It includes 61 individuals. Fish populations from both rivers are characterized by disturbed age structure and predominance of young individuals. The average body length by size class was calculated using a relationship between the average values of *L* (standard length) and *S* (scale radius). The analysis showed that fish grow faster in their first year. A back calculated standard length of the Chepinska River fish is as follows: year 1: 50 mm, 2: 82mm, 3: 131 mm an 4: 192 mm. In the Vacha River it is - 1: 42 mm, 2: 78 mm, 3: 118 mm, 4: 149 mm and 5: 175 mm. Two hundred mm long individuals in the Chepinska River have average weight 80g and in the Vacha River - 126g. As it concerns these two rivers, the study found that fish growth in length and weight is relatively low in comparison with many other Bulgarian water bodies.

Keywords: agritourism, Orpheus dace, size-age composition, growth in length, growth in weight

INTRODUCTION

Orpheus dace (*Squalius orpheus* Kottelat & Economidis 2007) is widely distributed in the Balkan Peninsula. The fish's range includes the Aegean catchment area in Bulgaria, Greece and Turkey (Kottelat and Freyhof 2007). Orpheus dace is widespread in rivers with constant and medium fast water flow; the species also thrives in some dams (Mikhailova, 1964, Marinov, 1986). This is one of the most abundant fish in the middle zone of the Maritsa River tributaries (Dikov *et al*., 1994; Kolev, 2013). During the warm period of the year the fish

[1]Vasil Kolev (corresponding author: vassilie@abv.bg) University of Forestry, Faculty of Forestry, Department of Hunting and Game Management, 10 Kliment Ochridski Blvd., 1797 Sofia, BULGARIA.

Notes: The authors declare that they have no conflicts of interest. Authorship Form signed online.
Recieved:15/08/2021 *Accepted:04/03/2022*

stays near the water jet in search of food. Orpheus dace is omnivorous, its diet includes many planktonic and demersal organisms: insects, insect larvae, leeches, worms. The fish also consumes larger animal organisms such as small frogs and small fish. Moreover, the species feeds on algae and fruits of coastal plants (Mikhailova, 1964). In winter, Orpheus dace hides in deep waters, but remains active for most of the cold period (Mikhailova, 1964). In spring and during the first half of the summer, the fish enter small and shallow streams for breeding. Sexual maturation and fertility of this species in the Struma River in Bulgaria have been studied by Mikhailova (1964). In 2021 Kolev has published research data about the fecundity of Sq. orpheus populations of the rivers Chepiska and Stryama. Data about the length growth of Orpheus dace in Bulgarian territory have also been published by Mikhailova (1964), Dikov and Zhivkov (1985), Marinov (1986), Dikov *et al*. (1994), Stefanova *et al*. (2008), Kolev and Raikova (2015). However, these studies lack data on species growth in the Chepinska and Vacha rivers.

In Bulgaria, recent research about Sq. orpheus has focused on the species' helminth parasites (Kirin et. al, 2019; Chunchukova et. al, 2020), while studies of species population biology have not been as popular. Nonetheless, in Turkey's European part, Saç et. al. (2020) have investigated the W-L (mass-length) ratio of Sq. orpheus of four rivers in the Turkish part of South Thrace and Strandja. The authors do not establish relevant population parmeters for each individual population - i.e. the population inhabiting each of these rivers. Instead, the scholars combine all available data and estimate the a and b coefficients of the W-L ratio for the combined four populations of the Orpheus dace (one of each river) altogether. In contrast, the present study takes the opposite approach - it focuses on a Sq. orpheus population, which inhabits one river, a single water body, in order to establish the population parameters for this particular habitat.

The aim of this study is to determine some of the most important population characteristics of Orpheus dace from the rivers Chepinska and Vacha: species' growth in length and in weight. The results will then be compared with relevant data published by other scientists, who have studied other rivers of the Aegean watershed.

MATERIAL AND METHODS

The research project studies the rivers Chepinska and Vacha; both are parts of the Maritsa River basin.

The Chepinska River originates in the West Rhodopes Mountains; its springs are located underneath the peak Mala Siutkia (2078.7 m a.s.l.) (Figure 1). In its upper reaches, the river flows to the Northwest and is called the Bistritsa River. Once it reaches the town of Velingrad, the river runs northwards and near the village of Vetren it enters the Upper Thracian Valley. The studied river flows into the Maritsa River near the village of Kovachevo (near the town of Pazardzhik). This Maritsa River tributary is 81.7 km long with a catchment area of 899.6 km^2. It is a medium sized mountain Bulgarian river (№ H-4 /14.09.2012

MOSV) with an average altitude of 1228 m. Declination of the river bed is 68%, and the Chepiska River's average flow rate is 18 m^3/s^{-1} (Stoyanov *et al.*, 1981; Hristova, 2012). In summer, the water temperature reaches 20° C (BD-IBR 2015).

The Vacha River marks the border between the Eastern and the Western parts of the Western Rhodope Mountains. It is a 111.5 km long river with a catchment area of 1644.7 km^2. The beginning of the Vacha River is the Buynovska River, which springs below Bukovik Peak (1805 m above sea level) in the Western Rhodope Mountains, near the border with Greece. The second studied river flows into the Maritsa River near the village of Kadievo. The river's waters are used to generate electricity through the Dospat-Vacha cascade. As a result, water outflow after the cascade is strongly influenced by an operation of a hydropower plant. This Maritsa River tributary belongs to the category of large mountain Bulgarian rivers (№ H-4 /14.09.2012 MOSV). Its average altitude is 1441 m. Declination of the river bed is 14%. The Vacha River's average flow rate is 9,3 m^3/s^{-1} (Stoyanov *et al.* 1981; Hristova, 2012).). In summer, water temperature in this river does not exceed 20° CBD-IBR 2015).

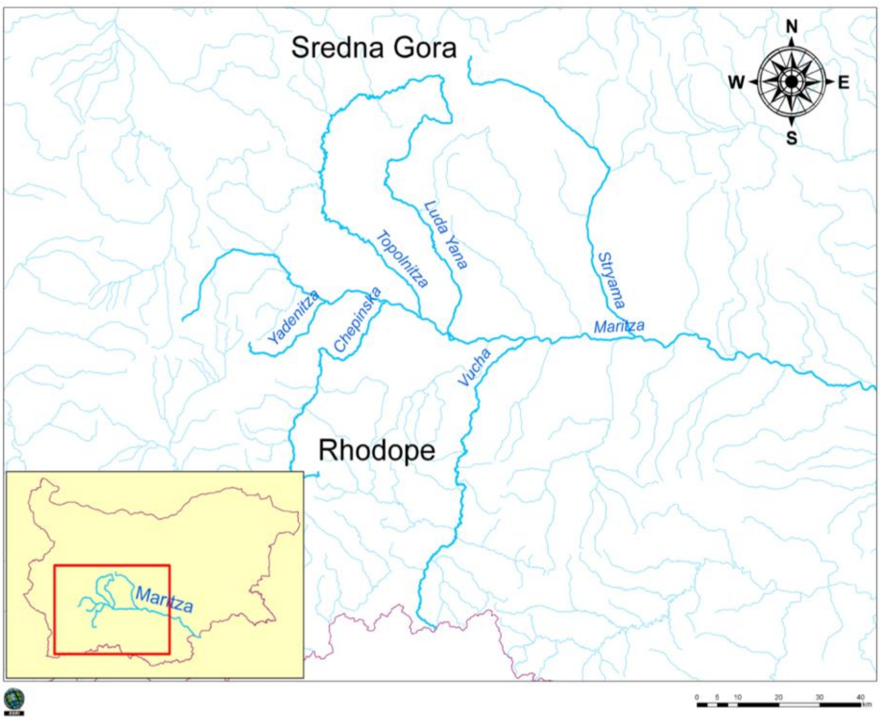

Fig. 1. Location of the rivers Chepinska and Vacha, Arc Map 10.0 (ESRI – ArcGIS 2013).

Specimens were collected in the spring and in the autumn of the period of 2006-2011. Using the method of electrofishing 470 Orpheus dace specimens were caught in the Chepinska River and 61 respectively in the Vacha River. A SAMUS 725G converter was used, providing up to 640 V direct current (DC), with a frequency of 50 Hz and output power reaching up to 200 W. The catch was performed according to an EN 14011: 2004 instruction (Water quality – Sampling of fish with electricity). Four sampling areas, located in different parts of the studied rivers, were used (Table 1).

Standard length (L) was measured with a 1 mm precision, while weight (W) was measured with a 1 g precision.

Table 1. Sampling areas along the rivers Chepinska and Vacha.

№	Location	Geographic coordinates		Alti-tude (m)	Date of sampling
		N	E		
1.	In the vicinity of the village of Kovatchevo	42°12'28,79"	24°10'54,69"	523	09.04.2011
2.	In the vicinity of the village of Lozen	42°11′09,62″	24°09′45,65″	240	08.04.2011 18.11.2011
3.	In the vicinity of the village of Yoakim Grouevo	42°06'59,28"	24°33'06,89"	182	12.10.2007
4.	In the vicinity of the town of Krichim	42°01'25,87"	24°28'22,49"	209	12.10.2007

More than ten scales ware collected from each Orpheus dace specimen. They were taken from underneath the dorsal fin; an equal number of scales were taken from the left and right side of the dorsal fin. Next, the scales were dried up and stored in small papers bags. The scales were then examined with a microscope Olympus CX 31, at 40× magnification. Each scale was sandwiched between two microscope slides. Fish age was then determined by counting the annual rings of a scale. For this purpose, the diagonal caudal radius of the scales was used.

Fish linear growth was determined via a back-calculation of the length *(L)* from the diagonal caudal radius of the scales (S) (Zhivkov, 1993). This relation is well described by a linear equation:

$$L = a + b.S \quad (1)$$

where:

L – Length of fish (mm)

S – Diagonal caudal radius of the fish scales (eyepiece micrometer scales divisions)

a, *b* – Equation Coefficients

Net weight (*W*) values were estimated, using the equation described by Ricker (1975) and applied by many authors (Zhivkov 1993, 1999, Raikova-Petrova and Zhivkov 1993, Kukushkin, 1997, Belomacheva *et al*. 2000).

$W = a.L^b$ (2)

where:

L – Length of the fish (mm)

W – Weight of the fish with entrails (g)

a, *b* – Equation Coefficients

A comparison of the length growth of different Orpheus dace's populations is made by ranking them according to the average lengths at the same age. The length of the last age group of the youngest population is used for comparison. (Zhivkov, 1972).

To compare the weight growth (*W*) of fish from different populations, a method proposed by Goldspind (1979), De Silva (1985), Zhivkov (1993, 1999) and Raikova-Petrova and Zhivkov (1993) is used. The relationship is expressed by the following equation:

$logW = loga + b.logL,$ (3)

where:

L – Length of fish (mm)

W – Weight of fish, together with the entrails (g)

a, *b* – Equation Coefficients

Equation 3 is obtained by taking the logarithm of the equation: $W = a.L^b$.

In order to obtain comparable values of *W* in equation 3, pre-selected rounded values of L (L = 50, L = 100, L = 150, L = 200, L = 250, L = 300, L = 350, L = 400, mm) are successively substituted on place of L. Using equation 3 with the listed values of *L (mm)* allows obtaining the corresponding values of the mass W - $W_{L=50}$, $W_{L=100}$, $W_{L=150}$, $W_{L=200}$, $W_{L=250}$, $W_{L=300}$, $W_{L=350}$, $W_{L=400}$. The so-obtained mass values ($W_{L=50}$, $W_{L=100}$, $W_{L=150}$, $W_{L=200}$, $W_{L=250}$, $W_{L=300}$, $W_{L=350}$, $W_{L=400}$) for each of the studied populations were then compared.

Due to the fact that some authors have measured total length (to the end of the caudal fin) and others have measured standard length (to the end of the scale cover) it is necessary to use both in the comparison tables.

The association degree between *L* and *S*, as well as between *W* and *L* variables, was determined by a correlation coefficient (r). All data were calculated by using MS-Excel 2010.

RESULTS AND DISCUSSION

The age composition of the Chepinska River's population is simple. There are four age groups, but young fish are the most abundant. Ninety six percent of the fish belongs to the first and second age groups. The presence of predominantly young fish is also well illustrated by the size of the catch. Most fish (87 % of the total sample) are less than 110 mm long (Figure 3, 5).

In the Vacha River five age groups are recorded. The small sample catch, however, definitely does not represent the whole variety of age and size groups, characteristic of the population. Therefore, it is not possible to clearly identify any trends and draw conclusions. (Figure 2, 4).

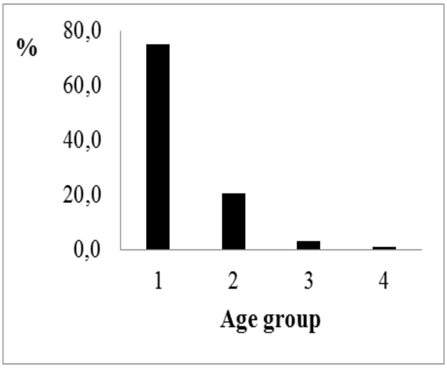

Fig. 2. Age structure of Orpheus dace from the Chepinska River

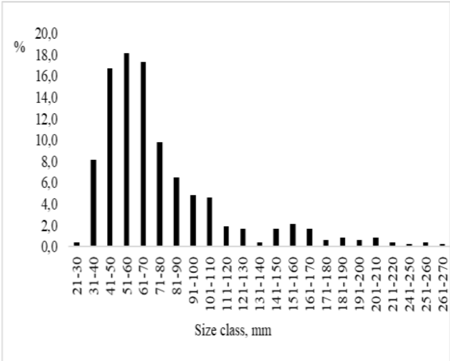

Fig. 3. Size classes of Orpheus dace from the Chepinska River.

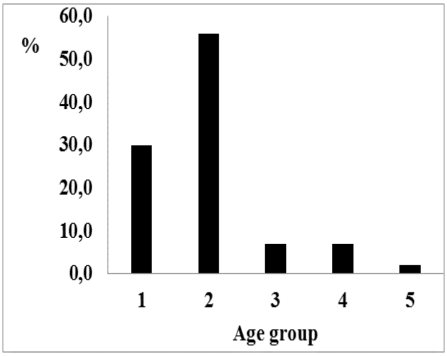

Fig. 4. Age structure of Orpheus dace from the Vacha River

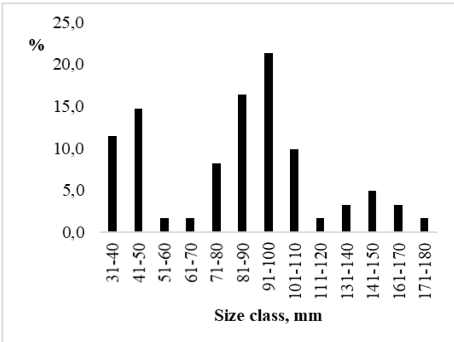

Fig. 5. Size classes of Orpheus dace from the Vacha River

The biggest specimen registered in the Chepinska River is 270 mm long (319 mm full length) and weighs 333 g (375g weight with entails). This is four-year-old fish. The smallest one is 27 mm long (34 mm full length) and weighs 0.2g (0.3 g weight with entails). This is an annual fish.

The biggest Orpheus dace caught in the Vacha River is 178 mm in length (210 mm full length) and weighs 81 g (91g weight with entails). This is the only five-year-old specimen caught in the Vacha River. The smallest one is 32 mm long (44 mm full length) and weighs 0.5g (0.8 g weight with entails). This is an annual fish.

The relationship between fish standard body length (L) and scale radius (S) (measured in divisions of the eyepiece – micrometer) is very well expressed by a linear function, which has a high degree of reliability (equation 4, the Chepinska River; equation 5, the Vacha River.

L = 15.28+2.0712·S; correlation r = 0.9964, n=470 (4)

L = 6.4981+2.5162·S; correlation r = 0.9960, n=61 (5)

In both studied rivers, a faster growth of Orpheus dace is observed in the first year of life.

Generally the species reaches bigger length in the Chepinska River. For all age groups, average fish length exceeds that of fish from the Vacha River. Average length of four-year-old specimens from the Chepinska River is greater than the average length of five-year-old specimens from the Vacha River (Tables 2, 3). In the both rivers, in 2004 and 2006, fish grew slightly faster.

Table 2. Back-calculated standard body length (L) of Orpheus dace from the Chepinska River.

Years	Age group	Back-calculated standard body length (mm)				Number
		L_1	L_2	L_3	L_4	
2007	I	51				5
2006	II	49	94			258
2005	II	35	77			169
2004	III	59	81	155		22
2003	IV	57	76	106	192	16
∑						470
Average body-length (L_{av}), mm		50	82	131	192	
Growth in length (t'), mm		50	32	49	62	

Table 3. Back-calculated standard body-length (L) of Orpheus dace from the Vacha River.

Years	Age group	Back-calculated standard body length (mm)					Number
		L_1	L_2	L_3	L_4	L_5	
2007	I	40					17
2006	II	40	91				30
2005	III	32	44	102			6
2004	IV	54	82	126	145		7
2003	V	44	95	125	152	175	1
∑							61
Average body-length (L_{av}), mm		42	78	118	149	175	
Growth in length (t'), mm		42	36	40	31	26	

The relationship between fish weight and length (L) is very well expressed by a parabolic function with a high degree of reliability. The general equation for the Chepinska River population is equation number 6 and for the Vacha River – number 7.

$W = 0.00001 \cdot L^{3.0002}$; $r = 0.9973$, n=470 (6)

$W = 0.000007 \cdot L^{3.1533}$; $r = 0.9997$, n=61 (7)

A comparison of mass growth rate between the two rivers indicates that there is a slightly faster mass accumulation for all age groups from the Vacha River. In 2004, in both rivers, mass rate growth is relatively higher, in comparison with other years. However, species' weight growth in both rivers is relatively slow (Tables 4, 5).

Table 4. Back-calculated body-weight (*W*) of Orpheus dace from the Chepinska River

Years	Age group	Back-calculated body-weight (g)				Number
		W_1	W_2	W_3	W_4	
2007	I	1.3				5
2006	II	1.2	8			258
2005	II	0.4	5			169
2004	III	2.1	5	38		22
2003	IV	1.8	4	12	71	16
∑						470
Average body weight (W_{av}). g		1.4	6	25	71	
Weight growth – (t'). g		1.4	4	19	46	

Table 5. Back-calculated body-weight (*W*) of Orpheus dace from the Vacha River

Years	Age group	Back-calculated body-weight (g)					Number
		W_1	W_2	W_3	W_4	W_5	
2007	I	1.2					17
2006	II	1.1	17				30
2005	III	0.5	2	24			6
2004	IV	3.1	12	48	75		7
2003	V	1.6	19	46	89	139	1
∑							61
Average body weight (W_{av}). g		1.5	13	39	81	139	
Weight growth – (t').g		1.5	11	27	42	58	

DISCUSSION

The age structure of the Orpheus dace' population in the Chepinska River is disturbed. The presence of mostly small and young fish is an indicator of a significant elimination of fish due to angling (mostly of larger sizes) (Pravdin, 1966). This observation is also confirmed by the low survival rates of Orpheus dace - 25% for in the Chepisnska River. As a result, most of the population in the river consists of replenishment (annual fish).

The length-growth of the Orpheus dace is relatively slow in the Chepinska River. Length-growth is fast in the first year, after which it slows down. A rapid increase in size in the first year of a fish's life allows it to escape the press of predators (Table 2). During the following year, length-growth decreases. This phenomenon is associated with a sexual maturation of a large number of individuals at this age (Nikolsky, 1965). The rate of weight growth of the Orpheus dace in Chepinska River increases with age. Since the populations is young, a delay in mass accumulation for older age group is not observed (Tables 4).

Similar results about fish's length-growth and mass accumulation are estimated to characterize the Vacha River's population of Orpheus dace (Tables 3, 5). Regrettably, the current study's small sample size does not allow for reliable conclusions to be drawn about the entire population.

A comparison of length-growth of Orpheus dace from different water bodies, using the Zhivkov's method (1972), shows that the species grows faster in dams, rather than in rives (Table 6).

Table 6. A comparison of average lengths at equal age of Orpheus dace from different water bodies of its habitat range.

Author/s and year	River Dam	Back-calculated standard body length (mm)										
		L_1	L_2	L_3	L_4	L_5	L_6	L_7	L_8	L_9	L_{10}	L_{11}
Dikov *et al.*, 1994	Arda River	58	104	137	159	-	-	-	-	-	-	-
Kolev and Raikova, 2015	Stryama River	58	83	121	162	192	-	-	-	-	-	-
Michailova, 1964	Struma River	83	115	148	175	202	215	-	-	-	-	-
Dikov and Zhivkov, 1985	Dzerman River	52	101	141	183	-	-	-	-	-	-	-
Present data, 2021	Chepinska River	50	82	131	192	-	-	-	-	-	-	-
Marinov, 1986	Chepinska River	61	115	152	-	-	-	-	-	-	-	-
Dikov *et al.*, 1994	Struma River	54	119	164	211	223	241	243	-	-	-	-
Dikov *et al.*, 1994	Mesta River	64	114	195	214	-	-	-	-	-	-	-
Stefanova *et al.*, 2008	Maritsa River	60	95	130	240							
Zhivkov, 1973	Batak Dam	96	163	215	247	272	294	318	352	379	397	406
Boyadgiev, 1966	Pyasachnik Dam	89	155	218	289	316	-	-	-	-	-	-
Marinov and Boyadjiev, 1967	Koprinka Dam	73	193	261	-	-	-	-	-	-	-	-

In all three dams: Batak, Pyasachnik and Koprinka, length-growth is faster than that in rivers. This finding can be explained by taking into account the influence of a larger number of predators, especially perch and pikeperch, found in the dams (Zhivkov, 1973) and consequently - the larger press of predators on fish populations. Growth conditions also have an impact. Orpheus dace grows faster in the dams Koprinka and Pyasachnik, which are located at an altitude of about 300 m in comparison with the Batak Dam, located at 1108 m above sea level. Thus, the two dams have longer warm period and more favourable temperatures (Table 6). In the rivers Struma and Mesta Orpheus dace grows faster in length than in the Maritsa River and its tributaries, the rivers: Arda, Chepinska and Stryama. A study by Marinov (1986) presents an exception to this trend, as it concerns the Chepinska River. However, the author studied only ten Orpheus dace specimens and the study's accuracy is lower in comparison with the present study, which includes 470 specimens from this river (Table 6).

In the Table 7 are presents the calculated masses of fish for the same length from different water courses, by means of the formula: $W = a.L^b$, according to above-mentioned method (Zhivkov, 1993, 1999).

Table 7. Comparison of the average mass (*W*) of Orpheus dace from different rivers, calculated at pre-selected rounded standard body length values (*L*).

Author/s and year	River. Dam	Equation of the whole Population	Average weight (W_L. g) calculated with the same rounded lengths (*L*. mm)				
			W_{50}	W_{100}	W_{150}	W_{200}	W_{250}
Present data, 2021	Chepinka	$W = 0.00001L^{3.0002}$	1.3	10	34	80	156
Dikov *et al.*, 1994	Arda	$W = 0.00005L^{2.7522}$	2.3	16	49	108	199
Kolev and Raikova, 2015	Stryama	$W =0.000009L^{3.1154}$	1.8	15	54	133	266
Dikov *et al.*, 1994	Struma	$W = 0.00003L^{2.9007}$	2.5	19	62	142	271
Zhivkov, 1973	Batak	$W =0.000007L^{3.1662}$	1.7	15	54	135	274
Dikov *et al.*, 1994	Mesta	$W = 0.00006L^{2.7793}$	3.2	22	67	149	277
Stefanova *et al.*, 2008	Maritsa	$W = 0.0148L^{3.0595}$	2.0	17	59	142	280
Mikhailova, 1964	Struma	$W = 0.00001L^{3.1175}$	2.0	17	61	149	299
Dikov and Zhivkov, 1985	Dzerman	$W = 0.0116L^{3.05}$	2.2	19	64	154	305

Legend: W_L – weight of the fish with rounded values of body length (50 to 250 mm)

Orpheus dace's mass increases faster in main watercourses: the rivers Struma, Mesta and Maritsa, in comparison with their tributaries: the rivers Arda, Stryama and Chepinska. Species mass growth is also relatively fast in the Batak Dam. Probably the greater weight of fish, with the same length from the rivers Maritsa, Struma and Mesta, as well as from the Batak dam, is a result of the richer food base there. Moreover, in the Maritsa River the speed of water flow is lower than in its smaller tributaries: Arda, Chepinska and Stryama. Water in the Batak Dam is stagnant. In such habitats fish use less energy for their movements.

CONCLUSIONS

The populations of Orpheus dace of the rivers Chepinska and Vacha are characterized by disturbed age structures. Fish stocks are predominated by 1- to 2-year old specimens. In recent years, there has been comparatively relatively less research focus on the biology of *Squalius orpheus*. In many Bulgatian rivers the fish's population structure has changed and younger fish dominate.

Compared to other Bulgarian water bodies, the linear growth of Orpheus dace of the rivers Chepinska and Vacha is relatively slow. Mass accumulation is also slow. Four-year-old specimens of both rivers reach an average weight of 70-80g.

ACKNOWLEDGMENTS

I am grateful to Prof. Dr. G. Raykova for her help in developing the research methodology. I am grateful to my colleagues I. Goranov and G. Gruychev for their participation in collecting materials for this study.

REFERENCES

ArcGIS(2013). Web site. Available at: http://www.arcgis.com/home/webmap/viewer.html

Chonchukova, M., Kirin, D., Kuzmanova, D. (2020). Helminth parasites of two cyprinid fishes from Topolnitsa River, Bulgaria. Agricultural university of Plovdiv, Department of agroecology and environmental protection. Scientific Papers. Series D. Animal Science. Vol. LXII, No. 1: 475-480

De Silva, S. (1985). Body condition and nutritional ecology of *Oerofchromus mossambicus* (Pisces, Cichlidae) populations of man-made lake in Sri Lanka. Journal of Fish Biology 27: 621–633.

Goldspind, C. (1979). The population density, growth rate and production of roach, *Rutilus rutilus*, in Tjeukemeer, the Netherlands. Journal of Fish Biology 15: 437–498.

Hristova, N. (2012). Rechni voidi na Bulgaria. Izdatelska kasta Top Press. 538 p. (in Bulgarian).

Boyadgiev, At. (1966). Ichthyofauna i ribostopansko izpolzvane na izovir Piyasachnik. Plovdiv, 5: 41–49 (in Bulgarian).

Dikov, Tz. & Zhivkov, M. (1985). Age. Lineary and Weight Growth of the Chub (*Leuciscus cephalus* L.) in the Dzerman River. Bulgarian Academy of Sciences. *Hydrobiology*, 24: 13–23

Dikov, Tz., Jankov, J., Jocev, St. (1994). Fish stocks in River of Bulgaria. *Pol. Arch. Hydrobiol.*, 43: 377–391.

Kirin, D., Chonchukova, M., Kuzmanova, D. (2019). Helminths and helminth communities of Orpheus dace (*Squalius Orpheus* Kottelat & Economidis, 2006) from Stryama River, Bulgaria. Agricultural university of Plovdiv, Department of agroecology and environmental protection. Scientific Papers. Series D. Animal Science. Vol. LXII, No. 1: 475-480

Kolev, V. (2013). Species composition of the ichthyofauna of some tributaries of the Maritza River. *Forest. Ideas, 19*. 2 (46): 129-139

Kolev, V. & Raikova, G. (2015). Age, growth rate and condition factor of the chub (*Squalius orpheus* Kottelat & Economis. 2006) in the Stryama River. *Forest. Ideas*, 2*1*. 2 (50): 269-276

Kolev, V. (2021). Fecundity of *Squalius orpheus* from the rivers Stryama and Chepinska. Macedonian journal of ecology and environment, Vol. 23. 1: 25-35

Kottelat, M. & Economis, P.S. (2006). *Squalius orpheus*. a new species of cyprinid fish from Evros drainage. Greece (Teleostei: Cyprinidae). *Ichthyol. exp.of freshwat.*, 17 (2): 181–186.

Kottelat, M. & Freyhof, J. (2007). Handbook of European Freshwater Fishes. Kottelat. Cornol. Switzerland and Freyhof. Berlin. Germany. 646 pp.

Marinov, B. & Byadjiev, At. (1967). Varhu stopanski cennite vidove ribi v iazovir "G. Dimitrov" (Koprinka), *Izvest. na inst. po ribn. stop. i oken. Varna*, 8: 359-360.

Marinov, B. (1986). *Taksonomia, binomia i faunistika na nakoi ot vidovete ot semeistvo Cyprinidae i Cottidae (Pisces) v Bulgaria*. Sofia University "St. Kliment Ohridski". Department of General and Applied Hydrobiology: 46–76 (in Bulgarian) (PhD thesis)

Mikhailova, L. (1964). Varhu biologiata na rechnia kefal (*Leuciscus cephalus* L.*)* v reka Struma Bulgarian Academy of Sciences. Institute of Zoology. Sofia, *Bull. of the inst. of zool. and museum*, 17: 125–156 (in Bulgarian).

Nikolsky, G. (1965). Teoria dinamiki stada rib. Nauka. Moskva: 80–115 (in Russian).

Pravdin, I. (1966). Rukovodstvo po izucheniu rib. Pishtchevaia promishlenost. Moskva. 376 pp. (in Russian).

Raikova-Petrova, G. & Zhivkov, M. (1993). Vazrast i temp na restej na bialata riba (*Stizostedion lucioperca* L.) v iazovir ohladitel Ovcharica. Bulgarian academy of sciences. *Hydrobiology*, 38: 67–80 (in Bulgarian).

Ricker, W. (1975). Computation and interpretation of biological statistics of fish populations. "Food industry". Moscow: 408 pp. (in Russian).

Saç, G., Gaygusuz, Ö., Gaygusuz, Ç., Özuluğ, G. (2020). Length-weight relationship of seven freshwater species from Turkish Trace. Journal of applied ichthyology. Vol. 35, 3: 808-811

Stefanova, E., Uzunova, E., Hubenova, T., Vasileva, P., Terziiski, D., Iliev, I. (2008). Age and Growth of the Chub. Leuciscus cephalus L. from the Maritza River (South Bulgaria). *Bulg. journ. of agric. science*, 14(2): 214–220.

Stoyanov, G., Gigova, V., Penchev, M., Ivanova, N., Hristova, D., Shishkova, I., Krastva, C. (1981). Hydrologichen spravochnik na rekite v Republika Bulgaria. Volume II–III, Balgarska academia na naukite. 526 p. (in Bulgarian).

Zhivkov, M. (1972). Critical analysis of some relative indice of the intensity of the fish growth. *Bull. of the inst. of zool. and museum*, 36:81-101.

Zhivkov, M. (1973). *Zakonomernosti i osobenosti v narastwaneto, sazriavaneto i plodovitostta na ribnite populacii v iazovir Batak*. Institute of Zoology. Sofia. 316 pp. (in Bulgarian). (PhD thesis)

Zhivkov, M. (1993). Comparative analysis of the age composition, growth rate and condition of carp (*Cyprinus carpio* L.) in three Bulgarian reservoirs. *Ichtiologia*, 25 (1):7-18

Zhivkov, M. (1999). *Factori, zakonomernosti i metodologichno znachenie na biologichnata izmenchivost pri sldkovodnite ribi.* Institute of Zoology. Sofia. 406 pp. (in Bulgarian). (DSc thesis)

Arif, A., Husna., Tuheteru, F.D., Rosnawati (2022). Shoots cuttings propagation of endangered and endemic tree species of Kalappia celebica Kosterm using the application of Rootone-f . Agriculture and Forestry, 68 (2): 121-131. doi:10.17707/AgricultForest.68.2.09

DOI: 10.17707/AgricultForest.68.2.09

Asrianti ARIF*, HUSNA, Faisal Danu TUHETERU, ROSNAWATI[1]

SHOOTS CUTTINGS PROPAGATION OF ENDANGERED AND ENDEMIC TREE SPECIES *Kalappia celebica* Kosterm USING THE APPLICATION OF ROOTONE-F

ABSTRACT

Kalappia celebica Kosterm is a member of the Fabaceae family and is included as monotypic species. The tree is one of the most important timber because has a high quality of wood, with dark brown color, making *K. celebica* has great performance thus increasing its economic value. However, its population has decreased with the increase in logging and wood harvesting, mining, and housing. Natural regeneration is also limited due to infrequent flowering periods and fruiting. Therefore, to improve plant material for replanting, it is crucial to do vegetative propagation, such as cutting and accelerating their rooting and growth using a growth regulator. This study aimed to determine the effect of rootone-f as a plant growth regulator on the rooting and growth of *K. celebica* cuttings. The study was designed using a randomized block design which consisted of 4 (four) treatments. The treatments used were untreated cuttings (control), application of 100 ppm, 200 ppm, and 300 ppm/rootone-f solution. The data recorded were analyzed using an analysis of variance (ANOVA). The results showed that the application of rootone-f treatments had a significant effect. There is a different response between untreated and treated cuttings. The treatment of rootone f produced better rooting and growth than untreated ones. There was a significant increase in the total of primary and secondary roots, length of roots, shoots number, leaf area, shoots dry weight, and roots dry weight of *K. celebica* cuttings at eight weeks after planting. The highest rooting and growth were reached by 200-300 ppm treatment. Rootone f application with concentrations of 200 ppm is the optimal dose that could be considered to produce high-quality seedlings of *K. celebica* from cuttings. The success of shoots cutting propagation for *K. celebica* will provide primary practice of *K. celebica* cultivation, support juvenile stage bypass, and contribute to conservation efforts for valuable, endemic, and threatened tree species.

Keywords: Cuttings, endangered species, growth regulator rootone-f, *K. celebica* Kosterm, propagation

[1] Asrianti Arif* (corresponding author: antyarf75@gmail.com), Husna, Faisal Danu Tuheteru, Rosnawati, Halu Oleo University, Kendari, INDONESIA

Notes: The authors declare that they have no conflicts of interest. Authorship Form signed online.
Recieved:04/12/2021 *Accepted:15/05/2022*

INTRODUCTION

Kalappia celebica Kosterm, called kalapi (*local name*), is the local and endemic plant that is widely distributed to Sulawesi Island, especially in Malili, Each Sulawesi and Kolaka, Abuki, Konawe, etc., Southeast Sulawesi, Indonesia (Arif *et al*., 2016; Arif and Uslinawaty, 2017). *K. celebica* belongs to the Fabaceae family and is categorized as monotypic species (Trethowan *et al*., 2019). The tree is one of the most important timber because it has a high quality of wood, with dark brown color make *K. celebica* has great performance thus increasing its economic value. It is commonly used in house constructions such as door and window frames, house walls, light construction, boat materials, bridges, etc. (Whitmore *et al*., 1989). However, *K. celebica* was listed as vulnerable species on IUCN red list (Trethowan *et al*., 2019; IUCN, 2022), with significant threats being logging and wood harvesting, mining, and housing. In the regulation of Ministry of Forestry No P57/2008, the Indonesian Government has declared that *K. celebica* should be conserved (Mardiastuti *et al*., 2008). There is no accurate information about *K. celebica* cuttings and still limited reports about replanting activities. Therefore, propagation such as generative and vegetative and replanting of *K. celebica* should be done. Approaches to generative and vegetative propagation can save many endangered or extinct species (Dunsin *et al*., 2016; Susilowati *et al*., 2018; Hendalastuti *et al*., 2010; Darma and Priyadi, 2019).

In a natural forest, the *K. celebica* population has limited due to logging and wood harvesting, and regeneration is merely limited due to infrequent flowering periods and fruiting. In addition, seed collection posed some problems, as seeds have a hard coat, thus poor viability and germination. One vegetative propagation that should be done is cutting. This method is the strategy to produce many high qualities of seedlings and faster tree growth (Husen and Pal, 2007). Besides that, this is a valuable method to produce seedlings when seeds are limited. The propagation techniques depend on characteristics and plant type itself. Cutting propagation was applied to more plants species which improved tree yield, quality, and good seedlings in *Hopea gregaria* Slooten (Tuheteru *et al*., 2020), *V. paradoxa* (Yeboah et al. 2020), guava (Qadri *et al*., 2018), *Corchoorus sp*. (Alam *et al*., 2017), *K. celebica* Kosterm (Arif *et al*., 2015), *Eucalyptus pellita* F. Muell (Sulichantini *et al*., 2014), *E. ganitrus* (Rahman and Rohandi, 2012).

In order to accelerate and increase the rooting and growth of cuttings, the use of hormones is required. Hormones are chemical compounds synthesized into the plant tissues to support the roots and shoot development (Monteuuis, 2016), regulate and stimulate plant growth (Dunsin *et al*., 2016). It can be produced in the growing organ of the plant and meristematic tissues (endogenous), and some are synthetic hormones or growth regulator substances (exogenous). Growth regulator hormone also contains auxin that would improve the division and elongation of cells. Thus it will accelerate roots formation (Choi *et al*., 2000; Truemand and Richardson, 2008; Fadli *et al*., 2017; Mabizela *et al*., 2017).

Synthetic hormones (exogenous hormones) are also known as growth regulator substances, for example rootone-f, which contains active compounds such as NAA, NAD, and IBA as well as thiram (Sudomo *et al.,* 2013). Rootone-f is a synthetic hormone that plays an essential role in rooting and growth regulation. It is beneficial to stimulate root growth and promote plant root initiation. Rootone-f, a growth regulator, is very active in accelerating initial roots formation and provides a better root length. The growth increased because rootone-f has several elements that can encourage growth and are more stable than other hormones. Tuheteru et al. (2020) proved that rootone f increased the number of secondary roots of *H. gregaria*. A study on using rootone-f to enhance the rooting and growth of *K. celebica* shoots cuttings is not recorded yet. Therefore, this research aimed to determine the effect of rootone-f on increasing the rooting and growth of *K. celebica* cuttings.

MATERIAL AND METHODS

Materials and tools

Two years *K. celebica* seedling collected from Tanggetada district, Kolaka Regency was cut its shoots with the height of about 10 cm, rootone f- PT Rhone-Poulence Agrocard (a commercial product of synthetic hormone for rooting stimulator), rice husk charcoal, sterilized fine sand, and cow manure as growth media, a tray for cutting growing, cutting scissors, electrical scale, oven, digital thermometer and hygrometer, transparent plastic and styrofoam for covering (to maintain humidity). The cover was created from styrofoam with 80 cm length x 70 cm width, line height in the middle was 25 cm, and both sides of 20 cm in height.

Preparation and cuttings planting

Shoots were cut from stocks of seedlings using sharp scissors, approximately 1 cm below its node. Then, it was soaked immediately in water to keep them fresh. Leaves were removed from the seedling in approximately ¼ parts to reduce transpiration. Rootone f solution was applied on the cutting base using dipped method for 10 minutes. Next, cuttings were planted into growth media in a tray (sterilized sand: manure: rice husk charcoal : 2: 1: 1 v/v) (Arif *et al*., 2015). In which every tray contained ten cuttings. Trays were put and arranged on benches randomly according to the randomized block design in the greenhouse of Indonesia Mycorrhiza Association branched Kendari Indonesia. Each tray was covered using transparent plastic to maintain humidity and avoid dryness. Cuttings were grown for two months, and the environmental condition recorded was about 29.8^{o}C for an average minimum temperature and 33.87^{o}C for an average maximum temperature. For maintenance, cuttings were poured with water using the sprayer one time a day or depending on the humidity (humidity maintained about ± 90%), and weeds were removed manually.

Experimental design

The experimental design used was Randomized Block Design (RBD), which consisted of untreated cuttings/ control, 100 ppm rootone-f, 200 ppm rootone-f, and 300 ppm rootone-f solution, and each treatment was repeated three times. Each treatment consisted of ten cuttings, and thus, the total cuttings were 120. Cuttings were grown in the greenhouse of the Indonesia Mycorrhiza Association branch Kendari, Southeast Sulawesi, Indonesia.

Data Collection

Parameters measured were the number of primary and secondary roots, which were manually counted, roots length, leaf area, shoot number, shoots, and roots dry weight. Shoots and roots dry weight were determined after drying them using an oven with temperatures of 70 ºC for 2 x 24 hours, then balanced with electrical balance. Measurements of data were conducted at the laboratory of the Forestry Department, Forestry and Environmental Science Faculty, Halu Oleo University. Additional data such as temperatures and humidity were also collected and measured using a digital thermometer and hygrometer.

Measurement of roots length

The roots length was calculated using *Grid Intersect Method* (Rowell, 1995) with the formula:

$$R = \lambda \times N,$$

where:
R: roots length;
λ=0.786 (grid 1 cm);
N: number of roots intersection with gridline

Data analysis

Data were analyzed using a one-way analysis of variance (ANOVA). Comparisons of means were done using Least Significant Differences (LSD) Test at the 5% probability level when the F values were significant. All statistical analyses were conducted using SAS 9.1.3 portable statistical software (Mattjik and Sumertajaya, 2002).

RESULTS AND DISCUSSION

The results showed that rootone f improved the rooting and growth of shoots cutting of *K. celebica* aged eight weeks. Rootone f treatments significantly affected the number of primary and secondary roots, roots length, shoot number, leaf area, shoots, and roots dry weight. Data showed that maximum rooting was produced by rootone f treated cuttings. In spite of rooting was also observed on untreated cuttings, but growth was lowest. Based on the LSD test, 200 and 300 ppm treatments were more and similarly effective than others (Table 1). Treatments of 200-300 ppm were increased about seven times on primary roots number, thirteen times on secondary roots number, and nine to fourteen times on roots length, respectively, than control.

Table 1. Effect of treatments on rooting growth of *K. celebica* cuttings after 8 weeks

Rootone-F (ppm) Treatments	Number of primary roots	Pi (%)	Number of secondary roots	Pi (%)	roots length (cm)	Pi (%)
Untreated	0.60±0.256 c	-	2.07±1.112 b	-	1.0±0.577 c	-
100	2.07±0.646 b	245	10.03±2.723 b	385	3.83 ± 1.123 bc	284
200	4.87±0.649 a	711	30.03±5.636 a	1353	10.35 ± 1.967 ab	939
300	5.07±0.719 a	745	29.73±5.136 a	1338	15.01±2.999 a	1407
Pr>F	**		*		*	

Average values followed by unequal letters in the same column were significant differences at the 0.05 LSD test level. Percentage of increasing (Pi), significant (*), very significant (**)

The use of rootone f also improves the growth of cutting shown in table 2. Treatments of rootone f 200 and 300 ppm increase shoot number and leaf area at eight weeks. Treatments of rootone f 300 ppm increased shoot number, which was different from other treatments. In the leaf area, treatments of 200 and 300 ppm rootone f were more and similarly effective in stimulating the leaf area. In contrast, untreated cuttings (control) were the poorest treatments that differed from others. Treatment of 300 ppm increased shoots number about six times than control, while treatment of 200 ppm improved leaf area about four times than control (Table 2).

Table 2. Effect of Rootone F treatments on shoots growth (number of shoots and leaf area) of *K. celebica* cuttings, after 8 weeks

Rootone-F (ppm) Treatments	Shoots number	Pi (%)	Leaf area (cm^2)	Pi (%)
Untreated	0.07± 0.046 c	-	0.81±0.357 b	-
100	0.23± 0.078 b	250	2.42±0.234 ba	200
200	0.33± 0.087 b	400	4.95±0.305 a	514
300	0.50±0.114 a	650	4.10±0.390 a	408
Pr>F	**		*	

Average values followed by unequal letters in the same column were significant differences at the 0.05 LSD test level. Percentage of increasing (Pi), significant (*), very significant (**)

Better growth was also presented by treatments of 200 and 300 ppm rootone f on the dry weight. It is shown that the treatment of 200 ppm is the best treatment with increasing shoots and roots dry weight, but no significant differences with 300 ppm treatment. In contrast, untreated cuttings (control) produced the lowest value (Table 3).

Table 3. Effect of Rootone f treatments on plant dry weight *K. celebica* cuttings after 8 weeks

Rootone-F (ppm) Treatments	Shoots dry weight (g)	Pi (%)	Roots dry weight (g)	Pi (%)
untreated	0.116±0.011 b	-	0.001±0.0005 c	-
100	0.174±0.015 b	49	0.006±0.001 b	408
200	0.258±0.020 a	120	0.014± 0.002 a	1106
300	0.257±0.24 a	119	0.013±0.002 a	1012
Pr>F	**		**	

Average values followed by unequal letters in the same column were significant differences at the 0.05 LSD test level. Percentage of increasing (Pi); significant (*); very significant (**)

There were significant differences in the number of primary and secondary roots, roots length, shoot number, leaf area, and plant dry weight due to the different treatments applied in the rooting of *K. celebica* cuttings. Rootone-f, as a growth regulator substance, stimulates and accelerates roots growth. The effect would be better when using the proper hormone concentration and suitable for plant species. This experiment showed that the addition of 200-300 ppm treatments produced better rooting and growth. It stimulated elongation and cell growth, thus increasing roots and shoot growth of *K. celebica* cuttings.

According to Small and Degenhardt (2018), hormones can enhance cell division and development of cells, including the structure and functions. Giving hormone in an optimal concentration will stimulate the growth and development of the roots (Akhtar *et al*., 2015; Okao *et al*. 2016; Maggioni *et al*., 2020). In addition, there was a correlation between endogenous auxin content and the ability of cuttings to form rooting (Henselova *et al*., 2002). Thankamani *et al*. (2020) also noticed that auxin could increase the activity of meristematic tissues and carbohydrates transport to the base of cuttings, thus improving the rooting. The presence of roots will give better growth for plants. Roots are crucial parts of a plant that play essential roles in soil nutrients and water uptake. In which nutrients and water supply are translocated to the leaves, which are involved in plant metabolism activities such as photosynthesis to produce carbohydrates (Lambers *et al*., 2008). In line with some research, *Duabanga mollucana* Blume cuttings (Supriyanto and Prakasa, 2011), *Anthocephalus cadamba* (Putra *et al*., 2014), and *H. gregaria* (Tuheteru *et al*. 2020) better rooting and growth was also achieved when cutting were treated with rootone f. Similarly, Sudomo *et al*. (2013) found that using rootone f 100 ppm increased shoots, roots length, and the number of roots on *Manglietia glauca* BI at three months old. Furthermore, cutting material taken from the juvenile seedling of *K. celebica* has produced better rooting. Danu *et al*. 2011 found that shoots cutting material obtained from seedling gave the highest survival than obtained from the young tree or mature tree.

Figure 1. Cuttings of *K. celebica* after soaked into rootone-f solution based on treatments, planted on media and covered with transparent plastic

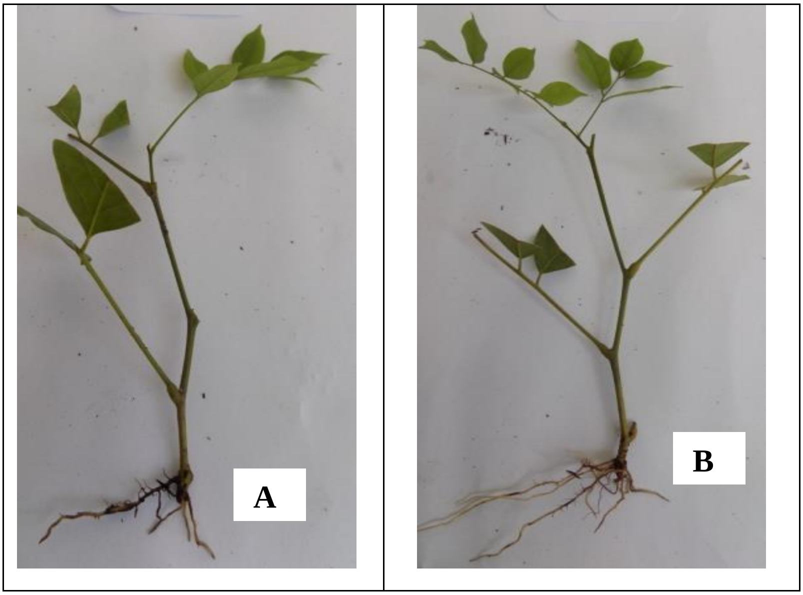

Figure 2. Appearance of *K. celebica* cuttings after 8 weeks of growth.
A: 200 ppm and B: 300 ppm of rootone-f

In contrast to untreated cuttings, the rooting and growth were the lowest. It was assumed that internal hormone is not adequate to promote the development of roots. According to Rahayu & Riendriasari (2016) that the sea bidara plant did not affected by rootone-f application (exogenous auxin) due to the adequacy of endogenous auxins. However, a high dose of the hormone also can bring adverse effects. This case was proved by Truemand and Richardson (2008) found that the highest amount of 8 g IBA/ kg powder caused leaf abscission and reduced leaf area or shoot dry weight on *C. torreliana* and *C. citriodora*. High concentrations of hormones have a negative impact, like oxidative stress, that effected in death of cells (Flasinski and Hac-Wydro, 2014).

Cuttings achieved the highest shoots number, leaf area and plant dry weight when applied 200-300 ppm of rootone-f. Rootone f stimulates cell division, resulting in growth and increased shoots number and leaf area. It will impact the rate of photosynthesis. An increase in growth will occur, indicated by an increase in plant dry weight. Enhancing the leaf area will also improve stomata for CO_2 fixation, and then the CO_2 assimilation rate would be better. Chlorophyll concentration also would be enhanced as increasing of the leaf area. Lambers *et al*. 2008 also noticed that adequate absorbed light was caused by improving leaf surface and chlorophyll concentration. Therefore, the photosynthetic rate would be increased, and the production of carbohydrates would be sufficient for the growth of roots and shoots. Devi et al. 2016 found that there was rising in leaves number (18.74), leaf area (3.76 cm^2), and content of chlorophyll (39.76%) of *Grewia asiatica* cuttings when treated with IBA 300 ppm and highest than other treatments. In addition, the presence of bud and shoots on cuttings, including meristematic tissues, will stimulate the production of hormones (Small and Degenhardt, 2018) and then circulate to the bottom or basal to form the roots.

Efforts to conserve *K. celebica* have been carried out, such as planting on gold mining land and propagation through root cuttings, seed germination, and shoot cuttings. The obstacle faced in supporting conservation efforts is the shortage of seedlings for planting. For this reason, shoot cuttings are a solution to overcome the problem of limited seeds by providing seedlings from cutting for planting in the field.

CONCLUSIONS

Application of Rootone-f has improved rooting and growth of *K. celebica* cuttings aged eight weeks. Using rootone-f as a growth regulator at concentrations of 200 ppm has been more efficient and could be considered to support *K. celebica* propagation and conservation program. The success of shoots propagation for *K. celebica* will provide the primary practice of *K. celebica* cultivation, support bypassing the juvenile stage, and contribute to conservation efforts for endemic and threatened tree species.

ACKNOWLEDGEMENTS

The authors are grateful to Ministry of research, Technology, and Higher Education Indonesia for providing financial assistance to carry out this work. We also thank to Liam Trethowan for improving the manuscript.

REFERENCES

Alam, M.A., Mollah, M.A.F., Rafiq, Z.A., Sarker, M.S.A, Rony, M.N.H., & Tareq, M.Z. (2017): Effect on plant age for cuttings on the growth and seed yield in late season jute under different planting spacings. *Journal Expt. Bioscience* 10(2): 1-8.

Akhtar, G., Akram, A., Sajjad, Y., Balal, R.M., Shahid, M.A., Sardar, A., Naseem, K., & Shah, S.M. (2015): Potential of growth plant regulators on modulating rooting of *Rosa centifolia*. *American Journal of Plant Science* 6(5): 659-665.

Arif, A., Tuheteru, F.D., & Husna. (2015): The concervation of endemic and endangered species of kalapi (*Kalappia celebica* Kosterm) through cuttings propagation and AMF potential assessment. pp 53-65.Proceedings ICSD, Universitas Mahasaraswati Press. Bali.

Arif, A., Tuheteru, F.D., Husna, Kandari, A.M., Mekuo, I.S., & Masnun. (2016). Status and culture of arbuscular mycorrhizal fungi isolated from rhizosphere of endemic and endangered species of kalapi (*Kalappia celebica* Kosterm). *European Journal Sustainable Development* 5(4): 395-402.

Arif, A. & Uslinawaty, Z. (2017): Pembangunan kebun pangkas dan teknik perbanyakan pupuk hayati fungi mikoriza dalam mendukung konservasi jenis terancam punah kalapi (*Kalappia celebica* Kosterm), University of Halu Oleo, Kendari. (Research Report)

Choi, B.J., Sang, C.K., & Choi, E.J. (2000): Effect of rooting promoters and light intensity on rooting and root growth of rose cuttings, *Horticultural science and Technology* 18(6): 815-818.

Darma, I.D.P., & Priyadi, A. (2019): Perbanyakan *Dacrycarpus imbricatus* (Blume) De Laub. dengan biji di Kebun Raya “Eka Karya” Bali, *Jurnal Hutan Tropis* 7(3): 310-316

Danu, A., Subiakto, & Abidin, A.Z. (2011) Pengaruh umur pohon induk terhadap perakaran stek nyamplung (*Calophyllum inophyllum* L.), *Jurnal Hutan Tanaman* 8(1).

Devi, J., Bakshi, P., Wali, V.K., Kour, K., & Sharma, N. (2016): Role of auxin and dates of planting on growth of cuttings raised plantlets of phalsa (*Grewia asiatica* L.). *The Bioscan* 11(1): 535-537.

Dunsin, O., Ajiboye, G., & Adeyemo, T. (2016): Effect of alternative hormones on rootability of *Parkia biglobosa*. *Journal of Scientia Agriculturae* 13(2): 113-118.

Fadli, A., Attaoui, A.E., Chetto, O., Boudoudou, D., Talha, B.A., Benkirane, R., & Benyahia, H. (2017): Propagation of citrus rootstocks by stem cutting using auxin pretreatments: the case of citrumello (*Citrus paradisi* Macf and *Poncirus trifoliate* (L.) Raf.). *Journal of materials and environmental sciences* 8(11): 4085-4093.

Flasinski, M., & Hac-Wydro, K. (2014): Natural vs synthetic auxin: studies on the interactions between plant hormones and biological membrane lipids. *Environ. Res*. 133, 123-134.

Henselova, M., Lux, A., & Masarovicova, E. (2002): Effect of growth regulators on rooting cuttings of Karwinskia species under in vivo condition. *Journal of Rostlinna Vyroba* 48(10): 471-476.

Hendalastuti, H.R., Subiakto, A., Siregar, I.Z., & Supriyanto. (2010): Uji pertumbuhan stek cemara Sumatra (*Taxus sumatrana* (Miguel) de Laub. Cuttings). *Jurnal Penelitian Hutan dan Konservasi Alam* 7(3): 289-298.

Husen, A., & Pal, M. (2007): Effect of branch position and auxin treatment on clonal propagation of *Tectona grandis* Linn. f. *Journal of New Forest* 34(3): 223-233.

IUCN. (2022): The IUCN red list of threaten species, *Kalappia celebica* Kosterm, version 2021-3. (available at https://www.iucnredlist.org)

Lambers, H., Chapin III, F.S., & Pons, T.L. (2008): Plant physiological ecology. Springer. 604 pp.

Mardiastuti, A., Kusrini, M.D., Mulyani, Y.A., Manullang, S., & Soehartono, T. (2008): Permenhut No. P.57/Menhut-II/2008 tentang arahan strategis konservasi spesies nasional 2008-2018. Penerbit Direktorat Jenderal Perlindungan Hutan dan Konservasi Alam

Mattjik, A.A., & Sumertajaya, I.M. (2002): *Perancangan percobaan dengan aplikasi SAS dan Minitab*. Penerbit IPB Press.

Maggioni, R.A., Vieira, L.M., Invernizzi, S.F., Carpanezzi, A.A., & Zuffellato-Ribas, K.C. (2020): Germination potential and vegetative propagation of *Aegiphila brachiata* Vell. *Verne* 26(2): 222-231.

Mabizela, G.S., Slabbert, M.M., Bester, C. (2017): The effect of rooting media, plant growth regulators and clone on rooting potential of honeybush (*Cyclopia subternata*) stem cuttings at different planting dates. *South African Journal of Botany* 110: 75-79.

Monteuuis, O. (2016): Micropropagation and production of forest tree. *In* Park, Y.S., Bonga, J.M., Moon, H.K., eds. *Vegetatif propagation of forest tree,* National Institute of Forest Science (NIFoS). p 32-55 Seoul, Korea.

Okao, M., Ogwal, L., Mutoni, G., Alip, S.O., Okullo, J.B.L., & Okia, C.A. (2016): Effect of mode of auxin application on rooting and bud break of shea tree (*Vitellaria* paradoxa) cuttings. *American Journal of Plant Sciences* 7(15): 2199-2208.

Putra, F., Indriyanto, & Riniarti, M. (2014): Keberhasilan stek pucuk jabon (*Anthocephalus cadamba*) dengan pemberian beberapa konsentrasi rootone f. *Jurnal Sylva Lestari* 2(2): 22-40.

Qadri, R., Azam, M., Khan, S.B., Khan, I., Haq, I.U., Yang, Y., Muzammil, M.J., Ghani, M.A., & Moazzam, M. (2018): Growth performance of guava cutting under different growing media and plant cutting taking height. *Bulgarian Journal of agriculture science* 24(2): 236-243.

Rahman, E., & Rohandi, A. (2012): Keberhasilan stek pucuk ganitri (*Elaeocarpus ganitrus* Roxb.) pada aplikasi antara media tanam dan hormon tumbuh. *Jurnal Penelitian Hutan Tanaman* 9(4): 219-225.

Rahayu, A.A.D. & Riendriasari, S.D. (2016): Pengaruh beberapa jenis zat pengatur tumbuh terhadap pertumbuhan stek batang bidara laut (*Strychnos ligustrina* Bl.) *Jurnal Perbenihan Tanaman Hutan*, 4(1): 25-31.

Rowell, D.L. (1995): *Soil Science*. Methods and application. Longman Scientific and Technical, Essex, UK.

Small, C.C., & Degenhardt, D. (2018): Plant growth regulators for enhancing revegetation success in reclamation: a review. *Ecological engineering* 118: 43-51

Sudomo, A., Rohandi, A., & Mindawati, N. (2013): Application of rootone f growth regulator substance on manglid cutting (*Manglietia glauca* BI). *Jurnal penelitian hutan tanaman* 10(2): 57-63.

Sulichantini, E.D., Sutisna, M., Sukartiningsih, & Rudiansyah. (2014): Clonal propagation of two clones *Eucalyptus pellita* F. Muell by mini cuttings. *International journal of science and engineering* 6(2):117-121.

Susilowati, A., Kholibrina, C.R., Rachmat, H.H, Elfiati, D., Aswandi, & Raeni, I.M. (2018): Short Communication: Macropropagation-an important tool for conservation of North Sumatran endangered tree species, *Dryobalanops aromatica*. *Biodiversitas* 19(5):1672-1675.

Supriyanto, & Prakasa, K.E. (2011): The effect of rootone-f plant growth regulator on the growth of *Duabanga mollucana* Blume cuttings. *Jurnal Silvikultur Tropika* 3(1): 59-65.

Thankamani, C.K., Prathyusha, K., Hamza, S., & Kandiannan, K. (2020): Enhancement of rooting and growth of bush pepper by jeevamruthum and tender coconut water. *Journal of plantation crop* 48(2):146-149.

Trethowan, L.A., Arif, A., Clark, R.P., Girmansyah, D., Kintamani, E., Prychid, C.J., Pujirahayu, N., Rosmarlinasiah, Brearley, F.Q., Utteridge, T.M.A., & Lewis, G.P. (2019): An enigmatic genus on an enigmatic island: the rediscovery of Kalappia on Sulawesi. *Ecology* 100(11): 1-4.

Truemand, S.J., & Richarson, D.M. (2008): Relationships between indole-3 butyric acid, photoinhibition and adventitious rooting of *Corymbia torelliana*, *C. citriodora* and F1 hybrid cuttings. *Tree and Forestry Science and Biotechnology* 2(1): 26-33.

Tuheteru, F.D., Arif, A., Husna, Basrudin, Albasri, & Danar. (2020): Keberhasilan stek pucuk pooti (Hopea gregaria Slooten) dengan pemberian rootone f. *Jurnal Perbenihan Tanaman Hutan* 8(1):25-32.

Whitmore, T.C., Tantra, I.G.M., & Sutisna, U. (1989): Tree flora of Indonesia check list for Sulawesi. Forest Research and Development Centre, Forestry of Department. Bogor.

Yeboah, J., Segbefia, M.A.D., Dadzie, A.E., Padi, F., Lowor, S.T., Agene, F.N., Owusu-Ansah, F., & Owusu-Ansah, B. (2020): Cuttings propagation of shea (*Vitellaria paradoxa* C.F. Gaertn) tree using shoot types and application of auxin. *Journal of Agriculture Science* 12(12): 213-220.

Cuong, L., Thang, B., Bolanle-Ojo, O.T., Bao, T., Tuan N., Sang T., Xu, X., Thanh, N. (2022): Enhancement of soil organic carbon by Acacia mangium afforestation in Southeastern region, Vietnam. Agriculture and Forestry, 68 (2): 133-155. doi:10.17707/AgricultForest.68.2.10

DOI: 10.17707/AgricultForest.68.2.10

Levan CUONG [1], Buivan THANG [2], Oluwasanmi Tope BOLANLE-OJO [2,3], Tranquang BAO [1], Nguyenthanh TUAN [1], Tranvan SANG [4], Xiaoniu XU [2]*, Nguyenminh THANH [1]*

ENHANCEMENT OF SOIL ORGANIC CARBON BY *ACACIA MANGIUM* AFFORESTATION IN SOUTHEASTERN REGION, VIETNAM

SUMMARY

The knowledge about dynamics of soil organic carbon (*SOC*) accumulation and its controls are critical in understanding of the C cycling in forest ecosystems. *Acacia mangium* Willd. is one of the most important fast-growing afforestation tree species in Vietnam, providing significant ecological, economic, environmental, and social benefits. The existing studies offered information limited on the distribution and regulation of *SOC* in the *A. mangium* plantations. The primary purpose of this study was to explore the variation trend of *SOC* and its driving factors in an age-sequence of three *A. mangium* plantation stands in Changriec Historical - Cultural Forest, Southeastern region, Vietnam. The study was conducted to estimate *SOC* content and storage, and soil physicochemical characteristics of three different–aged (4–, 7–, 11–year–old stands) *A. mangium* plantations. The *SOC* content increased significantly from young to older stand, and its maximum concentration occurred in the topsoil layer and decreased continually with increasing soil depth. The *SOC* stocks increased significantly with the stand age. The *SOC* stocks showed obvious surface aggregation, with more than 60% of *SOC* distributed in the soil of 0–30 cm depth. The soil total nitrogen content and soil texture (i.e., soil silt content) were identified as the major factors controlling the *SOC* distribution. The other parameters (i.e., plant biomass, soil *pH*, bulk density, available nitrogen, total phosphorus, available phosphorus, total potassium, and available potassium) also significantly influenced the distribution of *SOC*. These findings suggest that afforestation with *A. mangium* can facilitate *SOC* accumulation, improve soil nutrient regimes, and

[1]Levan Cuong, Tranquang Bao, Nguyenthanh Tuan, Nguyenminh Thanh, Faculty of Forestry, Vietnam National University of Forestry, Hanoi 100000, Vietnam

[2]Xiaoniu Xu (*Corresponding author: xnxu2007@ahau.edu.cn), BuivanThang, Oluwasanmi Tope Bolanle-Ojo, School of Forestry & Landscape Architecture, Anhui Agriculture University, Hefei 230036, Anhui, China

[3]Oluwasanmi Tope Bolanle-Ojo, Forestry Research Institute of Nigeria, P.M.B. 5054, Ibadan, Nigeria

[4]Tranvan Sang, Institute of Ecology and Works Protection, Vietnam Academy for Water Resources, Hanoi 100000, Vietnam

Notes: The authors declare that they have no conflicts of interest. Authorship Form signed online.

Recieved:20/12/2021 *Accepted:04/05/2022*

provide a new insight in understanding the factors controlling *SOC* in the Southeastern region of Vietnam.

Keywords: *Acacia mangium* plantations, Soil organic carbon, Environmental variables, Age-sequence, Vietnam

ABBREVIATIONS USED: *SOC* (soil organic carbon); *CS* (soil organic carbon storage); *DBH* (diameter at breast height); *H* (height); *TAGB* (total above-ground biomass); *TBGB* (total below-ground biomass); *BD* (bulk density); *TN* (total nitrogen); *TP* (total phosphorus); *TK* (total potassium); *AN* (available nitrogen); *AP* (available phosphorus); *AK* (available potassium).

INTRODUCTION

Soil is the largest terrestrial organic carbon (C) pool, holds three times as much C as the vegetation C pool and twice as much as the atmosphere (Batjes, 1996; Lal, 2004; Carvalhais *et al*., 2014). Soil C in the Forest ecosystem is a crucial part of the global C reservoir, containing 73% of the global *SOC* pool (Sombroek *et al*., 1993; Six *et al*., 2002b). Thus, minor changes in the C reservoir of forest soil will dramatically influence the global C balance, which impacts global climate change (Albaladejo *et al*., 2013). The *SOC* is principally determined by the balance between C inputs through litterfall and root turnover and loss of C primarily through organic matter decomposition, which processes are controlled by various environmental variables, including vegetation biomass (Wang *et al*., 2013; Zhang *et al*., 2018) and soil physicochemical properties such as soil *N* (Batjes, 1996; Cong *et al*., 2016), soil texture (Jobbágy and Jackson, 2000; Liu *et al*., 2016), soil *P* (Zu *et al*., 2011; Deng and Shangguan, 2017), soil *K* (Zu *et al*., 2011; Zhang *et al*., 2016), soil *pH* (Robson and Foy, 1990; Thomas, 1996; Chen *et al*., 2004), and soil *BD* (Hobley *et al*., 2015; Ngaba *et al*., 2020). Hence, understanding the *SOC* storage dynamics and the factors that control this process in forest ecosystems is critical for better C budget management and climate change mitigation options.

To date, studies on *SOC* content or storage following afforestation and stand age have been widely carried out worldwide, and showed contradictory results. Some scholars presented that the *SOC* decreased in the early stage of afforestation and then gradually increased with stand age (Pregitzer and Euskirchen, 2004; Zhaodi *et al*., 2018). Whereas others showed an increasing *SOC* in the early period after afforestation followed by a gradual decrease (Ali *et al*., 2019; Zhang *et al*., 2019), a stable *SOC* after afforestation (Simon *et al*., 2012), or no significant increase with stand development (Matthias and Arain, 2006; Yue *et al*., 2018). Nonetheless, according to most researches, *SOC* significantly increased with forest age (Cheng *et al*., 2015; Deng *et al*., 2017; Zhang *et al*., 2018). One possible interpretation to this discrepancy is that, in addition to stand age, several other factors impact *SOC* accumulation, such as tree species, forest types, climate conditions, soil physicochemical characteristics, and former land use (Smal and Olszewska, 2008; Noh *et al*., 2010).

Acacia mangium Willd. is one of the most principal afforestation tree species in some of the eight important forestry-ecological regions and Southeastern region in Vietnam (MARD, 2018), where it has been planted on more than 800,000 ha and comprises approximately 19% of all forested plantation areas in Vietnam (MARD, 2020). Its wood is suitable for the production of pulps, timbers, and household furniture (MARD, 2018). Besides producing woods for industries, *A. mangium* plantations also have a crucial role in providing environmental services such as C uptake and storage given by its high growth rate. Thus, a better knowledge of *SOC* dynamics of *A. mangium* plantations is of great importance in the accurate prediction of soil C storage and its influence on future climate change and forest management. Although there is abundant studies in *A. mangium* forests; growth and yield prediction (Shah Newaz and Millat-e-Mustafa, 2004), biomass accumulation and C storage (Hai *et al*., 2009; Lee *et al*., 2015; Cuong *et al*., 2020), wood properties (Jusoh *et al*. 2014), soil nutrients (Lee *et al*. 2015, Matali and Metali, 2015), biological N fixation (Lydie-Stella *et al*., 2017), and benefits and threats on biodiversity (Koutika and Richardson, 2019). Nevertheless, existing knowledge and studies have offered limited information on the distribution of *SOC* and its influencing factors in an age-sequence of *A. mangium* plantation forests, particularly in the Southeastern region of Vietnam. Therefore, the present study was designed to examine the *SOC* content and storage in an age-sequence of three *A. mangium* plantation stands (4-, 7-, and 11-years-old) in Southeastern region, Vietnam. The specific purposes of the study were to: (i) quantify the *SOC* content and stocks; and (ii) identify the controlling parameters of *SOC* variation in *A. mangium* plantations across three different ages in the Southeastern region. Our findings can strengthen understanding of C sink management in *A. mangium* forest soils and provide new insight into the unique relationship between *SOC* and influential environmental factors (i.e. plant biomass and soil physicochemical properties).

MATERIAL AND METHODS

Study site description

The study was conducted at the Chang Riec Historical - Cultural Forest (11°00′30″ to 11°35′13″N and 106°00′00″ to 106°07′10″E), located in Tay Ninh Province, Southeastern region, Vietnam (Figure 1). The study area has two distinct seasons: the dry season (December to April) and the rainy season (May to November). The annual mean temperature is 26.9°C with a yearly range of 25.2°C to 28.8°C. The annual mean precipitation is 1967 mm with average rainy days of 155 days (IBST, 2009). This study area terrain is relatively flat, with an altitude of 29-67 m a.s.l. and slopes of 3-5°. Soil type in this region is mainly grey-brown, developed on ancient alluvium, and soil depth over 100 cm. Soil's texture is loam (Cuong *et al*., 2020). The dominant tree species of the area consist of *A. mangium* Willd., *Acacia hybrid (Acacia auriculiformis* A. Cunn. ex Benth. × *A. mangium* Willd.*)*, *Dipterocarpus obtusifolius* Teijsm. ex Miq., *Tectona grandis* L.f., *Hopea* spp., and *Khaya senegalensis* (Desv.) A.Juss.. The plantation forests are composed of about 40% of the total forest area. *A. mangium* amounts to approximately 20% of the total plantations in this region and plays an important role in pulp and timber production. In this study, we selected three differently aged (4-, 7-, 11-years) *A. mangium* plantations, which were all covered by previous Cassava (*Manihot esculenta* Crantz) before afforestation. Additionally, no fertilization was applied after afforestation. The initial density of the experimental stands were 1000 trees·ha^{-1} (initial spacing, 4 m × 2.5 m), and thinning operations were carried out once, twice, and three times for the 4-, 7-, and 11-year-old stands, respectively. The diversity, healthy, and abundance of understory vegetation in the *A. mangium* plantations were found, particularly in the 7- and 11-year-old stands. The dominant species of understory vegetation in the *A. mangium* plantations include *Mallotus apelta* (Lour.) Müll. Arg., *Tetracera scandens* (L.) Merr., *Chromolaena odorata* (L.) R.M. King & H. Rob., *Saccharum arundinaceum* (Retz.), *Mimosa pudica* var. *tetrandra* (Willd.) DC., *Chrysopogon aciculatus* (Retz.) Trin., *Maesa perlarius* (Lour.) Merr., *Lygodium microphyllum* (Cav.) R. Br., *Dryopteris parasitica* (L.) Kuntze, *Helicteres angustifolia* var. *obtusa* (Wall. ex Kurz) Pierre, and *Cynodon dactylon* (L.) Pers (Cuong *et al*. 2020).

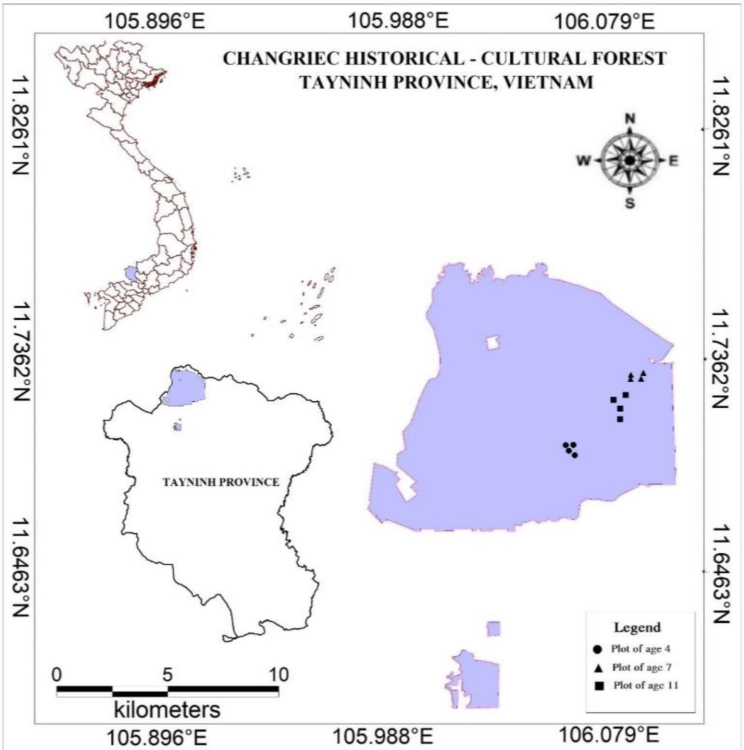

Figure 1. Map of experimental plots in Changriec Historical - Cultural Forest (Tayninh Province, Southeastern region, Vietnam)

Biomass estimation

Four plots of 40 m × 25 m were established in each *A. mangium* stands in February to April 2019 (Figure 1). The detailed descriptions of the study site and biomass estimation were given by Cuong *et al*. (2020) and is reproduced in Table 1.

Table 1. Biomass characteristics of *Acacia mangium* plantations at different stand ages

Measured variables			Stand age (years)		
			4	7	11
Plants		Stand area (ha)	2.6	2.2	3.6
		Mean *DBH* (cm)	13.78 ± 0.38^a	17.94 ± 0.86^b	21.78 ± 0.85^c
		Mean *H* (m)	14.72 ± 0.17^a	17.29 ± 0.56^b	18.60 ± 0.21^c
		Stand density (tree· ha^{-1})	888 ± 30^a	728 ± 22^b	610 ± 29^c
		Canopy density	0.83 ± 0.01^a	0.81 ± 0.01^b	0.79 ± 0.03^b
		Elevation (m a.s.l.)	38	40	40
		Soil depth (cm)	>100	>100	>100
	Above-ground biomass	Trees (Mg· ha^{-1})	55.08 ± 3.98^a	109.18 ± 4.44^b	175.17 ± 5.11^c
		Understory (Mg· ha^{-1})	4.05 ± 0.05^a	4.31 ± 0.05^b	4.80 ± 0.11^c
		TAGB (Mg· ha^{-1})	59.13 ± 3.98^a	113.49 ± 4.46^b	179.96 ± 5.07^c
	Below-ground biomass	Trees (Mg· ha^{-1})	17.64 ± 0.68^a	34.38 ± 1.43^b	35.40 ± 1.87^b
		Understory (Mg· ha^{-1})	0.82 ± 0.02^a	0.92 ± 0.02^b	1.19 ± 0.02^c
		TBGB (Mg· ha^{-1})	18.46 ± 0.67^a	35.30 ± 1.41^b	36.59 ± 1.87^c
		Litter biomass (Mg· ha^{-1})	11.43 ± 0.91^a	11.90 ± 0.55^{ab}	13.29 ± 1.16^b

Note. Values are means ± standard deviations (SD). *DBH*, diameter at breast height (1.3 m); *H*, tree height; *TAGB*, total above-ground biomass; *TBGB* total below-ground biomass. Means in a row, different lower-case letters are significantly different at $p<0.05$

Soil sampling and laboratory analysis

Five soil profiles were dug to a depth of 50 cm from the four corners and the center of each sample plot, and the samples were taken from four depths (0-10, 10-20, 20-30 and 30-50 cm) using a soil corer (5 cm inner diameter). Soil samples from the same layer in the same plot were mixed in equal volume proportions, air-dried and stored at room temperature. Meanwhile, soil *BD* samples were collected from different soil layers using a stainless-steel cutting ring (volume of 100 cm^3). Soil samples were analyzed at the Centre of Forestry Research and Climate Change laboratory at the Vietnam National University of Forestry (VNUF). Soil *pH* was measured with a *pH* meter at a soil:water ratio of 1:2.5. Soil *BD* was determined by drying the core samples at 105°C until constant weight (Blake and Hartge, 1986), while the pipette method was employed to measure the soil texture and compute the percentage of clay (<0.002 mm), silt (0.002–0.02 mm), and sand content (0.02–2 mm) (Van Reeuwijk, 2002). *SOC* content was analyzed by the potassium dichromate oxidation (external heat applied) method (Nelson and Sommers, 1982). The contents of soil *TN*, *TP*, *TK*, *AN*, *AP*, and *AK* were analyzed according to the Vietnam National Standard methods (TCVN 6498:1999 - ISO 11261:1995; TCVN 8940:2011; TCVN

8660:2011; TCVN 5255:2009; TCVN 5256:2009; TCVN 8662:2011) adopted by Cuong *et al*. (2017) and Thanh & Cuong (2017b). The soil *TN* concentration was determined by the modified Kjeldahl method after digestion with a mixture of $C_7H_6O_3$ and H_2SO_4. The soil *TP* content was determined by the colorimetric method after digestion with $HClO_4$ and H_2SO_4. The soil *TK* concentration was analyzed using the flame photometer method after digestion with $HClO_4$ and HF. The concentration of soil *AN* was measured by the alkaline hydrolysis-diffusion method. The soil *AN* content was reduced to NH_3 after adding a NaOH solution, then the NH_3 was diffused and absorbed by H_3BO_3 solution and titrated using H_2SO_4 to calculate the soil *AN* content. The concentration of soil *AP* was estimated using the Olsen method (the soil *AP* was extracted using $NaHCO_3$ followed by measurement via the molybdenum antimony colorimetric method). The content of soil *AK* was measured using the flame photometer method after extraction with CH_3COONH_4.

Calculation of soil carbon storage

The C storage in each soil layer was computed according to *SOC* content, soil *BD* and sampled depth. Coarse fractions (>2 mm) were very rare in the soil samples. Thus, the following equation was used to calculate *CS* (Deng *et al*. 2017; Thanh and Cuong 2017a; Wang *et al*. 2019):

$$CS_i = SOC_i \times BD_i \times d_i \times 10^{-1} \quad (1)$$

where: CS_i, soil carbon storage in the soil layer i ($Mg \cdot C \cdot ha^{-1}$); *i* represents the 0–10 cm, 10–20 cm, 20–30 cm, and 30–50 cm soil layers; SOC_i, soil organic carbon concentration of the soil layer i ($g \cdot kg^{-1}$); BD_i, soil bulk density of the soil layer i ($g \cdot cm^{-3}$); and d_i, soil thickness of the soil layer i (cm).

Statistical analyses

The effects of plantation age, soil depth and their interactions on *SOC* content and stocks, and soil physicochemical properties in *A. mangium* plantations were analyzed by two-way analysis of variance (ANOVA). Comparisons of *SOC* content and stocks, and soil physicochemical properties among three plantations, and four soil depths were tested by one-way ANOVA followed by Fisher's Least Significant Difference (LSD) test ($p < 0.05$). Before ANOVA analyses, we conducted tests for normality and homogeneity of variance.

Pearson's correlation was applied to understand the relationships between *SOC* contents and environmental factors (e.g., *TAGB, TBGB*, litter, *BD*, *pH*, *TN*, *TP*, *TK*, *AN*, *AP*, and *AK*). The environmental factors that had high weighted factor loadings were obtained by reducing the dimension of environmental factors using Principal Component Analysis (PCA); the effect of a possible linear correlation between variables was also eliminated (Fan *et al*., 2018). It should be noted that only principal components (PCs) having eigenvalues greater than 1 and factors having highly weighted factor loading (i.e., those with absolute values for factor loading within 10% of the maximum value) were retained for Stepwise

Multiple Regression Analysis (SMRA) (Tian *et al*., 2016; Fan *et al*., 2018). The SMRA was conducted using the filtered factors as inputs to determine the major factors that influence *SOC*. In the present study, both data processing and statistical analyses were carried out using SPSS 25.0 (IBM Corp, 2017) and R 3.5.2 (R Core Team, 2018) software packages.

RESULTS

C content in the soil layer

The two-way ANOVA analysis revealed the *SOC* was significantly affected by stand age (p<0.001). Besides, soil layer (p<0.001) and the interaction between stand age and soil layer (p<0.001) resulted in a significant effect on *SOC* (Figure 2a). Statistically significant differences were observed among different aged stands of different soil layers for *SOC* values (p<0.05). The *SOC* concentration decreased significantly with an increase in soil depth irrespective of stand age (p<0.05). In 0-10 cm soil layer, *SOC* ranged from 12.70 to 21.90 g· kg^{-1}, which was much greater than that of the other soil depths (10–20, 20–30, and 30–50 cm). *SOC* concentration at all soil depths increased significantly with stand age (p<0.05).

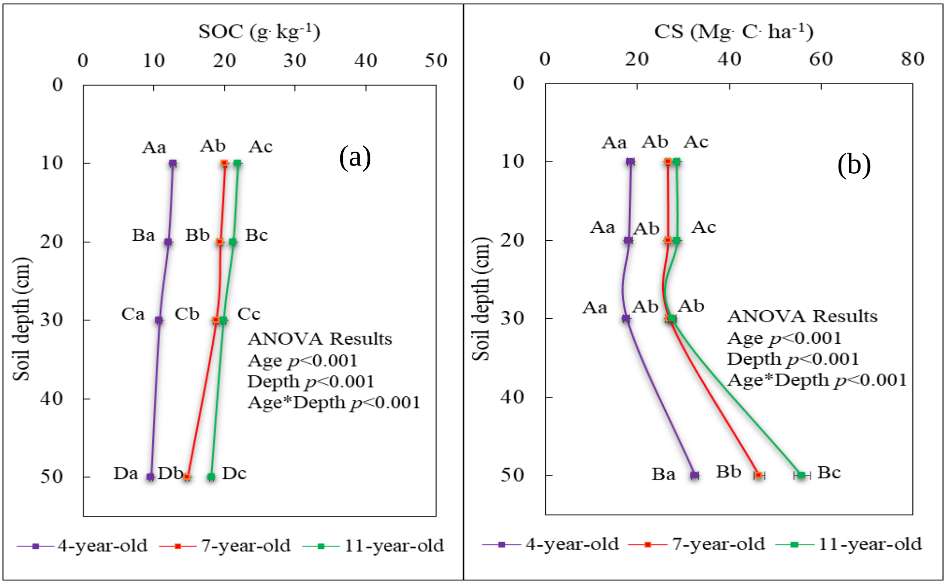

Figure 2. Variation of *SOC* (a) and *CS* (b) with stand age and soil depth. Error bars indicate standard deviation (SD). *Note*. *SOC*, soil organic carbon; *CS*, soil organic carbon stocks. Means with different uppercase and lowercase letters indicate significantly different between soil layers in the same stand ages and between stand ages in the same soil layers (p<0.05), respectively. Results (p-values) of two-way ANOVAs show the effect of stand age, soil depth and the interaction between stand age and soil depth on the *SOC* and *CS*

C storage in the soil layer

Figure 2b represents trends in the soil layer C stocks over an age-sequence of three *A. mangium* stands. Stand age (p<0.001) and soil layer (p<0.001) had significant influences on *CS*. Similarly, the interaction effect between stand age and soil depth demonstrated significant differences in *CS* (p<0.001). The *CS* of the 30-50 cm soil layer followed a significant increasing trend with the increase of stand age (p<0.05). Although the *CS* of the soil at 0–10 cm, 10–20 cm, and 20–30 cm increased with increasing forest age, the relationship was not significant. Summed *CS* from 0 to 50 cm soil depth was 86.86, 126.88, and 140.94 Mg· C· ha^{-1} in the 4-, 7-, and 11-year-old stands, respectively. The uppermost 30 cm of soil stocked a large proportion of C, and the *CS* in the 0–30 cm soil layer occupied 60.37%, 62.53%, and 63.33% of the total soil total C storage in the 0–50 cm soil layer for the three stands.

Basic soil physicochemical properties

There was a significant interaction between stand age and soil layer on soil physical properties (*BD*, clay, silt, and sand) (p<0.001, Figures 3a-3d). As described in Figure 3a, soil *BD* increased significantly as soil depth increased across all stand ages (p<0.05). The soil *BD* in 4-year-old stand was the highest among all stand ages at four soil depths (i.e., 0–10, 10–20, 20–30, and 30–50 cm) (p<0.05). However, there was no significant difference in soil *BD* between the 11- and 7-year-old stands at the 0–10 and 10–20 cm soil layers (p>0.05). Statistical analysis revealed significant differences in soil clay, silt, and sand contents between the three stand ages at the four soil depths (p<0.05, Figures 3b-3d). The changes of clay, silt, and sand contents showed a trend not obvious along with soil depth in all three stands. There were no significant differences in contents of soil clay, silt, and sand among the four soil depths at the same forest age (p>0.05), except for the clay content at the 11-year-old stand (p<0.05).

Soil chemical properties (*pH*, *TN*, *TP*, *TK*, *AN*, *AP*, and *AK*) were significantly influenced by both stand age and soil depth (p<0.001, Figures 4a-4d, and Figures 5a-5c). Similarly, the interaction among stand age and soil depth also significantly affected the chemical characteristics of the soil (p<0.001, Fig. 4b-4c, and Fig. 5a-5b) except for *pH*, *TK*, and *AK* (p=0.735, Figure 4a, p=0.987, Figure 4d, and p=0.956, Figure 5c, respectively). The soil *pH* value appeared an increasing trend with soil depth in the same forest age but was not significantly different among the four soil depths for any given age stand (p>0.05, Figure 4a). A significant decreasing trend was found as the stand age increased (p<0.05). The respective highest and lowest *pH* values were recorded in the 4- and 11-year-old stands for the four sampled soil depths. The contents of soil *TN*, *TP*, *TK*, *AN*, *AP*, and *AK* decreased significantly with increasing soil depth across the three stands, being higher in the superficial soil depth (0–10 cm) than in the other three deeper soil layers (10–20, 20–30, and 30–50 cm) (p<0.05, Figures 4b-4d, and Figures 5a-5c). Significant differences in soil *TN*, *TP*, *TK*, *AN*, *AP*, and *AK* concentrations were found among the three stand ages at all soil depths (p<0.05). These parameter values increased with stand age, being the highest in 11- year-old-stand and the lowest in 4- year-old-stand, and this trend was consistent at the four soil depths.

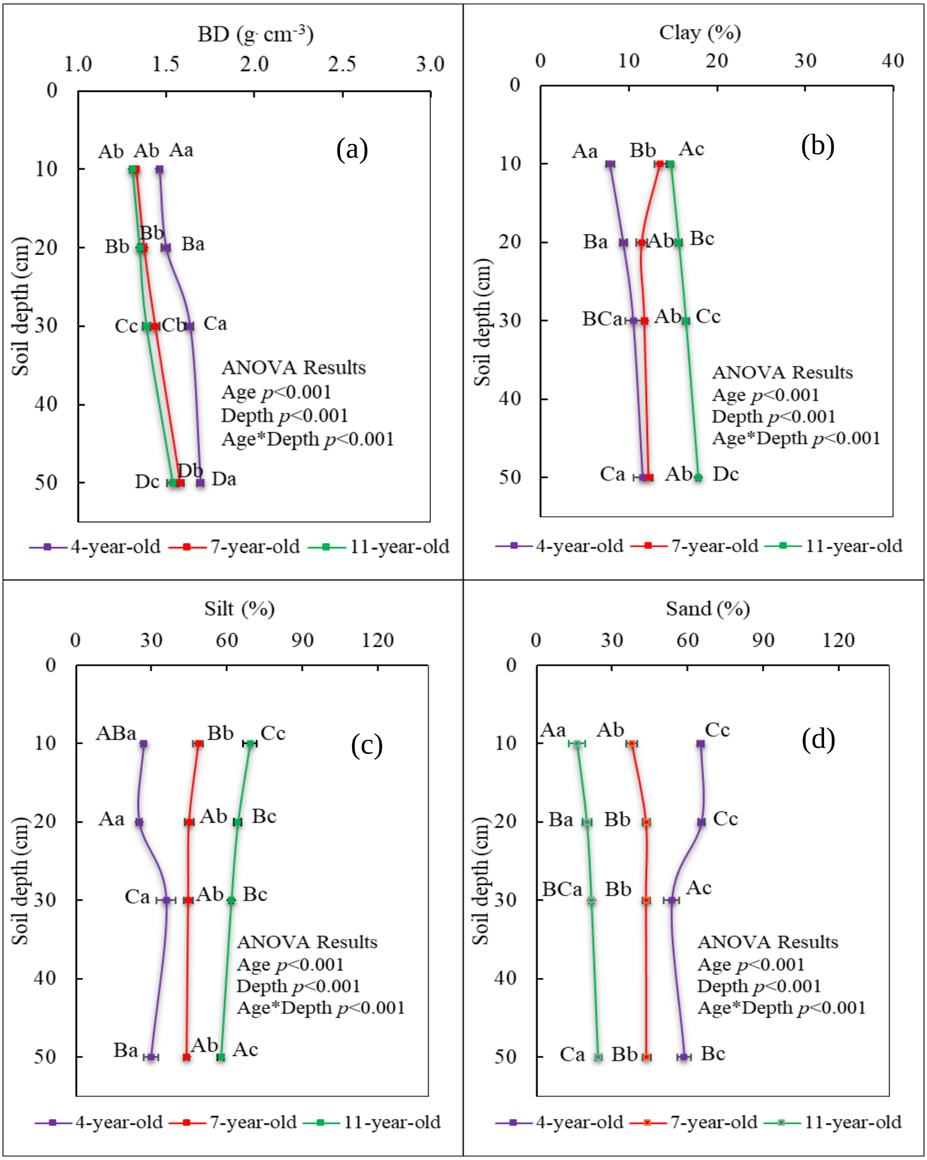

Figure 3. Variation of soil *BD* (a), clay (b), silt (c), and sand (d) with stand age and soil depth. Error bars indicate standard deviation (SD). *Note. BD*, bulk density. Means with different uppercase and lowercase letters indicate significantly different between soil layers in the same stand ages and between stand ages in the same soil layers (p<0.05), respectively. Results (p values) of two-way ANOVAs indicate the effect of stand age, soil layer, and their interaction on the soil *BD* and particle composition

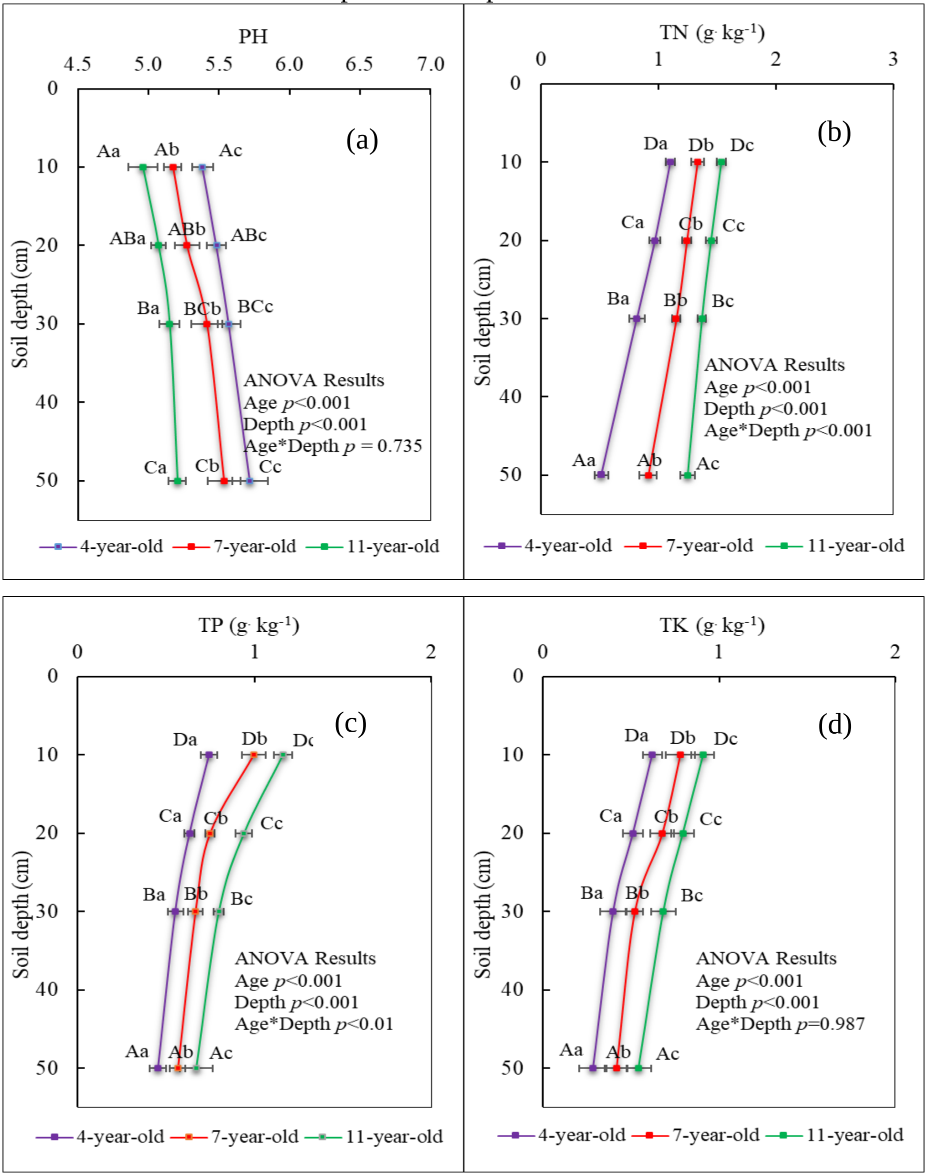

Figure 4. Variation of soil *pH* (a), *TN* (b), *TP* (c), and *TK* (d) with stand age and soil depth. Error bars indicate standard deviation (SD). *Note. TN*, total nitrogen; *TP*, total phosphorus; and *TK*, total potassium. Means with different uppercase and lowercase letters indicate significantly different between soil layers in the same stand ages and between stand ages in the same soil layers ($p<0.05$), respectively. Results (*p* values) of two-way ANOVAs indicate the effect of stand age, soil layer, and their interaction on the *pH*, *TN*, *TP*, and *TK*

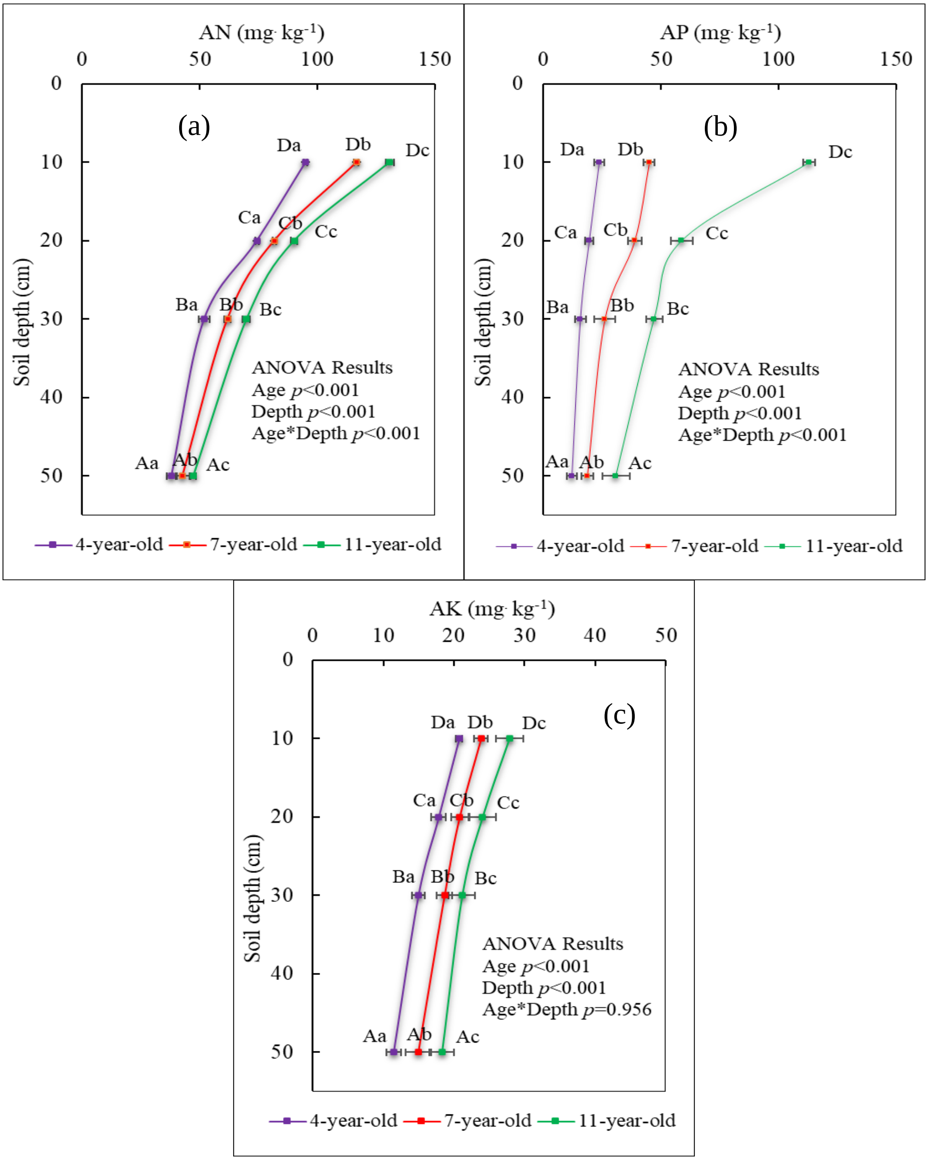

Figure 5. Variation of *AN* (a), *AP* (b), and *AK* (c) with stand age and soil depth. Error bars indicate standard deviation (SD). *Note*. *AN*, available nitrogen; *AP*, available phosphorus; and *AK*, available potassium. Means with different uppercase and lowercase letters indicate significantly different between soil layers in the same stand ages and between stand ages in the same soil layers ($p<0.05$), respectively. Results (p values) of two-way ANOVAs indicate the effect of stand age, soil layer, and their interaction on the *AN*, *AP*, and *AK*

Major factors controlling *SOC*

The correlation analysis showed that *SOC* was strongly and positively correlated with clay, silt, *TN*, *TP*, *TK*, *AN*, *AP*, and *AK* but significantly negatively correlated with *BD*, *pH*, and sand (p<0.01) (Table 2). Plant biomass factors including *TAGB*, *TBGB*, and litter were also significantly positively correlated with *SOC* (p<0.01).

Table 2. Pearson Correlation Coefficient Values (r) between soil organic carbon content and environmental variables at different stand ages of *Acacia mangium* forests

Environmental variables	*SOC* (g· kg^{-1})
TAGB (Mg· ha^{-1})	0.86**
TBGB (Mg· ha^{-1})	0.90**
Litter (Mg· ha^{-1})	0.53**
Clay (%)	0.68**
Silt (%)	0.87**
Sand (%)	-0.86**
BD (g· cm^{-3})	-0.86**
pH	-0.86**
TN (g· kg^{-1})	0.92**
TP (g· kg^{-1})	0.79**
TK (g· kg^{-1})	0.81**
AN (mg· kg^{-1})	0.58**
AP (mg· kg^{-1})	0.75**
AK (mg· kg^{-1})	0.80**

Note. *SOC*, soil organic carbon; *TAGB*, total above-ground biomass; *TBGB* total below-ground biomass; *BD*, bulk density; *TN*, total nitrogen; *TP*, total phosphorus; *TK*, total potassium; *AN*, available nitrogen; *AP*, available phosphorus; and *AK*, available potassium. ** indicates significant effects at p < 0.01

The PCA results revealed that the first principal component (PC1) explained 71.21% of the total variance of data obtained in the 12 study plots, whereas the second principal component (PC2) interpreted 17.19% (Figure 6). These results illustrated that the first two principal components contributed 88.40% of the standardized variance. The first principal component was mainly associated with variation in *TN*, *pH*, and silt, and the second was primarily related to *AN* and clay.

To find the best predictive variables that influence *SOC*, we conducted SMRA with PC1 (*TN*, *pH*, and silt), and PC2 (*AN*, and clay) as independent variables and *SOC* as the dependent variable. The regression model suggested that the soil *TN* and silt were the two most important factors controlling *SOC* and these factors exerted a significant positive effect (Table 3).

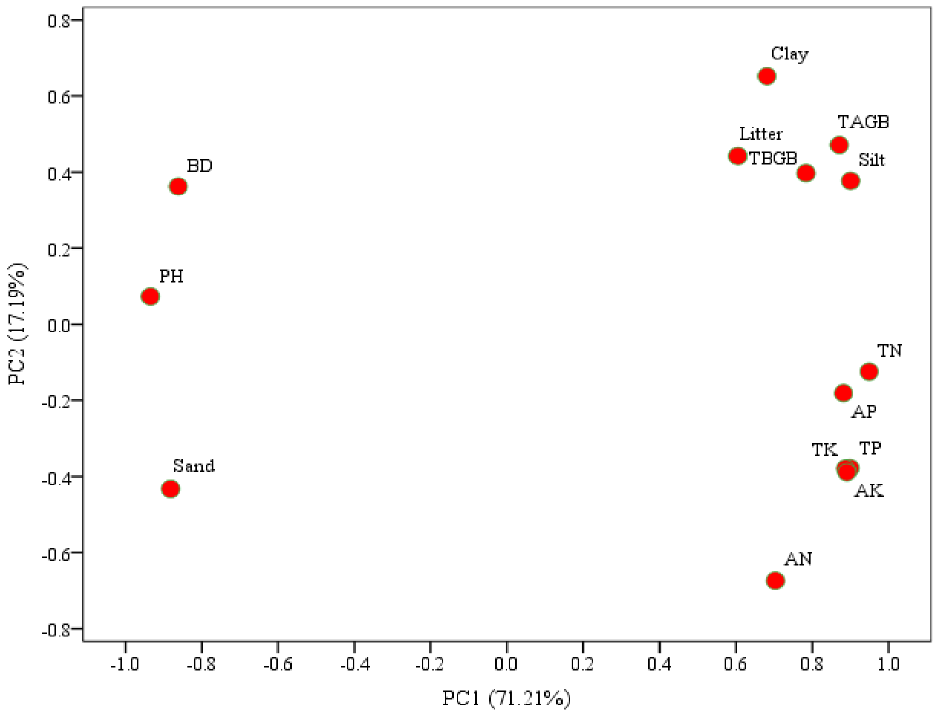

Figure 6. Principle component analysis (PCA) of the environmental variables

Table 3. Results of stepwise multiple linear regression analyses showing the dependence of soil organic carbon on environmental variables

Dependent variable	Explanatory variable	Coefficient estimate	*SE*	*t-value*	*p*-value	R^2
	Constant	1.103	0.804	1.371	0.177	
SOC	*TN*	9.077	1.114	8.149	<0.001	0.898
	Silt	0.113	0.022	5.122	<0.001	

Note. *SOC*, soil organic carbon; *TN*, total nitrogen; *SE*, standard error of the coefficient estimate

DISCUSSION

Soil organic carbon content and storage in *A. mangium* plantations

In the three age-sequence *A. mangium* stands of this study, the *SOC* concentration was the highest in the surface 0–10 cm soil layer and revealed a decreasing trend with increasing depth (Figure 2a). The *SOC* produced from the decomposition of root system and litter near the ground surface will get into the topsoil first, this could be responsible for the significant higher *SOC* content in the upper soil layer (Zhong and Qiguo, 2001; He *et al*., 2009; Laik *et al*., 2009; Thanh and Cuong, 2017a; Zhang *et al*., 2018). The concentration of C stored in the top three soil layers (0–10 cm, 10-20 cm, and 20–30 cm) and the deepest layer (30–50 cm) significantly increased with increased age of *A. mangium* plantations, probably due to the increase of litter productivity and slow decomposition in older stands (Herdiyanti and Sulistyawati, 2009; Ming *et al*., 2014).

Changes in *CS* following afforestation and stand age have been widely carried out in earlier studies. Interestingly, there were varied conclusions concerning the changes in *CS* after afforestation among former studies in the literature. Some researchers found no change in *CS* after afforestation (Zhang *et al*., 2017; Yue *et al*., 2018). Some researchers observed an increasing trend of *CS* in the plantations in the early stages after afforestation followed by a gradual decrease (Noh *et al*., 2010; Ali *et al*., 2019). Some researchers showed that there was an initial decline in *CS* after afforestation followed by a gradual increase (Li *et al*., 2011; Zhaodi *et al*., 2018). Some important factors, such as the choice of plant species used for plantation, forest type, soil cultivation method, soil properties, earlier land use and climate could explain the contradictory results reported in various studies. All these factors, independently or in combination could overshadow the effect of stand age on the accumulation of soil organic C (Noh *et al*., 2010; Zhang *et al*., 2019). In the current study, carbon storage in the mineral soil layer always increased significantly along with *A. mangium* stand development (Figure 2b). Hence, our study results demonstrate that afforestation with *A. mangium* resulted in a remarkable increase in soil organic C storage in Southeastern region. These findings may be attributed, at least in part, to the larger accumulation of soil organic matter (litter and roots) with the forest stand development (Thanh and Cuong, 2017a) and the annual soil respiration was far lower (Yang *et al*., 2007). Similar results were obtained by Hai *et al*. (2009), He *et al*. (2009), Zhao *et al*. (2014), Abaker *et al*. (2016), and Zhang *et al*. (2018), who also observed an increase of organic C in soil following afforestation. Furthermore, in terms of vertical distribution of *CS*, the results of our study illustrated that a large quantity of the *CS* was sequestrated in upper 0-30 cm of the mineral soil horizon in all stands, showing that greater amounts of *CS* were stoked in the topsoil layer. Approximately 60.37% to 63.33% of *CS* in the 0–50 cm range of soil was found in the 0–30 cm range (Figure 2b), where soils can be disturbed by human disturbances and natural erosion. Thus, research the vertical variability of *CS,* and protection of the topsoil from loss is important to promote C sequestration.

Factors influencing *SOC* across stand ages

Our findings revealed that soil *TN* and *AN* were strongly correlated with *SOC* (Table 2). In many ecosystems, it is well known that soil *C* and *N* are two closely associated biogeochemical processes (Hagedorn *et al*., 2003; Abaker *et al*., 2018). As one of the most essential nutrients for plant healthy growth, the quality and quantity of available *N* could impact the biomass productivity and the amount of plant litter, which is the dominant source of organic *C* (Bronson *et al*. 2004; Sam *et al*. 2006). *A. mangium* has a very high biological N-fixation capacity because of its symbiotic association with nodule-forming bacteria (Yang *et al*., 2009; Matali and Metali, 2015), it probably maintains the *N* inputs at our sites, and indirectly increase *SOC*. Partly due to their contribution, the increasing of the soil *N* contents likely affects the accumulation of *SOC (*Zhang *et al*., 2018), including *SOC* variation in the *A. mangium* forest land (Table 3).

In the present study, soil texture could play a crucial role in determining *SOC* accumulation. The variation in *SOC* in different age stands was positively correlated with clay and silt contents, while *SOC* was negatively correlated with sand content (Table 2). Additionally, silt content was the dominant factor influencing *SOC* (Table 3). Therefore, the present results corroborated previous empirical studies demonstrating that soil clay and silt contents contribute to *SOC* formation and preservation (Six *et al*., 2002a; Zhou *et al*., 2019). Fine particle proportions (clay and silt) and microaggregates can protect soil organic matter by stabilizing them against microbial mineralization (Paul, 1984; Baldock and Skjemstad, 2000). Moreover, fine soil particles can enhance water retention in soil and promote biomass production, increase litter input to soils (Burke *et al*., 1989; Yang *et al*., 2008).

Soil *pH* was the environment factor with high factor loading, which could interpret *SOC* variability to certain extents (Figure 6). As depicted in Table 2, *SOC* was significantly negatively correlated with soil *pH*. This result is congruent with the findings of the previous researches (Zhang *et al*., 2018; Zhaodi *et al*., 2018; Zhou *et al*., 2019). The soil *pH* primarily influences microbial respiration and activity, which directly affects soil organic matter formation and decomposition (Senechkin *et al*., 2014), since most microorganisms prefer to grow and metabolize with *pH* values ranging from 5.5 to 8.5 (Holguin *et al*., 2001; Zhou *et al*., 2005). In such *pH* range, more microorganism activities are available, therefore further contribute to higher *SOC* decomposition. The current research found *SOC* increased with a decrease in soil *pH*. The relatively low *pH* values are often related to low microbial activity that reduces the *SOC* decomposition (Lei *et al*., 2019). Thus, relatively low soil *pH* may enhance soil C accumulation in the *A. mangium* forest land.

The previous studies showed that *SOC* was significantly positively correlated with plant biomass (He *et al*., 2009; Sun and Guan, 2014), which was confirmed by the current study (Table 2). Other studies reported similar finding for some plantation forests in Vietnam (e.g., *A. mangium, A. auriculiformis, A. hybrid,* and *Eucalyptus urophylla*) (Hai *et al*., 2009). It also demonstrated the increase in biomass accumulated in the above- and below-ground components as the principal source of soil C inputs in forest ecosystems, which play a crucial role in *SOC* dynamics (Kristensen *et al*., 2008). The quantity and quality of aboveground litterfall determine *SOC* accumulation especially for the surface soil layer (Herdiyanti and Sulistyawati, 2009). Belowground root biomass plays a pivotal role in the accumulation of *SOC* across the soil profiles (Bauhus *et al*., 2000; Qu *et al*., 2011). Soil *BD* can be viewed as a key parameter of soil physical health that could affect soil structure, porosity, water-holding capacity, permeability and soil ventilation, and thus further influence the accumulation of *SOC* (Yu *et al*., 2019). In present study, significantly negative correlation between *SOC* and soil *BD* had been found (Table 2), which is in agreement with the results of previous studies (Thanh and Cuong, 2017a; Zhang *et al*., 2018). Plant growth and root penetration with organic matter returning can significantly improve soil structure and porosity and increase *SOC* content and impact soil *BD* (Ruehlmann and Krschens, 2009; Thanh and Cuong, 2017a; Wang *et al*., 2019). Soil *P* is a dominant nutrient that controls plant growth and development (Lei *et al*., 2019). Our results demonstrated that *SOC* was significantly positively correlated with soil *TP* and *AP* contents (Table 2). Lei *et al*. (2012) showed that *P* limitation might restrict *SOC* accumulation. It should be due to the availability of *P* regulating microbial growth and activities. Insufficient *P* supply may influence symbiotic *N* fixation (Augusto *et al*., 2013), and ultimately impact *SOC* accumulation. Another study demonstrated that the decomposition of *SOC* could promote the release of *P*, and the increased *P* availability had a contribution to the *SOC* accumulation (Qian *et al*., 2017). Available *K* could accelerate plant growth and simultaneously provide sufficient nutrient for the healthy root system in plants, increasing the number of plant residuals in the soil and increasing *SOC* (Sam *et al*. 2006). Our research also found a significant positive correlation of soil *K* contents (*TK* and *AK* contents) with *SOC* (Table 2), which might be associated with *K* released by the soil parent material with an increasing rate of weathering. Besides, the stand characteristic parameters such as stand density, canopy closure, mean *DBH*, and *H* may also contribute to interpreting the change of *SOC* in forests at different ages (Table 1).

CONCLUSIONS

The present study results provided an overall view of *SOC* distribution in an age-sequence of *A. mangium* forests (from 4- to 11-year-old plantations). To the best of our knowledge, this is the first report on the dynamics of *SOC* accumulation and the unique relationships between *SOC* and influential environmental variables for *A. mangium* forests in Southeastern region of Vietnam. Soil organic C content increased significantly with forest age. Moreover, *SOC* concentration primarily occurred in the topsoil and declined significantly with depth. Carbon storage in the mineral soil layer increased significantly with stand age. Soil organic C storage indicated obvious surface aggregation, with more than 60% of *CS* being in 0–30 cm depth. Soil *TN* content and soil texture (i.e., soil silt content) were the principal factors regulating the *SOC*. The findings provided by this study revealed that the *SOC* and nutrient regimes were substantially improved by afforestation with *A. mangium*, and provide valuable information for understanding the factors controlling *SOC* in the region.

ACKNOWLEDGEMENTS

This work was funded by the Chinese Government Doctoral Scholarship Foundation (2017GXZ025473) and the Doctoral Scholarship Foundation of Vietnam National University of Forestry (No.1872/QD/DHLN-TCCB). We would like to thank the Chang Riec Historical - Cultural Forest for providing invaluable information on the research site and permitting us to use the forests for this study. We would also like to thank the Dr. Dinh Mai Van and other researchers of the Centre of Forestry Research and Climate Change at VNUF for their support in laboratory analyses and for their comments to improve this manuscript.

REFERENCES

Abaker, W.E., Berninger, F., Saiz, G., Braojos, V., Starr, M. (2016). Contribution of *Acacia senegal* to biomass and soil carbon in plantations of varying age in Sudan. Forest Ecology and Management, 368: 71-80. doi:10.1016/j.foreco.2016.03.003.

Abaker, W.E., Berninger, F., Saiz, G., Pumpanen, J., Starr, M. (2018). Linkages between soil carbon, soil fertility and nitrogen fixation in *Acacia senegal* plantations of varying age in Sudan. PeerJ, 6: e5232. doi:10.7717/peerj.5232.

Albaladejo, J., Ortiz, R., Garcia-Franco, N., Navarro, A.R., Almagro, M., Pintado, J.G., *et al*. (2013). Land use and climate change impacts on soil organic carbon stocks in semi-arid Spain. Journal of Soils and Sediments, 13(2): 265-277. doi:10.1007/s11368-012-0617-7.

Ali, A., Ahmad, A., Akhtar, K., Teng, M., Zeng, W., Yan, Z., *et al*. (2019). Patterns of biomass, carbon, and soil properties in Masson pine (*Pinus massoniana* Lamb) plantations with different stand ages and management practices. Forests, 10(8): 645. doi:10.3390/f10080645.

Augusto, L., Delerue, F., Gallet-Budynek, A., Achat, D.L. (2013). Global assessment of limitation to symbiotic nitrogen fixation by phosphorus availability in terrestrial ecosystems using a meta-analysis approach. Global Biogeochem Cycles, 27(3): 804-815. doi:10.1002/gbc.20069.

Baldock, J.A. & Skjemstad, J.O. (2000). Role of the soil matrix and minerals in protecting natural organic materials against biological attack. Organic Geochemistry, 31(7-8): 697-710. doi:10.1016/S0146-6380(00)00049-8.

Batjes, N.H. (1996). Total carbon and nitrogen in the soils of the world. European Journal of Soil Science, 47(2): 151-163. doi:10.1111/j.1365-2389.1996.tb01386.x.

Bauhus, J., Khanna, P., Menden, N. (2000). Aboveground and belowground interactions in mixed plantations of *Eucalyptus* globulus and *Acacia mearnsii*. Canadian Journal of Forest Research, 30: 1886–1894. doi:10.1139/x00-141.

Blake, G.R. & Hartge, K.H. (1986). Bulk density. In: Klute A (ed) Methods of soil analysis part 1: physical and mineralogical methods, 2nd edn. American Society of Agronomy, Madison. pp. 363-375.

Bronson, K.F., Zobeck, T.M., Chua, T.T., Acosta-Martinez, V., Van Pelt, R.S., Booker, J.D. (2004). Carbon and nitrogen pools of southern high plains cropland and grassland soils. Soil Science Society of America Journal, 68(5): 1695-1704. doi:10.2136/sssaj2004.1695.

Burke, I.C., Yonker, C.M., Parton, W.J., Cole, C.V., Schimel, D.S., Flach, K. (1989). Texture, climate, and cultivation effects on soil organic matter content in U.S.

Grassland soils. Soil Science Society of America Journal, 53: 800-805. doi:10.2136/sssaj1989.03615995005300030029x.

Carvalhais, N., Forkel, M., Khomik, M., Bellarby, J., Jung, M., Migliavacca, M., *et al*. (2014). Global covariation of carbon turnover times with climate in terrestrial ecosystems. Nature, 514(7521): 213-217. doi:10.1038/nature13731.

Chen, CR., Xu, Z.H., Mathers, N.J. (2004). Soil carbon pools in adjacent natural and plantation forests of subtropical Australia. Soil Science Society of America Journal, 68(1): 282-291. doi:10.2136/sssaj2004.2820.

Cheng, J., Lee, X., Theng, B.K.G., Zhang, L., Fang, B., Li, F. (2015). Biomass accumulation and carbon sequestration in an age-sequence of *Zanthoxylum bungeanum* plantations under the Grain for Green Program in Karst regions, Guizhou Province. Agricultural and Forest Meteorology, 203: 88-95. doi:10.1016/j.agrformet.2015.01.004.

Cong, J., Wang, X., Liu, X., Zhang, Y. (2016). The distribution variation and key influencing factors of soil organic carbon of natural deciduous broadleaf forests along the latitudinal gradient. Acta Ecologica Sinica, 36(5): 333-339. doi:10.1016/j.chnaes.2016.06.002.

Cuong, L.V., Thanh, N.M., Long, L.V., Trang, B.T.T., Hieu, N.T. (2017). Some soil physical and chemical properties under natural forest cover in Tanphu protective forest, Dongnai Province. Journal of Forest Science and Technology, 6: 17-24 (in Vietnamese with English abstract)

Cuong, L., Hung, B., Bolanle-Ojo, O.T., Xu, X., Thanh, N., Chai, L., *et al*. (2020). Biomass and carbon storage in an age-sequence of *Acacia mangium* plantation forests in Southeastern region, Vietnam. Forest Systems, 29(2): e009. doi:10.5424/fs/2020292-16685.

Deng, L. & Shangguan, Z. (2017). Afforestation drives soil carbon and nitrogen changes in China. Land Degradation and Development, 28(1): 151-165. doi:10.1002/ldr.2537.

Deng, L., Han, Q.S., Zhang, C., Tang, Z.S., Shangguan, Z.P. (2017). Aboveground and belowground ecosystem biomass accumulation and carbon sequestration with *Caragana korshinskii* Kom plantation development. Land Degradation and Development, 28(3): 906-917. doi:10.1002/ldr.2642.

Fan, H., Zhao, W., Daryanto, S., Fu, B., Wang, S., Wang, Y. (2018). Vertical distributions of soil organic carbon and its influencing factors under different land use types in the desert riparian zone of downstream Heihe River basin, China. Journal of Geophysical Research, 123(14): 7741–7753. doi:10.1029/2018JD028268.

Hagedorn, F., Spinnler, D., Siegwolf, R. (2003). Increased in deposition retards mineralization of old soil organic matter. Soil Biology and Biochemistry, 35(12): 1683–1692. doi:10.1016/j.soilbio.2003.08.015.

Hai, VD., Trieu, D.T., Tiep, N.H., Bich, N.V., Duong, D.T. (2009). *Research on carbon sequestration potential and commercial value of some major types of plantation forests in Vietnam*. Final Project Report No. VAFS2009; Vietnamese Academy of Forest Sciences: Hanoi, Vietnam. 190 pp.

He, B., Liu, Y.H., Yu, H.G., Qin, W.M., Wei, S.H., Cai, S.W. (2009). Carbon density and storage of *Acacia mangium* plantation ecosystem in Nanning, Guangxi, China. Scientla Silvae Sinicae, 45(2): 6-11 (in Chinese with English abstract).

Herdiyanti, I. & Sulistyawati, E. (2009). Carbon stocks in *Acacia mangium* Willd. stands of different ages. In: Kanakaraju D, Kalu M, Ipor I, Lim CK, Lim PT, Roslan HA, Esa Y, Razali A, Ho WS, Mohamad S *et al*., editors. Proceedings of Conference on Natural Resources in the Tropics 3: Harnessing Tropical Natural Resources through Innovation and Technologies, 3–5 August 2009; Sarawak, Malaysia. Kota Samarahan, Malaysia: Universiti Malaysia Sarawak. pp. 679–685.

Hobley, E., Wilson, B., Wilkie, A., Gray, J., Koen, T. (2015). Drivers of soil organic carbon storage and vertical distribution in Eastern Australia. Plant and Soil, 390: 111–127.

Holguin, G., Vazquez, P., Bashan, Y. (2001). The role of sediment microorganisms in the productivity, conservation, and rehabilitation of mangrove ecosystems: an overview. Biology and Fertility of Soils, 33(4): 265-278.

IBM Corp. (2017). IBM SPSS Statistics for Windows, Version 25.0. Armonk, NY: IBM Corp.

IBST. (2009). Vietnam Building Code Natural Physical & Climatic Data for Construction. QCVN 02:2009/BXD. Institute for Building Science and Technology (IBST), Vietnam.

Jobbágy, E. & Jackson, R. (2000). The vertical distribution of soil organic carbon and its relation to climate and vegetation. Ecological Applications, 10:423-436. doi:10.1890/1051-0761(2000)010[0423:TVDOSO]2.0.CO;2.

Jusoh, I., Abu, Zaharin, F., Adam, N.S. (2014). Wood quality of *Acacia hybrid* and second-generation *Acacia mangium*. Bioresources, 9(1): 150-160. doi:10.15376/biores.9.1.150-160.

Koutika, L.S. & Richardson, D.M. (2019). *Acacia mangium* Willd: benefits and threats associated with its increasing use around the world. Forest Ecosystems, 6: 2. doi:10.1186/s40663-019-0159-1.

Kristensen, E., Bouillon, S., Dittmar, T., Marchand, C. (2008). Organic carbon dynamics in mangrove ecosystems: A review. Aquatic Botany, 89(2): 201-219. doi:10.1016/j.aquabot.2007.12.005.

Lal, R. (2004). Soil carbon sequestration to mitigate climate change. Geoderma, 123: 1-22. doi:10.1016/j.geoderma.2004.01.032.

Laik, R., Kumar, K., Das, D.K., Chaturvedi, O.P. (2009): Labile soil organic matter pools in a calciorthent after 18 years of afforestation by different plantations. Applied Soil Ecology, 42(2): 71-78. doi:10.1016/j.apsoil.2009.02.004.

Lee, K.L., Ong, K.H., King, P.J.H., Chubo, J.K., Su, D.S.A. (2015). Stand productivity, carbon content, and soil nutrients in different stand ages of *Acacia mangium* in Sarawak, Malaysia. Turkish Journal of Agriculture and Forestry, 39(1): 154-161. doi:10.3906/tar-1404-20.

Lei, L., Gundersen, P., Zhang, T., Mo, J. (2012). Effects of phosphorus addition on soil microbial biomass and community composition in three forest types in tropical China. Soil Biology and Biochemistry, 44(1): 31-38. doi:10.1016/j.soilbio.2011.08.017.

Lei, Z., Yu, D., Zhou, F., Zhang, Y., Yu, D., Zhou, Y., *et al*. (2019). Changes in soil organic carbon and its influencing factors in the growth of *Pinus sylvestris* var. mongolica plantation in Horqin Sandy Land, Northeast China. Scientific Reports, 9(1): 16453. doi:10.1038/s41598-019-52945-5.

Li, X., Yi, M.J., Son, Y., Park, P.S., Lee, K.H., Son, Y.M., *et al*. (2011). Biomass and carbon storage in an age-sequence of Korea pine (*Pinus koraiensis*) plantation forests in central Korea. Journal of Plant Biology, 54(1): 33–42. doi:10.1007/s12374-010-9140-9.

Liu, Y., Li, S., Sun, X. Yu, X. (2016). Variations of forest soil organic carbon and its influencing factors in East China. Annals of Forest Science, 73(2): 501-511. doi:10.1007/s13595-016-0543-8.

Lydie-Stella, K., Sogni, Viviane, T., Louis, M., Daniel, E. (2017). Nitrogen dynamics in a nutrient-poor soil under mixed-species plantations of Eucalypts and Acacias. Soil Biology and Biochemistry, 108: 84–90. doi:10.1016/j.soilbio.2017.01.023.

MARD. (2018). *Promulgating a list of major forestry tree species, recognition of varieties and seed sources, and management of main forestry tree seed materials*. No. 30/2018/TT-BNNPTNT. Ministry of Agriculture and Rural Development (MARD), Hanoi, Vietnam.

MARD. (2020). *Promulgation of the state of National forests*. No. 1558/QD-BNN-TCLN. Ministry of Agriculture and Rural Development (MARD), Hanoi, Vietnam.

Matali, S. & Metali, F. (2015). Selected soil physico-chemical properties in the *Acacia mangium* plantation and the adjacent heath forest at Andulau Forest Reserve. Malaysian Journal of Soil Science, 19: 45-58.

Matthias, P. & Arain, M.A. (2006). Above- and belowground ecosystem biomass and carbon pools in an age-sequence of *Temperate pine* plantation forests. Agricultural and Forest Meteorology, 140(1-4): 51-63. doi:10.1016/j.agrformet.2006.08.004.

Ming, A., Jia, H., Zhao, J., Tao, Y., Li, Y. (2014). Above- and belowground carbon stocks in an Indigenous tree (*Mytilaria laosensis*) plantation chronosequence in subtropical China. PLoS ONE, 9(10): e109730. doi:10.1371/journal.pone.0109730.

Ngaba, M.J.Y., Ma, X., Hu, Y. (2020). Variability of soil carbon and nitrogen stocks after conversion of natural forest to plantations in Eastern China. PeerJ, 8: e8377. doi:10.7717/peerj.8377.

Nelson, D.W. & Sommers, L.E. (1982). Total carbon, organic carbon and organic matter: In: A.L. Page, R.H. Miller and D.R. Keeney) Methods of soil analysis. Part 2 Chemical and Microbiological Properties. pp. 539-579. doi:10.2134/agronmonogr9.2.2ed.c29.

Noh, N.J., Son, Y., Lee, S.K., Seo, K.W., Heo, S.J., Yi, M.J., *et al*. (2010). Carbon and nitrogen storage in an age-sequence of *Pinus densiflora* stands in Korea. Science China Life sciences, 53(7): 822-830. doi:10.1007/s11427-010-4018-0.

Paul, E.A. (1984). Dynamics of organic matter in soils. Plant and Soil, 76: 275–285. doi:10.1007/978-94-009-6101-2_24.

Pregitzer, K.S. & Euskirchen, E.S. (2004). Carbon cycling and storage in world forests: biome patterns related to forest age. Global Change Biology, 10(12): 2052-2077. doi:10.1111/j.1365-2486.2004.00866.x.

Qian, J., Liu, J., Wang, P., Wang, C., Li, K., Shen, M. (2017). Riparian soil physicochemical properties and correlation with soil organic carbon of an inflowing river of Taihu Lake. IOP Conference Series: Earth and Environmental Science, 59: 012053. doi:10.1088/1755-1315/59/1/012053.

Qu, W.D., Chen, Y.M., Wang, L.L., Zhang, F., Zhang, X.W. (2011). Dynamics of soil organic carbon in *Caragana microphylla* forest and its relationships with environment factors in loess hilly region. Science of Soil and Water Conservation, 9(4): 72-77 (in Chinese with English abstract).

R Core Team. (2018). A language and environment for statistical computing. R Foundation for Statistical Computing, Vienna, Austria.

Robson, A.D. & Foy, C.D. (1990). Soil Acidity and Plant Growth. Soil Science, 150(6): 903.

Ruehlmann, J. & Körschens, M. (2009). Calculating the effect of soil organic matter concentration on soil bulk density. Soil Science Society of America Journal, 73: 876-885. doi:10.2136/sssaj2007.0149.

Sam, D.D., Que, D.N., Siem, T.N., Binh, N.N. (2006). *Forest soils, nutrition, and management*. Hanoi Agriculture Publishing House, Vietnam.

Shah Newaz, M. & Millat-e-Mustafa, M. (2004). Growth and yield prediction models for *Acacia mangium* grown in the plantations of the central region of Bangladesh. New Forests, 27: 81–88. doi:10.1023/A:1025086920175.

Senechkin, I.V., van Overbeek, L.S., van Bruggen, A.H.C. (2014). Greater fusarium wilt suppression after complex than after simple organic amendments as affected by soil *pH*, total carbon and ammonia-oxidizing bacteria. Applied Soil Ecology, 73: 148-155. doi:10.1016/j.apsoil.2013.09.003.

Simon, G.D., Alberti, G., Delle, Vedove, G., Zerbi, G., Peressotti, A. (2012). Carbon stocks and net ecosystem production changes with time in two Italian forest chronosequences. European Journal of Forest Research, 131(5): 1297-1311. doi:10.1007/s10342-012-0599-4.

Six, J., Conant, R.T., Paul, E.A., Paustian, K. (2002a). Stabilization mechanisms of soil organic matter: implications for c-saturation of soils. Plant and Soil, 24(2): 155-176. doi:10.1023/A:1016125726789.

Six, J., Callewaert, P., Lenders, S., De, Gryze, S., Morris, S.J., Gregorich, E.G., Paul, E.A., Paustian, K. (2002b). Measuring and understanding carbon storage in afforested soils by physical fractionation. Soil Science Society of America Journal, 66(6): 1981-1987. doi:10.2136/sssaj2002.1981.

Smal, H. & Olszewska, M. (2008). The effect of afforestation with Scots pine (*Pinus silvestris* L.) of sandy post-arable soils on their selected properties. II. Reaction, carbon, nitrogen and phosphorus. Plant and Soil, 305(1/2): 171-187. doi:10.1007/s11104-008-9538-z.

Sombroek, W.G., Nachtergaele, F.O., Hebel, A. (1993). Amounts, dynamics and sequestering of carbon in tropical and subtropical soils. Ambio, 22: 417-426.

Sun, L. & Guan, D.S. (2014). Carbon stock of the ecosystem of lower subtropical broadleaved evergreen forests of different ages in Pearl River Delta, China. Journal of Tropical Forest Science 26: 249-258.

Thanh, N.M. & Cuong, L.V. (2017a). Carbon storage in soil under *Acacia mangium* forest cover in Yenbai city, Yenbai Province. Science and Technology Journal of Agriculture & Rural Development, 2: 120-124 (in Vietnamese with English abstract).

Thanh, N.M. & Cuong, L.V. (2017b). Effects of plantation forest types to soil physical and chemical properties in Socson district, Hanoi city. Science and Technology Journal of Agriculture & Rural Development, 2: 133-139 (in Vietnamese with English abstract).

Thomas, G.W. (1996). Soil pH and soil acidity. Methods of Soil Analysis Part 3: Chemical Methods (ed. by DL Sparks). American Society of Agronomy and Soil Science Society of America, Madison. pp. 475-490.

Tian, F.P., Zhang, Z.N., Chang, X.F., Sun, L., Wei, X.H., Wu, G.L. (2016). Effects of biotic and abiotic factors on soil organic carbon in semi-arid grassland. Journal of soil science and plant nutrition, 16(4): 1087-1096. doi:10.4067/S0718-95162016005000080.

Van Reeuwijk, L.P. (2002). Procedures for Soil Analysis. 6th ed. ISRIC, FAO, Wageningen.

Wang, G., Guan, D., Peart, M.R., Chen, Y., Peng, Y. (2013). Ecosystem carbon stocks of mangrove forest in Yingluo Bay, Guangdong Province of South China. Forest Ecology and Management, 310: 539-546. doi:10.1016/j.foreco.2013.08.045.

Wang, Y., Liu, L., Yue, F., Li, D. (2019). Dynamics of carbon and nitrogen storage in two typical plantation ecosystems of different stand ages on the Loess Plateau of China. PeerJ, 7: e7708. doi:10.7717/peerj.7708.

Yang, Y.S., Chen, G.S., Guo, J.F., Xie, J.S., Wang, X.G. (2007). Soil respiration and carbon balance in a subtropical native forest and two managed plantations. Plant Ecology, 193(1): 71-84. doi:10.1007/s11258-006-9249-6.

Yang, Y., Fang, J., Tang, Y., Ji, C., Zheng, C., He, J., Zhu, B. (2008). Storage, patterns and controls of soil organic carbon in the Tibetan grasslands. Global Change Biology, 14(7): 1592-1599. doi:10.1111/j.1365-2486.2008.01591.x.

Yang, L., Liu, N., Ren, H., Wang, J. (2009). Facilitation by two exotic *Acacia*: *Acacia auriculiformis* and *Acacia mangium* as nurse plants in South China. Forest Ecology and Management, 257(8): 1786-1793. doi:10.1016/j.foreco.2009.01.033.

Yu, G., Jian, Z., Liming, W., Jiemin, G., Jianxiang, F., Hao, W., Guanghui, L. (2019). Distribution patterns and controlling factors for the soil organic carbon in four mangrove forests of China. Global Ecology and Conservation, 17: e00575. doi:10.1016/j.gecco.2019.e00575

Yue, J.W., Guan, J.H., Deng, L., Zhang, J.G., Li, G., Du, S. (2018). Allocation pattern and accumulation potential of carbon stock in natural spruce forests in Northwest China. PeerJ, 6: e4859-e4859. doi:10.7717/peerj.4859.

Zhang, L., Zhang, P., Yu, M., Wu, T. (2016). Soil organic carbon content and stocks in an age-sequence of *Metasequoia glyptostroboides* plantations in coastal area, East China. 4th International Conference on Sustainable Energy and Environmental Engineering (ICSEEE). pp. 1004-1012. doi:10.2991/icseee-15.2016.178.

Zhang, H., Wang, K., Zeng, Z., Du, H., Zeng, F. (2017). Biomass and carbon sequestration by *Juglans regia* plantations in the Karst regions of Southwest China. Forests, 8(4): 103. doi:10.3390/f8040103.

Zhang, H., Duan, H., Song, M., Guan, D. (2018). The dynamics of carbon accumulation in *Eucalyptus* and *Acacia* plantations in the Pearl River Delta region. Ann Forest Sci, 75(2):40. doi:10.1007/s13595-018-0717-7.

Zhang, X., Zhang, X., Han, H., Shi, Z., Yang, X. (2019). Biomass accumulation and carbon sequestration in an age-sequence of *Mongolian Pine* plantations in Horqin sandy land, China. Forests, 10(2): 197. doi:org/10.3390/f10020197

Zhao, J., Kang, F., Wang, L., Yu, X., Zhao, W., Song, X., *et al*. (2014). Patterns of biomass and carbon distribution across a chronosequence of Chinese Pine (*Pinus tabulaeformis*) forests. PLoS One, 9(4): e94966. doi:10.1371/journal.pone.0094966.

Zhaodi, W., Xiaodong, Y., Wei, W. (2018). Variation of soil carbon pools in *Pinus sylvestris* plantations of different ages in north China. Acta Ecologica Sinica, 38(3): 248-254. doi:10.1016/j.chnaes.2017.08.004

Zhong, L. & Qiguo, Z. (2001). Organic carbon content and distribution in soils under different land uses in tropical and subtropical China. Plant and Soil, 231(2): 175-185. doi:10.1023/A:1010350020951.

Zhou, L., Li, B.G., Zhou, G.S. (2005). Advances in controlling factors of soil organic carbon. Advances in Earth Science, 20(1): 99-105 (in Chinese with English abstract).

Zhou, W., Han, G., Liu, M., Li, X. (2019). Effects of soil pH and texture on soil carbon and nitrogen in soil profiles under different land uses in Mun River Basin, Northeast Thailand. PeerJ, 7: e7880. doi:10.7717/peerj.7880.

Zu, Y.G., Li, R., Wang, W.J., Su, D.X., Wang, Y., Qiu, L. (2011). Soil organic and inorganic carbon contents in relation to soil physicochemical properties in northeastern China. Acta Ecologica Sinica, 31(18): 5207–5216 (in Chinese with English abstract).

Krivokapić, S., Otović, M., Perović, S., Damjanović Vratnica, B. (2022). Total phenols, flavonoids, anthocyanins and antioxidant activity of wild pomegranate (Punica granatum l.) biowaste from Montenegro. Agriculture and Forestry, 68 (2): 157-165. doi: 10.17707/AgricultForest.68.2.11

DOI: 10.17707/AgricultForest.68.2.11

Slađana KRIVOKAPIĆ[*1], Milena OTOVIĆ[1], Svetlana PEROVIĆ[1], Biljana DAMJANOVIĆ VRATNICA[2]

TOTAL PHENOLS, FLAVONOIDS, ANTHOCYANINS AND ANTIOXIDANT ACTIVITY OF WILD POMEGRANATE (*Punica granatum* L.) BIOWASTE FROM MONTENEGRO

SUMMARY

In this paper, the content of total phenols, flavonoids, anthocyanins as well as antioxidant activity of 80% methanolic extracts of fruit peel and seeds of wild pomegranate (*Punica granatum* L.) collected from different localities of Montenegro were analyzed.

The obtained results showed a high level of presence of these bioactive substances with a high level of antioxidant activity. Among the samples, the dominant higher level of these bioactive substances was determined in the samples collected in the coastal region, while the smallest amount was detected in the samples collected from the locality Carev Laz, in that with higher altitude.

There was a negative correlation between the content of total phenols and flavonoids in the peel of wild pomegranate ($r = -0.57$), as well as a strong positive correlation between the amount of total phenols and antioxidant activity determined by the FRAP method ($r = 0.81$). In contrast to peel samples, in seed samples there was a positive correlation between the content of total phenols and flavonoids ($r = 0.67$). A high correlation was observed between antioxidant activity (FRAP method) and anthocyanin content ($r = 0.96$) as well as between antioxidant activity (DPPH method) and total phenols content ($r = 0.84$).

Keywords: *Punica granatum* L., phenols, flavonoids, anthocyanins, antioxidant activity, biowaste

INTRODUCTION

The organic part of municipal solid waste, also known as bio-waste, includes food scraps from households and garden waste (leaves, branches, grass).

[1] Slađana Krivokapić (*corresponding author: sladjanak@ucg.ac.me), Milena Otović, Svetlana Perović, University of Montenegro, Department of Biology, Faculty of Natural Sciences and Mathematics, MONTENEGRO;

[2] Biljana Damjanović Vratnica, University of Montenegro, Faculty of Metallurgy and Technology, MONTENEGRO

Notes: The authors declare that they have no conflicts of interest. Authorship Form signed online.

Recieved:17/02/2022 *Accepted:22/04/2022*

By developing strategies for its utilization, bio-waste can be an additional source of fertilizer for plants, but also a valuable source of secondary metabolites that can contribute to human health. Its recycling would reduce disposal costs and reduce its impact on air pollution (Vieira and Matheus, 2019; Mahro and Timm, 2007). In addition to the primary metabolites responsible for the growth, development and reproduction of each plant (Erb and Kliebenstein, 2020), plants also produce metabolites specific to each plant species. The production of secondary metabolites provides plants biotic and abiotic factors protection (Mazid, 2011). Phenols are a group of secondary metabolites that are distinguished by the level of biological capacity due to pronounced antioxidant, antimicrobial, antifungal and even anticancer activity (Viuda-Martos *et al*., 2010, Braga *et al*., 2005, Singh *et al*., 2018, Albrecht *et al*., 2004). Many studies have confirmed that the peel and seeds of wild pomegranate, as its biowaste, contains a large amount of phenols, flavonoids and anthocyanins (Radunić *et al*., 2017, Gadže *et al.*, 2012, Jacob *et al*., 2018, Kam *et al*., 2013). Tzulker *et al*. (2007) suggest that punicalagin is one of the main bioactive substances that contributes to the total antioxidant capacity of wild pomegranate fruit (*Punica granatum* L.). According to Gil *et al*. (2000), the wild pomegranate juice shows up to eight times stronger antioxidant activity than the juice of grapes, cranberries and oranges, and three times stronger than the activity of red wine and green tea. Derakhshan *et al*. (2018) in their study presented a positive correlation between phenolic composition and antioxidant activity. They also proved that temperature and environmental conditions have an impact on the amount of phenol and antioxidant activity.

The aim of this study was to determine the content of total phenols, flavonoids, anthocyanins, as well as antioxidant activity of peel and seeds of wild pomegranate (*Punica granatum* L.) collected from different localities of Montenegro.

MATERIAL AND METHODS

Plant material

For the purposes of this research, the fruits of wild pomegranate *(Punica granatum* L.) were collected in the period of October 2020 at six different localities of Montenegro: Bar (Šušanj), Budva, Cetinje (Carev Laz), Kotor (Škaljari), Kotor (Dobrota) and Podgorica (Brdo Gorica) (Table 1).

Table 1. Location of the sampling station

Locality	*Coordinates*	*Altitude*
Šušanj	42.11896N 19.10660E	71m
Budva	42.285978N 18.854130E	25m
Carev Laz	42.2220N 19.0610E	142m
Škaljari	42.416544N 18.768540E	11m
Dobrota	42.458932N 18.765057E	5m
Brdo Gorica	42.44832N 19.26640E	76m

Extraction of bioactive compounds

1g of each comminuted sample was dissolved in 10ml of 80% methanol in a test tube. Extraction was performed according to Sharayei *et al*. (2018), with certain modifications, in an ultrasonic water bath (ViMS Electric Serbia), at a constant temperature of 50°C with a frequency of 50KHz in a thirty-minute time interval. The extracts were filtered through Whatman filter paper and stored in sealed tubes in a refrigerator at 4° C until research.

Total phenolic content (TPC)

Determination of TPC was performed by the Folin-Ciocalteu method (Singleton and Rossi, 1965), according to Sarkhosh *et al*. (2009) by adding 10µl of extract, 100µl of Folin-Ciocalteu reagent and 1ml of distilled water to glass tubes. After 3 minutes, 0.5 ml of saturated sodium carbonate solution was added. The reaction mixture was vortexed and incubated in a water bath for 25-30 minutes at 50 ° C. Absorbance is measured spectrophotometrically at a wavelength of 765nm. The results are presented as milligrams of gallic acid equivalent per 100 grams of dry matter (mgGAE/100gDW).

Total flavonoids content (TFC)

Determination of TFC was performed by aluminum chloride colorimetric test according to Shams Ardecani *et al*. (2011) with certain modifications. Quantitative determination of total flavonoids were done by adding 1.2 ml of extract and 1.2 ml of 2% solution of aluminum chloride to glass tubes. The reaction mixture was incubated for 60 minutes at room temperature. Absorbance was measured spectrophotometrically at a wavelength of 420nm. An extraction solvent (80% methanol) was used as a blank. Results were presented as milligrams of quercetin equivalent per milliliter (mgQE/ml).

Total anthocyanins content (TAC)

Determination of total anthocyanins was performed by pH differential method according to Turfan *et al*. (2011). Two test tubes should be prepared for each test sample. 0.5ml of extract was added to the tubes in, and then 2ml of pH 1 buffer was added to one tube and 2mL of pH 4.5 buffer to the other. The reaction takes place for 20-30 minutes, at room temperature, in daylight. After that, the absorbance of each solution was measured at wavelengths of 500nm and 700nm. The results were presented as cyanidin-3-glucoside equivalents per gram (mgC3GE/g).

Antioxidant activity determined by FRAP method

Determination of antioxidant activity by FRAP (ferric reducing antioxidant power) method was performed according to Benzie and Strain (1996), with certain modifications (Sadeghi *et al*., 2009). The working (FRAP) reagent was incubated for 10 minutes at 37°C. Then 1ml of distilled water was added to one tube and the tubes were thermostated for 10 minutes at 37˚ C. 100µl of extract and 3 ml of heated working reagent (FRAP) were added to the tubes in succession. The mixtures were vortexed, thermostated for 10 min at 37° C, and then their absorbance was measured at 593 nm. The results are presented in µmol/l FRAP.

Antioxidant activity determined by DPPH method

Determination of antioxidant activity by DPPH method was performed according to Akpinar-Bayizit *et al*. (2016). 1ml of extract, 1ml of methanol and 0.5ml of DPPH solution were added to the glass tubes. The reaction takes place for 30 min in the dark, after which the absorbance is measured spectrophotometrically at a wavelength of 517 nm with a blank which is solvent for extraction (80% methanol). Due to background turbidity, the absorbance of the solution was measured first before the addition of DPPH, and then after the addition and development of a thirty-minute reaction, so the values are subtracted to make the results as accurate as possible. The results were presented as milligrams of trolox equivalent per 100 grams of dry matter (mgTE/100DW).

RESULTS AND DISCUSSION

Table 2 presents the content of total phenols, flavonoids, anthocyanins, as well as the antioxidant activity of the extract of the peel and seeds (*Punica granatum* L.). with a standard deviation of three measurements.

Table 2. Content of total phenols, flavonoids, anthocyanins and antioxidant activity of wild pomegranate peel samples (*Punica granatum* L.)

	Phenols (mgGAE/100gDW)	*Flavonoids (mgQE/ml)*	*Anthocyanins (mgC3GE/g)*	*FRAP (µmol/l FRAP)*	*DPPH (mgTE/100DW)*
Šušanj	701.54 ± 5.76	317.56 ± 1.53	0.45 ± 0.04	5714.28 ± 4.14	118.5 ± 3.23
Budva	750.66 ± 1.60	291.29 ± 8.93	0.90 ± 0.10	4859.34 ± 31.75	225.16 ± 2.24
Carev Laz	695.28 ± 0.88	275.11 ± 1.35	1.2 ± 0	4600 ± 5.35	205.16 ± 4.67
Škaljari	956.98 ± 4.80	236.88 ± 4.78	0.41 ± 0.008	6505.49 ± 3.53	223.5 ± 1.12
Dobrota	808.21 ± 1.83	304.52 ± 4.53	1.65 ± 0.27	5978.02 ± 8.41	226.83 ± 9.84
Brdo Gorica	905.05 ± 3.85	295.7 ± 1.35	0.53 ± 0.01	6109.89 ± 5.90	216.83 ± 1.26

According to the presented results, in methanolic extracts of wild pomegranate peel (*Punica granatum* L.), the highest amount of total phenols was recorded in the peel extract of Škaljari (956.98 ± 4.80 mgGAE/100gDW), while the lowest amount of total phenols was recorded in Carev Laz peel extracts – (695.23 ± 0.88 mgGAE/100gDW). The obtained results differ from the results of research on the content of total phenols in ethanolic extracts of wild pomegranate peel (*Punica granatum* L.) from the area of Iran, where the obtained results of research by Sarkhosh *et al*. (2009) and Derakhshan *et al*. (2018) range from 276 to 413 mgGAE/gDW and from 50.73 to 103.83 mgGAE/100gDW.

The most dominant content of total flavonoids in methanolic peel extracts was determined in the extract of the Šušanj locality, and the lowest in the peel extract of the Škaljari locality. The results range from 236.88 ± 4.78 to 317.77 ±

1.53 mgQE/g. The results obtained in this study differ from the results obtained in the study of Hajimahmoodi *et al*. (2013) where the values of determination of total flavonoids in aqueous extracts of fruit peel were presented and range from 11.46 to 23.06 mgCE/gDW. The obtained results were significantly lower compared to the results of this research, which is the result of the weak ability of water to allow the extraction of bioactive materials, as well as the use of conventional extraction methods. The obtained results of the content of total anthocyanins are in agreement with the results obtained in the research of Zhao *et al*. (2012) where the obtained values are in similar intervals. In their study, methanol was used as the extraction solvent in the same volume ratios as the test material as in this study.

The antioxidant activity of the tested extracts of wild pomegranate fruit peels was determined by two methods: FRAP and DPPH. Both methods have shown that the antioxidant capacity is at a high level. Determined by the FRAP method, the antioxidant activity of methanolic peel extracts ranges from 4600 ± 5.35 to 6505.49 ± 3.53μmol/l FRAP. The antioxidant activity of these results is relative to the study of Sharayei *et al*. (2018), where results range from 287 to 1950 μmol/l FRAP, significantly more dominant. The extraction was performed in the same way, with the ultrasonic type of extraction, with a ratio of solvent and test material of 1:10. However, water was used as the solvent. Determined by the DPPH method, the antioxidant activity of the tested extracts ranges from 118.5 to 226.83 mgTE/100gDW and is in accordance with the research of Kam *et al*. (2013) where the results range from 46 to 283 mgTE/100gDW.

Table 3 presents the content of total phenols, flavonoids, anthocyanins, as well as the antioxidant activity of wild pomegranate seed extract (*Punica granatum* L.). with a standard deviation of three measurements.

Table 3. Content of total phenols, flavonoids, anthocyanins and antioxidant activity of wild pomegranate seed samples (*Punica granatum* L.)

	Phenols (mgGAE/100gDW)	*Flavonoids (mgQE/ml)*	*Anthocyanins (mgC3GE/g)*	*FRAP (μmol/l FRAP)*	*DPPH (mgTE/100DW)*
Šušanj	120.12 ± 7.60	23.88 ± 1.18	4.09 ± 0.06	473.92 ± 0.02	106.83 ± 2.86
Budva	110.64 ± 1.75	31.18 ± 0.98	3.54 ± 0.20	326.53 ± 0.40	23.5 ± 4.10
Carev Laz	89.07 ± 2.52	12.11 ± 0.15	2.73 ± 0.39	260.77 ± 3.45	45.16 ± 0.85
Škaljari	189.77 ± 7.81	39.61 ± 1.58	4.34 ± 0.56	476.19 ± 2.86	161.83 ± 4.06
Dobrota	120.12 ± 5.30	15.05 ± 0.43	3.47 ± 0.38	349.2 ± 8.61	105.16 ± 1.02
Brdo Gorica	142.05 ± 3.17	15.2 ± 0.30	3.99 ± 0.19	453.51 ± 1.84	101.83 ± 3.40

As in determining the content of total phenols in peel extracts, the largest and smallest amounts are recorded in samples from the same localities, which leads to the conclusion that with increasing height, the amount of total phenols decreases. The obtained results are in accordance with the results of the research of Gözlekçi *et al*. (2011) where the obtained values of the research range from 125.3 to 177.4 mgGAE/100gDW, while the amount of total phenols compared to the research of Peng *et al*. (2019) where the obtained values range from 62 to 68 mgGAE/100gDW, more dominantly expressed.

The amount of total flavonoids in seed extracts ranges from 12.11 ± 1.58 to 39.61 ± 0.15 mgQE/g, where the highest amount of flavonoids was recorded in the extract of the locality Škaljari, and the lowest in the extract of the locality Carev Laz, as well as the content of total phenols. As in the case of total phenols and flavonoids, the highest amount of total anthocyanins was recorded in the extract of the locality Škaljari, and the lowest in the extract of the locality Carev Laz and the results are in the range from 2.73 ± 0.56 to 4.34 ± 0.39 mgC3GE/g. In relation to the research of Parseh and Shahablavasani (2019) where the content of total anthocyanins of wild pomegranate seed extract is 28 mgC3GE / g, the obtained results of this research deviate and the content of total anthocyanins is lower.

The antioxidant capacity of the seed extract determined by the DPPH method shows values ranging from 23.5 ± 4.10 to 161.83 ± 4.06 mgTE/100gDW. The strongest antioxidant capacity was recorded in the extract of the locality Škaljari, and the lowest in the extract of the locality Budva. The antioxidant capacity of the Carev Laz extract is 45.16 mgTE/100gDW, so it is again concluded that the antioxidant capacity, as well as the amount of total phenols, decreases with increasing altitude. Determined by the antioxidant method FRAP, the strongest antioxidant capacity was recorded in the seed extract of Škaljari, and the lowest in the extract of Carev Laz and Budva. The results range from 260.77 to 476.19 µmol/l FRAP and deviate from the results presented in the study by Sadeghi *et al*. (2009). Sadeghi *et al*. examined the antioxidant capacity of the seeds of six different varieties of wild pomegranate from Iran. Results range from 2.76 to 3.45 µmol/l FRAP. However, in this study the ratio of solvent to test sample was 1: 100 and water and ethanol, weaker solvents compared to methanol, were used as solvent.

Comparing the presented results with the results of Radunić *et al*. (2017) paper which talks about the content of phenols, flavonoids and anthocyanins of wild pomegranate (*Punica granatum* L.) juice from the territory of the Mediterranean part of Croatia, which states that the content of total phenols is 679.6 mg/100gDW, total flavonoids 393.6 mg/100g DW and total anthocyanins 81.06 mg/100gDW we conclude that the peel is a part of the fruit that is really rich in secondary metabolites, specifically phenols and that according to the above work it can match the juice.

Table 4 presents a correlation analysis of the content of total phenols, flavonoids, anthocyanins, as well as the antioxidant activity of samples of wild pomegranate fruit peel (*Punica granatum* L.).

There was a negative correlation between the content of total phenols and flavonoids in the fruit peel of wild pomegranate ($r = -0.57$), as well as a strong positive correlation between the amount of total phenols and antioxidant activity determined by FRAP method ($r = 0.81$).

Table 5 presents a correlation analysis of the content of total phenols, flavonoids, anthocyanins, as well as the antioxidant activity capacity of samples of wild pomegranate seeds (*Punica granatum* L.).

Table 4. Pearson's correlation coefficient ($p < 0.05$) for total phenols, flavonoids, anthocyanins and antioxidant capacity of wild pomegranate peel samples

	Phenols	*Flavonoids*	*Anthocyanins*	*FRAP*	*DPPH*
Phenols	1				
Flavonoids	-0.57	1			
Anthocyanins	-0.35	0.24	1		
FRAP	**0.81***	-0.21	-0.37	1	
DPPH	0.52	-0.5	0.39	0.04	1

*Bold values represent strong correlations ($p < 0.05$)

Table 5. Pearson's correlation coefficient ($p < 0.05$) for total phenols, flavonoids, anthocyanins and antioxidant capacity of wild pomegranate seed samples

	Phenols	*Flavonoids*	*Anthocyanins*	*FRAP*	*DPPH*
Phenols	1				
Flavonoids	0.36	1			
Anthocyanins	0.83	0.63	1		
FRAP	0.77	0.45	**0.96***	1	
DPPH	**0.84***	0.35	0.74	0.79	1

*Bold values represent strong correlations ($p < 0.05$) between the content of total phenols and flavonoids ($r = 0.67$). A high correlation was observed between antioxidant activity (FRAP method) and anthocyanin content ($r = 0.96$) as well as between antioxidant activity (DPPH method) and total phenol content ($r = 0.84$).

CONCLUSIONS

Comparing the results of total phenols, flavonoids, anthocyanins and antioxidant activity of samples of fruit peel and seed of wild pomegranate (*Punica granatum* L.) collected from six different localities of Montenegro, it is noted that a larger amount of these bioactive substances contains samples collected at lower altitudes, in fact those collected from coastal localities from the territory of Škaljari and Šušanj predominantly, and the smallest amount collected from higher altitudes, from the locality Carev Laz. According to the results obtained in this study, along with numerous other studies with similar research point, it is concluded that wild pomegranate biowaste is a valuable source of bioactive substances and that further research should focus on testing its effects in vivo.

REFERENCES

Akpinar-Bayizit, A., Ozcan, T., Yilmaz-Ersan, L., & Yildiz E. (2016). Evaluation of antioxidant activity of pomegranate molasses by 2,2-Diphenyl-l-Picrylhydrazyl (DPPH) method. International Journal of Chemical Engineering and Applications, 7(1), 71-74.

Albrecht, M., Jiang W. & Kumi-Diaka J. (2004). Pomegranate extracts potently suppress proliferation, xenograft growth, and invasion of human prostate cancer cells. Journal of Medicinal Food, 7, 274–283.

Braga, L.C., Shupp, J.W., Cummings, C., Jett, M., Takahashi, J.A., Carmo, L.S., Chartone-Souza, E., Nascimento, A.M. (2005). Pomegranate extract inhibits Staphylococcus aureus growth and subsequent enterotoxin production. Journal of Ethnopharmacology 96, 335–339.

Derakhshan, Z., Ferrante, M., Tadi, M., Ansari, F., Heydari, A., Hosseini, M. S., Sadrabad, E. K. (2018). Antioxidant activity and total phenolic content of ethanolic extract of pomegranate peels, juice and seeds. Food and Chemical Toxicology, 114, 108–111.

Erb, M., & Kliebenstein, D. J. (2020). Plant secondary metabolites as defenses, regulators, and primary metabolites: the blurred functional trichotomy. Plant Physiology, 184, 39-52.

Hajimahmoodi, M., Moghaddam G., Ranjbar, A., Khazani H., Sadeghi, N., Oveisi M. & Jannat, B. (2013). Total Phenolic, Flavonoids, Tannin Content and Antioxidant Power of Some Iranian Pomegranate Flower Cultivars (*Punica granatum* L.). American Journal of Plant Sciences, 4(9), 1815-1820.

Gadže, J., Voća, S., Čmelik, Z., Mustać, I., Ercisli, S. & Radunić, M. (2012). Physico-chemical characteristics of main pomegranate (Punica granatum L.) cultivars grown in Dalmatia region of Croatia. Journal of Applied Botany and Food Quality 85, 202 – 206.

Gil, M. I., Tomás-Barberán, F. A., Hess-Pierce, B., Holcroft, D. M., & Kader, A. A. (2000). Antioxidant Activity of Pomegranate Juice and Its Relationship with Phenolic Composition and Processing. Journal of Agricultural and Food Chemistry, 48(10), 4581–4589.

Gözlekçi, S., Saraçoglu, O., Onursal, E., & Özgen, M. (2011). Total phenolic distribution of juice, peel, and seed extracts of four pomegranate cultivars. Pharmacognosy Magazine, 7(26), 161.

Jacob, J., Lakshmanapermalsamy, P., Illuri, R., Bhosle, D., Sangli, G. K., & Mundkinajeddu, D. (2018). *In vitro* Evaluation of Antioxidant Potential of Isolated Compounds and Various Extracts of Peel of *Punica granatum* L. Pharmacognosy research, 10(1), 44–48.

Kam, A., Li, K. M., Razmovski-Naumovski, V., Nammi, S., Chan, K., & Li, G. Q. (2013). Variability of the Polyphenolic Content and Antioxidant Capacity of Methanolic Extracts of Pomegranate Peel. Natural Product Communications, 8(6), 707 – 710.

Mahro, B. & Timm, M. (2007). Potential of Biowaste from the Food Industry as a Biomass Resource. Life Sci., 7, 457 – 468.

Mazid, M., Khan, T. A. & Mohammad, F. (2011). Role of secondary metabolites in defense mechanisms of plants. Biology and Medicine, 3(2), 232-249.

Parseh, H. & Shahablavasani, A. (2019). Comparing total anthocyanins, total phenolics and antioxidant activities of extracts (aqueous, organic and anthocyanin) obtained from pomegranate (peel, juice, and seed) and antimicrobial activity of peel extracts on the four pathogenic bacteria. Journal of Food and Bioprocess Engineering, 2(1), 7-12.

Peng, Y. (2019). Comparative analysis of the biological components of pomegranate seed from different cultivars. International Journal of Food Properties, 22(1), 784–794.

Radunić, M., Gadže, J., Lozo, K., Šimera, E & Špika, M. J. (2017). Pomological traits, phenol and flavonoid content and antioxidant activity introduced the pomegranate (*Punica granatum* L.) cultivars grown in the Mediterranean part of Croatia. Pomologia Croatica, 21(3-4).

Sadeghi, N., Jannat, B., Oveisi, M. R., Hajimahmoodi M., & Photovat M. (2009). Antioxidant activity of Iranian pomegranate (*Punica granatum* L.) seed extracts. Journal of Agricultural Science and Technology, 11(5), 633-638.

Shams Ardecani, M. R., Hajimahmoodi, M., Oveisi, M. R., Sadeghi, N., Jannat, B., Ranjbar, A. M., Gholam, N., & Moridi, T. (2011). Comparative antioxidant activity and total flavonoid content of Persian pomegranate (*Punica granatum* L.) cultivars. Iranian Journal of Pharmaceutical Research: IJPR, 10(3), 519–524.

Sharayei, P., Azarpazhooh, E., Zomorodi, S., & Ramaswamy, H. S. (2018). Ultrasound assisted extraction of bioactive compounds from pomegranate (Punica granatum L.) peel. LWT - Food Science and Technology.

Singh, B., Singh, J. P., Kaur, A., & Singh, N. (2018). Antimicrobial potential of pomegranate peel: a review. International Journal of Food Science & Technology.

Turfan, Ö., Türkyılmaz, M., Yemiş, O., & Özkan, M. (2011). Anthocyanin and colour changes during processing of pomegranate (*Punica granatum* L., cv. Hicaznar) juice from sacs and whole fruit. Food Chemistry, 129(4), 1644–1651.

Tzulker, R., Glazer I., Bar-Ilan I., Holland D., Aviram M. & Amir R. (2007)**.** Antioxidant activity, polyphenol content and related compounds in different fruit juices and homogenates prepared from 29 different pomegranate accessions. Journal of Agricultural Food and Chemistry, 55, 9559–9570.

Vieira, V. H. A. de M., & Matheus, D. R. (2019). Environmental assessments of biological treatments of biowaste in life cycle perspective: A critical review. Waste Management & Research, 1-16.

Viuda-Martos, M., Fernández-López, J., & Pérez-Álvarez, J. A. (2010). Pomegranate and its Many Functional Components as Related to Human Health: A Review. Comprehensive Reviews in Food Science and Food Safety, 9(6), 635–654.

Zaynab, M., Fatima, M., Sharif, Y., Zafar, M. H., Ali, H., & Khan, K. A. (2019). Role of primary metabolites in plant defense against pathogens. Microbial Pathogenesis, 103728.

Vasylyshyna, O., Chernega, A. *(2022). The effect of food coating treatment on the change of chlorogenic and caffeic acid content in cherry fruits in period of storage. Agriculture and Forestry, 68 (2): 167-174. doi:10.17707/AgricultForest.68.2.12*

DOI: 10.17707/AgricultForest.68.2.12

Olena VASYLYSHYNA[1], Andrii CHERNEGA[1]

THE EFFECT OF FOOD COATING TREATMENT ON THE CHANGE OF CHLOROGENIC AND CAFFEIC ACID CONTENT IN CHERRY FRUITS IN PERIOD OF STORAGE

SUMMARY

The article detected the effect of pre-treatment of cherry fruits with solutions of chitosan and salicylic acid on the content of chlorogenic and caffeic acid. The research have been conducted at the research station of pomology named after L.P. Symyrenko of the Institute of Horticulture of NAAS with cherry fruits of varieties 'Alpha' and 'Pamiat Artemenko'. For studies of 15 trees of each variety the day before harvest, sprayed with a solution of 1% chitosan; 1% chitosan with salicylic acid (100 mg L^{-1}). Fruits were removed at the consumer stage of ripeness from four different places of the crown from each tree of a certain variety and type of processing, placed in boxes weighing 5 kg for storage at a temperature of 1±0.5 °C and relative humidity of 95 ± 1%. Unprocessed cherry fruits were taken as a control. It was found that pre-treatment of cherry fruits with solutions of polysaccharide compositions contributed to the significant preservation of phenolic substances. Moreover, the most effective was the treatment of fruits with a solution of chitosan with salicylic acid, in which the loss of phenolic substances was 5.0−5.5%, including chlorogenic – 10.0−11.0% and caffeic acid – 36.8−40.1%.

Keywords: period of storage, coating treatment, phenolic substances, cherry fruits, chitosan

INTRODUCTION

Tart cherry is widely used in the food industry, and some are excellent for fresh consumption. The beneficial effects of fresh tart cherry consumption on health has also been proven. To increase the fresh consumption of cherry tart we need to provide longer availability of fresh fruit. Tart cherries are non-climatic fruits, therefore harvested fruit can be stored for a few days without significant decay. Appropriate storage, preserving nutritional value of fruits and inhibiting

[1]Olena Vasylyshyna, Andrii Chernega*(corresponding author: elenamila@i.ua), Uman National University of Horticulture, Institutska 1, Uman city, 20301, UKRAINE.
Notes: The authors declare that they have no conflicts of interest. Authorship Form signed online.
Recieved:20/11/2021 *Accepted:01/06/2022*

decay should be developed by using pre- and postharvest technologies. Chitosan has been found to be an effective preharvest treatment against decaying fungi in cherry. Different biofungicides effectively reduced the incidence of monilia-rot and other postharvest diseases. Several authors' research has shown that it is better to apply MAP with high (10%) CO_2 content during the storage of tart cherry than normal atmosphere. The not completely anaerobic conditions with increased CO_2 level in combination with cooling can slow the quality of deterioration of the fruit. There are few observations on pre- and postharvest technologies in the case of tart cherry, therefore, more research is necessary to develop successful storage technology methods that have been successfully applied to similar fruits. By achieving the most suitable storage technology, it would be possible to increase shelf-life, which would positively influence the increase in the consumption of fresh tart cherry (Mihaly *et al.*, 2019).

Shows the results of the research into marketability evaluation of sour cherry (*Prunus cerasus L.*) fruits, treated with chitosan solution. Fruits were treated with 0.5 % or 1 % chitosan solution, and stored at 5 °C. After 21 days of storage of sour cherry fruits the mass loss made up 4.6 % with 85.5 % output of marketable products (Vasylyshyna, 2018).

Polyphenols are a large group of secondary metabolites of the plant with a broad spectrum of biological action, exhibiting antioxidant activity. Studies have shown that the content of polyphenolic compounds and antioxidant activity of stone fruits depends on the characteristics of the variety (Goncalves *et al.*, 2004; Dziadek *et al.*, 2019).

The most important component of stone fruits, especially cherries, are phenolic substances, the content of which, depending on varietal characteristics and place of cultivation, varies significantly from 321 to 3370 mg / 100 g. - glucorutinoside, cyanidin-3-rutinoside and cyanidin-3-glucoside. Up to 40% of the amount of phenols is the content of flavan-3-oils and about 25% - flavonols and phenolic acids with the advantage of quercetin-3-rutinoside and chlorogenic acid, respectively (Wojdyło *et al.*, 2014; Yezhov *et al.*, 2019; Vasylyshyna, 2020).

In period of storage, the content of chlorogenic and caffeic acids changes. Thus, after six months of storage, the concentration of polyphenolic compounds of carrots of Nantes variety decreased caffeic acid by 64.6%, chlorogenic by 37.9% (Augqpole *et al.*, 2017).

The content of caffeic acid in the fruit due to its fungitoxic properties accelerates the process of suberinization, as well as helps to preserve them in period of transportation and storage.In response to damage to the fruit increases the content of chlorogenic acid. Which stimulates the formation of wound periderm. In contrast, caffeic acid inhibits these processes. Studies (Demyanets, *et al.*, 1974; Vasylyshyna, 2016) have shown that on the third day after injury there is a maximum accumulation of chlorogenic acid, after which its content decreases. In contrast, the maximum accumulation in the wound zone of caffeic acid occurs after 14 days.

Chlorogenic acid is thought to be a chemical barrier to the passage of microorganisms and provides reliable protection against damage. In addition, the appearance of darkening of the skin (tan) and pulp of the fruit is explained by the enzymatic oxidation of chlorogenic acid (Demyanets, *et al.*, 1974; Vasylyshyna, 2016).

There is an inverse correlation between the content of chlorogenic acid and the degree of browning of the fruit. More resistant to browning fruits are characterized by a high content of chlorogenic acid and its economical consumption (Vasylyshyna, 2016).

Protection of fruits from damage and economical consumption of chlorogenic and caffeic acid is possible only with proper organization of storage of fruits and vegetables. Polysaccharide-based preparations are now used for post-harvest ripening: chitosan, salicylic acid, and others (Rassa, *et al.*, 2013; Giméneza, *et al.*, 2016; Adiletta, *et al.*, 2019).

The purpose of the study was to study the effect of pretreatment with a solution of chitosan and salicylic acid on the change in the content of chlorogenic and caffeic acid in period of storage of sour cherry.

MATERIAL AND METHODS

Methods the research was conducted during 2018 year on the basis of the research station of pomology named after L.P. Symyrenko of the Institute of Horticulture of NAAS with cherry fruits of varieties Alpha and Pamiat Artemenko. For studies of 15 trees of each variety the day before harvest, sprayed with a solution of 1% chitosan; 1% chitosan with salicylic acid (100 mg L^{-1}). Fruits were removed at the consumer stage of ripeness from four different places of the crown from each tree of a certain variety and type of processing, placed in boxes weighing 5 kg for storage control fruits 15 days and experiment – 30 days at a temperature of 1±0.5 °C and relative humidity of 95±1%. Unprocessed cherry fruits were taken as a control. The experiment was repeated three times.

Phenolic compounds. The content of phenolic substances was determined by the Folin-Chocalteu method (Fruits, vegetables and products, 2006). Total phenolic content was determined spectrophotometrically KFK-2 (Russia), according to the Folin–Ciocalteu. Briefly, 1.0 mL of the sample was pipetted into a 10 mL volumetric flask containing 0.5 mL of Folin–Ciocalteu reagent (The Folin–Ciocalteu reagent be prepared by dissolving 100 g sodium tungstate (VI) dihydrate and 25 g sodium molybdate (VI) dihydrate with 700 ml distilled water, 100 ml concentrated hydrochloric acid, and 50 ml of 85% phosphoric acid to which is added 150 g of lithium sulphate hydrate), 5 mL of distilled water and 1.5 mL of Na_2CO_3 solution (w = 20 %), and the volume was made up with distilled water. After one hours, the absorbance of blue coloration was measured at λ = 670 nm against a blank sample. The measurements were compared to a standard curve of prepared rutin solutions (50, 100, 150, 250, 500 mg L^{-1}) and expressed as milligrams of rutin per 100 g ± SD. All measurements were performed in triplicate.

Chromatography. The content of chlorogenic and caffeic acid was determined by high performance liquid chromatography with diode matrix detector (chromatograms with absorption spectra) on a Waters 2998 instrument (USA) (Guidelines for methods of quality control, 2004). For research, an analytical column dimensions 250 mm × 4.6 mm filled with sorbent Diaspher-110-C18 (6 µm). Injection volume of a sample was 0.7-1.0 mL/minute. For the preparation of eluents used the mobile phase consisted of water, acetonitrile (“Cryochrome”) and formic and orthophosphoric acid solution (1:1:0.1). The extracts were filtered and diluted with water (1: 5) before analysis. The relative content of chlorogenic and caffeic acid is defined as the ratio of the area of the chromatographic peak and the sum of the peak planes of all identified acids (*Guidelines for methods of quality control*: P 4.1.1672-03, 2004).

Statistical analysis. Data were expressed as mean ± stan-dard deviation; for mathematical data processing the value of $p<0.05$ was regarded as statistically significant. Two-way analysis of variance (ANOVA) was used to deter-mine the significance of differences. The statistical analyses were performed STATISTICA 6.

RESULTS AND DISCUSSION

The content of phenolic substances in fresh cherry fruits was significant and was at the level of 2270−2280 mg/100 g (Fig. 1). During storage, its content decreased by 5.9−6.1%. In the treated cherry fruits with chitosan solution, the losses decreased to the level of 5.6–5.7%, and they were the smallest when used for pre-treatment of a compatible solution of chitosan with salicylic acid - 5.0–5.5%.

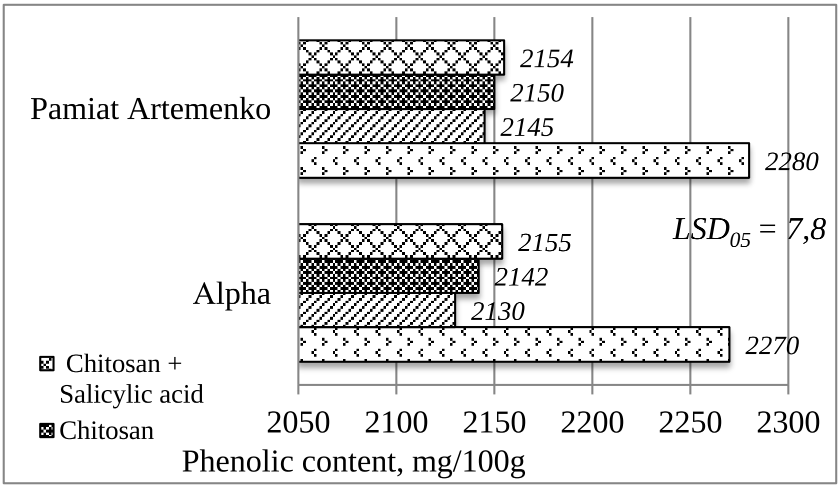

Figure 1. Change in the phenolic content of cherry fruits in period of storage

Their content chlorogenic acid in fresh cherries of the Pamiat Artemenko and Alpha varieties was at the level of 301 and 308 mg/100 g, respectively (Fig.

2). After storage, itscontent in the control version decreased by 1.5 times, and in pre-treated cherries, losses were lower and at the level of 13.6–14.9% in chitosan and 10.0–11.0% in chitosan and salicylic acid.

Similar to chlorogenic acid, there were changes in caffeic acid (Fig. 3). In particular, its content in fresh cherry fruits was at the level of 30.4–35.2 mg /100 g. During storage, it decreased by 1.9–2.0 times, and cherry fruits, pre-treated with polysaccharide compositions, had losses of caffeic acid at the level of 1.6–1.7 times.

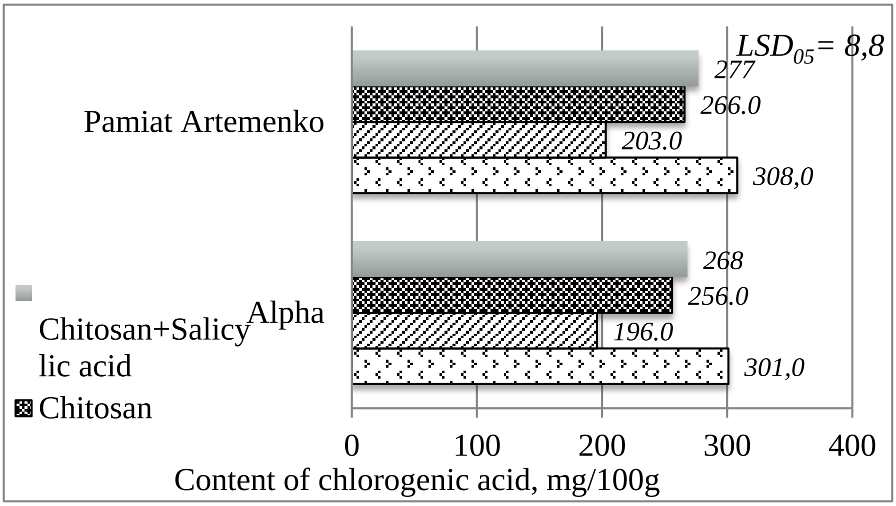

Figure 2. The content of chlorogenic acid in cherry fruits at the end of storage

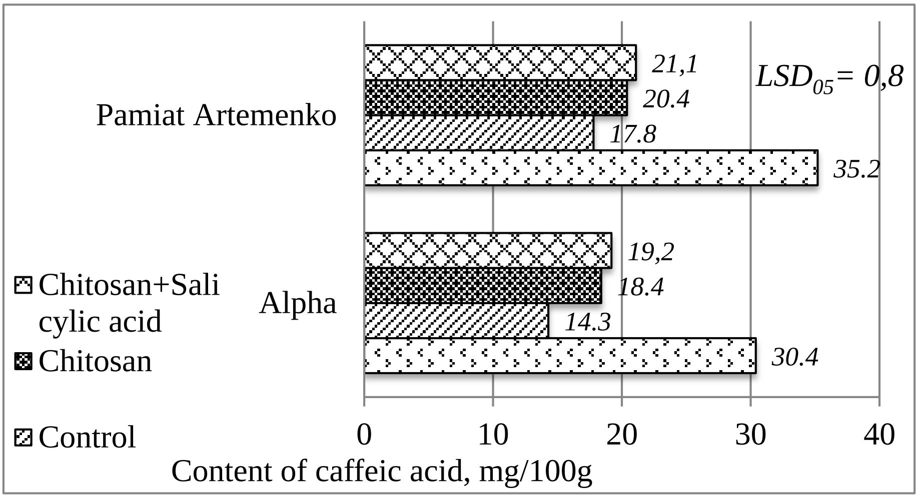

Figure 3. The content of caffeic acid in cherry fruits at the end of storage

As a result of the conducted researches the significant content of phenolic substances in cherry fruits was established - at the level of 2270–2280 mg /100 g, of which 301−308 mg/100g are chlorogenic, and 30.4−35.2 mg/100 g - caffeic acid.

During fruit storage, the content of phenols decreased by 5.9−6.1%, including chlorogenic acid by 1.5 and caffeic acid by 1.9−2.0 times.

Strong correlations (r = 0.75–0.97) were found between the content of phenolic substances, chlorogenic and caffeic acids and the corresponding regression equations were derived (Fig. 4).

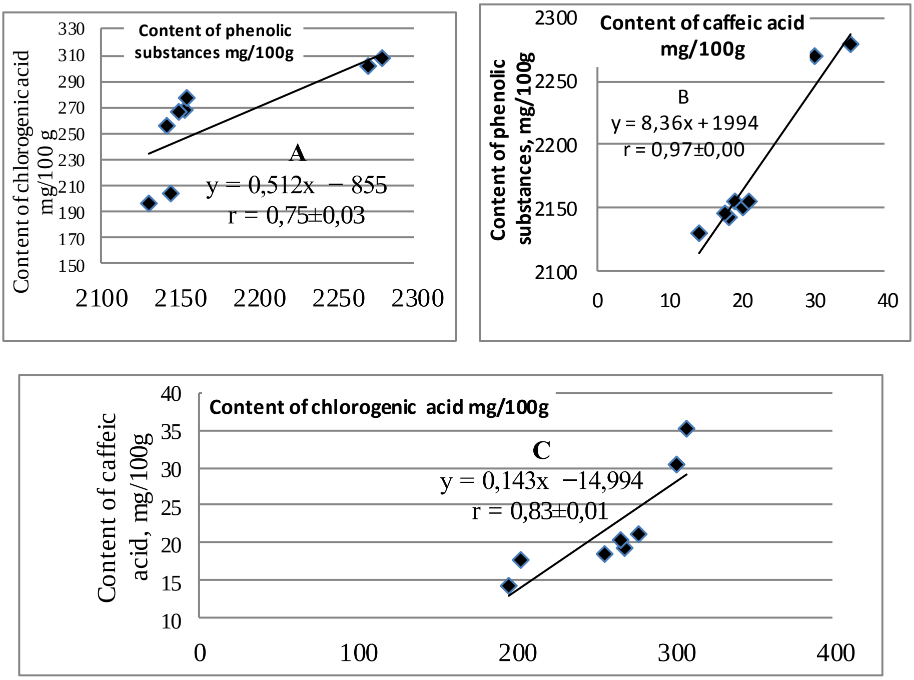

Figure 4. Correlation between the content of phenolic substances and chlorogenic acid (A); content caffeic acid and phenolic substances (B); content chlorogenic acid and caffeic acid (C) in cherry fruits

Were found between the content of phenolic substances, chlorogenic and caffeic acids strong correlations.

DISCUSSION

New storage technology, it would be possible to increase shelf-life, which would positively influence the increase in the consumption of fresh tart cherry (Mihaly *et al*., 2019). The results of the research Vasylyshyna (2018) into evaluation of sour cherry (Prunus cerasus L.) fruits, treated with chitosan solution, and stored at 5 °C after 21 days of storage of sour cherry fruits the mass loss made up 4.6 % and the quality of the chemical composition of cherry fruits changed.

Because sour cherries have unique anthocyanin content, and they are rich in phenolic compounds 2270–2280 mg/100 g. Our variability between sour cherry in total phenolics and anthocyanins confirming the results of Pedisic *et al*. (2010), Wojdylo *et al*. (2014), Stan *et al*. (2015). A significant part (25%) of the content of phenolic substances is accounted for by flavonols and phenolic acids with a predominance of chlorogenic acid (Yezhov *et al*, 2019). Phenolic acid contents generally decreased during storage by 5.9–6.1%, including chlorogenic acid by 1.5 and caffeic acid by 1.9–2.0 times. The data obtained by us are similar to the results of research performed Goncalves *et al*. (2007), Augqpole *et al*. (2017) on the reduction of chlorogenic and caffeic acid in period of storage of fruit.

And cherry fruits, pre-treated with polysaccharide compositions in chitosan and salicylic acid, had losses of caffeic acid at the level of 1.6–1.7 times of chlorogenic acid of 10.0–11.0%. According to research more resistant to browning fruits are characterized by a high content of chlorogenic and caffeic acid and its economical losses Demyanets, *et al*. (1974).

The obtained results are a consequence of the fact that the solutions used for fruit pretreatment form an additional barrier on the fruit surface, slowing down the intensity of transpiration processes and reducing the degradation of phenolic compounds (Krasniewska *et al.*, 2017).

CONCLUSIONS

Preservation of phenolic substances pretreatment of cherry fruits with solutions of polysaccharide compositions contributed. The most effective was the treatment of fruits with a solution of chitosan with salicylic acid in which the loss of phenolic substances was 5.0–5.5%, including chlorogenic - 10.0–11.0% and caffeic acid - 36.8–40.1%.

Therefore, in practice the content of chlorogenic and caffeic acids in the fruit during storage can determine the quality and suitability for fresh storage. To preserve the quality of cherry fruits before storage, they must be treated with a solution of 1% chitosan and 100 mg L^{-1} salicylic acid.

REFERENCES

Adiletta, G., Zampella, L., Coletta, C., Petriccione, M. (2019). Chitosan coating to preserve the qualitative traits and improve the antioxidant system in fresh figs (*Ficus carica* L.). Agriculture, 9(4): 84–96. DOI: 10.3390/agriculture9040084

Augqpole, I., Kince, T., Cinkmanis, I. (2017). Changes of polyphenol compound concentrations in hybrids of carrots of Nante sort during storage. Proceedings. Latvian Academy of Sciences, 71(6): 492–495. DOI: 10.1515/prolas-2017-0085

Demyanets, E.F., Rybak, H.M. (1974). Lesions of apple fruits by browning of the skin during long-term storage, depending on the content of some phenolic substances. Physiology and biochemistry of cultivated plants, 3: 293. (in Russian)

Dziadek, K., Kopec, A., Tabaszewska, M. (2019). Potential of sweet cherry (*Prunus avium L.*) by-products: bioactive compounds and antioxidant activity of leaves and petioles. European Food Research and Technology, 245: 763–772. DOI: 10.1016/j.lwt.2011.12.015

Fruits, vegetables and products of their processing. Methods for determining the content of polyphenols: DSTU 4373: 2005. Kyiv: Derzhspozhyvstandart of Ukraine, 2006: 6.

Giméneza, M.J., Valverdea, J.M., Valero, D., Zapata, P.J., Castillo, S., Serrano, M. (2016). Postharvest methyl salicylate treatments delay ripening and maintain quality attributes and antioxidant compounds of 'Early Lory' sweet cherry. Postharvest Biology and Technology, 117: 102−109. DOI: 10.1016/j.postharvbio.2016.02.006

Goncalves, B., Landbo, A.-K., Knudsen, D., Silva, A. P., Moutinho-Pereira, J., Rosa, E. (2004). Effect of ripeness and postharvest storage on the phenolic profiles of cherries (*Prunus avium L.).* Journal of Agricultural and Food Chemistry, 52 (3): 523–530. DOI: 10.1021/jf030595s

Goncalves, B., Silva, A.P., Moutinho-Pereira, J., Bacelar, E., Rosa, E., Meyer, A.S. (2007). Effect of ripeness and postharvest storage on the evolution of colour and anthocyanins in cherries (*Prunus avium L*.). Food Chemistry, 103: 976–984. DOI:10.1016/j.foodchem.2006.08.039

Guidelines for methods of quality control and safety of biologically active food additives. P 4.1.1672-03. Ministry of Health of Russia, Moscow, 2004: 237.

Krasniewska, K., Scibisz, I., Gniewosz, M., Mitek, M., Pobiega, K., Cendrowski, A. (2017). Effect of pullulan coating on postharvest quality and shelf-life of highbush blueberry (*Vaccinium corymbosum L*.). Materials, 10 (8): 965−970. DOI: 10.3390/ma10080965

Mihaly,K., Kovacs,C., Takacs, F., Sandor, E (2019). Pre- and postharvest technologies to extend the shelf life of Prunus cerasus. Acta agrarian Debreceniensis, (1): 85−89. DOI: 10.34101/actaagrar/1/2376

Pedisic, S., Dragovi-Uzelac, V., Levaj, B., Skevin, D. (2010). Effect of vaturity and geographical region on anthocyanin content of sour cherries (*Prunus cerasus var. marasca*). Food Technol. Biotechnol, 48 (1): 86–93.

Rassa, M., Ghasemnezhad, M., Zareh, S., Sajedi, R.H. (2013). Effect of chitosan coating on maintenance of aril quality, microbial population and PPO activity of pomegranate (*Punica granatum* L. Cv. Tarom) at cold storage temperature. Journal Science of Food and Agriculture, 93 (2): 368−374. DOI: 10.1002/jsfa.5770. Epub 2012 Jul 20.

Stan, A., Popa, M.E. (2015). Pretreatment and freezing storage effect on antioxidant capacity of sour cherries and correlation with color changes. Romanian Biotechnological Letters, 20(5): 10826−10834.

Vasylyshyna, O.V. (2016). Changes in biologically active substances, chlorogenic and caffeic acids in cherry fruits during storage in their treatment with antimicrobial substances. Visnyk of Uman National University of Horticulture. Uman, 2: 35−38.

Vasylyshyna, O.V. (2018). The quality of sour cherry fruits (*Prunus cerasus L.),* treated with chitosan solution before storage. Acta agriculturae Slovenica, 111(3): 633−637.

Vasylyshyna, O. (2020). Changing the antioxidant activity of cherry fruits during storage by means of pre-treatment with polysaccharide compositions. Bulletin of the Transilvania University of Brasov, 13 (62): 157−164. DOI: 10.31926/but.fwiafe.2020.13.62.2.14

Wojdyło, A., Nowicka, P, Laskowski, P., Oszmiański, J. (2014). Evaluation of sour cherry (*Prunus cerasus L*.) fruits for their polyphenol content, antioxidant properties, and nutritional components. Journal of Agricultural and Food Chemistry, 62: 12332−12345. DOI: 10.1021/jf504023z

Yezhov, V.M., Grynyk, I.V. (2019). Biochemical aspects of selection of fruit crops of the genus *Prunus L.* Horticulture, 74: 5−15.

Marić, D., Burzanović, K., Marić, S. (2022). Variability of length weight relationship and condition factor of the European eel (Anguilla anguilla l.) – case study from the Lake Skadar (Montenegro). Agriculture and Forestry, 68 (2): 175-191. doi: 10.17707/AgricultForest.68.2.13

DOI: 10.17707/AgricultForest.68.2.13

Drago MARIĆ[1], Katarina BURZANOVIĆ[2], Stevan MARIĆ[3*]

VARIABILITY OF LENGTH WEIGHT RELATIONSHIP AND CONDITION FACTOR OF THE EUROPEAN EEL (*Anguilla anguilla* L.) – CASE STUDY FROM THE LAKE SKADAR (MONTENEGRO)

SUMMARY

The results presented contribute to the knowledge about the length-weight relationships (LWR) of the European eel (*Anguilla anguilla*). When using the results presented in this study, it should borne in mind that the samples were taken during the year and the number of fish examined was relatively large. LWRs parameters are calculated for the two different length classis and found significant. In the present study, bigger specimens (45 cm) of European eel have value of growth coefficient b = 3.25. This value is significantly higher than the b = 3 showing that weight of this fish increases more than cube of its length (positive growth coeffient). The lesser specimens (<45 cm) of European eel have value of growth coefficient b = 2.54, and this value is significantly smaler than the b = 3. The relationship between total length (TL) and weight (W) was described by the equation:

Length <45 cm (n = 320), $Y = 0.0098x^{2.5398}$ $R^2 = 0.8362$

Length ≥45.1 cm (n = 346), $Y = 0.0007x^{3.2525}$ $R^2 = 0.8971$

The values of condition factor (CF) were ranged from 0.13-0.25 (average 17.0-18.5) and smalest were found in the December.

Analysis of the total sample, of any species, cannot show by what rule the population grows, if infrapopulation variability is present, because the studied value will depend on the number of individual subgroups. The estimations of LWRs shall be helpful in future works on by catch of fish species in Skadar Lake in Montenegro and Albania.

Keywords: European eel, LWR, CF, infrapopulation variability, seasonal cycle

---

[1]Drago Marić, University of Montenegro, Department of Biology, Faculty of Sciences, P.O. Box 328, 20000 Podgorica, MONTENEGRO.
[2]Katarina Burzanović, Ministry for Agriculture, Forestry and Water management, Directory for Fisheries, Rimski trg, 46, 81000 Podgorica, MONTENEGRO.
[3]Stevan Marić* (Coresponding autor: stevanmaric@nparkovi.me), National Parks of Montenegro, 81000 Podgorica, MONTENEGRO.

Notes: The authors declare that they have no conflicts of interest. Authorship Form signed online.
Recieved:10/03/2022 *Accepted:22/05/2022*

INTRODUCTION

The European eel (*Anguilla anguilla*) is found and exploited in most European water bodies and a number of sites in northern Africa (Dekker, 2000). It inhabits the basin of Skadar Lake and small tributaries of the Adriatic Sea in Montenegro (Marić, 2019). European eel landings have decreased rapidly throughout Europe since the 1960s (ICES, 2019). The same applies for the Skadar Lake of Montenegro, where European eel the permanent decrease (R^2 = 0.76) over the entire period (70 years), (Marić, 2018).

Fishery management of European eel (*A. anguilla*) has received increasing attention by both the scientific community and fisheries agencies in the last years (ICES, 2019). *A. anguilla* has been recently listed in Annex B of CITES, and the European Council adopted a regulation (EC 1100/2007) aimed at recovering the stock through the drawing up of Eel Management Plans (EMPs) at a river basin scale. Montenegro has no long-term management plans. Basic information about this species is missing. Some biological characteristics are partial or analyzed on a small number of specimens, e.g. abundance, length-weight rationship, conditions, etc.

The length-weight relationship is very important for proper exploitation and management of the population of fish species (Anene, 2005). These data are needed to estimate growth rates, length and age structures, and other components of fish population dynamics (Kolher *et al*. 1995). Length-weight relationships allow fisheries scientists to convert growth-in-length equations to growth-in-weight in stock assessment models, estimate biomass from length frequency distributions, compare life history and morphological aspects of populations inhabiting different regions and calculate fish condition (Petrakis & Stergiou 1995; Vaslet *et al*. 2008; De Giosa *et al*. 2014; Özpiçak *et al*. 2018 Froese & Pauly 2020 and etc). The length-weight relationships of some fishes in Montenegrin waters have been studied, e.g. Milošević & Marić (2012); Milošević *et al*. (2012); Marić & Rakočević (2015); Marić & Burzanović (2021) studied the length-weight relationships of some fish species (e.g. *Rutilus* spp., *C. carpio*, *S. farioides*, *A. scoranza*) in the Skadar Lake watershad. In fisheries science, the condition factor is used in order to compare the "condition", "fatness" or wellbeing of fish. It is based on the hypothesis that heavier fish of a particular length are in a better physiological condition (Bagenal, 1978). Condition factor is also a useful index for monitoring of feeding intensity, age, and growth rates in fish (Le Cren, 1951; Weatherley 1972; Marić & Burzanović 2021). It is strongly influenced by both biotic and abiotic environmental conditions and can be used as an index to assess the status of the aquatic ecosystem in which fish live (Anene, 2005; Simon, 2007).

Insufficient knowledge of the growth pattern, as well as the condition of the *A. anguilla* in this lake is the main reason-goal of studying this species in this paper. The aim of this study was to evaluate the length-weight relationship and condition of the native European eel population from the Skadar Lake.

Consideration of the life-history strategies of the European eel should be of great significance to fisheries management, restoration and monitoring.

MATERIAL AND METHODS

Area and habitat study

Skadar Lake is a karst lake created by inundation of a karstic field. It is situated on the border of Montenegro and Albania, ⅔ of the lake belongs to Montenegro (Figure 1). It is situated between 18^o 41' and 19^o 47' of eastern geographical longitude and between 42^o 58' and 40^o 10' of northern geographical latitude, with the surface area that fluctuates seasonally from approximately 370 to 540 km^2 and water level also varies seasonally from 4.7 to 9.8 m above sea level. The shape of lake is elongated oval with peak width of circa 14 km at average water level, and it is approximately 44 km long (NW-SE direction), with the mean depth of 5 m (Beeton, 1981).

Figure **1.** Map of the Skadar Lake and the European eel distribution (marked with orange lines) in Montenegro.

Waters from the watershed reach the lake by ground or underground water courses, through a number of sublacustrine springs (so called “oka” – “eye”). The largest tributary of Skadar Lake is the Moraca River which brings around 62% of water, while the waters flow away from the lake into the sea by the Bojana River; its average flowing through is over 300 m^3/sec. Average monthly water temperatures range 5-7 ^oC in winter, to 25-28 ^oC in summer. During the summer the transparency of lake waters is 2-3 meters, but in winter it increases reaching up to 5 meters (Petrović, 1981; Kastratović, 2018).

The lake represents one of the most important centers of biodiversity for Western Balkan and SouthEastern Europe (Marić & Rakočević 2010) with more than 100 species of water birds (Vizi, 2018) and 41 (34 autohtonusand 7 alohtonus) fish species (Marić, 2019). Fish in this watershed have significant economic potential. A large number of species are important mainly for sports–recreational fishing, whereas a lesser number are economically useful in terms of gaining profit. If we observe the lake in its entirety, it should be stated that there is little precise and reliable data on the catch of fish (Marić, 2018).

The average chlorophyll a concentration indicates mesotrophic conditions in Lake Skadar, but during midsummer, when the highest phytoplankton abundance and biomass occurs, the trophic level of the lake increases to eutrophy (Rakočević, 2018).

Data

Data of 666 specimens of European eel (*A. anguilla*) were collected in the Skadar Lake. Fishes were collected during autumn (early December), Spring (March and April) and summer (August) i.e. 5 samples were collected in 2014-2015. Sampling was carried out from boats by means of 4.0 kW electric stunning devices; these devices supplied continuous pulsating current (direct current), along rocky shores and the borders of reed areas. Sampling was conducted from March 2014 to April 2015. All eels were killed by freezing and then it were immediately freshly measured. Total length (cm) of each fish was measured from the tip of the snout (mouth closed) to the extended tip of the caudal fin using a measuring board (±0.1 mm). Body weight (fresh) was recorded to the nearest gram using electronic balance (±0.1 g).

The relation between the weight and the length is given by the equation $W = aL^b$, where *W* is the total weight in grams, *L* the total length in centimetres, *a* the factor and *b* the exponent (Ricker, 1975). The parameters *a* and *b* of the *L-W* relationships were estimated by the power functions (regression method). The deviation of regression coefficient *b* from 3 was tested by calculating t value, t = (*b*-3)/*Sb*, where Sb was given as: $Sb = \sqrt{}\ [(SW / SL) - b^2]$ / n-2, where *SW* is the variance of the body weight, *sL*, the variance of the total length and n the sample (Lawson *et al*. 2013). Because the LWR for the same fish species is often different between adults and juveniles (Safran, 1992; Marić & Rakočević 2015; Marić & Burzanović 2021), the LWR relationships were calculated separately by length groups. Four size classes were established units and included: eel less than 40 cm TL, those between 40.1 - 45.0 cm TL, than 45.1 - 50.0 cm TL and those greater than 50.1 cm TL.

Condition factor (CF) of the eels was calculated using the formula of Fulton (1904): CF = W^x 100/L^3, where, CF - Condition factor; W – total weight of body (in g); L – total lenght of body (in cm), the factor 100 is used to bring K close to unity (Froese, 2006). The coefficient of determination (R^2) was used as an indicator of the quality of the regression (Scherrer, 1984).

Statistical methods used for data analysis included the usual calculations of means and standard deviations. Analysis of variance (ANOVA) and the Tukey HSD test were used to assess differences between observed variables (mean length, mean condition factor and *b* the exponent) in the different periods (five). A t-test was used for testing significant of the coefficient of determination and the significant difference of *b* values from 3, which represent isometric growth. The statistical analyses, e.g. two-way ANOVA and t-test, were performed with the statistical program SPSS (Statistical Package for the Social Sciences) version 9.0. All the statistical analyses were considered at a significance level of 5%; 1% or % 0.1 (P <0.05; P <0.01 or P <0.001).

Ethical Statement

This study does not need any formal consent as the experimental fish because fishing is carried out commercially in Montenegro.

RESULTS AND DISCUSSION

Table 1. reports the basic statistics of length (TL) and weight (W) data (by year) for the 2014-2015 European eel samples from the Skadar Lake. The sample was composed of 666 specimens. The TL and W of the specimens analyzed varied between 30.0 and 67.0 cm, 51.5 and 740.0 g, respectively.

Table **1**. Basic statistics of length, weight, standard deviation (±) and n data (by year) from eel samples from March 2014 to April 2015

Periods	N	TL: Min-max	W: Min-max	TL and W: Average
March (total)	118	40.0 - 67.0	120.0-740.0	53.08 (293.06)
March > 45	103			52.58 ±6.15 (±SD)
June (total)	209	31.1 - 60.0	53.8 - 408.4	42.81 (153.87)
June>45	79			50.14 ±3.78
August (total)	144	30.0 - 64.5	51.5 - 500.0	43.68 (164.84)
August >45	52			50.9±5.06
December (total)	116	40.1 - 63.0	105.0 - 580.0	49.73 (229.79)
December >45	76			52.18 ±5.84
April (total)	120	32.5 - 61.0	55.8 - 553	48.09 (214.30)
April>45	73			53.58 ±5.28

Average length of the investigated eel from five periods ranged from 42.81 to 53.08 mm and body weight from 153.78 to 293.06 g. ANOVA show a statistically significant difference (P < 0.01) between five periods (f = 3.75., P =

0.005.,) for total length. Post Hoc Tukey (Tukey's HSD) test show a statistically significant difference between April and June (Q = 5.01, P = 0.004), than April and August (Q = 3.9, P = 0.048). No signfcant differences were found between the average leigth of the investigated European eel biger than 45 cm from five periods ($P > 0.05$).

The Fulton's condition faktor (CF) varied from 0.13 to 0.25 (Table 2). The condition faktor undergoes minor changes in specimens belonging to different size classes. ANOVA show a statistically significant difference ($P < 0.01$) between five periods (f = 5.54., P = 0.002) for CF.

Table **2**. The monthly values of the condition factor for eel from March 2014 to April 2015

Periods	N	Min	Max	Average (SD)
Mart (total)	102	0.15	0.25	0.183 (0.022)
June (total)	209	0.14	0.23	0.184 (0.019)
August (total)	119	0.13	0.23	0.181 (0.02)
December (total)	116	0.14	0.22	0.175 (0.02)
April (total)	120	0.13	0.22	0.178 (0.019)

The smallest values of condition factor were recorded in the specimens from period December (Table 2). Post Hoc Tukey (Tukey's HSD) test show a statistically significant difference between three group/pairs: June vs December (Q = 5.97, P = 0.00027), June vs April: Q = 4.14, P = 0.02914), and August vs December (Q = 4.09, P = 0.03256). Differences is not significant at $p < 0.01$ between five periods in specimens large than 45 cm.

The number of individuals sampled (N), the length and weight ranges, parameters a and b of the length-weight relationships and the determination coefficient (R^2) for the five periods are given in Table 3. According to LWRs determined for yearly data (2014-2015) the *A. anguilla*, exhibited pozitive allometric growth for specimens biger than 45 cm, because b value was always bigger than 3 for each month of observation (Table 3). The length-weight relationship for the pooled data (N = 346) is presented in Fig. 3.

The relationship between total length and weight showed a strong pozitive correlation ($R^2 > 0.90$, $P < 0.001$, Table 3) for all size classes > 45 cm Tl. Within the size range of length lesser then 40 cm and weight lesser then 150g, the European eel appeared not to follow the cube law (b = 2.56 - 2.85). This value of b was significantly lesser than 3 ($P < 0.001$). In size classis of length lesser than 45 cm (and 200 g) value of b varied between 2.8677 - 2.7966. The allometric exponent b of size classis lesser than 45 cm is greater than that of size classis lesser than 40cm, buth both exhibited negative gowth parern, which shows that they increase in weight at a comparatively lower rate than the larger fish. The relationship between Total length and weight showed pozitive correlation (R^2 = 0.678 - 0.94, $P < 0.01$, Table 3) for all size clasis.

Table **3**. Values of α and b parameters and R^2 in separate size length for months/periods

Periods	N	*a*	*b*	R^2
March (45 - 70 cm)	102	0.0006	3.2843	0.9232
June (30 - 40 cm, < 120 g)	58	0.0078	2.5910	0.8125
June (30 - 45 cm)	130	0.0030	2.8677	0.8709
June (40 - 50 cm)	120	0.0018	2.9943	0.7818
June (45 - 60 cm)	79	0.0004	3.3977	0.9053
June (50 - 60 cm)	31	0.0005	3.3578	0.678
August (30 - 40 cm < 120 g)	36	0.0085	2.5621	0.7616
August (30 - 45)	67	0.0037	2.7966	0.8565
August (40 - 50 cm)	50	0.0019	2.9771	0.7688
August (40 - 65 cm)	80	0.0009	3.1815	0.9393
August (45 - 65 cm)	52	0.0007	3.2331	0.9172
December (40 - 50 cm)	65	0.0013	3.0677	0.7406
December (45 - 67)	76	0.0010	3.2188	0.9157
December (50 -70 cm)	51	0.0008	3.1871	0.9329
April (30 - 40 cm)	20	0.0019	2.8484	0.8700
April (45 - 65 cm)	73	0.0008	3.1881	0.9002

The figure 2 and 3 show that in relation to length, fish of the 45 - 67 cm group increase in weight at a higher rate than fish of the smaller size groups (< 45). The t-tests shoued that the regression coefficients of the length-weight relationship in both length group differed significantly from 3.

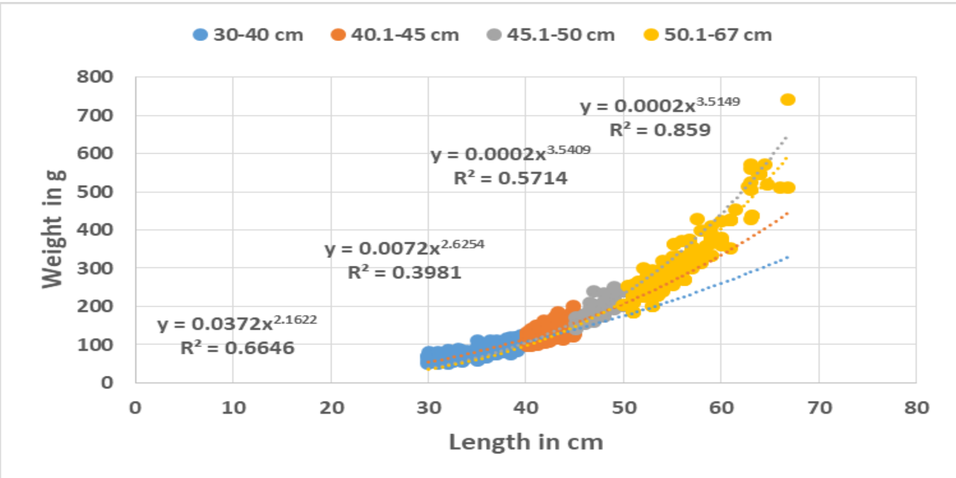

Figure **2**. Length-weight relationship for European eel for four length classes

Data from Table 3 as well as figure 2 showed that the same equation would not fit the data for the entire length range and that break occurred around the 45 cm. This break, a change in growth, also shows the coefficient of determination (R^2) and it is the smallest (greater variability in weight) in individuals from the length groups of 40 - 45 cm. R^2 values of 0.40 and 0.46 are at the limit of statistical significance (0.05 < P < 0.01), which shows a large irregularity in the growth of individuals from this length group.

After analysis in multiple size classis, it proved to be justified to single out only two groups (Figure 3). The first group is a group of specimens < 45 cm long and 200 g. weight and the second group are individuals > 45 cm Tl. We concluded that no single regression would adequately describe the length-weight relationship for the European eel in Skadar Lake and separate estimates were therefore made for two different length classes (groups), as mentioned below:
Length <45 cm (n = 320), $Y = 0.0098x^{2.5398}$ $R^2 = 0.8362$
Length ≥45.1 cm (n = 346), $Y = 0.0007x^{3.2525}$ $R^2 = 0.8971$

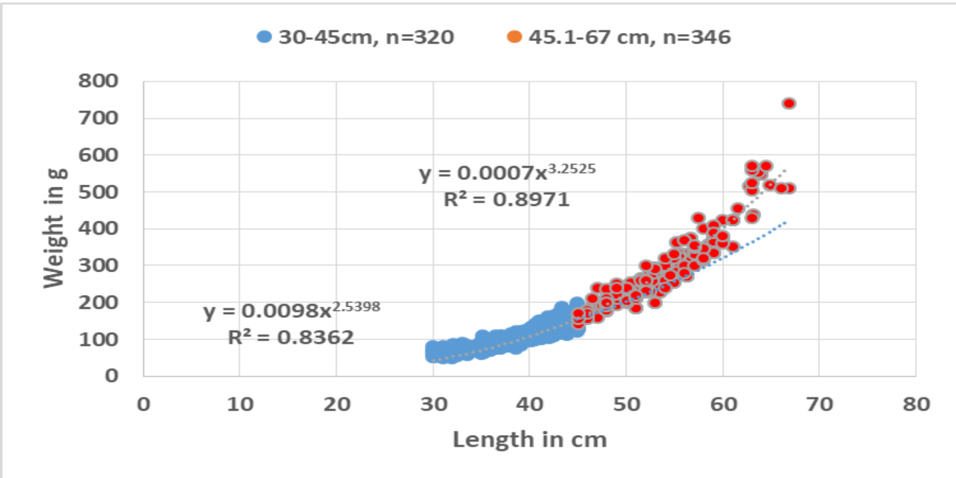

Figure **3**. Length-weight relationship for European eel for two size classis

DISCUSSION

There are many studies on biology of European eel in fresh waters (for example: Tesch, 1977; Dekker, 2004; Bevacqua, 2008; Castaldelli *et al*. 2014; Silm *et al*. 2017), but the ecology and biology of European eel in Montenegrin waters has received comparatively little attention. Unfortunately, there is no even data about the weigth-length relationship and the condition of European eel in this area. A common practice in freshwater fisheries biology is to scrutinize fish condition as an indicator of wellbeing and for comparing populations or stocks. The weight–length relationship and condition factor of the European eel, *A, anquilla*, were studied in specimens from Skadar Lake during the five period. A lot of work on the ratio of length and weight has been done on European eel found in the world, but in many works the dependence on length has not been analyzed (https://www.fishbase.se/ Search.php). There are only two studies regarding the biology of fishes from the Skadar Lake drainage, in terms of growth related to differences in the length range (Marić & Rakočević 2015; Marić & Burzanović 2021).

The condition of fish and their related length-weight relationship are widely used parameters which enhance the understanding of their general state, growth, survival, maturity and reproduction (Richter *et al*. 2000; Frose, 2006; Kharat *et al*. 2008; Milošević & Marić 2012). These parameters are also broadly used in the estimation of weight from the length, conversion of growth in length equations to growth in weight equations in stock assessment models, estimation of biomass from the length, indication of sex and differences between regions, and for comparison of the individuals of the same species (Bagenal & Tesch 1978; Gonçalves *et al*. 1997; Rawat *et al*. 2014).

The current paper presents data on the weigth-length relationship and the condition of European eel in Skadar Lake, during the annual cycle are analyzed in detail. Also, variability in relation to size was analyzed in detail. The LWR value was found to vary exclusively with body size (Table 3, Fig. 2) without varying beyond the corresponding range of allometry for the analyzed group during the annual cycle. As detailed research or research in this way has generally not been done, it represent the first data on this species in Skadar Lake. For the population from Skadar Lake, Milošević & Mrdak (2016) report LWR data and state that the population has negative allometry as a growth model. However, the data from that work show that both small (11.2 cm and 2.3 g) and larger specimens (79.5 cm and 930.5 g) were analyzed in the sample. For young European eels that are being prepared or already on their way to freshwater, Hegediš (2007) states the values for LWR, i.e. coefficient *b* less than 3 (about 2.6), which corresponds to negative allometry as a growth model, which was also found in this paper for European eels less than 40 cm. The results of our research differ significantly from most of the available data in the literature. In the literature and in the fish base, data are presented for all specimens together, for the population, and not by length. Often these results are shown on a small number of specimens, which is not in line with the recommendations suggested (100 specimens) by Froese (2006) and as such can give a distorted picture of the growth of this and other species. Length-weight relationships are not constant over the year and Length-weight relationships parameter may vary significantly due to biological, food availability, temporal and sampling factors, health and sex (Bagenal & Tesch 1978; Froese, 2006). Data from this paper were made on a large number of specimens, over 660, (at least 100 per period) and are in accordance with the recommendation of Froese (2006). They show that specimens up to 45 cm have negative allometry, and larger specimens have positive allometry at all times of the year. Partial analysis by length groups in the range of 10 cm per group, and even less (5 cm) if represented with a satisfactory number of specimens, showed that even the number of specimens in the group affects the value of the coefficient *b*, or the pattern of allometric-isometric growth. There are a lot of data in the literature, for several species, which show that many factors affect the value of *b* (Castadelli *et al*. 2014; Boulenger *et al*. 2015; Rawat *et al*. 2014). To study variability among populations and determine causes, intra-population variability must be analyzed first, i.e. by groups as done in this paper. Such an analysis shows a sharp boundary of differences between individual groups. Young specimens up to 45 cm were found to have negative allometry as a growth model. Separate length classes from 40 to 50 cm, depending on the season, have negative allometry to isometry (b = 2.9771 to 3.0677), however, all groups of 45 – 50 cm or larger than 45 cm have positive allometry. It should be noted that the youngest age class has not been studied, as well as that Hegediš (2007) states negative allometry for it. All this suggests that young individuals up to 45 cm grow according to the principle of negative allometry. It is interesting to note that the literature (Dekker *et al*. 1998) states that the limit value for the minimum allowable measure is usually 45 cm, although in some countries the minimum length allowed for hunting is 40 cm. This limit value (45) could be a good indicator for legislation in terms of illegal lengths in economic hunting.

According to many authors (Penàz & Tesch 1970; Poole & Reynolds 1996; Holmgren *et al*. 1997; Rawat *et al*. 2017), the growth of females in fish is significantly different from that of males. If we analyze the biology of this species (e.g. Tesch 1977; Dekker *et al*. 1998; Bevacqua *et al*. 2006; Melià *et al*. 2006; Silm *et al.* 2017), it can be seen that males mature first, i.e. they mature at shorter lengths, while in some (Dekker *et al*. 1998; Fernéndez-Delgado *et al*. 2006) it is stated that all specimens in freshwater larger than 45 cm are females. In the Asi River in Turkey, males larger than the above mentioned dimensions have been found, but they are few and this is explained by the good conditions for this species in the abovementioned river (Yalçin-Özdilek *et al*. 2006). According to van Ginneken *et al*. (2007) yellow eels grow and feed in continental waters in this pre-reproductive stage for a variable number of years, until they reach maturation size (around 400 mm for males and 600 for females). Boulenger *et al*. (2015) report mainly negative allometry for males and positive for females for many European waters (six countries, 13 basins). Isometry was found in only some waters and positive allometry for males in one. This means that males grow more slowly, i.e. that they are smaller in size than females, but also that they mature earlier and go to spawn (Dekker *et al*. 1998; Yalçin-Özdilek *et al*. 2006; van Ginneken *et al*. 2007). Because of all these differences when comparing, Kangur (1998), Matthews *et al*. (2003) analyzed only female growth. According to these data, our results would indicate that all specimens larger than 45 cm in Skadar Lake are females.

In terms of age, i.e. specimens of which age remain in lagoons and freshwaters, there is great disagreement. According to some, males live up to 4 - 5 years in freshwater, and females longer, while according to others, both males and females live more than ten years; even the age of over 50 is stated (Poole & Reynolds 1996; Simon, 2015). As sex and age were not studied in this paper, only on the basis of LWR can it be assumed that specimens with positive growth allometry are females. In contrast, specimens less than 40 cm would be young specimens in which the silvering process does not occur or is just beginning, and in specimens 40 to 45 cm the maturation process is likely to occur, primarily in males. This assumption for support also has a very large variability within this group, so at the same lengths we find specimens over 50% heavier than each other. This inequality is likely to affect the differences in LWR between periods in this length class (Table 3). If we keep in mind that mature specimens, primarily males (Dekker *et al*. 1998; Yalçin-Özdilek *et al*. 2006), go to spawn during the autumn period (November-December), it is logical to assume that poorly fed immature specimens, of the same length, remain in Lake Skadar until the next spawning season. The lowest value of CF was recorded in December (0.17) and the differences compared to other periods are statistically significant. According to Fernéndez-Delgado *et al*. (2006) European eel growth stagnates during the winter. The above mentioned could indicate that European eels that are up to 40 cm long are at least one year younger than those that are 40 - 45 cm long. It could also be assumed that European eels up to 45 cm long are significantly younger than those whose lengths are greater than 45 and 50 cm, respectively. If we add to this the already mentioned data that the growing eels are probably females, then it is understandable that there are these differences in the growth pattern (negative and positive allometry) between the studied groups in Skadar Lake. All of the above indicates that the values and form of growth (*b*) of an eel population may be good indicators of multiple biological characteristics that are indirectly studied and concluded. These results are suitable for the estimation of length-weight relationship since, the values of *b* are within the range of values of this parameter usually estimated in fishes, which according to Froese (2006) lies between 2.5 and 3.5.

In studies of population dynamics high condition factor values shows of favorable environmental conditions (such as: habitat and prey availability) and low values indicate less favorable environmental conditions (Blackwell *et al*. 2000). Analysis of the seasonal trend in the condition factor (CF) of the European eel in Lake Skadar reveals that august is the most favourable season, and that the population displays its worst condition in winter. In summer, the greater availability of food and the favourable weather conditions permit rapid growth and the accumulation of reserves of fat; this justifi as the high value of CF recorded in this period. Beside the specimens from November that have the lowest nutrition, the specimens from April also have lower values compared to other periods. As it is known, and already mentioned above, that European eels migrate to the sea during late autumn and early winter for spawning (Dekker *et al*. 1998; Davidsen *et al*. 2011; Monteiro *et al*. 2020), it can be assumed that those that are better fed in that period already migrated, and those who are less fed remained, so CF is therefore significantly different from those from the period of March, June and August. Condition factor compares the wellbeing of a fish and is based on the hypothesis that heavier fish of a given length are in better condition (Bagenal & Tesch 1978). Certain differences between March of one year and April of the other can be attributed to the differences in the external environment in which these groups grew and fed. According to Castaldelli *et al*. (2014), due to reduced competition, after migrations in November and December, European eels have more favorable conditions for growth, so the differences found in eels in Skadar Lake in the periods of March of one year and April of the other may be due to reduced number in that period, in this case in March 2015. There are no precise data on the number of European eels in Skadar Lake, and data on general conditions in the studied period are scarce, so they are not suitable for further comparison.

In many species, CF has higher values in the autumn (late autumn) period than in others, although this depends on the species, more often on the spawning period. Cyprinid species have the highest CF just before spawning (Erk'akan *et al*. 2013; Milošević & Marić 2012; etc.), which is in spring, while salmonid species have the highest CF just in the period when the eel has the lowest value (Rawat *et al*. 2014; Jan *et al*. 2018). In this case, specimens with lower CF than others will probably not spawn, ie. go to spawn that year precisely because of poor nutrition and they remain for at least another vegetative year. Therefore, poorly fed specimens remain in fresh water during the winter period, when, as a rule, there is less food in Skadar Lake (Rakočević, 2018). This has the effect that CF increases significantly during the spring period, so in spring and summer it has significantly higher values than during autumn and winter. According to Fernéndez-Delgado *et al*. (2006) the growth of eels stagnates during the winter, although it is generally known that in continental waters during the winter all fish have a slow growth or the growth is interrupted (Marić, 2019). According to Bagenal & Tesch (1978), the higher nutrition of a group indicates that the conditions in a given water facility are more favorable for that age group than for others. For European eels from Skadar Lake, therefore, the conditions are more favorable for larger specimens. As it is known that large European eels feed on fish (Rasmussen & Therkildsen 1979; Barak & Mason 1992; Mann & Blackburn 1991; Golani *et al*. 1988; Yalçin-Özdilek & Solak 2007), and that there is a higher number of fish species in Skadar Lake, including those that do not grow more than 10-15 cm (Marić, 2019), it is clear that the conditions for feeding of large European eels in Skadar Lake are very favorable. Also, as most species in this lake spawn during the spring (Marić, 2019), then the concentration of young fish is the highest, which represents ideal conditions for feeding of eels, but also other species. No statistically significant differences were found between the smaller and larger ones in that period, and all groups had a high CF (0.18).

CONCLUSIONS

The data showed that the same equation LWRs would not fit the data for the entire length range for the *A. anguilla*. After analysis in multiple size classis, it proved to be justified to single out only two groups and that break occurred around the 45 cm. The first group is a group of specimens < 45 cm long and 200 g. weight (negative allometric growth) and the second group are individuals > 45 cm TL (pozitive allometric growth). This break, a change in growth, also shows the coefficient of determination (R^2) and it is the smallest in individuals from the length groups of 40-45 cm, which shows a large irregularity (greater variability in weight) in the growth of individuals from this length group. The condition faktor undergoes minor changes in specimens belonging to different size classes. ANOVA show a statistically significant difference ($P < 0.01$) between five periods (f= 5.54, p = 0.002) for CF. The smallest values of condition factor were recorded in the specimens from period December. Differences is not significant at $P < 0.01$ between five periods in specimens large than 45 cm. The results presented contribute to the knowledge about the weight-length relationships of the European eel. When using the results presented in this study, it should borne in mind that the samples were taken during the year and the number of fish examined was relatively large. The estimations of LWRs shall be helpful in future works on by catch of fish species in the Skadar Lake in Montenegro and Albania.

ACKNOWLEDGEMENTS

We thank two anonymous reviewer, whose constructive comments greatly improved this paper.

Funding: This research received no funding.

REFERENCES

Anene, A. (2005). Condition factor of four Cichlid species of a man-made lake in Imo State, Southeastern Nigeria. *Turkish Journal of Fisheries and Aquatic Sciences*, 5 (1), 43–47.

Bagenal, T.B. & Tesch, F.W. (1978). Conditions and growth patterns in fresh water habitats. *Blackwell Scientific Publications*, Oxford, UK. pp. 75- 89.

Barak, N.A.E. & Mason, C.F. (1992). Population density, growth and diet of eels, *Anguilla anguilla* L., in two rivers in eastern England. *Aquaculture and Fisheries Management*, 23, 59-70.

Beeton, A.M. (1981). Physical conditions of Lake Skadar and its Basin. General introduction. In:Karaman G.S. & Beeton, A.M. (Eds.) The biota and limnology of Lake Skadar. University Veljko Vlahović, Institute of Biological and Medicine Research Titograd, Smithsonian institution, Washington, DC, USA, pp. 15–17.

Bevacqua, D., Melià, P., Crivelli, A.J., De Leo, G.A. & Gatto, M. (2006). Timing and rate of sexual maturation of European eel in brackish and freshwater environments. *Journal of Fish Biology*, 69, 200-208.

Bevacqua, D. (2008). A Modelling Approach for Conservation Of European Eel (*Anguilla Anguilla*) and Related Fisheries. Ph. D. Thesis. Univeristà Degli Studi Di Parma. 87 pp.

Blackwell, B., Brown, M.L. & Willis, D.W. (2000). Relative weight (Wr) status and current use in fisheries assessment and management. *Review in Fisheries Sciences*, 88, 1-44.

Boulenger, C., Acou, A., Trancart, T., Crivelli, A.J. & Feunteun, E. (2015). Length–weight relationships of the silver European eel, *Anguilla anguilla* (Linnaeus, 1758), across its geographic range, *Journal Applied Ichthyology*, 31(2), 1-4.

Castaldelli, G., Aschonitis, V., Lanzoni, M., Gelli, F., Rossi, R. & Fano, E.A. (2014). An update of the length–weight and length–age relationships of the European eel (*Anguilla anguilla*, Linnaeus 1758) in the Comacchio Lagoon, northeast Adriatic Sea, Italy. *Journal of Applied Ichthyology*, 30(3), 558–559.

Davidsen, J.G., Finstad, B., Økland, F., Thorstad, E.B., Mo, T.A. & Rikardsen, A.H. (2011). Early marine migration of European silver eel *Anguilla anguilla* in northern Norway. *Journal of Fish Biology*, 78 (5), 1390–1404. https://doi.org/10.1111/j.1095-8649.2011.02943.x

De Giosa, M., Czerniejewski, P. & Rybczyk, A. (2014). Seasonal Changes in Condition Factor and Weight-Length Relationship of Invasive *Carassius gibelio* (Bloch, 1782) from Leszczynskie Lakeland, *Poland Advances in Zoology*, 2014, 1-7. https://doi.org/10.1155/ 2014/678763.

Dekker, W. Van Os, B. & Van Willigen, J.A. (1998). Minimal and maximal size of eel. *Bulletin Français de la Pêche et de Pisciculture, Conseil Supérieur de la Pêche*, Paris (France), 349, 195-197.

Dekker, W. (2000). Fractal geometry of the European eel stock. *ICES Journal of Marine Science*, 57(1), 109–121.

Dekker, W. (2004). Slipping through our hands – population dynamics of the European eel. (PhD thesis). Amsterdam, the Netherlands: University of Amsterdam, 186 pp. Retrieved from http://www.diadfish.org/doc/these_2004/dekker_thesis_eel.pdf

Erk'akan, F., Innal, D. & F. Özdemir, F. (2013). Length–weight relationships for five Cyprinid species in Turkey. *Journal of Applied Ichthyology*, 30, 12-13.

Fernéndez Delgado, C., Hernando Jose, A., Herrera, M. & Bellido, M. (2006). Age and growth of yellow eels, *Anguilla anguilla*, in the estuary of the Guadalquivir River (south-west Spain). *Journal of Fish Biology*, 34(4), 561 – 570.

Froese, R. (2006). Cube law, condition factor and weight-length relationships: history, meta-analysis and recommendations. *Journal of Applied Ichthyology*, 22, 241-253.

Froese, R. & Pauly, D. (eds.) (2020). FishBase. World Wide Web electronic publication. www.fishbase.org, version (12/2020).

Fulton, TW. (1904). The rate of growth of fishes. Twenty-second Annual Report Part III. *Fisheries Board of Scotland*, Edinburgh, 3,141-241.

Golani, D., Shefler, D. & Gelman, A. (1988). Aspects of Growth and Feeding Habits of the Adult European Eel (*Anuguilla anguilla*) in Lake Kinneret (Lake Tiberias), Israel. *Aquaculture*, 74, 349-354.

Gonçalves, J.M.S., Bentes, L., Lino, P.G., Ribeiro, J., Canario, A.V. M. & Erzini, K. (1997). Weight-length relationship for selected fish species of the small-scale demersal fisheries of the south and south-west coast of Portugal. *Fisheries Research* 30, 253-256.

Hegediš, A. (2007). Migracija i odlike staklaste jegulje (*Anguilla anguilla*) kao limitirajući faktori za ribnjačko gajenje. Doktorska disertacija, Univerzitet u Novom Sadu, Novi Sad. 117 pp.

Holmgren, K., Wickstrom, H. & Clevestam, P. (1997). Sex related growth of European eel, *Anguilla anguilla*, with focus on median silver eel age. *Canadian Journal of Fisheries and Aquatic Sciences*, 54 (12), 2775-2781 https://doi.org/10.1139/f97-181.

ICES (2019). Joint EIFAAC/ICES/GFCM Working Group on Eels (WGEEL). ICES Scientific Reports, 1:50. 177 pp. http://doi.org/10.17895/ices.pub.5545

Jan, M., Jan, N. & Ahmed, I. (2018). Length Weight Relationship (LWR) and Condition Factor (K) of Brown Trout, *Salmo trutta fario. Journal of Ecophysiology and Occupational Health,* 18 (3-4), 73-79. DOI 10.18311/jeoh/2018/19992.

Kharat, S.S., Khillare, Y.K. & Dahanukar, N. (2008). Allometric scaling in growth and reproduction of a freshwater loach *Nemacheilus mooreh* (Sykes, 1839). *Electronic Journal of Ichthyology*, 4(1), 8–17.

Kangur, A. (1998). European eel, *Anguilla anguilla* (L.) fishery in Lake Võrtsjärv: current status and stock enhancement measures. *Limnologica*, 28(1), 95–101.

Kastratović, V. (2018). The water and sediment chemistry of Lake Skadar. In: Pešić, V., Karaman, G. & Kostoanoy, A. (Eds.): Lake Skadar/Shkodra Environment. The Handbook of Environmental Chemistry, *Springer,* Berlin, Heidelberg, pp 121-151. DOI https://doi.org/10.1007/ 698_2017_233

Lawson, E.O., Akintola, S.L. & Awe, F.A. (2013). Length-Weight Relationships and Morphometry for Eleven (11) Fish Species from Ogudu Creek, Lagos, Nigeria. *Advances in Biological Research* 7 (4), 122-128, DOI:10.5829/idosi.abr.2013.7.4.73190

Le Cren, E.D. (1951). The length-weight relationship and seasonal cycle in gonad weight and condition in the pearch (*Perca fluviatilis*). *Journal of Animal Ecology.* 20, 201-219. https://doi. org/10.2307/1540

Mann, R.H.K. & Blackburn, J.H. **(**1991). The biology of the eel *Anguilla anguilla* (L.) in an English chalk stream and inter-actions with juvenile trout *Salmo trutta* L. and *Salmo salar* L. *Hydrobiologia*, 218(1), 65-76.

Marić, D. & Rakočević, J. (2010). Biodiverzitet. M. Burić (Ed.), Životna sredina i održiv razvoj Podgorica: Crnogorska akademija nauka i umjetnosti. [Biodiversity. In M. Burić (Ed.), Environment and Sustainable Development. Podgorica: Montenegrin Academy of Sciences and Arts], 2, pp. 113–150.

Marić, D. & Rakočević, J. (2015). Some Life - History Traits of the Adriatic Beown Trout, *Salmo farioides* (Karaman, 1938) (Salmonidae) from the Morača River (Montenegro). *Acta zoologica bulgarica*, 67(2), 249–257.

Marić, D. (2018). The Ichthyofauna of Lake Skadar/Shkodra: Diversity, Economic Significance, Condition, and Conservation Status. In Pešić, V. *et al.* (eds.), The Skadar/Shkodra Lake Environment. Hdb Env Chem, Springer International Publishing AG pp. 363-381.

Marić, D. (2019). Fauna slatkovodnih riba (Osteichthyes) Crne Gore. CANU, Posebna izdanja (Monografije i studije). Knjiga 149. Odjeljenje prirodnih nauka. Knjiga 48. Podgorica, 419 pp.

Marić, D & Burzanović, K. (2021). Are there one or two stocks of Bleak - *Alburnus scoranza* Bonaparte, 1845 in the Lake Skadar (Montenegro). *Ecologica Montenegrina* 40, 80-92.

Matthews, M.A., Evans, D.W., McClintock, C.A., & Moriarty, C. (2003). Age, growth, and catch-related data of yellow eel *Anguilla anguilla* (L.) from lakes of the Erne catchment, Ireland. American Fisheries Society Symposium, 2003, pp 207–215.

Melià, P., Bevacqua, D., Crivelli, A.J., De Leo, G.A. & Gatto, M. (2006). Sex differentiation of the European eel in brackish and freshwater environments: a comparative analysis. *Journal of Fish Biology* 69, 1228-1235.

Milošević, D. & Marić, D. (2012). Length- weight relationship and condition factor of *Cyprinus carpio* from Skadar Lake (Montenegro) during spawn-ing period. *Agriculture and Forestry*, 52, 53-60.

Milošević, D., Pešić, V., Petrović. D., Pavićević, A., & Marić, D. (2012). Length- weight relationship and condition factor of two sympatric *Rutilus* (Rafinesque, 1820) species from Lake Skadar (Montenegro). *Archives of Biological Sciences*, 64, 991-994.

Milošević, D. & Mrdak, D. (2016). Length- weight relationship of nine fish species from Skadar Lake (Adriatic catchment area of Montenegro) *Journal of Applied Ichthyology,* 32, 1331–1333.

Monteiro, R.M., Domingos, I., Almeida, P.R., Costa, J.L., Alexandre, C.M. & Quintella, B.R. (2020). Migration and escapement of silver eel males, *Anguilla anguilla*, from a southwestern European river. *Ecology of Freshwater Fishes,* 29(4), 679-692.

Özpiçak, M., Saygın, S., Hançer, E., Aydın, A., Yılmaz, S. & Polat, N. (2018). Length-weight and length-length relationships of chub (*Squalius cephalus*, L., 1758) inhabiting a few inland waters of the Middle Black Sea Region. *Ege Journal Fisheries and Aquatic Sciences*, 35(2): 175-179.

Penàz, M. & Tesch, F.-W. (1970). Geschlechtsverhaltnis und Wachstum beim Aal (*Anguilla anguilla*) an verschiedenen Lokalitaten von Nordsee und Elbe. *Berichte der Deutschen Wissenschaftlichen Kommission für Meeresforschung* 21, 290–310.

Petrakis, G. & Stergiou, K.I. (1995). Weight-length relationships for 33 fish species in Greek waters. *Fisheries Research*, 21(3-4), 465-469.

Petrović, G. (1981). Chemical investigations of water and sediment of Lake Skadar. In: Karaman GS, Beeton AM (eds) The biota and limnology of Lake Skadar. University Veljko Vlahović, Institute of Biological and Medicine Research Titograd, Smithsonian institution, Washington, DC, USA, pp 68–96.

Poole, W.R. & Reynolds, J.D. (1996). Growth rate and migration of the Eel *Anguilla anguilla* L., *Journal of Fish Biolology*, 48(4), 633-642.

Rakočević, J. (2018). The phytoplankton and trophic state of Lake Skadar/Shkodra. In Pešić, V. *et al.* (eds.), The Skadar/Shkodra Lake Environment. Hdb Env Chem, Springer International Publishing AG. pp 153-168.

Rasmussen, G. & Therkildsen, B. (1979). Food, growth, and production of *Anguilla anguilla* L., in a small Danish stream. *Rapports et Proces- Verbaux des Reunions, Conseil International pour L exploration de la Mer,* 174, 115-123.

Rawat, M.S., Bantwan, B. & Singh, D. (2017). Study on the fecundity of brown trout (Salmo trutta fario L.) in River Asiganga, Uttarkashi (Uttarakhand), India. *International Journal of Fisheries and Aquatic Studies*, 5(1), 167-172.

Rawat, M.S., Bantwan, B., Singh, D. & Gusain, O.P. (2014). Length-weight relationship and condition factor of Brown trout (*Salmo trutta fario*) from river Asiganga, Uttarakhand (India). *Journal of Environmental Conservation*, 15, 41-6.

Richter, H.C., Luckstad, C., Focken, U. & Becker, K. (2000). An improved procedure to asses fish condition on the basis length-weight relationship. *Archive of Fishery and Marine Research*, 48, 255-264.

Ricker, W.E. (1975). Computation and Interpretation of Biological Statistics of Fish *Populations. Bulletin - Fisheries Research Board of Canada*, 191, 382 pp.

Safran, P. (1992).Theoretical analysis of the weight–length relationships in the juveniles. *Marine Biology*, 112(4), 545–551.

Scherrer, B. (1984). Biostatistique. Gae¨tan Morin E´ diteur. Chicoutimi, Canada, 850 pp.

Silm, M., Bernotas, P., Haldna, M., Järvalt, A. & Nõges, T. (2017). Age and growth of European eel, *Anguilla anguilla* (Linnaeus, 1758), in Estonian lakes. *Journal of Applied Ichthyology,* 1–6. DOI: 10.1111/jai.13314

Simon, J. (2007). Age, growth, and condition of European eel (*Anguilla anguilla*) from six lakes in the River Havel system (Germany). *ICES Journal of Marine Science*, 64, 1414–1422.

Simon, J. (2015). Age and growth of European eels (*Anguilla anguilla*) in the Elbe River system in Germany. *Fisheries Research*, 164, 278-285.

Tesch, F.W. (1977). *The eel*. Chapman & Hall, London, 434 pp.

Yalçin-Özdilek, Ş., Gümüş, A. & Dekker, W. (2006). Growth of European eel in a Turkish river at the south eastern limit of its distribution. *Electronic Journal of Ichthyology*, 2, 55-64.

Yalçın-Özdilek, Ş. & Solak, K. (2007). The Feeding of European eel, *Anguilla anguilla* L. in the River Asi, Turkey. *Electronic Journal of Ichthyology*, 1, 26-34.

van Ginneken, V., Dufour, S., Sbaihi M., Balm, P., Noorlander, K., de Bakker, M., Doornbos, J., Palstra, A., Antonissen, E., Mayer, I. & van de Thillart, G. (2007). Does a 5500-km swim trial stimulate early sexual maturation in the European eel (*Anguilla anguilla* L.)? *Comparative Biochemistry and Physiology a-Molecular & Integrative Physiology*, 147(4), 1095-1103

Vaslet, A., Bouchon-Navaro, Y., Louis, M. & Bouchon, C. (2008). Weight-length relationships for 20 fish species collected in the mangroves of Guadeloupe (Lesser Antiles). – *Journalof Applied Ichthyology*, 24, 99-100.

Vizi, O. (2018). Ornithological features of Skadar Lake. In: Pešić, V., Karaman, G. & Kostoanoy, A. (Eds.): Lake Skadar/Shkodra Environment. The Handbook of Environmental Chemistry, SPRINGER, Berlin, Heidelberg, 415-445 pp.

Weatherley, A.H. (1972). Growth and ecology of fish populations. Academic Press, Inc. (London), pp 80-86.

Llupa, J., Gašić, U., Brčeski, I., Demertzis, P., Tešević, V., Topi, D. (2022). LC-MS/MS characterization of phenolic compounds in the quince (Cydonia oblonga Mill.) and sweet cherry (Prunus avium L.) fruit juices. Agriculture and Forestry, 68 (2): 193-205. doi: 10.17707/AgricultForest.68.2.14

DOI: 10.17707/AgricultForest.68.2.14

Jonilda LLUPA[1]*, Uroš GAŠIĆ[2], Ilija BRČESKI[3], Panagiotis DEMERTZIS[1], Vele TEŠEVIĆ[3], Dritan TOPI[4]

LC-MS/MS CHARACTERIZATION OF PHENOLIC COMPOUNDS IN THE QUINCE (*CYDONIA OBLONGA MILL.*) AND SWEET CHERRY (*PRUNUS AVIUM L.*) FRUIT JUICES

SUMMARY

Quince and sweet cherry are two common edible fruit-producing trees of temperate regions of Euroasia. The phenolic profiles of juices from quince and sweet cherry fruit extracted by the cold-pressing were analyzed by Ultra-High-Performance Liquid Chromatography (UHPLC). Chromatographical results identified 31 phenolic compounds while quantified thirteen for fruit juices. The quantitative data indicate that the predominant phenolic was 5-O-caffeoylquinic acid in quince (8.343 mg L-1) and cherry juice (6.407 mg L-1). Total Flavonoids (TF), Total Phenolic Content (TPC), and Total Antioxidant Capacity (TAC) were also investigated. In both fruit juices, the TF values varied between 0.30-0.97 g L-1 (Catechin Equivalent) and TPC between 0.36 to 0.94 g L-1 (Gallic Acid Equivalent). It is worth noting that the quince fruit juices possessed a higher TPC and TFC compared to sweet cherry fruit juices.

Keywords: quince, sweet cherry, fruit juices, phenolic compounds, antioxidant, cold-pressing

INTRODUCTION

Tree fruits present an essential source of nutrients such as carbohydrates, lipids, and non-nutrient phytochemicals like polyphenols, associated with health benefits (Wojdyło, Oszmianski, & Bielicki, 2013). Besides the water and the common primary metabolites such as carbohydrates as the main ingredients; fruits comprise a complex composition of several hundred substances,

[1]Jonilda Llupa* (Corresponding author: jonilda.llupa@gmail.com), Panagiotis Demertzis, Laboratory of Food Chemistry and Food Microbiology, Department of Chemistry, University of Ioannina, GR-45110 Ioannina, GREECE
[2]Uroš Gašić, Institute for Biological Research "Siniša Stanković"- National Institute of Republic of Serbia, University of Belgrade, Bulevar Despota Stefana 142, 11060 Belgrade, SERBIA
[3]Ilija Brčeski, University of Belgrade, Faculty of Chemistry, Studentski Trg 12-16, 11000 Belgrade, SERBIA
[4]Dritan Topi, University of Tirana, Faculty of Natural Sciences, Department of Chemistry, Blvd. Zogu 1, No. 25/A, Tirana, ALBANIA
Notes: The authors declare that they have no conflicts of interest. Authorship Form signed online.
Recieved:11/04/2022 *Accepted:15/06/2022*

characterized by many secondary plant metabolites such as phenolic compounds, organic acids, amino acids, and minerals (Paredes-Lopez, Cervantes-Ceja, Vigna-Perez, & Hernandez-Perez, 2010). Recent evidence of an association between a healthy diet and fruit consumption by identifying edible fruits as an essential source of polyphenols (Manach, Scalbert, Morand, Remesy & Jimenez, 2004). Despite the common characteristics, specific fruits own their specific phytochemical composition pattern. A quantitative and qualitative correlation among the fruit phenolics with the tree variety, climate, and agriculture practices has already been proved. The presence of over 224 compounds is analyzed in orange juice, including flavones, carotenoids, flavanones, anthocyanins, and flavanols (McKay &Wilson, 2016). Fifty-six phenolic compounds are identified and quantified in strawberry fruits (Gasperotti, Masuero, Mattivi & Vrhovsek, 2015).

Quinces (*Cydonia oblonga* Mill.) belong to the *Rosaceae* family, specifically the *Maloideae* subfamily, and originate in Central Asia. Fruits are preferred for non-directly consumption because of hardness and astringency, but to prepare liqueur, jam, or marmalade (Wojdyło, Oszmianski, & Bielicki, 2013). The fruit is highly evaluated due to rich polyphenols content exerting antioxidant effects (Silva, Andrade, Ferreres, Domingues & Seabra, 2002; Fattouch *et al*. 2007), and anti-inflammatory activity in the human body (Szajdek & Borowska, 2008; Basu & Penugonda, 2009; McKay & Wilson, 2016). Sweet cherry (*Prunus avium* L.) and sour cherry (*Prunus cerasus* L.), belonging the *Rosaceae* family, are widely consumed. (Blando & Oomah, 2019). Their red color is associated with the presence of anthocyanin compounds (Sokół-Łętowska, Kucharska, Hodun & Gołba, 2020). Their consumption contributes to modulating blood glucose levels by lowering blood pressure, body protection from oxidative stress and anti-inflammatory activity ((Kelley, Aldkins, & Laugero, 2018; Blando & Oomah, 2019; Sokół-Łętowska, Kucharska, Hodun & Gołba, 2020).

Used for a long time as fresh and conserved specific fruits from local communities, nowadays together with juice fruits and other fruit confections such as jam, marmalades, jelly, juice, and cakes are widely infused to consumers diet globally. Fruit juice is a reliable source of bioactive compounds, such as phenolic compounds. Among them, cherry and quince juices are well-known as excellent sources. Studies on examining the polyphenol content in cherry juices have revealed a plethora of phenolic classes: anthocyanins, which include (-)-epicatechin (flavanol), neo-chlorogenic, chlorogenic, and 3-coumaroylquinic acid (hydroxycinnamic acids), as well as quercetin and kaempferol glycosides (flavonols) (Bonerz, Würth, Dietrich & Will, 2007).

Quince fruit has gained much attention because of its high antioxidant capacity resulting from phytochemicals, including phenolic compounds such as hydroxycinnamic acid and proanthocyanidins. The cold-pressing technique enables the transfer of most primary and secondary metabolites found in the original ripped and sound fruit, from the fruit to the juice through the fruit crush at room temperatures, at a low speed. The extraction process generates almost no heat and preserves the juice's nutritional quality (Miguel, Dandlen, Antunes, Neves & Martins, 2004). Another critical factor associated with the juice nutritional value is the quality of storage conditions, mainly temperature and time (Gholamreza, Kitipong, Supaart, 2019).

Nowadays, studying of phenolic compounds both as bulk matrix as well as individually is of primary importance to researchers. Applying the liquid chromatography separation technique enables identifying and quantifying phenolic compounds. The major limitation is that the compound identification is achieved only by retention time and UV spectra. In recent years, to overcome this problem, applying liquid chromatography coupled with tandem mass spectrometry (LC-MS/MS) has taken ground for the proper characterization of phenolic compounds in fruit juice.

In addition, noise reduction and sensitivity improvements are achieved by exploiting multiple reactions monitoring (MRM) scan mode (Hossain, Rai, Brunton, Martin-Diana & Barry-Ryan, 2010). This study aimed to evaluate the phenolic composition of cold-pressed fruit juices and provide relevant information on foods with high antioxidant content.

MATERIAL AND METHODS

Plant material and juice extraction

Quince (*Cydonia oblonga* Mill.) and sweet cherry (*Prunus aviums* L.) fruits were harvested at an optimum ripeness according to the season. Fruit coloring and peel were determining factors to the ripeness. The harvesting period was July 2018 and October 2018 for sour cherry and quince, respectively. The fruits were harvested at plantation orchards (40° 81′ N; 20° 74′ E), and (51° 99′ N; 20° 16′ E) from Korça region with plain elevation 850 m above sea level. Harvesting, transportation, preservation (in a controlled atmosphere and temperature 0-20 °C) to the laboratory were performed on the same day.

In this study, the cold-pressing method was employed to produce sweet cherry and quince juices. Overall, the cold extraction method was employed to 20 kg fruit of sweet cherry and quince, respectively. Juice extractions were processed in duplicate for both fruits. Finally, 1000 mL fruit juice was preserved in a dark bottle, 4°C, until laboratory analysis. According to the 2001/112/EC Directive, the 'fruit juice' is obtained from the edible part of the ripped fruit through an extrusion and served or marketed as unfermented fresh or preserved, or fermentable liquid product (Directive 2012/12/EU, 2012).

Chemicals and reagents

Analyses were performed using analytical grade chemicals and reagents. Methanol Sodium carbonate, Sodium nitrite, Aluminum chloride, Gallic Acid, Folin-Ciocalteu reagent, and DPPH assay were obtained from Sigma Aldrich Chemical Co. (Steiheim, Germany). Deionized water from Milli-Q, (Merck-Millipore, Darmstadt, Germany) were used throughout the test analysis.

Quantification of Total Phenolic Content

The modified Folin-Ciocalteu procedure was applied to determine Total Phenolic Content (TPC) by Shimadzu UV-1280 UV-VIS spectrophotometry (Ljekočević *et al.* 2019). Overall, the juice sample was filtered by a 0.45 μm Captiva filter. A sample aliquot (0.25 mL), appropriately diluted, and Gallic acid standard solutions were mixed with 6 mL of deionized water. Further, Folin-Ciocalteu reagent (1.25 mL) was added and gently mixed. After 5 minutes, a volume of 1.0 mL of sodium carbonate (7.5%) was pipetted into the test tube and further vortex. Analyses were performed in triplicate, and absorbance was measured at 765 nm. The TPC was expressed as mg Gallic Acid Equivalent per liter (mg GAE L^{-1}).

Quantification of Total Flavonoids Content

The total flavonoids were analyzed according to the colorimetric assay proposed by Kim *et al*. (2003). A volume of 1.2 ml deionized water was pipetted to the test tube with 0.3 ml of the fruit juice sample. Consecutively, were pipetted a volume of 0.09 ml of 5% sodium nitrite, followed by 0.09 ml of $AlCl_3$ solution (10%). The test tube was incubated at a temperature of 25°C, for 6 minutes. A volume of 1 ml of sodium hydroxide (1 M) was added to the mixture. Immediately, the reaction mixture volume was made to 2.4 ml with deionized water. The mixture was thoroughly vortexed, and absorbance was measured at 510 nm. The calibration curve was produced by using aqueous solutions of known concentrations varied 0.05; 0.1; 0.2; 0.3, and 0.4 mg/cm^3. The results were expressed as g Catching equivalents (CEQ)/ L of juice sample.

Radical Scavenging Activity Determination

The scavenging activity assay method was compiled by Silva *et al.* (2004). A sample volume of 0.2 ml (0.100; 0.050; 0.020; 0.005 and 0.001 mg mL^{-1}) mixed with DPPH solution (1.8 mL) (0.04 mg L^{-1} in ethanol) incubated for 30 minutes in the darkroom. The absorbance measurements were performed at 517 nm. The calibration curve was prepared using Trolox (0.01, 0.025, 0.05, 0.075 and 0.1 mg mL^{-1}). Measurements were performed in triplicates. The scavenging activity was calculated through the following equation:

$$\text{DDPH scavenging activity (\%)} = 100 \times (A_c - A_s)/A_c$$

where: A_c-the control absorbance, and A_s -sample absorbance. IC50 calculated values denote the sample concentration required to decrease the absorbance at 517 nm by 50%). Presentation of the DPPH values was expressed as mg Trolox L^{-1}.

Solid-phase extraction

Vacuum device SPE Vacuum Manifold Baker SPE-12G using Oasis HLB bcc/200 μm cartridges were employed for extraction. 5 mL of MeOH followed by 5 mL of deionized water was applied for the cartridge conditioning.

A fruit juice sample (5 mL) passed through the cartridge, washed with 2 mL of water, and eluted with 2 mL of MeOH. Samples were collected and consecutively analyzed by LC-MS/MS.

LC-MS/MS characterization of phenolic compounds

LC-MS/MS analysis was performed using the Accela 600 UHPLC system connected to an LTQ OrbiTrap XL mass spectrometer (Thermo Fisher Scientific, Bremen, Germany) in negative ionization mode (heated electrospray ionization–HESI). The analytical column used for separation was Syncronis C18 (50 × 2.1 mm, 1.7 μm particle size). The exact UHPLC conditions and MS parameters have been reported (Vasić *et al*., 2019). Xcalibur software (version 2.1, Thermo Fisher Scientific, Waltham, MA, USA) was used for instrument control and data analysis. The molecule editor program, ChemDraw (version 12.0, Cambridge Soft, Cambridge, MA, USA), was used to draw the structures and calculate the exact masses of compounds of interest. Tentative identification of some compounds with no available standards was confirmed using previously reported MS fragmentation data (Stojković *et al*. 2020).

Phenolic compounds were identified by direct comparison with commercial standards. The total amounts of each compound were evaluated by calculation of the peak areas and are expressed as mg/kg. The limits of detection (LOD) and quantification (LOQ) were calculated using standard deviations of the responses (SD) and the slopes of the calibration curves (S) according to the formulas: LOD = 3(SD/S) and LOQ = 10 (SD/S) (Kostić *et al*. 2019).

RESULTS AND DISCUSSION

Total phenolics and flavonoids estimation

Edible fruits have historically held a place in the consumer’s diet. Sweet cherries composition in phenolic compounds is distinguished among other fruits. Their presence is essential and directly influences the fruit juice quality by contributing into organoleptic characteristics, affecting the color, astringency, and aroma. They are essential in preventing chronic diseases like cancer and cardiovascular and neurodegenerative diseases. All these effects are attributed to the antioxidant properties of these molecules. This study has quantified the phenolic compound by the total phenolic content (TPC), total flavonoids content (TFC), together with DPPH radical scavenging activity of fruit juices from sweet cherry and quince fruits grown in Eastern region of Korca, Albania. The results are shown in Table 1.

Total phenolic content measured by Folin-Ciocalteu method, gives an estimate of different phenolic compounds including phenolic acids, flavonols and others. The TPC values were compared with data from literature, (Prvulovic *et al*., 2012; Tianyi *et al*., 2021). The TPC value from sweet cherry grown in Serbia show similarity 76 ± 4.85 mg GAE/100g (Prvulovic *et al*., 2012), and Australian grown sweet cherry 0.87 ± 0.09 mg GAE/g (Tianyi *et al*., 2021). Sweet cherry comprises another important source of flavonoids.

Table 1. Total phenolic, anthocyanin content and DPPH radical scavenging activity of fruit juices.

Fruit juice	Total phenolic content[a](mg GAE g^{-1})	Total flavonoids content[a] (g CEQ g^{-1})	DPPH radical scavenging activity[a] ($IC_{50\%}$)
Sweet cherry	0.60 ± 0.04^b	0.58 ± 0.04^c	10.92 ± 0.24^d
Quince	0.94 ± 0.02^b	0.97 ± 0.05^c	5.78 ± 0.13^d

[a]The results are displayed as mean ± standard deviation (n=3); [b-d]shows that means in a row are different at significant level ($p<0.05$) using One-way analysis of variance (ANOVA) and Tukey's test[c] DPPH (IC50%) mg Trolox L^{-1}, GAE-Gallic acid equivalent, CEQ-Catechin Equivalent.

De Sourza (2014) presented the TFC in sweet cherry grown in Brasil (59.92 ± 3.76 mg QE/100g. Tianyi *et al* (2021) presented data on TFC 0.31 ± 0.05 mg QE/g and 0.47± 0.01 mg QE/g. Variations in reported data are influenced by a number of agro-climatic factors, such as cultivar, land latitude of the orchards. Accordingly, the TPC and TFC of quince juice were about 1.5-fold, higher compared with sweet cherry juice. In a study, Fattouch *et al*. (2007) concluded that TPC range from 37 - 47 mg/g in quince pulp. Another study showed TPC content 6.3, 2.5, and 0.4g/kg for quince peel, pulp, and seeds, respectively (Magalhaes *et al*., 2009). In another study the TPC in Japanese quince fruit ranged from 3906 to 4550 mgGAE/100 g (Urbanaviciute *et al*., 2020).

Evaluation of anti-DPPH radical activity

The results of the anti-DPPH radical assay confirmed that the fruit juices had significant antioxidant capacities. The results supported a correlation between anti-DPPH radical activity and total phenolic content. As shown in Tab. 1, the antioxidant properties of quince juice were $IC_{50\%}$ 5.78, while the cherry juice showed antioxidant capacity $IC_{50\%}$ 10.92. Individual antioxidants do not exert separately but in concert with other antioxidants (Strazzulo *et al*., 2007). Such interactions can affect total antioxidant capacity, producing synergistic or antagonistic effects (Niki & Noguchi, 2000). A study of quince fruit methanolic extracts (pulp, peel, and seed) showed that peel extract presented the highest antioxidant capacity. The $IC_{50\%}$ values of quince pulp, peel, and jam extracts were correlated with the caffeoylquinic acid's total content (Silva *et al*. 2004). More recently, phytochemicals exerting anti-oxidative properties have taken the focus.

LC-MS/MS phenolic compound identification and quantification

Thirty-one phenolic compounds were identified in both fruit juices through UHPLC analysis including *hydroxybenzoic acids* (6): Dihydroxybenzoic acid hexoside, Protocatechuic acid, Dihydroxybenzoic acid hexosyl-pentoside, p-Hydroxybenzoic acid, Ellagic acid, Vanillic acid; *hydroxycinnamic acids* (14): Caffeoylquinic acid hexoside, 3-O-Caffeoylquinic acid, Caffeic acid hexoside, 3-O-p-Coumaroylquinic acid, 4-O-Caffeoylquinic acid, 3-O-Feruoylquinic acid, Caffeic acid, Coumaric acid hexoside, 5-O-Caffeoyl-quinic acid, 5-O-p-Coumaroylquinic acid, Caffeoylshikimic acid, 4-O-Feruoylquinic acid, 4-O-p-Coumaroylquinic acid, p-Coumaric acid; *flavan-3-ols* (2): Catechin and Epicatechin; *procyanidins* (2): Procyanidin dimer B type isomer 1, and Procyanidin dimer B type isomer 2; *flavonols* (6): Quercetin 3-O-(6"-rhamnosyl) glucoside, Quercetin 3-O-glucoside, Kaempferol 3-O-(6"-rhamnosyl) glucoside, Quercetin 3-O-pentoside, Quercetin 3-O-rhamnoside, and Quercetin; and *dihydrochalcone* (1): Phloretin 2'-O-glucoside, with specific retention times (Table 2). Each phenolic compound was identified based on the exact mass and respective MS2, MS3 and MS4 fragments m/z. These findings were consulted with Phenolic compounds Mass spectra databank.

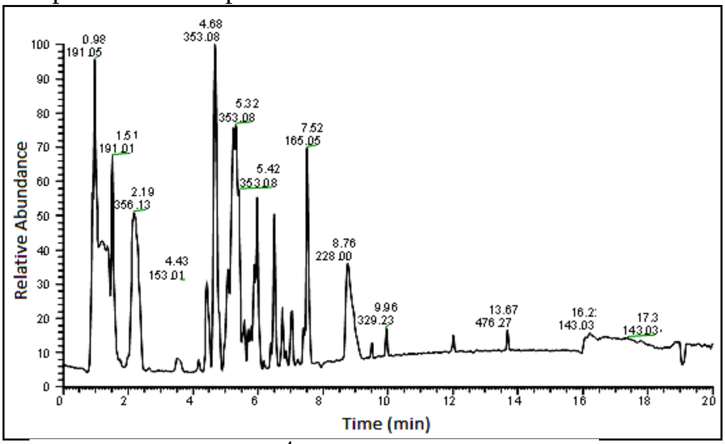

Figure 1. LC-MS/MS^4 Chromatogram of Quince

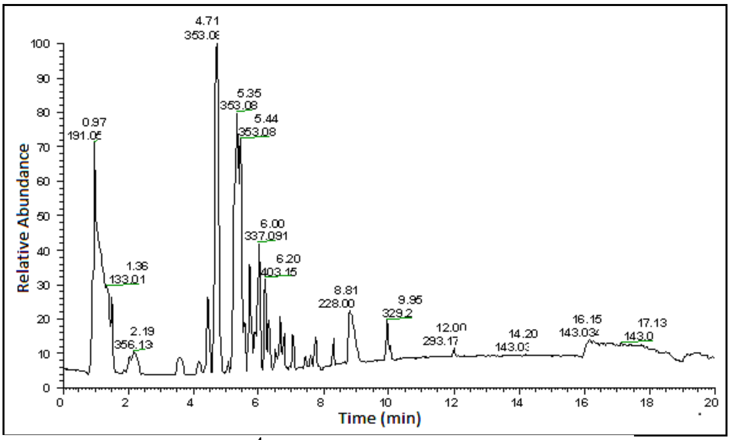

Figure 2. LC-MS/MS^4 Chromatogram of Cherry Juice

Table 2. Phenolic compounds detected and quantified in cherry and quince juices by LC–MS/MS^4 in negative ionization mode.

No	t_R, min	Compound name	Molecular formula [M–H]$^-$	Calculated mass, [M–H]$^-$, m/z	Exact mass, [M–H]$^-$, m/z	Δ ppm	MS^2 Fragments, m/z (% Base Peak)	MS^3 Fragments, m/z (% Base Peak)	MS^4 Fragments, m/z (% Base Peak)	Cherry	Quince
Hydroxybenzoic acids											
1.	3.92	Dihydroxybenzoic acid hexoside	$C_{13}H_{15}O_9^-$	315.07216	315.07207	0.29	153(100) 152(50) 109(15) 108(10)	109(100)	123(25) 109(10) 85(10) 81(100)	+	+
2.	4.44	Protocatechuic acid*	$C_7H_5O_4^-$	153.01933	153.01932	0.07	109(100) 95(75) 79(20) 59(10)	81(100) 68(25) 65(15)	–	1.145	1.265
3.	4.58	Dihydroxybenzoic acid hexosyl-pentoside	$C_{18}H_{23}O_{13}^-$	447.11441	447.11434	0.16	315(100) 285(10) 153(10)	153(100) 123(10)	123(100)	+	+
4.	5.37	*p*-Hydroxybenzoic acid*	$C_7H_5O_3^-$	137.02442	137.02423	1.39	109(10) 93(100)	93(10)	–	0.827	0.716
5.	6.79	Ellagic acid	$C_{14}H_5O_8^-$	300.99899	300.99890	0.30	284(40) 271(60) 257(100) 229(85) 185(40)	229(100) 213(20) 185(85)	201(100) 185(95) 157(30) 145(20) 129(10)	–	+
6.	6.93	Vanillic acid*	$C_8H_7O_4^-$	167.03498	167.03484	0.84	153(10) 152(80) 124(10) 123(100) 108(20)	108(100)	79(100)	2.945	6.478
Hydroxycinnamic acids											
7.	4.53	Caffeoylquinic acid hexoside	$C_{22}H_{27}O_{14}^-$	515.14008	515.13977	0.60	353(40) 341(100) 335(30) 323(10) 191(15) 179(45)	179(100) 135(10)	135(100)	+	+
8.	4.72	3-*O*-Caffeoylquinic acid	$C_{16}H_{17}O_9^-$	353.08781	353.08656	3.54	191(100) 179(30) 135(10)	173(75) 127(100) 111(40) 93(60) 85(90)	109(30) 99(40) 85(100)	+	–
9.	5.24	Caffeic acid hexoside	$C_{15}H_{17}O_9^-$	341.08781	341.08658	3.61	179(100) 135(10)	135(100)	107(100) 79(20)	+	+
10.	5.27	3-*O*-*p*-Coumaroylquinic acid	$C_{16}H_{17}O_8^-$	337.09289	337.09201	2.61	191(10) 173(10) 163(100) 119(10)	119(100)	119(100)	+	+
11.	5.33	4-*O*-Caffeoylquinic acid	$C_{16}H_{17}O_9^-$	353.08781	353.08624	4.45	191(60) 179(75) 173(100) 135(15)	115(20) 111(50) 93(100) 71(20)	–	+	+
12.	5.55	3-*O*-Feruoylquinic acid	$C_{17}H_{19}O_9^-$	367.10346	367.10220	3.43	193(100) 134(10)	149(25), 134(100)	106(100)	+	
13.	5.97	Caffeic acid*	$C_9H_7O_4^-$	179.03498	179.03464	1.90	135(100)	135(60), 117(15), 107(100) 91(55), 79(15)	–	0.672	0.553
14.	5.45	Coumaric acid hexoside	$C_{15}H_{17}O_8^-$	325.09289	325.09277	0.37	289(20) 265(20) 187(40) 163(80) 145(100) 119(10)	117(100)	–	+	–
15.	5.80	5-*O*-Caffeoyl-quinic acid*	$C_{16}H_{17}O_9^-$	353.08781	353.08627	4.36	191(100) 179(5)	173(75) 127(100) 111(40) 93(60) 85(90)	109(40) 99(50), 85(100)	8.343	6.407
16.	6.00	5-*O*-*p*-Coumaroylquinic acid	$C_{16}H_{17}O_8^-$	337.09289	337.09128	4.78	191(100) 179(5) 163(10)	173(75) 127(100) 111(40) 93(60) 85(90)	109(30) 99(40), 85(100)	+	+
17.	6.06	Caffeoylshikimic acid	$C_{16}H_{15}O_8^-$	335.07724	335.07608	3.46	179(100) 135(25)	135(100)	107(100)	+	+
18.	6.24	4-*O*-Feruoylquinic acid	$C_{17}H_{19}O_9^-$	367.10346	367.10330	0.44	193(10) 191(5) 173(100)	155(20) 111(20) 93(100) 71(20)	–	+	–
19.	6.38	4-*O*-*p*-Coumaroylquinic acid	$C_{16}H_{17}O_8^-$	337.09289	337.09238	1.51	191(5) 173(100) 163(10)	115(20), 111(50), 93(100), 71(20)	–	+	+

20.	6.78	*p*-Coumaric acid*	$C_9H_7O_3^-$	163.04007	163.03984	1.41	119(100)	119(60) 101(20) 93(25) 91(100) 72(10)	–	0.636	0.191
		Flavan-3-ols									
21.	5.39	Catechin*	$C_{15}H_{13}O_6^-$	289.07176	289.07126	1.73	271(5) 245(100) 205(40) 179(15) 125(5)	227(30) 203(100) 187(25) 175(10) 161(20)	188(70) 185(20) 175(100) 161(40) 157(10)	0.413	0.725
22.	5.92	Epicatechin*	$C_{15}H_{13}O_6^-$	289.07176	289.07095	2.80	271(5) 245(100) 205(40) 179(15) 125(5)	227(35) 203(100) 187(30) 175(15) 161(25)	188(60) 185(20) 175(100) 161(35) 157(15)	0.918	1.911
Procyanidins											
23.	4.97	Procyanidin dimer B type isomer 1	$C_{30}H_{25}O_{12}^-$	577.13515	577.13440	1.30	559(15) 451(25) 425(100) 407(50) 289(30) 287(10)	407(100) 381(5) 287(5) 273(10)	389(30) 297(30) 285(100) 281(90)	+	+
24.	5.60	Procyanidin dimer B type isomer 2	$C_{30}H_{25}O_{12}^-$	577.13515	577.13330	3.21	559(5) 451(20) 425(100) 407(50) 289(20) 287(10)	407(100) 381(10) 273(10)	389(40) 297(40) 285(100) 243(75)	+	+
Flavonols											
25.	6.50	Quercetin 3-*O*-(6''-rhamnosyl) glucoside*	$C_{27}H_{29}O_{16}^-$	609.14611	609.14447	2.69	343(5) 301(100) 300(30) 271(10) 255(5)	273(25) 257(20) 179(100) 151(75)	151(100)	0.450	2.104
26.	6.73	Quercetin 3-*O*-glucoside*	$C_{21}H_{19}O_{12}^-$	463.08820	463.08710	2.38	301(100) 300(30)	273(25) 257(20) 179(100) 151(75)	151(100)	0.527	0.960
27.	6.85	Kaempferol 3-*O*-(6''-rhamnosyl) glucoside	$C_{27}H_{29}O_{15}^-$	593.15119	593.15112	0.12	285(100) 284(10)	257(100) 241(30) 229(40) 213(30) 151(5)	255(10) 239(30) 229(100) 163(40)	–	+
28.	6.97	Quercetin 3-*O*-pentoside	$C_{20}H_{17}O_{11}^-$	433.07763	433.07724	0.90	343(5) 301(80) 300(100)	271(100) 255(60) 179(10) 151(10)	243(100) 227(80) 215(20) 199(20)	–	+
29.	7.25	Quercetin 3-*O*-rhamnoside*	$C_{21}H_{19}O_{11}^-$	447.09329	447.09222	2.39	301(100) 300(35) 284(20)	273(25) 257(20) 179(100) 151(75)	151(100)	0.034	0.077
30.	8.83	Quercetin*	$C_{15}H_9O_7^-$	301.03538	301.03534	0.13	271(50) 255(20) 179(100) 151(80) 107(5)	151(100)	107(100) 83(10)	1.612	1.861
Dihydrochalcon											
31.	7.60	Phloretin 2'-*O*-glucoside*	$C_{21}H_{23}O_{10}^-$	435.12967	435.12784	4.21	274(5) 273(100)	167(100) 125(5) 123(5)	125(10) 123(100)	0.325	0.596
*Identification with standard. Other compounds were tentatively identified by MS fragmentation; Δ ppm – mean mass accuracy; + stands for detected and – stands for not detected compound. t_R - retention time.									Σ	18.846	23.844

A number of these phenolics are found in olive oil and red wines (Topi, Guclu, Kelebek & Selli, 2020). Among them, thirteen phenolic compounds were quantified. Despite their species variation, apple juices comprise an essential source of phenolic compounds (Soler, Soriano & Mañes, 2009). Grapefruit also contains many phytochemicals, including twenty carotenoids, particularly beta-carotene and lycopene, as well as 13 polyphenols, mostly naringin and narirutin (McKay & Wilson, 2016). Besides vitamin C, citrus fruits are rich in flavanones and carotenoids (Baghurst, 2003; Manners, 2007; Topi, 2020). Even their fermented products, such as wines, are rich in phenolic compounds (Topi, Kelebek, Guclu, & Selli, 2021).

5-*O*-caffeoylquinic acid was the main phenolic compound identified in sweet cherry juice. Meanwhile important levels of protocatechuic and vanillic acid from hydroxybenzoic acids group; and quercetin from flavonol group were quantified. Sokół-Łetovska *et al*. (2020) examined the fruit chemical composition of 21 sour cherry cultivars in Poland and found neochlorogenic, chlorogenic, and *p*-coumaric acids dominant in cherry fruit. Other publication identifies quercetin, kaempferol, isorhamnetin rutinosides, and glucosides as dominant constituents in sweet cherry cultivars (Levaj, Dragović-Uzelac, Ganić, Banović & Kovačević, 2010; Cao, Jiang, Lin, Li & Sun, 2015). According to the literature, sour cherry fruits contain glucose, fructose, sucrose, organic acids, and malic acid. Among phenolic compounds, the main group is phenolic acids, with 5-caffeoylquinic, *p*-coumaric, and 3-caffeoylquinic most relevant. Flavanols and flavonols are also important phenolic groups present in cherry fruit (Sut, Dall'Acqua, Poloniato, Maggi, & Malagoli, 2019).

5-*O*-caffeoylquinic acid and vanillic acid were the main phenolic compounds quantified in quince juice. In addition, significant amount of quercetin and its glucosides (table 2) were present. In a study, Magalhaes and colleagues (2009) evaluated the phenolic compounds' profile of the quince fruit (peel, pulp, and seeds) and showed that 5-O-caffeoylquinic acids were major phenolic while seeds were rich in 6,8-di-*C*-glucosyl chrysoeriol. Similarly, chlorogenic acid (5-*O*-caffeoylquinic acid, 37%) and rutin (36%) were primary phenolics (Fattouch *et al*., 2007).

CONCLUSIONS

Phenolic compounds in quince and sweet cherry cold-pressed juice were successfully estimated by liquid chromatography tandem mass spectrometry, as well as spectrophotometry. Quince juice had the highest TPC and TFC values compared to sweet cherry juice. Regarding to antioxidant scavenging activity was fond that inverse value, with sweet cherry possessing higher anti-DPPH radical activity comparing with quince juice. Phenolic acids were the main phenolic class in both investigated fruit juices—with a significant correlation with total phenolic content. According to LC-MS/MS4 analysis, a total of 31 phenolic compounds were identified including 6 hydroxybenzoic acids, 14 hydroxycinnamic acids, two flavan-3-ols, six flavonols, and one dihydrochalcone.

REFERENCES

Baghurst, K. (2003). Composition of citrus fruits, other fruits, fruit juices, soft and sports drinks. In: The Health Benefits of Citrus Fruits. *Health Sciences & Nutrition, CSIRO*, Sydney, Australia, p. 36.

Basu, A., & Penugonda, K. (2009). Pomegranate juice: a heart-healthy fruit juice. *Nutrition Reviews,* 67, 49-56.

Blando F., & Oomah B. D. (2019). Sweet and sour cherries: Origin, distribution, nutritional composition, and health benefits. *Trends in Food Science and Technology*, 86, 517–529. DOI: 10.1016/j.tifs.2019.02.052.

Bonerz, D., Würth, K., Dietrich, H., & Will, F. (2007). Analytical characterization and the impact of aging on anthocyanin composition and degradation in juice from five sour cherry cultivars. *European Food Research and Technology*, 224, 355–364.

Cao, J., Jiang, Q., Lin, J., Li, X., Sun, C., & Chen, K. (2015). Physicochemical characterization of four cherry species (*Prunus spp.*) grown in China. *Food Chemistry*. 173, 855–863.

Directive 2012/12/EU, (2012). Directive 2012/12/EU of the European Parliament and of the Council of 19 April 2012 amending Council Directive 2001/112/EC relating to fruit juices and certain similar products intended for human consumption. *Official Journal of the European Union*, L 115, p. 1-12.

Fattouch, S., Caboni, P., Coronea, V., Tuberoso, C. I. G., Angioni, A., Dessi, S., Marzouki, N. & Cabras, P. (2007). Antimicrobial Activity of Tunisian Quince (*Cydonia oblonga Miller*) Pulp and Peel Polyphenolic Extracts. *Journal of Agricultural and Food Chemistry,* 55, 963–969.

Gasperotti, M., Masuero, D., Mattivi, F., & Vrhovsek, U. (2015). Overall dietary polyphenol intake in a bowl of strawberries: The influence of *Fragaria* spp. In nutritional studies. *Journal of Functional Foods,* 18, 1057-1069.

Gholamreza, K., Kitipong, A., & Supaart, S. (2019). Effect of cold-pressed and normal centrifugal juicing on quality attributes of fresh fruit juices: do cold-pressed juices harbor a superior nutritional quality and antioxidant capacity? *Heliyon,* 5(6), e01917.

Hossain, M. B., Rai, D. K., Brunton, N. P., Martin-Diana, A. B., & Barry-Ryan, C. (2010). Characterization of phenolic composition in *Lamiaceae* spices by LC-ESI-MS/MS. *Journal of Agriculture and Food Chemistry*, 58, 10576–0581.

Kelley S.D., Adkins Y., & Laugero D.K. (2018). A Review of the health benefits of cherries. *Nutrients*, 10, 368. DOI: 10.3390/nu10030368.

Kim, D. O., Jeong, S. W., & Lee, C. Y. (2003). Antioxidant capacity of phenolic phytochemicals from various cultivars of plums. *Food Chemistry,* 81, 321-326.

Kostić, A., Milinčić, D., Gašić, U., Nedić, N., Stanojević, S., Tešić, Ž., & Pešić, M. (2019). Polyphenolic profile and antioxidant properties of bee-collected pollen from sunflower (*Helianthus Annuus* L.) plant. *LWT - Food Science and Technology*, 112, 108224.

Levaj, B., Dragović-Uzelac, V., Ganić, K. K., Banović, M., & Kovačević, D. B. (2010). Polyphenols and volatiles in fruits of two sour cherry cultivars, some berry fruits, and their jams. *Food Technology and Biotechnology*, 48, 538–547.

Ljekočević, M., Jadranin, M., Stanković, J., Popovic, B., Nikićević, N., Petrović, A., & Tešević, V. (2019). Phenolic composition and DPPH radical scavenging activity of plum wine produced from three plum cultivars. *Journal of the Serbian Chemical Society*, 84(2), 141-151.

Magalhaes, A. S., Siva, B. M., Pereira, J. A., Andrade, P. B., Valentao, P. & Carvalho, M. (2009). Protective effect of quince (*Cydonia oblonga* Miller) fruit against oxidative hemolysis of human erythrocytes. *Food and Chemical Toxicology*, 47, 1372–1377.

Manach, C., Scalbert, A., Morand, C., Rémésy, C. Jiménez, L. (2004). Polyphenols: food sources and bioavailability. *The American Journal of Clinical Nutrition*, 79/5, 727–747, https://doi.org/10.1093/ajcn/79.5.727.

Manners, G. D. (2007). Citrus Limonoids: Analysis, Bioactivity, and Biomedical Prospects. *Journal of Agricultural and Food Chemistry.* 55, 8285-8294.

McKay, D.L. & Wilson, T. (2016). Cranberry Juice: Effects on Health. In: Beverage Impacts on Health and Nutrition, Wilson T. und & N. J. Temple, N. J. Eds. Humana Press, Totowa, NJ, USA, p. 101-114.

Niki, E., & Noguchi, N. (2000). Evaluation of antioxidant capacity. What capacity is being measured by which method? *IUMBM Life*, 50, 323–329.

Paredes-Lopez, O., Cervantes-Ceja, M. L., Vigna-Perez, M., & Hernandez-Perez, T. (2010). Berries: improving human health and healthy aging, and promoting quality life − a review. *Plant Foods for Human Nutrition*, 65, 299−308.

Prvulović, D., Popović, M., Malenčić, D., Ljubojević, M., Barać, G., Ognjanov, V. (2012). Phenolic content and antioxidant capacity of sweet and sour cherries. *Studia UBB Chem*. 57, 175– 181.

Silva, B. M., Andrade, P. B., Valentao, P., Ferreres, F., Seabra, R. M., & Ferreira, M. A. (2004). Quince (*Cydonia oblonga Miller*) fruit (pulp, peel, and seed) and jam: antioxidant activity. *Journal of Agricultural and Food Chemistry*, 52, 4705–4712.

Silva, B.M., Andrade, P.B., Ferreres, F., Domingues, A. L., & Seabra, R. M. (2002). Phenolic profile of quince fruit (*Cydonia oblonga Miller*) (pulp and peel). *Journal of Agricultural and Food Chemistry*, 50, 4615–618.

Sokół-Łętowska, A., Kucharska, A. Z., Hodun, G., & Gołba, M. (2020). Chemical Composition of 21 Cultivars of Sour Cherry (*Prunus cerasus*) Fruit Cultivated in Poland. *Molecules*, 25 (19), 4587.

Soler, C., Soriano, J. M., & Mañes, J. (2009). Apple-products Phytochemicals and Processing: A review. *Natural Product Communications*, 4, 659-670.

Stojković, D., Drakulić, D., Gašić, U., Zengin, G., Stevanović, M., Rajčević, N., & Soković, M. (2020). *Ononis spinose* L. an edible and medicinal plant: UHPLC-LTQ-Orbitrap/MS chemical and biological activities of the herbal extract. *Food & Function*, 11, 7138-7151.

Strazzulo, G., De Giulio, A., Tommonaro, G., La Pastina, C., Poli, A., Nicolaus, B., De Prisco, R., & Saturnino, C. (2007). Anti-oxidative Activity and Lycopene and β-Carotene Contents in Different Cultivars of Tomato (*Lycopersicon Esculentum*). *International Journal of Food Properties*, 10, 321–329.

Sut, S., Dall'Acqua, S., Poloniato, G., Maggi, F. & Malagoli, M. (2019). Preliminary evaluation of quince (Cydonia oblonga Mill.) fruit as extraction source of antioxidant phytoconstituents for nutraceutical and functional food applications. *J Sci Food Agric*. 99(3), 1046-1054. DOI: 10.1002/jsfa.9271.

Szajdek, A., & Borowska, E.J. (2008). Bioactive Compound and Health-Promoting Properties of Berry Fruits: A review. *Plant Foods for Human Nutrition*, 63, 147-156.

Topi, D. (2020). Volatile and chemical compositions of freshly squeezed sweet lime (*Citrus limetta*) juices. *Journal of Raw Materials and Processed Foods*, 1(1), 22-27.

Topi, D., Guclu, G., Kelebek, H., & Selli, S. (2020). Comparative elucidation of phenolic compounds in Albanian olive oils using LC-DAD-ESI-MS/MS. *Journal of Liquid Chromatography & Related Technologies*. 43, 203–212. DOI: 10.1080/10826076.2019.1711117.

Topi, D., Kelebek, H., Guclu, G., & Selli, S. (2021). LC- DAD- ESI- MS/MS characterization of phenolic compounds in wines from Vitis vinifera '*Shesh i bardhë*' and '*Vlosh*' cultivars. *Journal of Food Processing and Preservation*, e16157.

Vasić, V., Gašić, U., Stanković, D., Lušić, D., Vukić-Lušić, D., Milojković-Opsenica, D., Tešić, Ž., & Trifković, J. (2019). Towards better quality criteria of European honeydew honey: Phenolic profile and antioxidant capacity. *Food Chemistry,* 274, 629–641.

Wojdyło, A., Oszmianski, J. and & Bielicki, P. (2013). Polyphenolic Composition, Antioxidant Activity, and Polyphenol Oxidase (PPO) Activity of Quince (*Cydonia oblonga* Miller) varieties. *Journal of Agriculture and Food Chemistry*, 61, 2762−2277.

Tianyi, H., Vigasini, S., Hanjing, W., Amrit, BK, Abdur, R., Fahad, A.A., & Hafiz, A.R.S. (2021). Determination and Characterization of Phenolic Compounds from Australia-Grown Sweet Cherries (*Prunus avium* L.) and Their Potential Antioxidant Properties. *ACS Omega*, 6(50), 34687-34699. DOI: 10.1021/acsomega.1c05112.

de Souza, V. R., Pereira, P. A., da Silva, T. L., de Oliveira Lima, L. C., Pio, R., Queiroz, F. (2014). Determination of the bioactive compounds, antioxidant activity and chemical composition of Brazilian blackberry, red raspberry, strawberry, blueberry, and sweet cherry fruits. *Food Chemistry*. 156, 362−368.

Urbanavičiūtė, I., Mindaugas, L., Bobinas, Č., Šarkinas, A., Rezgienė, A. & Viskelis, P. (2020). Japanese Quince (*Chaenomeles japonica*) as a potential source of phenols: Optimization of the extraction parameters and assessment of antiradical and antimicrobial activities. *Foods*. 9. 10.3390/foods9081132.

Sabri, E., Spalevic, V., Boukdir, A., Karaoui, I., Ouallali, A., Mincato, R.L., Sestras, P. (2022). Estimation of soil losses and reservoir sedimentation: A case study in Tillouguite Sub-basin (High Atlas-Morocco). Agriculture and Forestry, 68 (2): 207-220. doi:10.17707/AgricultForest.68.2.15

DOI: 10.17707/AgricultForest.68.2.15

Elmouatassime SABRI[1], Velibor SPALEVIC[2], Ahmed BOUKDIR[1], Ismail KARAOUI,[1] Abdessalam OUALLALI[3], Ronaldo Luiz MINCATO[4], Paul SESTRAS[5]

ESTIMATION OF SOIL LOSSES AND RESERVOIR SEDIMENTATION: A CASE STUDY IN TILLOUGUITE SUB-BASIN (HIGH ATLAS - MOROCCO)

SUMMARY

Dam siltation has become a serious problem in arid and semi-arid countries under climate variability, where soil erosion and siltation represent a major challenge that face the industry of dams. In Morocco the policy of dam construction is one of the main keys in sustainable development, but unlikely, the dam siltation caused by soil erosion still present a big constraint. This study was carried out in the sub-basin of Tillouguite upstream the Bin El Ouidane dam in the High Atlas, in the region of Beni Mellal Khenifra, Morocco. The study aims to estimate the production of erosion material: soil losses, and the real soil losses rate - sediment yield, in Bin El Ouidane dam, using a combination of IntErO model - Intensity of Erosion and Outflow, GIS - Geographic information System and RS - Remote sensing. The study requires data which are collected from meteorological stations, soil data analysis, satellite images and observations during field missions. As a result, the production of erosion material in the Tillouguite sub-basin is estimated at 10,015,354 m^3yr^{-1}, the coefficient of the deposit retention is estimated at 0.283, and the real soil losses rate is around 2,838,489 m^3yr^{-1}. Given that the specific real soil losses rate is estimated at 910.02 $m^3km^2yr^{-1}$, and based on Gavrilovic classification, the sub-basin of Tellouguite is considered with a high potential of soil erosion risk, due to large bare land, and the steep land slope in the sub basin - factors that affect the storage capacity of Bin El Ouidane Dam. All the findings are a measurable indicators that are inviting policy makers to initiate appropriate measures for the protection of land degradation, all in line with the sustainable development policies in Morocco.

Keywords: Dam siltation, Soil erosion, IntErO Model, Land Use, Soil erosion, GIS, Remote Sensing.

[1] Elmouatassime Sabri (corresponding: sabri.elmouatassime@gmail.com), Ahmed Boukdir, Ismail Karaoui, Sultan MoulaySlimane University, Department of Geology, Beni Mellal, MOROCCO;
[2] Velibor Spalevic, Biotechnical faculty, University of Montenegro, Podgorica, MONTENEGRO;
[3] Abdessalam Ouallali, GPE department,, Faculty of Sciences and Techniques of Mohammedia, Hassan II University of Casablanca, MOROCCO;
[4] Federal University of Alfenas, UNIFAL-MG, Alfenas, Minas Gerais, BRAZIL; Paul Sestras, Faculty of Civil Engineering, Technical University of Cluj-Napoca, Cluj-Napoca, ROMANIA.
Received: 29/04/2022 Accepted: 24/06/2022

INTRODUCTION

Soil is a three-phase system that consists of solid particles, liquid, and gas, but also species that create a dynamic and complex ecosystem and is among the most precious resources to humans. On the other hand, soil erosion by water is acknowledged as a primary concern in the degradation of soil quality and functionality (Billi, & Spalevic, 2022; Saggau *et al*, 2022; Stefanidis *et al*., 2022; Lense *et al*, 2022; Chalise *et al*, 2019; Spalevic *et al*, 2017; Borrelli *et al*., 2016; Lal, 2014). The ever-growing availability of earth observation (EO) data and the well-established use of geographic information systems (GIS) during the last decades leads to the development of automated geospatial workflows for the estimation and mapping soil losses (Dominici *et al*., 2021; Stefanidis *et al*., 2021). It is a major global soil degradation threat to land, freshwater, and oceans; but also to the reservoirs constructed for agriculture production needs, energy, and other water supply matters (Stefanidis & Stefanidis, 2012). The sustainable reservoir management is rarther important for sustainable water resources management due to reported trends in drought conditions to mountainous and semi-mountainous areas (Stefanidis & Alexandridis, 2021; Myronidis *et al*., 2012). This process of degradation has continued to grow as a problem over time, with increasing sediment mobilization; decreasing reservoirs retention capacity (Spalevic *et al*., 2020). For over a century the scientific community has been addressing the processes governing soil erosion, the occurrence of accelerated soil erosion, and its negative associated socio-environmental impacts (Bennett and Chapline, 1928; Smith, 1914; Borrelli *et al*., 2021). Some researchers demonstrated in their studies the effect of vegetation cover and lithology on the detachment, mobilization and transport capacity of sediments (Khaledi Darvishan *et al*., 2019; Spalevic *et al*., 2019; Behzadfar *et al*., 2018; Kavian *et al*., 2018; Behzadfar *et al*., 2017; Behzadfar *et al*., 2014; Spalevic *et al*., 2013). Soil degradation and decreased water resources negatively affect agricultural production and have a negative impact on a country's economy (Ouallali *et al*., 2018). The United Nations Sustainable Development Goals (SDGs) acknowledge the significance of soil resources for sustainable development and advocate their protection in order to meet the ambitious goal of zero land degradation by 2030. This task must be integrated evaluated under the context of climate change for near and far future climate projections (Stefanidis et al., 2021). Our goal is to contribute with our research to the local demand and needs in relation to the dam siltation estimation of soil losses and reservoir sedimentation by using Global Inventions for the future Local Interventions.

The dam siltation which results the storage capacity loss is a natural phenomenon and depends on climatic conditions, relief, soil characters and land use (Costea *et al*, 2022; Felix *et al*, 2021; Chalise & Kumar, 2020; Andjelkovic *et al*, 2018). It is accelerated and intensified with human activity such as agricultural practices, grazing and deforestation. In Morocco the dam siltation is still the biggest problem and is facing the dam construction policies, including sustainable development policy. This phenomenon requires costly investments to solve problems caused by siltation. Due to siltation, dams in Morocco lost 10% of their storage capacities, where nearly 75 Mm^3 of soil reaches reservoirs every year, and some dams such as Khattabi, Dkhila, Sidi Driss, Sidi Said Maâchou and Nakhla, have already reached their maximum storage capacities because of the soil erosion problem.

Some solutions, including forestation are implemented in order to decrease the soil losses rate and reduce the nuisance of siltation on the storage capacity of dams, but unlikely and despite more than six decades of research, sedimentation is still probably the major problem faced by the dam industry.

The Bin El Ouidane dam is the third large dam in Morocco, with 1.5 Billion m^3 of the initial storage capacity, and is considered as important key in energetic and agricultural national plans, where the dam produces almost 12% of national hydroelectric energy production and irrigates the plain of Tadla, including two irrigated perimeters of Bni Amir and Bni Moussa, with a total surface of 105,500 ha (Karaoui *et al*., 2018).

The strategic importance of Bin El Ouidane dam brings the intention and interest of researchers to siltation and soil erosion problem in the watershed of Oued El A bid upstream the Bin El Ouidane dam. The objective of the research was identification of erosion critical areas based on soil erodibility, including related geographical factors in the Tillouguite sub-basin, High Atlas, Morocco.

MATERIAL AND METHODS

Study area. Morocco, in Northern Africa, bordering the North Atlantic Ocean and the Mediterranean Sea. The Position of this area is strategic with the location along Strait of Gibraltar, and it is the only African country to have both Atlantic and Mediterranean coastlines. This study was carried out in the sub-basin of Tillouguite, with a total surface of 2954 km^2, which forms alongside the sub-basins the big watershed of Oued EL Abid with a surface of 6073 km^2 (Figure 1).

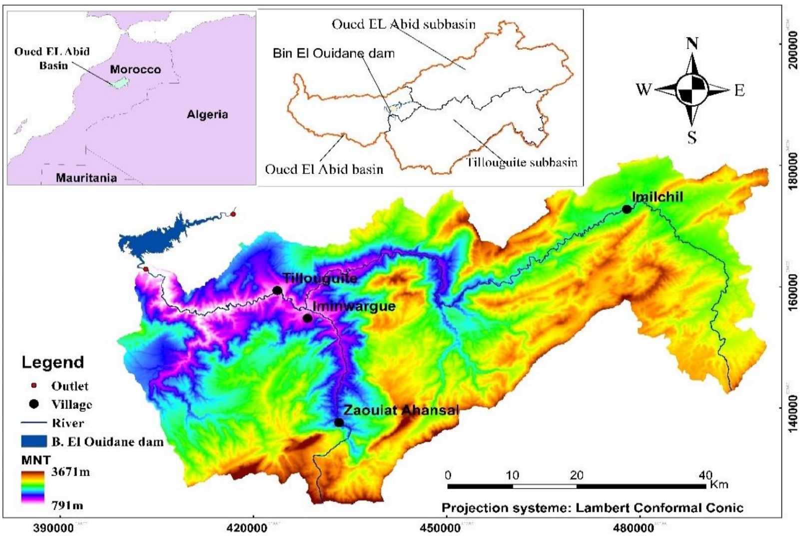

Figure 1. Study area of the sub-basin of Tillouguite, Morocco.

The region of Beni Mellal-khenifra is located between the High Atlas and the plain of Tadla. The main river in Tillouguite sub-basin is Oued assif-Ahansal, which aliments with the river of Oued El Abid the Bin El Ouidane Dam.

In term of geology, the sub-basin of Tillouguite is a part of High Atlas, which is formed mainly of carbonate grounds, belonging to the Jurassic, which gives it the character of having very high mountain ranges, where the elevation varies from 791m to 3671m (Sabri *et al*., 2018; Sabri *et al*., 2019).

The average annual precipitation according to the four meteorological stations is Ait Ouchen: 419.6 mm, TiziNisly: 453.0 mm, Zaouite Ahansal: 369.8 mm and Tellouguite: 395.3 mm. A semi-arid climate is observed in the sub-basin, with 6 months of rainy season and 6 months of dry season, where over 90% of annual precipitations is during the winter and spring seasons (Figure 2).

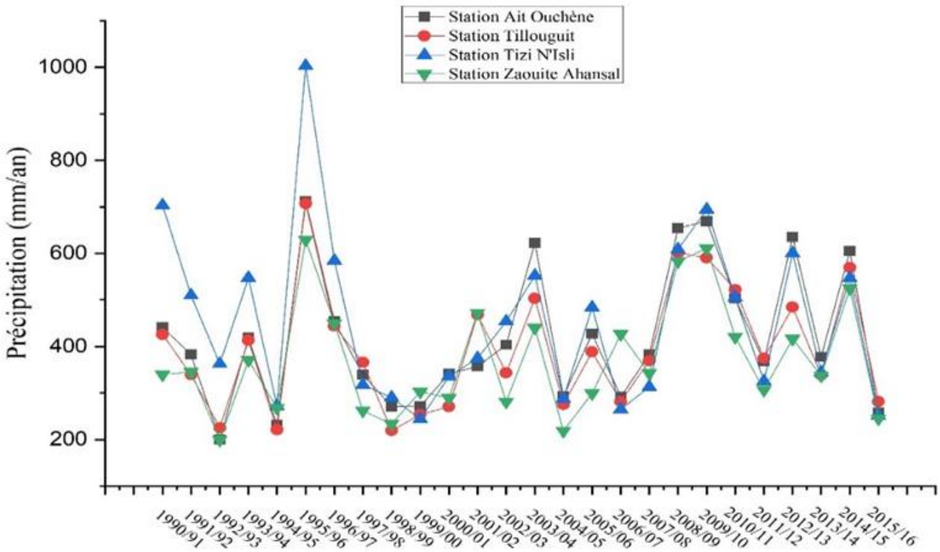

Figure 2. Precipitations in sub-basin of Tillouguite, Morocco (period: 1991-2016)

The temperature data has obtained from 4 meteorological stations measurements during 15 years, between 1991 and 2016. Where the maximum and minimum temperature ranges observed in the watershed are 26 °C to 45 °C and -9 °C to 8 °C, respectively.

The sub-basin of Tillouguite is characterized by 6 types of land use, including bare lands, which covers alongside pasture lands, the quasi totality of the sub-basin, dense forests and sparse forests, which have known a high rate of degradation in the last 20 years, and culture (Figure 3).

The soil map of Tillouguite sub-basin is generated based on the soil map of Morocco (1: 1.500.000) by Wladimir Cavalla in 1950 who was in charge of the mission on behalf the National Center for Scientific Research at the Center of agronomic research of Morocco in 1950 (Figure 4).

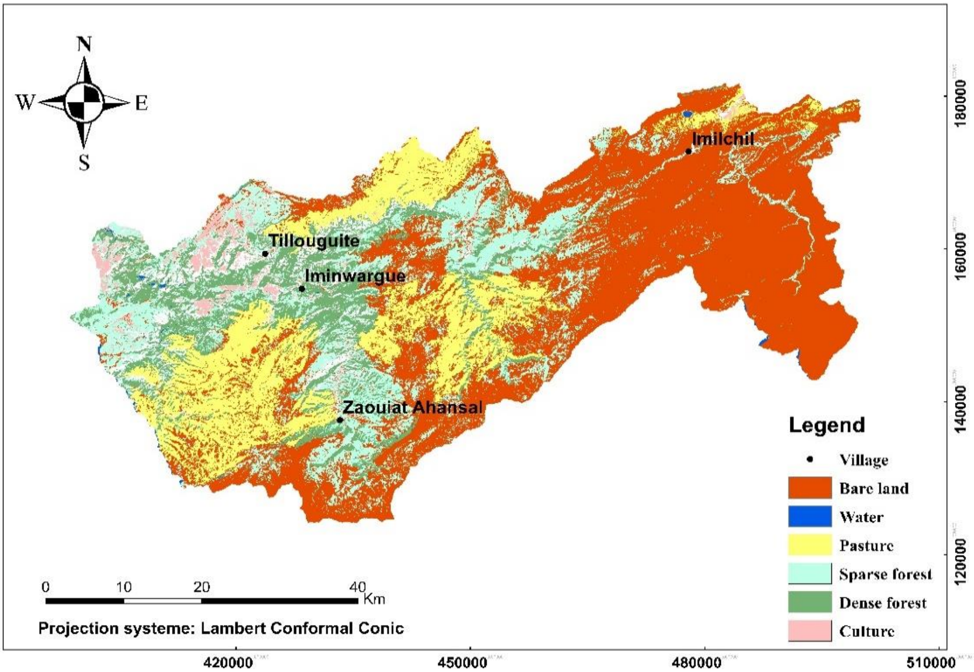

Figure 3: Land use in the sub-basin of Tillouguite, Morocco.

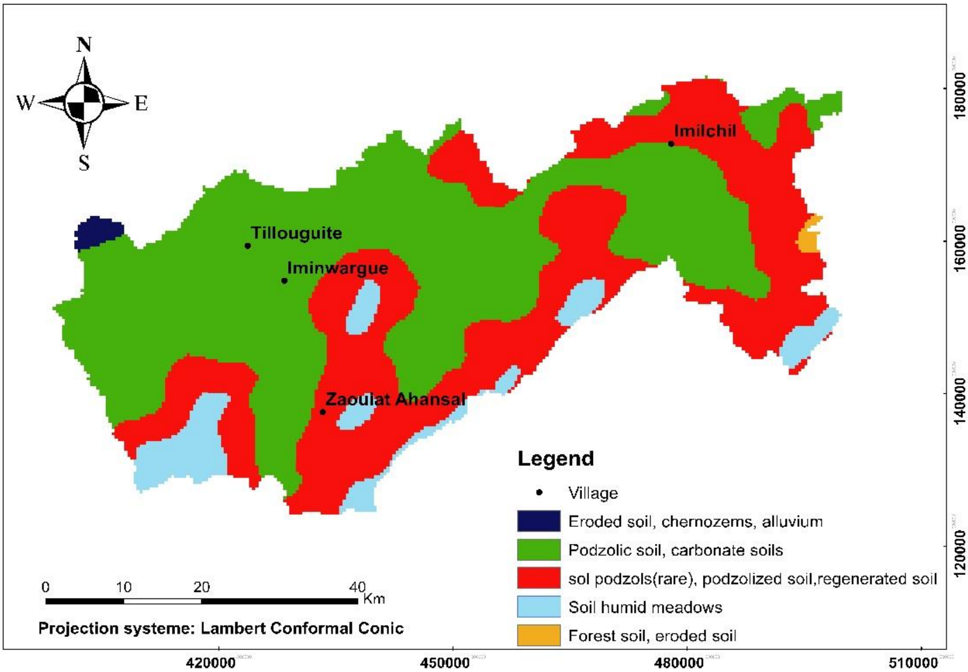

Figure 4: Types of soil in Tillouguite Sub-basin.

Method. With an increased abundance of observed data and the aim of mapping spatially distributed soil erosion rates with a better understanding of their mechanics (Cook, 1937), scientists are developing quantitative soil-erosion prediction equations based on physical factors such as climate, soil characteristics, vegetation type, and topography (Zingg, 1940) for a century. Several mathematical models classified as empirical, conceptual, or process-oriented have been developed to predict soil erosion processes at different spatial and temporal scales (Merritt *et al*., 2003; Morgan and Nearing, 2011; Nearing, 2013). Batista *et al*. (2019) reported that today “there is no shortage of soil erosion models, model applications, and model users' but there is still acknowledge gap on the validity, quality, and reliability of the modelling application results”.

Despite the significant progress made in model development and input parameterization, output uncertainties persist due to the non-linear relationships and thresholds at play between driving factors and the subsequent erosion processes, as well as the difficulties of upscaling model findings from the local scale to larger ones (Borrelli *et al*., 2021.; DeVente and Poesen, 2005).

Today, with the well-established use of geospatial technologies like Geographic Information Systems (GIS), spatial interpolation techniques, and the ever-growing range of environmental data; soil-erosion models play an increasingly important role in the design and implementation of soil management and conservation strategies (Panagos *et al*., 2015). The applications of soil erosion models are growing (Auerswald *et al*., 2014), alongside the scale of their application (Borrelli *et al*., 2017, Naipal *et al*., 2018). These models play an important role as tools to support decision-makers in policy evaluations (Borrelli *et al*., 2021; Olsson and Barbosa, 2019).

Accurate information on the existing land-use pattern and its spatial distribution is a prerequisite for soil conservation planning and assessment of the soil erosion rate. It is essential for the development of adequate erosion prevention measures for sustainable management of land and water resources (Thakur et al, 2018).

In this study we used the IntErO model, which is based on EPM- Erosion Potential Model (Gavrilovic S., 1972). The EPM was created to estimate the annual sediment yield and the transport of sediments based on physical, climate, geological and hydrological characteristics of the river basin such as the temperature, the mean annual rainfall, the soil use, the soil properties and some other factors in the watershed scale, with arid and semi-arid climate, where it has been used in Europe, Middle-Est, North-Africa, America, under arid and semi-arid climate. In recent times the EPM is repeatedly applied in several watersheds in the Mediterranean area, especially in the South East Europe - Balkan region (Kostadinov *et al*., 2006; Tazioli, 2009; Dragicevic *et al*., 2017; Tavares *et al*., 2019; Tosic *et al*, 2019.; Spalevic *et al*., 2020; Dragicevic *et al*., 2022), and also in arid and semi-arid areas of the south-western USA (Gavrilovic Z., 1988).

The method was based on the factors affecting erosion in a watershed, which are dependent on the temperature, the mean annual rainfall, the soil use, the geological properties, and some other factors in the watershed scale (Gholami *et al*, 2013; Khaledi Darvishan *et al*., 2017).

The Intensity of Erosion and Outflow - IntErO program package was developed to predict the runoff peak discharge, the intensity of soil erosion, and the sediment yield in a variety of watershed forms. The model was tested in different countries such as Bosnia & Herzegovina, Bulgaria, Croatia, Czech Republic, Italy, Iran, Montenegro, Macedonia, Serbia, Slovenia, Morocco, Brazil and Nepal, in arid and semi-arid climate (Mohammadi *et al*., 2021; Ouallali *et al*, 2018).

In this study we used IntErO model specifically, to estimate the soil losses in the sub-basin of Tillouguite and sediment yield in the Bin El Ouidane dam, based on the following equations:

$$W_{yr} = T_i \cdot H_{yr} \cdot \pi \cdot \sqrt[2]{Z^3} \cdot F \qquad \text{Equation 1}$$

$$T_i = \sqrt[2]{\frac{t_0}{10}} + 0.1 \qquad \text{Equation 2}$$

$$Z = Y \cdot X_a \cdot (\varphi + \sqrt[2]{I_{sr}}) \qquad \text{Equation 3}$$

$$G_{yr} = W_{yr} \cdot R_u \qquad \text{Equation 4}$$

$$R_u = \frac{(O \cdot D)^{0.5}}{0.25 \cdot (Lv \cdot 10)} \qquad \text{Equation 5}$$

where: W_{yr} = Annual erosion (m^3 km-^{2} yr-^{1}); T_i = Coefficient of temperature (dimensionless); H_{yr} = Mean annual rainfall (mm yr^{-1}); Z = Coefficient of erosion (dimensionless); F = Basin area (km^2); t_0 = Mean air temperature (°C yr^{-1}); Y = Soil resistance to erosion (dimensionless); x_a = Coefficient of soil use and management (dimensionless); φ = Coefficient of visible erosion features (dimensionless); I_{sr} = Mean slope (%); G_{yr} = Sediment production (m^3 km^{-2} yr^{-1}); Ru = Coefficient of retention (dimensionless); O = Basin length (km); D = Difference in basin elevation (m) and; Lv = Length of main stream (km).

Based on the data mentioned we obtained the data needed to run the IntErO program package. The input data needed for modelling of soil erosion processes and runoff are presented in the table below (Table 1).

Table 1: Modelling inputs data for Tillouguite sub-basin, Morocco.

Inputs	**Symbol**	**Value**	**Unit**
River basin area	F	2954	km²
The length of the watershed	O	457.84	km
Natural length of the main watercourse	Lv	154.12	km
The shortest distance between the fountainhead and mouth	Lm	99.23	km
The length of the main watercourse with tributaries	ΣL	55594	km
River basin length measured by a series of parallel lines	Lb	120	km
The area of the bigger river basin part	Fv	1603.45	km²
The area of the smaller river basin part	Fm	1350.55	km²
Altitude of the first contour line	h0	700	m
Equidistance	Δh	110	m
The lowest river basin elevation	Hmin	650	m
The highest river basin elevation	Hmax	3226	m
A part of the basin with very permeable product from rocks	fp	0.46	
A part of the basin area consisted of medium permeable rocks	fpp	0.22	
A part of the basin consisted of poor water permeability rocks	fo	0.32	
A part of the river basin under forests	fs	0.09	
A part of the basin under grass, pastures and orchards	ft	0.07	
A part under bare land, plough-land and ground without grass	fg	0.84	
The volume of the torrent rain	hb	165.5	mm
Average annual air temperature	t0	16.8	°C
Average annual precipitation	Hyr	450	mm
Types of soil products and related types	Y	1.3	
coefficient of the river basin planning	Xa	0.84	
Numeral equivalents of visible erosion process	φ	0.61	

RESULTS AND DISCUSSION

After preparing the inputs required for IntErO model, the model was run and came out with outputs data which is shown in Table 2.

Based on the results, we concluded that there is a possibility of the appearance of large flood waves. The value of the coefficient G of 18.91 indicates a very high density of the hydrographic network in the sub-basin. The value of 73.48% indicates the existence of steep slopes in the sub-basin. The value of the Z coefficient of 1.695 indicates that the watershed belongs to category I of destruction. The results indicate also that the force of the erosion process is excessive in the sub-basin.

Table 2: Modelling results for Tillouguite sub-basin, Morocco.

Results	**Symbol**	**Value**	**Unit**
Coefficient of the river basin form	A	0.54	-
Coefficient of the watershed development	m	0.89	-
Average river basin width	B	23.99	km
(A)symmetry of the river basin	a	0.91	-
Density of the river network of the basin	G	18.91	-
Coefficient of the river basin tortuousness	K	1.88	-
Average river basin altitude	Hsr	2223.58	m
Average elevation difference of the river basin	D	1432.58	m
Average river basin decline	Isr	73.48	%
The height of the local erosion base of the river basin	Hleb	2908	m
Coefficient of the erosion energy of the basin's relief	Er	123.86	-
Coefficient of the region's permeability	S1	0.78	-
Coefficient of the vegetation cover	S2	0.95	-
Water retention in inflow	W	9363.25	m
Energetic potential of water flow during torrent rains	2gDF^½	3600.58	m km s
Temperature coefficient of the region	T	1.33	
Coefficient of the river basin erosion	Z	1.695	
Production of erosion material in the river basin	Wyr	1001535	$m^3\ yr^{-1}$
Coefficient of the deposit retention	Ru	0.283	
Real soil losses	Gyr	2838489	$m^3\ yr^{-1}$
Real soil losses per km^2	Gyr (km^2)	910.02	$m^3 km^2 yr^{-1}$

Bathymetric measurements at the Bin El Ouidane dam have reported that the sediment yield rate is 5 million m^3 per year. Where previous studies, in the watershed of Oued El Abid using the USLE/RUSLE model (Wischmeier and Smith, 1978; Williams, 1975; Renard, 1991), estimated the soil losses at 8.000.000 $m^3\ yr^{-1}$ and the sediment yield at 5.200.000 $m^3\ yr^{-1}$ (Sabri *et al*., 2016).

Being a spatially explicit model is the biggest advantage of the RUSLE whereas the IntErO calculates sediment yield collectively for the whole basin. Where the RUSLE model is more focused with the calculation of soil loss only, the IntErO also computes maximum outflow from the river basin, asymmetry of the river basin and coefficients of river basin form, watershed development, river basin tortuousness, region’s permeability, and vegetation cover; these parameters are also of paramount importance in determining the soil loss of a landscape. A major advantage of IntErO over RUSLE is it calculates both the sediment delivery ratio and sediment yield but RUSLE does not. RUSLE only calculates gross soil erosion rates which may or may not include soil that is lost from the river basin as not all the erosion materials generated get lost from the basin but sediment yield measured by the IntErO is the actual volume of soil leaving the river basin (Chalise *et al*., 2019).

Other study using the IntErO model in the sub-basin of Oued El Abid estimated the soil losses at 3.960.115 m^3 yr^{-1}, and the sediment yield in the dam of Bin El Ouidane at 1.200.000 m^3 yr^{-1} (Sabri *el al*., 2019). The results of this study came out with the sediment yield in the watershed of Oued El Abid, upstream of the dam of Bin El Ouidane, which gathers both sub-basins of Oued El Abid and Tillouguite, and is estimated at 4.100.000 m^3 yr^{-1}, which is about 10% less than the bathymetric measurement in the Bin El Ouidane dam.

CONCLUSION

This study shows the effectiveness of the combination of RS, GIS and IntErO model to estimate the soil losses and sediment yield, based on data, which have obtained from satellite images analyses and meteorological stations measurements, but also on data from soil analysis and field observations.

The sediment production in the region of the Bin El Ouidane dam, that counts the results from the two sub-basins of the El Abid and Tillouguite, is estimated at 4.1 Mm^3 $year^{-1}$, and shown close match of the results obtained by modelling and the bathymetry studies.

This study also confirms the effectiveness of the IntErO model in assessing the soil loss in a North African country that is outside of the Balkan Peninsula where the IntErO model is frequently used. The research approved the technical capability of IntErO model in soil erosion modelling and sedimentation estimation, under semi-arid climate in large spatial scale. Also, this study could provide important support to decision makers and planners to simulate scenarios to reduce soil erosion in the watershed of Oued El Abid and plan interventions against storage capacity loss in the dam of Bin El Ouidane, but also to the other river basins with similar physical-geographic conditions all over the World.

REFERENCES

Andjelkovic, A.; Ristic, R.; Janic, M.; Djekovic, V. and Spalevic, V. (2017). Genesis of Sediments and Siltation of the accumulation Duboki Potok of the Barajevska River Basin, Serbia. Journal of Environmental Protection and Ecology, 18(4), 1735-1745.

Auerswald, K.; Fiener, P.; Martin, W.; Elhaus, D. (2014). Use and misuse of the K factor equation in soil erosion modeling: an alternative equation for determining USLE nomograph soil erodibility values. Catena 118, 220–225. https://doi.org/10.1016/j.catena.2014.01.008.

Batista, P.V.G.; Davies, J.; Silva, M.L.N.; Quinton, J.N. (2019). On the evaluation of soil erosion models: are we doing enough? Earth-Science Rev. 197, 102898.

Behzadfar, M.; Djurovic, N.; Simunic, I.; Filipovic, M. and Spalevic, V. (2014). Calculation of soil erosion intensity in the S1-6 Watershed of the Shirindareh River Basin, Iran. 2015; p.207-213. International scientific conference: Challenges in Modern Agricultural Production, December 11, 2014, Skopje, Macedonia. Book of Proceedings, p. 273. Institute of agriculture. ISBN 978-9989-9834-9-8, COBISS.MK-ID 99839242

Behzadfar, M.; Sadeghi, S.H.; Khanjani, M.J.; Hazbavi, Z. (2017). Effects of rates and time of zeolite application on controlling runoff generation and soil loss from a soil subjected to a freeze-thaw cycle. International Soil and Water Conservation Research, 5 (2), 95-101. https://doi.org/10.1016/j.iswcr.2017.04.002

Behzadfar, M.; Spalevic, V.; Billi, P.; Chalise, D.; Mincato, R.; Sabri, E.; Sestras, P.; Kalonde, P. (2018). Calculation of soil erosion intensity and runoff in the S7-8-int basin of the Shirindareh Watershed in Iran. Book of Proceedings, Green Room Sessions 2018 International Geo Eco-Eco Agro Conference, Podgorica, Montenegro, 111-116.

Bennett, H.; Chapline, W. (1928). Soil erosion: A national menace. United States Department of Agriculture (USDA).

Billi, P.; Spalevic, V. (2022). Suspended sediment yield in Italian rivers. Catena 212(2022), 106119. DOI: 10.1016/j.catena.2022.106119

Borrelli, P.; Alewell, C.; Alvarez, P.; Anache, J.; Baartman, J.; Ballabio, C.; Bezak, N.; Biddoccu, M.; Cerda, A.; Chalise, D.; Chen, S.; Chen, W.; De Girolamo, A.; Gessesse, G.D.; Deumlich, D.; Diodato, N.; Efthimiou, N.; Erpul, G.; Fiener, P.; Panagos, P. (2021). Soil erosion modelling: A global review and statistical analysis. Science of The Total Environment. 146494. 10.1016/j.scitotenv.2021.146494.

Borrelli, P.; Paustian, K.; Panagos, P.; Jones, A.; Schütt, B.; & Lugato, E. (2016). Effect of good agricultural and environmental conditions on erosion and soil organic carbon balance: A national case study. Land Use Policy, 50, 408–421.

Borrelli, P.; Robinson, D.A.; Fleischer, L.R.; Lugato, E.; Ballabio, C.; Alewell, C.; Meusburger, K.; Modugno, S.; Schütt, B.; Ferro, V.; Bagarello, V.; Van Oost, K.; Montanarella, L.; Panagos, P. (2017). An assessment of the global impact of 21st century land use change on soil erosion. Nat. Commun. 8, 2013.

Chalise, D.; Kumar, L. (2020). Land use change affects water erosion in the Nepal Himalayas. Plos One, 15(4): e0231692. doi.org/10.1371/journal.pone.0231692

Chalise, D.; Kumar, L.; Spalevic, V.; Skataric, G. (2019). Estimation of Sediment Yield and Maximum Outflow Using the IntErO Model in the Sarada River Basin of Nepal. Water, 11, 952.

Cook, H.L. (1937). The nature and controlling variables of the water erosion process. Soil Sci. Soc. Am. J. 1, 478–494.

Costea, A.; Bilasco, S.; Irimus, I.-A.; Rosca, S.; Vescan, I.; Fodorean, I.; Sestras, P. (2022). Evaluation of the Risk Induced by Soil Erosion on Land Use. Case Study: Guruslau Depression. Sustainability 2022, 14, 652.

De Vente, J.; Poesen, J. (2005). Predicting soil erosion and sediment yield at the basin scale: scale issues and semi - quantitative models. Earth - Sci. Rev. 71, 95–125.

Dominici, R., Larosa, S., Viscomi, A., Mao, L., De Rosa, R., & Cianflone, G. (2020). Yield erosion sediment (YES): A PyQGIS plug-in for the sediments production calculation based on the erosion potential method. Geosciences, 10(8), 324.

Dragicevic, N.; Karleusa, B.; Ozanic, N. (2017). Erosion Potential Method (Gavrilovic method) sensitivity analysis. Soil & Water Res., 12: 51-59.

Dragicevic, S.; Kostadinov, S.; Novkovic, I.; Momirovic, N.; Langovic, M.; Stefanovic, T.; Radovic, M.; Tosic, R. (2022). Assessment of Soil Erosion and Torrential Flood Susceptibility: Case Study—Timok River Basin, Serbia. In book: The Lower Danube River, Hydro-Environmental Issues and Sustainability. 10.1007/978-3-031-03865-5_12.

Felix, F.C.; Avalos, F.A.P.; De Lima, W.; Candido B.M.; Silva M.L.N. & Mincato R.L. (2021). Seasonal behavior of vegetation determined by sensor on an unmanned aerial vehicle. An Acad Bras Cienc 93, e20200712. DOI 10.1590/0001-3765202120200712

Gavrilovic, S. (1972). Inzenjering o bujicnim tokovima i eroziji. Izgradnja. Beograd.

Gavrilovic, Z. (1988). The use of empirical method (erosion potential method) for calculating sediment production and transportation in unstudied or torrential streams. In: White, W. R. (ed.), International Conference on River Regime; 411–422. Chichester.
Gholami, L.; Sadeghi, S.H.R.; Homaee, M. (2013). Straw mulching effect on splash erosion, runoff and sediment yield from eroded plots. Soil Science Society of America Journal, 77, 268–278.
Karaoui, I.; Arioua, A.; Boudhar, A.; Hssaisoune, M.; Sabri, E.; Ait Ouhamchich, K.; Elhamdouni, D. (2018). Evaluating the potential of sentinel-2 satellite images for water quality characterization of artificial reservoirs: the bin el ouidane reservoir case study (Morocco). Meteorol. Hydrol. Water Manag. 7(1), 31–39.
Kavian, A.; Gholami, L.; Mohammadi, M.; Spalevic, V.; Falah Soraki, M. (2018). Impact of Wheat Residue on Soil Erosion Processes. Notulae Botanicae Horti Agrobotanici Cluj-Napoca, 46(2), 553-562.
Khaledi Darvishan A.; Behzadfar M.; Spalevic V.; Kalonde P.; Ouallali A.; Sabri E. (2017). Calculation of sediment yield in the S2-1 watershed of the Shirindareh river basin, Iran, Agriculture and Forestry, 63(3), 23-32.
Khaledi Darvishan, A.; Mohammadi, M.; Skataric, G.; Popovic, S.; Behzadfar, M.; Rodolfo Ribeiro Sakuno, N.; Luiz Mincato, R.; Spalevic, V. (2019). Assessment of soil erosion, sediment yield and maximum outflow, using IntErO model (Case study: S8-IntA Shirindarreh Watershed, Iran). Agriculture and Forestry, 65(4), 203-210.
Kostadinov, S.; Zlatic, M.; Dragovic, N. & Gavrilovic, Z. (2006). Soil erosion in Serbia and Montenegro. In Boardman, J.; Poesen, J. (eds), Soil Erosion in Europe. John Wiley & Sons, Ltd; London, 271-277.
Lal, R. (2014). Desertification and soil erosion. Global environmental change. Cham: Springer. https://doi.org/10.1007/978-94-007-5784-4_7
Lense, G.H.E.; Servidoni, L.E.; Parreiras, T.C.; Santana, D.B.; Bolleli, T.M.; Ayer, J.E.B.; Spalevic, V.; Mincato, R.L (2022). Modeling of soil loss by water erosion in the Tietê River Hydrographic Basin, São Paulo, Brazil. Semina: Ciênc. Agrár. Londrina, v. 43, (4), 1417-1436
Merritt, W.S.; Letcher, R.A.; Jakeman, A.J. (2003). A review of erosion and sediment transport models. Environ. Model. Softw. https://doi.org/10.1016/S1364-8152(03)00078-1.
Mohammadi, M.; Khaledi Darvishan, A.K.; Spalevic, V.; Dudic, B.; Billi, P. (2021). Analysis of the Impact of Land Use Changes on Soil Erosion Intensity and Sediment Yield Using the IntErO Model in the Talar Watershed of Iran. Water 2021, 13, 881.
Morgan, R.P.C.; Nearing, M.A. (2011). Handbook of erosion modelling, Handbook of Erosion Modelling. doi:https://doi.org/10.1002/9781444328455.
Myronidis, D., Stathis, D., Ioannou, K., & Fotakis, D. (2012). An integration of statistics temporal methods to track the effect of drought in a shallow Mediterranean Lake. Water Resources Management, 26(15), 4587-4605.
Naipal, V.; Ciais, P.; Wang, Y.; Lauerwald, R.; Guenet, B.; Van Oost, K. (2018). Global soil organic carbon removal by water erosion under climate change and land use change during AD 1850–2005. Biogeosciences 15, 4459–4480.
Nearing, M.A. (2013). Soil erosion and conservation, in: Environmental Modelling: Finding Simplicity in Complexity: Second Edition. pp. 365–378. doi: https://doi.org/10.1002/9781118351475.ch22.
Olsson, L.; Barbosa, H. (2019). Chapter 4: land degradation, in: Climate Change and Land. pp. 4–186.

Ouallali, A,; Aassoumi, H.; Moukhchane, M.; Moumou, A.; Houssni, M.; Spalevic, V.; Keesstra, S. (2020). Sediment mobilization study on Cretaceous, Tertiary and Quaternary lithological formations of an external Rif catchment, Morocco, Hydrological Sciences Journal, 65(9), 1568-1582.

Panagos, P.; Borrelli, P.; Robinson, D.A. (2015). Common agricultural policy: tackling soil loss across Europe. Nature 526, 195.

Sabri, E.; Boukdir, A.; El Meslouhi, R.; Mabrouki, M.; El Mahboul, A.; Romaric Ekouele Mbaki, V.; Zitouni, A.; Baite, W.; Echakraoui, Z. (2016). Predicting soil erosion and sediment yield in Oued El Abid watershed, Morocco, Athens Journal of Sciences, DOI: 10.30958/ajs.4.3.4. 4(3): pp 225-243.

Sabri, E.; Boukdir, A.; Karaoui, I.; Skataric, G.; Nacka, M.; Khaledi Darvishan, A.; Sestras, P.; Spalevic, V. (2019). Modelling of soil erosion processes and runoff for sustainable watershed management: Case study Oued El Abid Watershed, Morocco. Agriculture & Forestry, 65 (4), 241-250.

Sadeghi, S.H.R.; Gholami, L.; Khaledi Darvishan, A.V. (2013). Suitability of MUSLT for storm sediment yield prediction in Chehelgazi watershed, Iran. Hydrological Sciences Journal, 58(4), 892-897.

Saggau, Philipp, Kuhwald, Michael, Hamer, Wolfgang; Duttmann, R. (2021). Are compacted tramlines underestimated features in soil erosion modelling? A catchment-scale analysis using a process-based soil erosion model. Land Degradation and Development. 33 (3), 452-469, 10.1002/ldr.4161.

Smith, J.R. (1914). Soil erosion and its remedy by terracing and tree planting. Science (80). 39, 858–862. doi:https://doi.org/10.1126/science.39.1015.858.

Spalevic, V.; Djurovic, N.; Mijovic, S.; Vukelic-Sutoska, M.; Curovic, M. (2013). Soil Erosion Intensity and Runoff on the Djuricka River Basin (North of Montenegro). Malaysian Journal of Soil Science. 17, 49-68.

Spalevic, V.; Lakicevic, M.; Radanovic, D.; Billi, P.; Barovic, G.; Vujacic, D.; Sestras, P.; Khaledi Darvishan, A. (2017): Ecological-Economic (Eco-Eco) modelling in the river basins of Mountainous regions: Impact of land cover changes on sediment yield in the Velicka Rijeka in Montenegro. Notulae Botanicae Horti Agrobotanici Cluj-Napoca: 45(2):602-610.

Spalevic, V. (2019). Assessment of Soil Erosion Processes by Using the IntErO Model: Case Study of the Duboki Potok, Montenegro. Journal of Environmental Protection and Ecology, 20(2), 657–665.

Spalevic, V.; Barovic, G.; Vujacic, D.; Curovic, M.; Behzadfar, M.; Djurovic, N.; Dudic, B.; Billi, P. (2020). The Impact of Land Use Changes on Soil Erosion in the River Basin of Miocki Potok, Montenegro. Water 2020, 12, 2973.

Stefanidis, P., & Stefanidis, S. (2012). Reservoir sedimentation and mitigation measures. Lakes & Reservoirs: Research & Management, 17(2), 113-117.

Stefanidis, S., & Alexandridis, V. (2021). Precipitation and potential evapotranspiration temporal variability and their relationship in two forest ecosystems in Greece. Hydrology, 8(4), 160.

Stefanidis, S., Chatzichristaki, C., & Stefanidis, P. (2021). An ArcGIS toolbox for estimation and mapping soil erosion. J. Environ. Prot. Ecol, 22, 689-696.

Stefanidis, S., Alexandridis, V., Chatzichristaki, C., & Stefanidis, P. (2021). Assessing soil loss by water erosion in a typical Mediterranean ecosystem of northern Greece under current and future rainfall erosivity. Water, 13(15), 2002.

Stefanidis, S.; Alexandridis, V.; & Ghosal, K. (2022). Assessment of Water-Induced Soil Erosion as a Threat to Natura 2000 Protected Areas in Crete Island, Greece. Sustainability, 14(5), 2738.

Tavares, A.S.; Spalevic, V.; Avanzi, J.C.; Nogueira, D.A.; Silva, M.L.N.; Mincato,R.L. (2019). Modeling of water erosion by the erosion potential method in a pilot subbasin in southern Minas Gerais. Semina: Ciencias Agrarias, 40(2), 555-572.

Tazioli, A. (2009). Evaluation of erosion in equipped basins: Preliminary results of a comparison between the Gavrilovic model and direct measurements of sediment transport. Environmental Geology, 56(5), 825-831.

Thakur, A.; Poonam.; Nema, A.K. (2018). Models for soil conservation planning based on soil erosion and deposition rates. Journal of Soil and Water Conservation, 17(4), 400-406.

Tosic, R.; Lovric, N.; Dragicevic, S. (2019). Assessment of the Impact of Depopulation on Soil Erosion: Case Study – Republika Srpska (Bosnia and Herzegovina). Carpathian Journal of Earth and Environmental Sciences. 14. 505-518.

Wischmeier, W.H.; Smith, D.D. (1978). Predicting rainfall erosion losses-a guide to conservation planning. In Predicting Rainfall Erosion Losses-A Guide to Conservation Planning; USDA, Science and Education Administration: Hyattsville, MD, USA, 1978.

Zingg, R.W. (1940). Degree and length of land slope as it affects soil loss in runoff. J. Agric.Eng. 21, 59–64.

Barakat, A., El Harti O., Ennaji, W. (2022). Environmental pollution from heavy metals in soils surrounding the abandoned mine of Tansrift (Central High-Atlas, Morocco). Agriculture and Forestry, 68 (2): 221-245. doi:10.17707/AgricultForest.68.2.16

DOI: 10.17707/AgricultForest.68.2.16

Ahmed BARAKAT*[*1], Oumaima EL HARTI[1], Widad ENNAJI [1]

ENVIRONMENTAL POLLUTION FROM HEAVY METALS IN SOILS SURROUNDING THE ABANDONED MINE OF TANSRIFT (CENTRAL HIGH-ATLAS, MOROCCO)

SUMMARY

In this study, the heavy metal (HM) pollution status, possible sources, and potential ecological and health risk of heavy metals in soils around the Tansrift abandoned mine (Central High Atlas, Morocco) were investigated using the coefficient variation (CV), principal component analysis (PCA), enrichment factor (*EF*), geoaccumulation index (I_{geo}), Pollution Load Index (*PL*I), potential ecological risk index (*RI*), and total hazard index (*HI*). A total of 25 surface soil samples were collected and analyzed to determine the soil proprieties of magnetic susceptibility (MS), organic matter (OM) contents, texture, and the HM (Cd, Cr, Cu, Pb, and Zn) concentrations. The average metal concentrations of 7.74 (Cd), 64.19 (Cr), 333.59 (Cu), 29.95 (Pb), and 58.12 (Zn) mg/kg in soils are higher, except for Pb, than that of the local background and worldwide guidelines. The MS result showed that the soil magnetic material consisted of multidomain (MD), superparamagnetic (SP), and stable single domain (SSD) particles, which were derived from both natural and anthropogenic sources. Moreover, the statistical analysis indicated that Cu originated mainly from anthropogenic and lithologic sources such as agricultural practices, soil parent materials, and mineral dust and wastes from the Tansrift mine. In contrast, agricultural activities are the predominant origin for Cd, Cr, and Zn. *EF* values revealed a significant HM contamination of samples soils, which is in the order of Cd>Cu>Cr>Zn>Pb. The I_{geo} and *PLI* results attested that soils were significantly affected by Cd, Cr and Cu toxic metal and, to a lesser degree, by Pb and Zn. According to the *RI* levels (12.07-1540.37), 40% of sampling sites were at considerable to high ecological risk, mainly influenced by Cd and Cu. Based on the *HI* values, the non-carcinogenic risk of HMs in studied soils could be neglected for adults but not for children. These findings showed the adverse HM effects on the environmental

[1]Ahmed Barakat[*] (Corresponding author: a.barakat@usms.ma), Oumaima El Harti, Widad Ennaji. Geomatics, Georesources and Environment Laboratory, Faculty of Sciences and Techniques, Sultan Moulay Slimane University, MOROCCO.

Notes: The authors declare that they have no conflicts of interest. Authorship Form signed online.

Recieved:17/03/2022 *Accepted:06/06/2022*

quality of soils and the need to implement protective management strategies in the study area.

Keywords: Tansrift abandoned mine, Mining and agricultural activities, Soil proprieties, HM concentrations, Pollution status, Ecological and health risks

INTRODUCTION

Heavy metals (HM) are known environmental pollutants because they are not readily degraded. Also, HM bioaccumulation via the food chain will promote human health hazards such as cancer and nervous system problems (Alomary & Belhadj, 2007; Madzin *et al*., 2015). Also, HMs with concentrations above the threshold levels can cause various effects on the microbiological balance of soils and consequently on their fertility (Barbieri, 2016). So, the properties of HMs in urban and agricultural soils have been gaining increasing attention over the last few decades. Numerous scientific studies have been focused on heavy metal pollution of soil worldwide. They reported that HMs mainly enter environments due to natural processes, anthropogenic activities, or both. Natural sources include weathering of soil and rock parents, while anthropogenic sources are mostly from industrial activities (Huang, 2021; Long *et al*., 2021; Yang *et al*., 2018), vehicle and domestic emissions (El Baghdadi *et al*., 2012; Hanfi *et al*., 2020; Roy *et al*., 2019), mining (Stefanowicz *et al*., 2020; Zhao *et al*., 2020), and agricultural production (Ennaji *et al*., 2020; Yan *et al*., 2020; Yang *et al*., 2018). Therefore understanding the source of HMs is essential to prevent pollution and formulate effective control strategies.

Mining activities are recognized as one of the greatest substantial causes of soil HM pollution affecting surrounding environmental compartments (Atibu *et al*., 2018; Sun *et al*., 2018; Wu *et al*., 2021). In recent decades, the environmental concerns produced by mining activities have attracted growing attention worldwide (Chun *et al*., 2021; Punia, 2021; Sun *et al*., 2018). Several studies have shown that mining activities polluted the surrounding area through inappropriate exploitation and uncontrolled dumping of the mine tailings (Abouian Jahromi *et al*., 2020; Sun *et al*., 2018; Wang *et al*., 2019). Due to its high geological complexity, mining activity in Morocco has enjoyed since its independence the multiplication of large projects concerning phosphates base and precious metals. Resources minerals are gradually extracted and exploited to meet the economic demands, but sometimes without appropriate management of mining tailings. Thereby, several uncontrolled mining areas having very significant concentrations of heavy metal (HM), including Pb, Zn, Cu, Cr, and Cd, have even now undesirable effects on the environmental aspects (El Azhari *et al*., 2017; Leila *et al*., 2021; Midhat *et al*., 2019; Nouri & Haddioui, 2015). These HM pollutants in impoverished heaps and tailings were generally very mobiles due to their smaller dimensions and reactivity linked to the chemical nature of sulfides and sulfates. So, if it is not managed correctly, it could become a pollution source of water, groundwater and soil (Azzeddine & El Hassan, 2020; Bouzekri *et al*., 2020; Moyé *et al*., 2017; Nassiri *et al*., 2021a; Zouhri *et al*., 2019). It can then cause potential risk to human health via direct inhalation, ingestion, and dermal contact absorption (De Miguel *et al*., 2007; Tang *et al*., 2021; Yang *et al*., 2018). Therefore, evaluating the potential environmental impact of Tansrift uncontrolled mining tailing allows residents and authorities to take protective measures.

In the light of the above, this study was conducted with the objectives to evaluate the HM (Cd, Cr, Cu, Pb, and Zn) contamination levels in soils surrounding the Tansrift abandoned mine using some environmental indices, to identify the possible sources of HMs using multivariate statistical methods, and to determine ecological risk level using the potential ecological and health risk indices. This assessment could also provide support and information for properly managing of the areas with a possible risk for residents and the general population.

MATERIAL AND METHODS

Study area

The study area is the Tansrift abandoned mine (32°12'1.72''N, W6°17'59.09''W) which closed in 1978. The Tansrift Village lies to the northeast of Ouaouizeght Town, Azilal Province, in the central High Atlas of Morocco (Fig. 1).

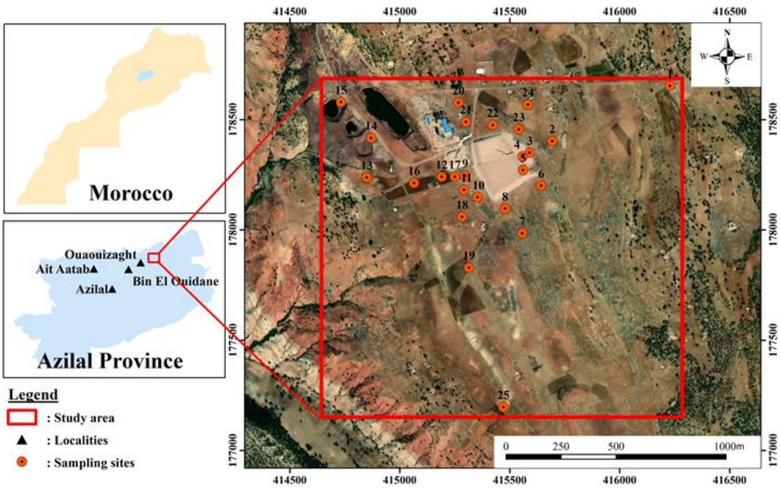

Fig. 1. Location of study area and soil samples.

During the mining years of the Tansrift abandoned mine, 650 000 tons of 1.5% Cu ore were surface mined from outcrops of copper-bearing sandstone. Since its closure, the tailings have been piled up on the mountainside with no protective measures. This area has an altitude of 1448 m and has a warm Mediterranean climate with dry summer. The long-term average annual temperature and precipitation are 19.2°C and 353.8 mm, respectively. With land formerly forest now agricultural and the steep slope of the area, the surface runoff and wind cause substantial surface erosion in the mining area. Fine tailings are easily transported by surface runoff and wind, entering the arable soils and streams of the mining area.

Geologically, the Tansrift area is located just south of the fault (Aghbala-Afourar accident) between the two synclinal structures of Ouaouizarth and Taguelft, having a Bajocian limestone frame and filled with Jurassic-Cretaceous Red Layers (Monbaron, 1988). The area is characterized by a sedimentary series of subsident platforms (transition to the High Atlas basin) comprising: (i) lower to middle Lias carbonate ensemble visible in the Jbel Ghnim to the northwest of the mine, (ii) alternations of red marl and limestone banks, (iii) Bajocian limestone bars visible at the Bin El Ouidane dam, (iv) Middle Jurassic to the Lower Cretaceous continental detrital ensemble of the "Red Layers", and (v) Aptian to the Eocene alternation of silts and red marls with dolomitic carbonate banks (Charrière *et al*., 2005; Haddoumi *et al*., 2010; Mojon *et al*., 2009). The Cu lenticular-shaped copper mineralization is hosted in the Jurassic-Cretaceous Red Layers as paleo-channels occupied mainly by sandstones and sometimes gray to yellowish arkoses (Ibouh *et al*., 2016). The Cu mineralization is mostly with chalcocite, chalcopyrite, pyrite, bornite, covellite, and rarely proustite. At the surface, it is primarily turned to supergene malachite and azurite.

Sampling and analysis

A study that focuses exclusively on HM contamination assessment of agricultural soil that is lacking in the Tansrift mine area. So, in the present study, the HM pollution status, possible sources, and potential ecological and health risk of heavy metals in soils around the Tansrift abandoned mine were investigated using various determining methods (physico-chemical analyses of soils, environmental indices, statistical analysis).

Samples of 25 surface tailings and agricultural soils (0–20 cm) were randomly collected in the study area in Marsh 2020 (Fig. 1). Three surface soil samples were also collected far from the Tansrift mine disturbance to establish the reference for soil HMs. The sampling site locations were obtained using a handheld global positioning system (GPS) (Fig. 1). The collected samples (0.5-1 kg) were stored in separate plastic self-sealing bags and marked and transported to the laboratory. The samples were dried, crushed, and sieved to less than 2 mm to remove coarse debris (Marguí *et al*., 2005). The samples are then used to measure the soil physical parameters of organic matter (OM), soil particle size (sand, silt, and clay), and magnetic susceptibility (MS). The OM content was determined by ignition at 550°C for 5 h in a muffle furnace and comparing pre- and post-ashing weights. The sand, silt, and clay contents were determined using the Robinson pipette method according to the NF X31–107 certified method (AFNOR, 2003). The soil texture is then predicted according to the USDA soil texture classes. The magnetic proprieties including the mass-specific low- and high-frequency magnetic susceptibilities (χlf and χhf at 470 and 4700 Hz) of sampled soils were measured by a Bartington Susceptibility Meter (Model

MS2B) with a dual-frequency sensor at the Georesources and environment laboratory of Sultan Moulay Slimane University., The frequency-dependent susceptibility (χfd) was thus calculated from the measured χlf and χhf (Dearing, 1996) by the application of Eq. (1) (Suresh *et al*., 2011):

$$\chi_{FD}\% = [(\chi_{LF} - \chi_{HF})/\chi_{LF}]x100 \tag{1}$$

The χfd is used to predict the presence of ultrafine superparamagnetic particles of ferrimagnetic components released by anthropogenic sources.

The concentrations of HMs (Cd, Cr, Cu, Zn, and Pb) and Fe in all soil samples were determined by applying the three-acid method (Allen, 1986). Tri-acid mixture (HNO3–HF–HCl) was added to the beaker containing soil sample and heated at 100-110°C until the solution becomes transparent. The resulting solution was finally maintained to 50 ml using deionized water and stored at room temperature before being placed in the Inductively Coupled Plasma Atomic Emission Spectroscopy (ICP-AES) analyzer of a National Center for Scientific and Technical Research (CNRST) laboratory accredited ISO 9001 and ISO 17025. To ascertain the accuracy of the analysis and to ensure quality assurance and control (QA/QC), reagent blanks, duplicate tests and standard deviation of <5% were used for HM analyses (Essien *et al*., 2019). The detection limit for the studied element was 10-1 µg.l-1. The analysis of background samples has been carried out using the same approach.

All analysis data were statistically analyzed using IBM SPSS Statistics software. A Shapiro-Wilk test was used to assess the normality of data, which is an assumption to be met in data for statistical tests. Pearson correlation coefficients were determined to quantify the relationships among HM contents and magnetic properties. The coefficient of variation (CV) and the principal component analysis (PCA) were performed to identify the potential sources of HMs.

Assessment of heavy metal contamination

To assess the HM pollution of soils in the study area, environmental factors, namely enrichment factor (EF), geoaccumulation index (I_{geo}), pollution load index (PLI), and potential ecological risk index (RI), were employed as they generally are considered to be more efficient tools in environmental quality assessments (Barakat *et al*., 2012; Barakat *et al*., 2020; El Baghdadi *et al*., 2012; Ennaji *et al*., 2020; Hilali *et al*., 2020; Mirzaei *et al*., 2020; Oumenskou *et al*., 2018a; Yu *et al*., 2017).

The EF index is introduced to evaluate the anthropogenic HM pollution degree and is obtained by the application of Eq. (2) proposed by Selvaraj *et al*. (2004) (Table 1). C_n and C_{ref} represent the concentrations of given examined metal and given reference element, respectively. Fe was used in the present study as the reference element for geochemical normalization (Salati and Moore, 2010) because it is the major element included in this study. EF values are generally interpreted as follows:

$$EF = \begin{cases} < 1 = \text{minimal enrichment or no enrichment} \\ 1-3 = \text{minor enrichment} \\ 3-5 = \text{moderate enrichment} \\ 5-20 = \text{significant enrichment} \\ 20-40 = \text{very high enrichment} \\ > 40 = \text{extremely high enrichment} \end{cases} \quad (3)$$

The I_{geo} index is employed to evaluate the anthropogenic heavy metal contamination in soils by comparing metal content in the sample with the geochemical background (Müller, 1979). I_{geo} is calculated as expressed in Eq. (4) (Table 1). Ci is the obtained metal concentration, Bi is the background concentration of analyzed metal, and 1.5 factor is used to attenuate lithogenic variations in background concentrations. According to the I_{geo} values, the soil pollution by HMs are classified as follows (Müller, 1979):

$$Igeo = \begin{cases} \leq 0 = \text{no contamination} \\ 0-1 = \text{slight contamination} \\ 1-2 = \text{moderate contamination} \\ 2-3 = \text{moderate to severe contamination} \\ 3-4 = \text{severe contamination} \\ 4-5 = \text{severe to extreme contamination} \\ > 5 = \text{exteme contamination} \end{cases} \quad (5)$$

The *PLI* index is proposed by Tomlinson *et al*. (1980) to assess the degree of HM contamination in samples by involving all elements concentrations. It was computed by applying Eqs. (6) and (7), where n is the number of determined heavy metals (Table 1). CF represents the contamination factor of the metals. The CF and PLI values are categorized according to respectively Hakanson (1980) and Zhang *et al*. (2018) as follows:

$$CF = \begin{cases} < 1 = \text{low contamination} \\ 1-3 = \text{moderate contamination} \\ 3-6 = \text{considerable contamination} \\ > 6 = \text{very high contamination} \end{cases} \quad (8)$$

$$PLI = \begin{cases} < 1 = \text{unpolluted soil} \\ 1-2 = \text{moderately polluted soil} \\ 2-3 = \text{highly polluted soil} \\ > 3 = \text{extremely polluted soil} \end{cases} \quad (9)$$

Description of the toxicity degree of HMs in the present study was carried out using the potential ecological risk index (RI) developed by Hakanson (1980). The RI index is calculated following Eqs. (10) and (11) as represented in Table 1:

E_r^i is the single potential ecological risk of HM i at the sampling site r, and T_i is the metal toxic factor for HM i. According to Hakanson (1980), the T_i values of Cd = 30; Cu = Pb = Ni = 5, Cr = 2, and Zn = 1 were used in this study. The E_r^n values and the RI index are generally grouped into the following levels (Hakanson, 1980):

$$E_r^n = \begin{cases} < 40 = \text{low risk} \\ 40 - 80 = \text{moderate risk} \\ 80 - 160 = \text{considerable risk} \\ 160 - 320 = \text{high risk} \\ \geq 320 = \text{very high risk} \end{cases} \quad (12)$$

$$RI = \begin{cases} < 150 = \text{low risk} \\ 150 - 300 = \text{moderate risk} \\ 300 - 600 = \text{considerable risk} \\ \geq 600 = \text{high risk} \end{cases} \quad (13)$$

The potential health risk by HMs, including non-carcinogenic effects on adults and children, was evaluated using a health risk quotient (HQ_i) and the total hazard index (HI). The two indices were calculated using Eqs. (14), (15) and (16) as given in Table 1.

Table 1. Pollution indices used in the present study.

Index name	pH	EC (µS/cm)
EF	$EF = (C_n/C_{ref})_{sample} \,/\, (C_n/C_{ref})_{background}$	Eq. (2) (Selvaraj *et al*. 2004)
Igeo	$I_{geo} = log_2\,(C_i/1.5B_i)$	Eq. (4) (Müller, 1979)
PLI	$CF = C_i/B_i$ $PLI = (CF_1 x CF_2 x \ldots . x CF_n)^{1/n}$	Eq. (6) (Müller, 1979) Eq. (7) (Tomlinson *et al*. 1980)
RI	$RI = \sum E_r^i$ $E_r^i = T_i x CF$	Eq. (10) (Müller, 1979) Eq. (11) (Hakanson 1980)
HI	$ADD_i = \frac{C_i x IR x EF x ED x CF}{BW x AT}$ $HQ_i = \frac{ADD}{RfD_i}$ $HI = \sum_{i=1}^{n} HQ_i$	Eq. (14) Eq. (15) Eq. (16)

ADD_i represents the average daily intake (mg/kg/day) of HMs through soil particle ingestion, Ci is the concentration of heavy metal i in soil (mg/kg), IR is the ingestion rate of soil/dust for children (200 mg/day) and adult (100 mg/day) (EPA, 2011), EF is the exposure frequency (350 days/year), ED is the exposure duration (6 years for children and 30 years for adults), BW is the body weight of the exposed individual (15 kg for children and 70 kg for adult), AT is the exposure period for non-carcinogenic effects (2190 days for children and 10950 days for adult), and CF is the conversion factor (10-6 kg/mg), and RfD representing the means reference oral dose, is 0.001, 0.003, 0.04, 0.0035, 0.3 and 0.7 mg.day/kg for Cd, Cr, Cu, Pb, Zn, and Fe, respectively (Leung *et al*., 2008). HQ and HI were classified into two levels: HQ or HI<1: no potential non-carcinogenic risk from HM accumulation, and HQ or HI> 1: significant non-carcinogenic health risk due to HMs.

RESULTS AND DISCUSSION

Physical parameters

The physical parameters and HM contents were determined at all soil samples around the Tansrift mine. The descriptive statistics of physical proprieties are presented in Table 2.

Table 2. Summary of descriptive statistics for soil physical properties.

Statistics	OM (%)	Grain size			χ_{fd} (%)	χ_{lf}
		Sand (%)	Silt (%)	Clay (%)		10^{-8} m^3 kg$^-$
Min	0.32	8.80	34.10	5.41	0.26	1.88
Max	9.36	31.60	52.00	14.95	12.38	463.65
Mean	4.06	17.23	48.47	10.52	5.09	111.82
SD	2.60	6.18	3.45	1.96	3.45	155.72
CV (%)	63.92	35.86	7.11	18.60	67.72	139.25

According to the USDA soil particle size classification, the texture of the soil samples was mostly silty sand indicating that soils of Tansrift are composed of coarse particles (Table 2). The sampled soil ranges of sand, silt and clay percentages were 8.80-31.60%, 34.10-52%, and 5.41-14.95%, respectively. Silt is the dominant facies in the sampled soils, followed by sand and clay in decreasing order. The samples collected near to the mining tailings showed sand to silty sand facies.

OM is a key factor inducing redox potential and biological processes in soils, including the control of the comportment of chemical species as HMs, through ion exchange adsorption, complexation or chelation reactions. In general, maximum adsorption of cationic HMs occurs at elevated OM levels. Then, OM is an important parameter for assessing HM pollution. The OM contents were in the range of 0.32 to 9.36%, with an average of 4.6%, which pertained to soils low in organic matter (Table 2).

As shown in Table 2, the MS values were in the ranges of 1.88×10^{-8}-463.65×10^{-8} m^3 kg^{-1} with a mean of 111.82×10^{-8} m^3 kg^{-1}, and 1.87×10^{-8}-456.82×10^{-8} m^3 kg^{-1} with a mean of 105.59×10^{-8} m^3 kg^{-1} for χ_{lf} and χ_{hf} frequency magnetic sensitivity, respectively. The slightly higher values of χ_{lf} than those of χ_{lf} revealed the presence of the superparamagnetic minerals (Dearing, 1996). Gautam *et al.* (2004) have described four categories of soils based on their MS values as follows: 'lowly magnetic' (MS<$10\times10^{-8}m^3kg^{-1}$), 'moderately magnetic' (MS $10{-}100\times10^{-8}m^3kg^{-1}$), and 'highly magnetic' (MS>$100\times10^{-8}m^3kg^{-1}$). According to Gautam *et al.* (2004) classification, the studied samples from the Tansrift area would be lowly, moderately, and highly magnetic, with the proportion of 15%, 55%, and 30%, respectively.

According to Hanesch and Scholger (2002), the MS values above $20\times10^{-8}m^3kg^{-1}$ are believed to be highly endangered by pollution. About 50% of the studied samples showing χ_{LF} values beyond this threshold value revealed anthropogenic stresses on the soil in the study area. Supported by CV coefficients (Table 2) below 139.25%, a tremendous spatial variation of MS might be explained by an enhancement in magnetic material contents derived from mining extraction.

Soils had χ_{fd} values ranging from 0.26% to 12.38%, with an average value of 5.09%. The χ_{fd} can be used to describe the magnetic grain variation in soils and to detect the possible presence of a superparamagnetic (SP) mineral fraction (Dearing, 1996). As predicted by the model of Dearing *et al*. (1996), χ_{fd} lower than 2%, between 2 and 10%, and greater than 10 % indicated a predominance of multidomain (MD) grains, a mixture of stable single domain (SSD) and superparamagnetic (SP) grains, and a predominance of SP gains, respectively. From this model, about 25% of the samples are dominated by coarse MD grains, 65% are a mixture of SP and SSD grains, 5% are dominated by SP grains, and 5% showed erroneous χ_{fd} values. The soil magnetic particles in the surface soil were commonly smaller like SP and PSD, as reported by Meena *et al*. (2011) and Poggere *et al*. (2018).

Regarding the χ_{fd} result, the studied samples are predominated by the three types of magnetic assemblages: MD, SP, and SSD, suggesting that MS values in studied soils might be attributed, in addition to pedogenic processes, to anthropogenic magnetic materials. The anthropogenic materials are suspected from the Tansrift mine environment as dust and erosion by water and wind of mining tailing. Also, the absence of significant correlations between χ_{lf} and χ_{fd} seems to agree with the χ_{lf} results, attesting a dominant portion of ferrimagnetic minerals in soils, and an anthropogenic influence, as mining tailings, on the MS enhancement in studied soils.

Heavy metal contents

The Cd, Cr, Cu, Pb, Zn, and Fe contents varied among sites, with values between 0.15 and 42.90 mg/kg, 16.55 and 215.03 mg/kg, 13.88 and 2444.45 mg/kg, 2.60 and 118.95 mg/kg, 12.98 and 144.68 mg/kg, and 952.25 and 4740.80 mg/kg, with a means of 7.74, 64.19, 333.59, 29.95, 58.12, 2273.92 mg/kg, respectively (Table 3). The HMs and soil physical properties were distributed differently between samples. The contents of Cd (100%), Cr (100%), Cu (67%), and Zn (68%) exceeded the local corresponding background values (Oumenskou *et al*. 2018b) in almost all sampling sites. They were also the two most abundant heavy HMs, with minimum concentrations exceeding the WHO and FAO guidelines (Chiroma *et al.*, 2014). Pb showed values exceeding the local background values and WHO guidelines in 9.14 times and 64.00, respectively. The Fe values remained below their corresponding background value, implying no enhancement in the iron contents of soils. The highest concentrations of HMs were recorded in samples closer to the mine wastes and in those located further away. This observation suggested that the studied soils received an important quantity of metallic pollutants directly associated with the mining activities.

To evaluate the degree of soil spatial variability, the coefficient of variation (CV) has been used, knowing that CV ≤ 15% indicates weak variability; 15% < CV < 100% indicates medium variability; CV ≥ 100% means substantial variability. From the CV results, Cr, Pb, Zn, and Fe were moderately spatially distributed, while Cd and Cu showed strong spatial variability. This disparity in the Cd and Cu concentrations can be attributed to the types and nature of metal sources. Also, their contents in surface soil have a very significant relative value compared to agricultural soils originating from other areas in the region (Barakat *et al.*, 2020; El Baghdadi *et al.*, 2012; Ennaji *et al.*, 2020; Hilali *et al.*, 2020; Oumenskou *et al.*, 2018a) (Table 3). They might be suspected of agricultural and industrial activities, urbanization, and wastewater reuse for crop irrigation.

Table 3. Basic statistics of HM concentrations (mg/kg) in studied soil samples (n=25) and in other studied farmlands of the region.

Samples	**Concentrations**						
	Cd	Cr	Cu	Pb	Zn	Fe	
Min	0.15	16.55	13.88	2.60	12.98	952.25	
Max	42.90	215.03	2444.45	118.95	144.68	4740.80	
Mean	7.74	64.19	333.59	29.95	58.12	2273.92	
SD	8.33	42.71	620.73	28.53	30.40	864.86	
CV (%)	107.67	66.53	186.08	95.25	52.31	38.03	
Earth's soil	0.11	84	26	29	60	3.2	Taylor (1964)
Earth's crust	0.6	100	50	14	75	4.1	Taylor (1964)
FAO/WHO	3	100	100	100	300	2.78	Chiroma *et al.* (2014)
Local Background	0.85	25.21	31.40	32.54	43.76	1.21	Oumenskou *et al.* (2018b)
Urban soil of Beni Mellal City	0,76	44,58		183,12	127,45	30160	El Baghdadi *et al.* (2012)
Peri-urban soils of Beni-Mellal city	2.20	140.41	37.24	31.45	154.63	33700	Barakat *et al.* (2020)
Northeast area of Tadla plain	0.92	32.72	138.10	31.72	162.11	19249.27	Ennaji *et al.* (2020)
Beni Moussa irrigated perimeter	4.89	77.77	87.40	109.66	75.98	26248.18	Hilali *et al.* (2020)
Beni Amir irrigated perimeter	8.77	57.06	25.95	33.32	294.71	23891.57	Oumenskou *et al.* (2018b)

Analysis of HM sources

Before statistical analysis, the data distribution was evaluated using the Shapiro-Wilk test; and since the distribution was not normal, the data were log-transformed. The correlation between soil proprieties, magnetic parameters, and HM contents was analyzed to determine the origin of HMs in the study area. Table 4 presented the Pearson correlation coefficient (R^2) among all analyzed parameters and metal elements.

Table 4. Pearson correlation among HM concentrations and magnetic proprieties.

	Zn	**Cd**	**Cr**	**Cu**	**Pb**	**Fe**	**χ_{FD} (%)**	**χ_{LF} (10^{-8} m^3 kg^{-1})**
Zn	1							
Cd	**0.58**	1						
Cr	**0.85**	**0.78**	1					
Cu	0.05	0.10	0.04	1				
Pb	0.06	0.03	-0.04	**0.70**	1			
Fe	0.07	**-0.27**	-0.14	**0.35**	**0.33**	1		
χ_{FD} (%)	0.09	**0.30**	**0.20**	**0.20**	**0.35**	-0.06	1	
χ_{LF} (10^{-8} m^3 kg^{-1})	0.07	**0.22**	0.15	**-0.33**	0.04	**-0.23**	0.11	1

Positive and significant correlations were observed between sand and Cu and between clay and Fe. In contrast, sand with Fe and clay with Cu and Pb showed negative and significant correlations indicating that the contents of these metals were affected by sand and clay contents in the studied samples. The other metal elements showed very low correlation coefficients with sand, silt, and clay, oscillating between -0.02 and 0.16. Therefore, all the correlations mentioned above prevent us from concluding the relationships between soil grain size distribution and HM concentrations.

The highest positive correlation was also recorded among Cd, Cr, and Zn, implying that these cations were derived from similar potential sources. Significant positive correlations were observed between Cu, Pb, and Fe, revealing thus that these elements might have common sources. Moreover, Cd exhibited a negative correlation with Fe, reflecting that Cd and Pb share different sources.

Highly significant correlations between HM concentrations and PLI were observed, with the R^2 coefficient increased in an order of 0.31 (Cr)<0.33 (Cd)<0.35 (Zn)<0.42 (Fe)<0.80 (Pb)< 0.88 (Cu). The results attested that metal pollution in the study area was greatly affected by Cu exploitation, even though there might have been natural sources.

The χ_{lf} magnetic susceptibility showed a significant positive correlation with Cd and Cr and a significant negative correlation with Cu and Fe. Such correlations are so weaker between χ_{lf} and contents of Zn and Pb. Similar observations were made by Beckwith *et al*. (1986), which reported that the correlation between HMs and MS is lost when the sediment samples having low MS are added to the statistical analysis. This may explain why the correlation of

MS with some HMs in the present study is so low. Some previous works indicated that the correlation between MS and HM accumulation is complex and varies by assessed areas and pollutant sources (Lu *et al*., 2007; Schmidt *et al*., 2005). Schmidt *et al*. (2005) stated that a significant correlation between MS and a given HM occurs if only samples above a threshold value of 2 % more than the mean or 52% below the median of all samples.

The χ_{fd} values showed a significant positive correlation with Cd, Cr, Cu, and Pb, a weaker positive relation with Zn, and a significant negative correlation with Fe. From this, it is assumed that Cd, Cr, Cu, and Pb may be mainly added through mining tailings and dust at the studied area, while the concentration of Fe could be primarily linked to the parent material of soils. Fe is an omnipresent element in the environment, but its content in soils is generally low (<0.1%). Thus, there is often little direct connection between magnetic susceptibility and Fe content in soils (Maher, 1998). Liu *et al*. (2003b) suggested that the MS of soils formed in sedimentary rocks frequently increases with an increase in χ_{fd} frequency-dependent susceptibility. This explained the close relationships between χ_{fd} and HM contents in studied soils developed from sedimentary rocks. The heavy metals are due to natural particles present in the bedrock and ore wastes and dust brought into the topsoil environment.

Among soil-magnetic parameters, there are no significant positive correlations between χ_{lf} and χ_{fd} in studied soils, which did not exceed R^2 of 0.11. The absence of a significant positive correlation revealed that a magnetic enhancement might cause the MS variations due to mining pollution.

For more evaluation of sources of the HMs, PCA was performed on log-transformed data that are non-normal distributed. Based on the grouping of HMs using varimax rotation factor analysis, four components with eigenvalue >1 were calculated and described 79.72% of cumulative percentage for the soils (Table 5, Fig. 2). According to Liu *et al*. (2003a), the component loadings were classified as ‘strong’, ‘moderate’, and ‘weak’, corresponding to absolute loading values of 40.75, 0.75–0.50, 0.50–0.30, respectively.

PC1 that produced 25.08% of the total variance was strongly positively correlated with Cr, Zn, and Cd and weakly positively loaded with Cu. This finding suggested that these elements are highly associated with each other. The primary sources of these elements are probably the dust fallout and gaseous emissions from the Cu ore mining and processing. Cd and Co frequently occur as an accompanying mineral of Cu ores (Esmaeili *et al*., 2014; Yang *et al*., 2020). Besides, the application of agrochemicals like phosphate fertilizers and pesticides could be another source for the high content of these HMs. PC2 accounting 22.50% of variance showed moderate to strong positive factor loadings with OM and sand variables and moderate to strong negative loading with Fe and clay variables. Local normality of Fe content might be derived from the weathering of parent material and subsequent pedogenesis. This finding is consistent with the positive between Fe and clay that clays can also influence. PC3, explaining for 19.53% of the data variance, had strong positive loadings on Cu, Pb, and Fe. The result suggested that these HMs is derived from the same source.

Table 5. Rotated principal component matrix and factor loadings for HMs in sampled soils.

	Principal component (PC)			
	1	2	3	4
Cr	**0.93**	0.10	0.02	-0.03
Zn	**0.90**	-0.14	0.07	-0.22
Cd	**0.87**	0.01	0.10	0.13
Pb	0.02	0.01	**0.86**	0.07
Cu	**0.23**	0.15	**0.81**	0.16
Fe	-0.07	**-0.48**	**0.67**	**-0.39**
OM	0.10	**0.56**	-0.15	0.01
Sand	-0.07	**0.91**	0.04	**-0.32**
Clay	0.10	**-0.91**	**-0.25**	-0.12
Silt	-0.08	-0.10	0.11	**0.95**
Eigenvalue	2.51	2.25	1.95	1.26
% of total variance	25.08	22.50	19.53	12.61
Cumulative variance (%)	25.08	47.58	67.11	79.72

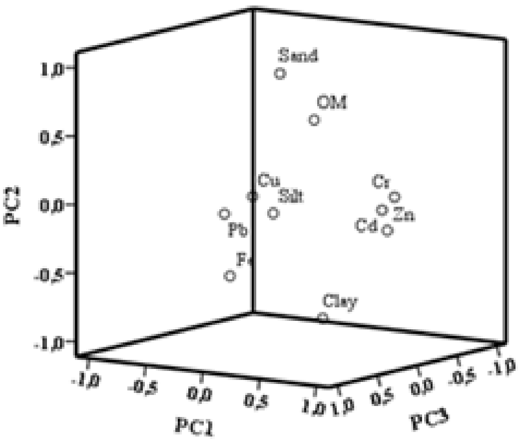

Fig. 2. Varimax-rotated components of the HMs in studied soils.

Since the contents of Pb and Fe in the study area do not exceed their contents in background soils, it can be inferred a major natural lithologic origin of the HMs of PC3. As the study area is located at and near the copper deposit and vicinity of the abandoned mine, the source of these elements could be lithogenic and related to ore extraction (waste minerals, tailings, and mine drainage). PC4, explaining for 12.61% of the data variance, mainly loaded silt and weakly negatively loaded sand and Fe, suggesting that it originated from weathering of the parent material of soils.

A cluster method is employed to assess the spatial variability and identify similarities among the sampling stations, and the obtained results are presented as a dendogram in Fig. 3. According to Fig. 3, all soil samples could be grouped in three clusters, with 14 samples in cluster 1, 3 samples in cluster 2, and 8 samples in cluster 3.

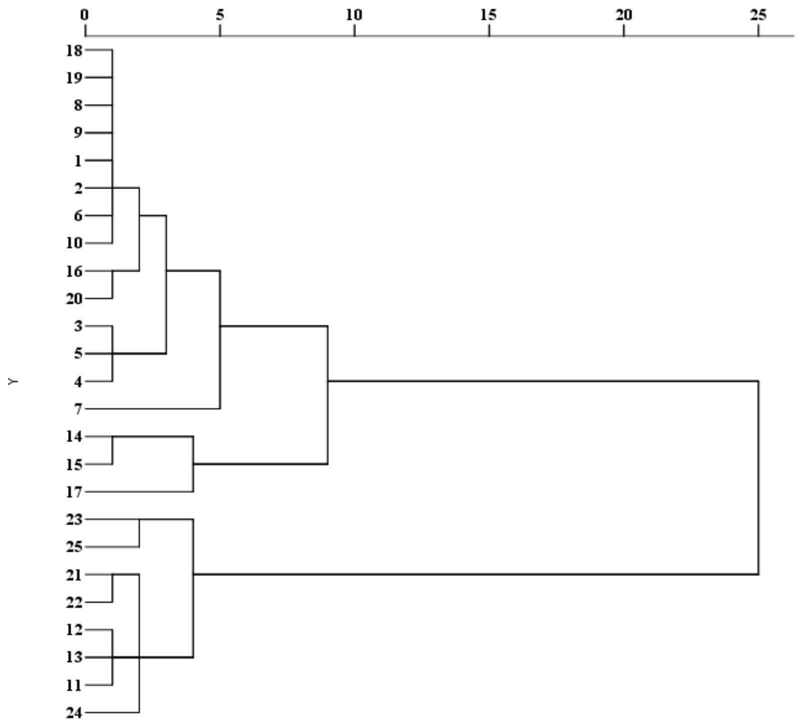

Fig. 3. Clustering tree of sampling sites based on the ward method.

The distribution patterns of soil samples based on their HM concentrations indicated spatial heterogeneity. Some highly polluted samples are located near or far away from abandoned mine wastes. This variation in the spatial distribution is probably controlled by the wind and water transport of the HM pollutants from the abandoned mine site.

HM contamination assessment

The effects of mining activities were further assessed using a few environmental, ecological, and health risk indices, namely *EF*, I_{geo}, *PLI*, *RI*, and *HI*. The results are presented in Tables 6, 7 and 8.

Table 6. Descriptive statistics of *EF*, I_{geo} and *PLI* values.

	EF					I_{geo}					***PLI***
	Cd	Cr	Cu	Pb	Zn	Cd	Cr	Cu	Pb	Zn	
Min	0.18	0.66	0.44	0.08	0.30	-3.09	-1.19	-1.76	-4.23	-2.34	0,39
Max	50.47	8.53	77.85	3.66	3.31	5.07	2.51	5.70	1.29	1.14	6,93
Mean	9.10	2.55	10.62	0.92	1.33	1.93	0.54	0.75	-1.20	-0.35	2,31
SD	9.80	1.69	19.77	0.88	0.69	1.64	0.78	2.35	1.25	0.74	1,58
CV (%)	107.67	66.53	186.08	95.25	52.31	84.90	144.23	311.75	-104.17	-210.81	68,49

Table 7. Statistical attributes of E_r^i and *RI* for ecological hazard of HMs in studied soil samples.

	E_r^i					***RI***
	Cd	Cr	Cu	Pb	Zn	
Min	5.29	1.31	2.21	0.40	0.30	12.07
Max	1514.12	17.06	389.24	18.28	3.31	1540.37
Mean	273.07	5.09	53.12	4.60	1.33	337.21
SD	294.01	3.39	98.84	4.38	0.69	322.96
CV (%)	107.67	66.53	186.08	95.25	52.31	95.77

Table 8. *HQ* and *HI* for non-carcinogenic risk of HMs in studied soil samples.

	HQ					***HO***
	Cd	Cr	Cu	Pb	Zn	
Child						
Min	1.92E-03	7.36E-02	4.63E-03	9.90E-03	5.77E-03	1.36E-01
Max	5.48E-01	9.56E-01	8.15E-01	4.53E-01	6.43E-02	1.78E+00
Mean	9.89E-02	2.85E-01	1.11E-01	1.14E-01	2.58E-02	6.35E-01
SD	1.07E-01	1.90E-01	2.07E-01	1.09E-01	1.35E-02	4.22E-01
CV (%)	1.08E+02	6.65E+01	1.86E+02	9.52E+01	5.23E+01	6.64E+01
Adult						
Min	2.05E-04	7.56E-03	4.75E-04	1.02E-03	5.92E-04	1.40E-02
Max	5.88E-02	9.82E-02	8.37E-02	4.66E-02	6.61E-03	1.84E-01
Mean	1.06E-02	2.93E-02	1.14E-02	1.17E-02	2.65E-03	6.57E-02
SD	1.14E-02	1.95E-02	2.13E-02	1.12E-02	1.39E-03	4.37E-02
CV (%)	1.08E+02	6.65E+01	1.86E+02	9.52E+01	5.23E+01	6.65E+01

The *EF* values of Cd varied between 1.48 and 643.51, indicative of significant contamination (20% of all samples) and very to extremely high contamination (72% of all samples) of sampled soils. The *EF* of Cr with values of 4.96-108.75 involved that 84% and 8% of all soil samples showed, respectively, significant enrichment and very- to extremely high enrichment. *EF* for Cu oscillated between 2.60 to 382.66 in soil samples. It indicated moderate, significant, and extremely high enrichment of Cu for 20%, 40%, and 28% of all samples. *EF* for Pb with values of 0.64-21.83 indicated that the sampled soils are minor, moderate, and significant enriched in Pb in 36%, 32%, and 28% of sampling sites. *EF* for Zn ranging between 2.49 and 39.08 revealed that 20% and 64% of all samples exhibited moderate and significant enrichment, respectively. The area surrounding the Tansrift mine tailings recovered high contamination that was in decreasing order Cd>Cu>Cr>Zn>Pb. Regarding *EF* results, it is significantly apparent that anthropogenic factors significantly impacted the sampled soils.

The results of the I_{geo} values (Table 6, Fig. 4) indicate that the studied soils were not polluted, slightly, moderately, moderately to severely polluted, severely polluted by Cd in 8%, 12%, 28%, 28%, and 20% of sites, respectively. The I_{geo} values of Cr classified the studied samples as not polluted (20% of all sites), slightly (60% of all sites), and moderately (12% of all sites). Moreover, the I_{geo} of Cu indicated that 56% and 44% of soil samples were respectively unpolluted and slightly to extremely polluted. Concerning I_{geo} of Pb, and Zn, the studied samples were mainly classified as unpolluted to slightly polluted. From the I_{geo} results, we acknowledge that the study area was greatly affected by Cd, Cr, and Cu and, to a lesser degree, by Pb and Zn, which might be mainly associated with mining. However, the naturally occurring source should not be neglected.

PLI used to evaluate the degree of HM pollution in the study area ranged from 0.39 to 6.93, with a mean of 2.31 (Table 6). Only 12% were not polluted among the entire soil samples, while 88% were polluted. As given in Fig. 5, the degree of pollution included moderately polluted, highly polluted, and extremely polluted, with the respective proportion being 48%, 16%, and 24% of analyzed samples. These *PLI* results combined with the I_{geo} results attested that HM pollution in the study area was affected by human activities.

The results of ecological indices of HMs in soils of the Tansrift are presented in Table 7. The results showed that the mean monomial potential ecological risk (E_r^i) was in the following order: Cd>Cu>Cr>Pb>Zn. The highest E_r^i of Cd was in a range of 5.29 and 1514.12, indicating significant risks of this metal. Cu had E_r^i varying between 2.21 and 389.24, indicating relatively high risks. E_r^i of Cr, Pb, and Zn were less than 18.3, suggesting quite low risks. The *RI* of the HMs in the studied soils ranged between 12.07 and 1540.37 (Table 7). According to the RI values, the studied soil samples are lowly, moderately, considerably, and highly contaminated, with the proportion being 24%, 36%, 24%, and 16%, respectively. Used for soil contamination health risk assessment, *HQ* values estimated for each element and the comprehensive non-carcinogenic risk index (*HI*), are given in Table 8. The *HQ* values of HMs for adult and children decreased in the Cr>Pb>Cu>Cd>Zn sequence. The *HI* values for adult were lower than 1, indicating no non-carcinogenic risk for the adult population, whereas, for children, four samples (S7, S10, S23, and S25) showed *HI* values exceeding 1. This finding indicated that the non-carcinogenic risk of HMs in the study area could be neglected for adult, but it could not be ignored for children health.

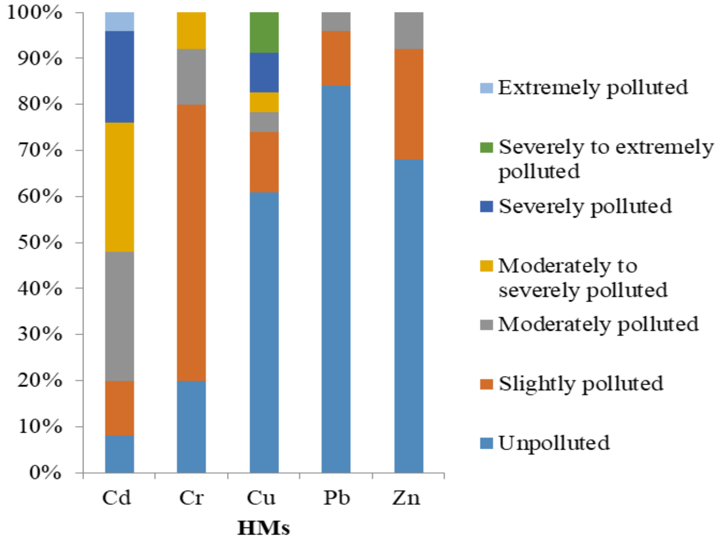

Fig. 4. HM pollution levels of the studied soils based on I_{geo} values.

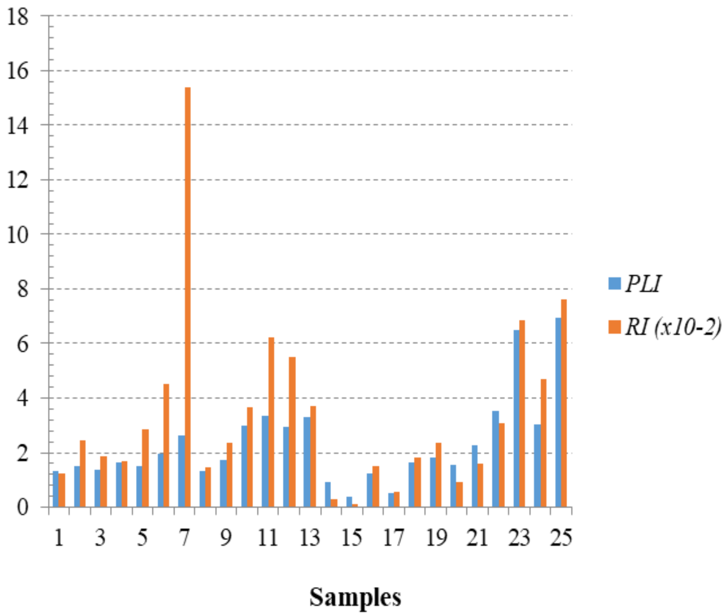

Fig. 5. *PLI* and *HI* values in soils near the Tansrift mine, Morocco.

Overall the obtained results in this study showed that the natural environment surrounding the Tansrift abandoned mine in the Azilal Province

(Morocco) is contaminated by HMs (Cd, Zn, Cr, Cu, and Pb). The HMs sources in question are closely connected to copper mine and the heaps of waste rock remaining after ore mining that are sources of HM from weathering and dusting.

Surface soil contents of Cd (100%), Cr (100%), Cu (67%), and Zn (68%) at the Tansrift area has a very high relative value compared to the corresponding average background values. The analyzed HMs were found to be the most polluting heavy metals in soils in Morocco. Reviews showed that metallic materials derived from different sources, including weathering of parent materials, agricultural activities, industrial activities, traffic, and mining activities (Barakat *et al*., 2019; Bouzekri *et al*., 2019; El Azhari *et al*., 2017; El Baghdadi *et al*., 2012; Ennaji *et al*., 2020; Hilali *et al*., 2020; Khafouri *et al*., 2021; Oumenskou *et al*., 2018b). In the study area, high concentrations of HMs added to high spatial variation indicated anthropogenic inputs for heavy metals. These high average concentrations are higher than those reported in agricultural soil samples of Tadla plain in central Morocco reported by Barakat *et al*. (2019), Ennaji *et al*. (2020) and Oumenskou *et al*. (2018b). Some previous case studies in Morocco focused on certain HMs in soils adjacent to the ore mines reported that the ore processing and the mineral residues affected the metallic mineral contents in the surrounding environments (El Amari *et al*., 2014; El Hamiani *et al*., 2015; Khafouri *et al*., 2021; Midhat *et al*., 2019). They reported that threats of HM pollution of the surrounding ecosystems of the abandoned Pb mines are strictly due to water and wind erosion that moved from the abandoned waste particles enriched in some HMs. Tuo *et al*. (2014) reported that the wind and water erosion of the surface soil produced a decrease in the content of fine particles and an increase in coarse particle content. This outcome is consistent with the coarse granulometry of the tailings evaluated in the field, suggesting that the tailings in the study area could be mobilized to the nearby environment under erosion. It is also supported by the fact that some soil samples located away from the mine site showed significant HM concentrations, and the magnetic properties result subsequently confirmed it. The type of magnetic material in the samples soils contained an admixture of MD, SP, and SSD grains, which is suspected of a combination of lithogenic and anthropogenic magnetic particles. Previous studies reported that the size of topsoil magnetic particles derived from anthropogenic is significantly coarser (Hu *et al*., 2007; Poggere *et al*., 2018).

Moreover, the lower correlation coefficients between χlf and HMs implied that HM contents in the soils are not controlled only by magnetic grains but can be affected by fertilization (Hu *et al*., 2007). Also, the PCA analysis finding attested that HMS in studied soils originated from different sources (lithogenic and anthropogenic) and confirmed the MS findings. The results of Igeo, PLI, and RI indices, calculated from spatially different soil samples, were also indicative of pollution driven by HMs in the Tansrift area. Cd, Cr, and Cu are considered the major contributors to contamination and toxicity in the investigated area. Many previous studies have been realized at other mines in Morocco and also reported abnormal accumulations of HMs accompanied by significant toxicity in soils and watercourse sediments, which often act simultaneously as a carrier and as secondary sources of pollutants in both the soil-plant and aquatic systems (Boularbah *et al*., 2006; Bouzekri *et al*., 2019; El Azhari *et al*., 2017; El Khalil *et al*., 2008; Khafouri *et al*., 2021; Nassiri *et al*., 2021b). In all of this, findings of the present investigation led to interesting conclusions on HM concentrations and their environmental toxicity in soils surrounding the Tansrift abandoned mine. Thus, based upon these conclusions, more attention should be paid to HM contamination of soils in the investigated area.

In summary, combining the analyses, the study area should be managed prior, and the protection of children should be prioritized. Therefore, the identification of priority control components from our study can help policymakers to form more effective exposure reduction and management measures. We also recommend implementing protective measures such as informing the local population about the health consequences and exposures.

CONCLUSIONS

The present study investigated the contents, contamination, and ecological and health risks of HMs in farmlands surrounding the abandoned mine of Tansrift (Central High Atlas, Morocco). The results showed that the HM concentrations followed the order of Cu>Cr>Zn>Pb>Cd, and the contents of Cd (100%), Cr (100%), Cu (67%), and Zn (68%) exceeded the local corresponding background values. Multivariate statistics suggested that Cu had anthropogenic and lithologic origins as agricultural practices, soil parent materials, and mineral dust and wastes from the Tansrift mine, while agricultural activities mainly governed cd, Cr, and Zn. Using cluster analysis, the polluted samples are heterogeneously spatially distributed, conforming that different sources contributed to the accumulation of HMs in soils. As regards *EF* results, significant contamination by HMs was recovered in decreasing order Cd>Cu>Cr>Zn>Pb. The I_{geo} revealed that the study area was greatly affected by Cd, Cr, and Cu toxic metal and, to a lesser degree, by Pb and Zn. According to I_{geo} values, the study area appeared more affected by Cd, Cr, and Cu toxic metal and, to a lesser degree, by Pb and Zn. The *PLI* values (0.39-6.93) used to evaluate the degree of HM pollution in the study area ranging between 0.39 and 6.93 showed that 88% of the soil samples were polluted. The potential ecological risk of HMs order was Cd>Cu>Cr>Pb>Zn. The criteria of ecological risk on Cd and Cu were significant risk, and the other metals were low risk. The *HI* values indicated that the non-carcinogenic risk of HMs in studied soils could be neglected for adult, but not for children.

To end, this study indicated that special actions could be carried out at the study area to reduce the inputs of HMs in agricultural lands. Furthermore, the study demonstrated that the adopted methodology combining soil proprieties' measurements, multivariate statistical analysis, and environmental indices could be a reliable tool to evaluate the HM pollution status and identify their origins and ecological impacts.

ACKNOWLEDGMENTS

We are grateful to H. Mosaid for his help in the figure conception.

REFERENCES

Abouian Jahromi, M., Jamshidi-Zanjani, A. & Khodadadi Darban, A. (2020). Heavy metal pollution and human health risk assessment for exposure to surface soil of mining area: a comprehensive study. *Environmental Earth Sciences*, 79(14), 1-18.

AFNOR. (2003). Norme Française NF X31-107. Qualité du sol Determination de la distribution granulométrique des particles du sol Méthode á la pipette. In: Association Française de Normalisation La Plaine Saint-Denis, France.

Allen, S. (1986). Chemical analysis. *Methods in plant ecology*, 285-344.

Alomary, A. A. & Belhadj, S. (2007). Determination of heavy metals (Cd, Cr, Cu, Fe, Ni, Pb, Zn) by ICP-OES and their speciation in Algerian Mediterranean Sea sediments after a five-stage sequential extraction procedure. *Environ. Monit. Assess.*, 135(1), 265-280. doi:10.1007/s10661-007-9648-8

Atibu, E. K., Lacroix, P., Sivalingam, P., Ray, N., Giuliani, G., Mulaji, C. K.,... Poté, J. (2018). High contamination in the areas surrounding abandoned mines and mining activities: An impact assessment of the Dilala, Luilu and Mpingiri Rivers, Democratic Republic of the Congo. *Chemosphere,* 191, 1008-1020. doi:https://doi.org/10.1016/j.chemosphere.2017.10.052

Azzeddine, K. & El Hassan, T. 2020. Assessment of Metallic Contamination of Water Resources in the Area Around the Abandoned Mining Site of Ouixane (North East Morocco). Paper presented at the Proceedings of the 4th Edition of International Conference on Geo-IT and Water Resources 2020, Geo-IT and Water Resources 2020.

Barakat, A., El Baghdadi, M., Rais, J. & Nadem, S. (2012). Assessment of heavy metal in surface sediments of Day River at Beni-Mellal region, Morocco. *Research Journal of Environmental and Earth Sciences,* 4(8), 797-806.

Barakat, A., Ennaji, W., Krimissa, S. & Bouzaid, M. (2019). Heavy metal contamination and ecological-health risk evaluation in peri-urban wastewater-irrigated soils of Beni-Mellal city (Morocco). *Int. J. Environ. Health Res*, 1-16.

Barakat, A., Ennaji, W., Krimissa, S. & Bouzaid, M. (2020). Heavy metal contamination and ecological-health risk evaluation in peri-urban wastewater-irrigated soils of Beni-Mellal city (Morocco). *Int. J. Environ. Health Res,* 30(4), 372-387. doi:10.1080/09603123.2019.1595540

Barbieri, M. (2016). The importance of enrichment factor (EF) and geoaccumulation index (Igeo) to evaluate the soil contamination. *J Geol Geophys,* 5(1), 1-4.

Boularbah, A., Schwartz, C., Bitton, G. & Morel, J. L. (2006). Heavy metal contamination from mining sites in South Morocco: 1. Use of a biotest to assess metal toxicity of tailings and soils. *Chemosphere*, 63(5), 802-810.

Bouzekri, S., El Hachimi, M. L., Touach, N., El Fadili, H. & El Mahi, M. (2019). The study of metal (As, Cd, Pb, Zn and Cu) contamination in superficial stream sediments around of Zaida mine (High Moulouya-Morocco). *Journal of African Earth Sciences,* 154, 49-58.

Bouzekri, S., El Hachimi, M. L., Kara, K., El Mahi, M. & Lotfi, E. M. (2020). Metal pollution assessment of surface water from the abandoned Pb mine Zaida, high Moulouya-Morocco. *Geosystem Engineering,* 23(4), 226-233. doi:10.1080/12269328.2020.1772125

Charrière, A., Haddoumi, H. & Mojon, P.-O. (2005). Découverte de Jurassique supérieur et d'un niveau marin du Barrémien dans les « couches rouges » continentales du Haut Atlas central marocain: implications paléogéographiques et structurales. *Comptes Rendus Palevol,* 4(5), 385-394. doi:https://doi.org/10.1016/j.crpv.2005.04.009

Chiroma, T., Ebewele, R. & Hymore, F. (2014). Comparative assessment of heavy metal levels in soil, vegetables and urban grey waste water used for irrigation in Yola and Kano. *International refereed journal of engineering and science,* 3(2), 01-09.

Chun, S.-J., Kim, Y.-J., Cui, Y. & Nam, K.-H. (2021). Ecological network analysis reveals distinctive microbial modules associated with heavy metal contamination of abandoned mine soils in Korea. *Environmental Pollution,* 289, 117851. doi:https://doi.org/10.1016/j.envpol.2021.117851

De Miguel, E., Iribarren, I., Chacón, E., Ordoñez, A. & Charlesworth, S. (2007). Risk-based evaluation of the exposure of children to trace elements in playgrounds in Madrid (Spain). *Chemosphere,* 66(3), 505-513. doi:10.1016/j.chemosphere.2006.05.065

Dearing, J. A., Hay, K. L., Baban, S. M., Huddleston, A. S., Wellington, E. M. & Loveland, P. (1996). Magnetic susceptibility of soil: an evaluation of conflicting theories using a national data set. *Geophys. J. Int.,* 127(3), 728-734.

El Amari, K., Valera, P., Hibti, M., Pretti, S., Marcello, A. & Essarraj, S. (2014). Impact of mine tailings on surrounding soils and ground water: Case of Kettara old mine, Morocco. *Journal of African Earth Sciences,* 100, 437-449.

El Azhari, A., Rhoujjati, A., El Hachimi, M. L. & Ambrosi, J.-p. (2017). Pollution and ecological risk assessment of heavy metals in the soil-plant system and the sediment-water column around a former Pb/Zn-mining area in NE Morocco. *Ecotoxicol. Environ. Saf.,* 144, 464-474. doi:https://doi.org/10.1016/j.ecoenv.2017.06.051

El Baghdadi, M., Barakat, A., Sajieddine, M. & Nadem, S. (2012). Heavy metal pollution and soil magnetic susceptibility in urban soil of Beni Mellal City (Morocco). *Environmental Earth Sciences,* 66(1), 141-155. doi:10.1007/s12665-011-1215-5

El Hamiani, O., El Khalil, H., Sirguey, C., Ouhammou, A., Bitton, G., Schwartz, C. & Boularbah, A. (2015). Metal concentrations in plants from mining areas in South Morocco: health risks assessment of consumption of edible and aromatic plants. *CLEAN–Soil, Air, Water,* 43(3), 399-407.

El Khalil, H., El Hamiani, O., Bitton, G., Ouazzani, N. & Boularbah, A. (2008). Heavy metal contamination from mining sites in South Morocco: monitoring metal content and toxicity of soil runoff and groundwater. *Environ. Monit. Assess.,* 136(1), 147-160.

Ennaji, W., Barakat, A., El Baghdadi, M. & Rais, J. (2020). Heavy metal contamination in agricultural soil and ecological risk assessment in the northeast area of Tadla plain, Morocco. *Journal of Sedimentary Environments,* 5(3), 307-320. doi:10.1007/s43217-020-00020-9

EPA, U. (2011). Exposure Factors Handbook 2011 Edition (Final Report). US Environmental Protection Agency, Washington, DC, EPA/600/R-09/052F.

Esmaeili, A., Moore, F., Keshavarzi, B., Jaafarzadeh, N. & Kermani, M. (2014). A geochemical survey of heavy metals in agricultural and background soils of the Isfahan industrial zone, Iran. *CATENA,* 121, 88-98. doi:https://doi.org/10.1016/j.catena.2014.05.003

Essien, J. P., Inam, E. D., Ikpe, D. I., Udofia, G. E. & Benson, N. U. (2019). Ecotoxicological status and risk assessment of heavy metals in municipal solid wastes dumpsite impacted soil in Nigeria. *Environmental Nanotechnology, Monitoring & Management,* 11, 100215.

Haddoumi, H., Charrière, A. & Mojon, P.-O. (2010). Stratigraphie et sédimentologie des «Couches rouges» continentales du Jurassique-Crétacé du Haut Atlas central (Maroc): implications paléogéographiques et géodynamiques. *Geobios,* 43(4), 433-451.

Hakanson, L. (1980). An ecological risk index for aquatic pollution control.a sedimentological approach. *Water Res.,* 14(8), 975-1001. doi:https://doi.org/10.1016/0043-1354(80)90143-8

Hanesch, M. & Scholger, R. (2002). Mapping of heavy metal loadings in soils by means of magnetic susceptibility measurements. *Environ. Geol.,* 42(8), 857-870. doi:10.1007/s00254-002-0604-1

Hanfi, M. Y., Mostafa, M. Y. & Zhukovsky, M. V. (2020). Heavy metal contamination in urban surface sediments: sources, distribution, contamination control, and remediation. *Environmental monitoring and assessment,* 192(1), 1-21.

Hilali, A., El Baghdadi, M., Barakat, A., Ennaji, W. & El Hamzaoui, E. H. (2020). Contribution of GIS techniques and pollution indices in the assessment of metal pollution in agricultural soils irrigated with wastewater: case of the Day River, Beni Mellal (Morocco). *Euro-Mediterranean Journal for Environmental Integration,* 5(3), 52. doi:10.1007/s41207-020-00186-8

Hu, X.-F., Su, Y., Ye, R., Li, X.-Q. & Zhang, G.-L. (2007). Magnetic properties of the urban soils in Shanghai and their environmental implications. *Catena,* 70(3), 428-436.

Huang, Y. (2021). Chinese ENGOs and the Heavy-Metal Pollution of the Consumer-Electronics Industry: Exploring the Constraining Factors. *East Asia,* 38(1), 21-37.

Ibouh, H., Hibti, M. & El Amari, K. (2016). LA MINE DE TANSRIFT: UN EXEMPLE DE RED BEDS CRETACES DU HAUT ATLAS CENTRAL MAROC, CONTEXTE GEOLOGIQUE.

Khafouri, A., Talbi, E. H. & Abdelouas, A. (2021). Assessment of Heavy Metal Contamination of the Environment in the Mining Site of Ouixane (North East Morocco). *Water Air Soil Pollut.,* 232(10), 1-27.

Leila, B., Loubna, B. & Ali, B. (2021). Impacts of mining activities on soil properties: case studies from Morocco mine sites. *Soil Science Annual,* 71(4), 395-407.

Leung, A. O., Duzgoren-Aydin, N. S., Cheung, K. & Wong, M. H. (2008). Heavy metals concentrations of surface dust from e-waste recycling and its human health implications in southeast China. *Environ. Sci. Technol.,* 42(7), 2674-2680.

Liu, C.-W., Lin, K.-H. & Kuo, Y.-M. (2003a). Application of factor analysis in the assessment of groundwater quality in a blackfoot disease area in Taiwan. *Sci. Total Environ.,* 313(1), 77-89. doi:https://doi.org/10.1016/S0048-9697(02)00683-6

Liu, Q., Banerjee, S. K., Jackson, M. J., Chen, F., Pan, Y. & Zhu, R. (2003b). An integrated study of the grain size dependent magnetic mineralogy of the Chinese loess/paleosol and its environmental significance. *Journal of Geophysical Research: Solid Earth,* 108(B9).

Long, Z., Huang, Y., Zhang, W., Shi, Z., Yu, D., Chen, Y.,... Wang, R. (2021). Effect of different industrial activities on soil heavy metal pollution, ecological risk, and health risk. *Environmental Monitoring and Assessment,* 193(1), 1-12.

Lu, S., Bai, S. & Xue, Q. (2007). Magnetic properties as indicators of heavy metals pollution in urban topsoils: a case study from the city of Luoyang, China. *Geophys. J. Int.,* 171(2), 568-580.

Madzin, Z., Shai-in, M. F. & Kusin, F. M. (2015). Comparing Heavy Metal Mobility in Active and Abandoned Mining Sites at Bestari Jaya, Selangor. *Procedia Environmental Sciences,* 30, 232-237. doi:https://doi.org/10.1016/j.proenv.2015.10.042

Maher, B. A. (1998). Magnetic properties of modern soils and Quaternary loessic paleosols: paleoclimatic implications. *Palaeogeography, Palaeoclimatology, Palaeoecology,* 137(1), 25-54. doi:https://doi.org/10.1016/S0031-0182(97)00103-X

Marguí, E., Queralt, I., Carvalho, M. & Hidalgo, M. (2005). Comparison of EDXRF and ICP-OES after microwave digestion for element determination in plant specimens from an abandoned mining area. *Anal. Chim. Acta,* 549(1-2), 197-204.

Meena, N. K., Maiti, S. & Shrivastava, A. (2011). Discrimination between anthropogenic (pollution) and lithogenic magnetic fraction in urban soils (Delhi, India) using environmental magnetism. *Journal of Applied Geophysics,* 73(2), 121-129.

Midhat, L., Ouazzani, N., Hejjaj, A., Ouhammou, A. & Mandi, L. (2019). Accumulation of heavy metals in metallophytes from three mining sites (Southern Centre Morocco) and evaluation of their phytoremediation potential. *Ecotoxicol. Environ. Saf.,* 169, 150-160.

Mirzaei, M., Marofi, S., Solgi, E., Abbasi, M., Karimi, R. & Riyahi Bakhtyari, H. R. (2020). Ecological and health risks of soil and grape heavy metals in long-term fertilized vineyards (Chaharmahal and Bakhtiari province of Iran). *Environ. Geochem. Health,* 42(1), 27-43. doi:10.1007/s10653-019-00242-5

Mojon, P.-O., Haddoumi, H. & Charrière, A. (2009). Nouvelles données sur les Charophytes et Ostracodes du Jurassique moyen-supérieur-Crétacé inférieur de l'Atlas marocain. *Carnets de géologie*.

Monbaron, M. (1988). Un serpent de mer: le problème de la datation des" Couches rouges" du Haut-Atlas marocain: le point de la situation.

Moyé, J., Picard-Lesteven, T., Zouhri, L., El Amari, K., Hibti, M. & Benkaddour, A. (2017). Groundwater assessment and environmental impact in the abandoned mine of Kettara (Morocco). *Environmental Pollution,* 231, 899-907. doi:https://doi.org/10.1016/j.envpol.2017.07.044

Müller, G. (1979). Schwermetalle in den Sedimenten des Rheins-Veränderungen seit 1971.

Nassiri, O., Rhoujjati, A. & El Hachimi, M. L. (2021a). Contamination, sources and environmental risk assessment of heavy metals in water, sediment and soil around an abandoned Pb mine site in North East Morocco. *Environmental Earth Sciences,* 80(3), 96. doi:10.1007/s12665-021-09387-y

Nassiri, O., Rhoujjati, A. & Hachimi, M. L. E. (2021b). Contamination, sources and environmental risk assessment of heavy metals in water, sediment and soil around an abandoned Pb mine site in North East Morocco. *Environmental Earth Sciences,* 80(3), 1-20.

Nouri, M. & Haddioui, A. (2015). Human and animal health risk assessment of metal contamination in soil and plants from Ait Ammar abandoned iron mine, Morocco. *Environ. Monit. Assess.,* 188(1), 6. doi:10.1007/s10661-015-5012-6

Oumenskou, H., El Baghdadi, M., Barakat, A., Aquit, M., Ennaji, W., Karroum, L. A. & Aadraoui, M. (2018a). Assessment of the heavy metal contamination using GIS-based approach and pollution indices in agricultural soils from Beni Amir irrigated perimeter, Tadla plain, Morocco. *Arabian Journal of Geosciences,* 11(22), 692. doi:10.1007/s12517-018-4021-5

Oumenskou, H., El Baghdadi, M., Barakat, A., Aquit, M., Ennaji, W., Karroum, L. A. & Aadraoui, M. (2018b). Assessment of the heavy metal contamination using GIS-based approach and pollution indices in agricultural soils from Beni Amir irrigated perimeter, Tadla plain, Morocco. *Arab. J. Geosci.,* 11(22). doi:10.1007/s12517-018-4021-5

Poggere, G. C., Inda, A. V., Barrón, V., Kämpf, N., de Brito, A. D. B., Barbosa, J. Z. & Curi, N. (2018). Maghemite quantification and magnetic signature of Brazilian soils with contrasting parent materials. *Applied Clay Science,* 161, 385-394.

Punia, A. (2021). Role of temperature, wind, and precipitation in heavy metal contamination at copper mines: a review. *Environmental Science and Pollution Research,* 28(4), 4056-4072. doi:10.1007/s11356-020-11580-8

Roy, S., Gupta, S. K., Prakash, J., Habib, G., Baudh, K. & Nasr, M. (2019). Ecological and human health risk assessment of heavy metal contamination in road dust in the National Capital Territory (NCT) of Delhi, India. *Environmental Science and Pollution Research,* 26(29), 30413-30425.

Schmidt, A., Yarnold, R., Hill, M. & Ashmore, M. (2005). Magnetic susceptibility as proxy for heavy metal pollution: a site study. *Journal of Geochemical Exploration,* 85(3), 109-117.

Selvaraj, K., Mohan, V. R. & Szefer, P. (2004). Evaluation of metal contamination in coastal sediments of the Bay of Bengal, India: geochemical and statistical approaches. *Mar. Pollut. Bull.,* 49(3), 174-185.

Stefanowicz, A. M., Kapusta, P., Zubek, S., Stanek, M. & Woch, M. W. (2020). Soil organic matter prevails over heavy metal pollution and vegetation as a factor shaping soil microbial communities at historical Zn–Pb mining sites. *Chemosphere,* 240, 124922.

Sun, Z., Xie, X., Wang, P., Hu, Y. & Cheng, H. (2018). Heavy metal pollution caused by small-scale metal ore mining activities: A case study from a polymetallic mine in South China. *Sci. Total Environ.,* 639, 217-227.

Suresh, G., Ramasamy, V., Meenakshisundaram, V., Venkatachalapathy, R. & Ponnusamy, V. (2011). Influence of mineralogical and heavy metal composition on natural radionuclide concentrations in the river sediments. *Applied radiation and isotopes: including data, instrumentation and methods for use in agriculture, industry and medicine,* 69(10), 1466-1474. doi:10.1016/j.apradiso.2011.05.020

Tang, X., Wu, X., Xia, P., Lin, T., Huang, X., Zhang, Z. & Zhang, J. (2021). Health risk assessment of heavy metals in soils and screening of accumulating plants around the Wanshan mercury mine in Northeast Guizhou Province, China. *Environmental Science and Pollution Research*, 1-14.

Taylor, S. (1964). Abundance of chemical elements in the continental crust: a new table. *Geochimica et cosmochimica acta,* 28(8), 1273-1285.

Tomlinson, D. L., Wilson, J. G., Harris, C. R. & Jeffrey, D. W. (1980). Problems in the assessment of heavy-metal levels in estuaries and the formation of a pollution index. *Helgoländer Meeresuntersuchungen,* 33(1), 566-575. doi:10.1007/BF02414780

Tuo, D. F., Xu, M. X., Ma, X. X. & Zheng, S. Q. (2014). [Impact of wind-water alternate erosion on the characteristics of sediment particles]. *Ying Yong Sheng Tai Xue Bao,* 25(2), 381-386.

Wang, P., Sun, Z., Hu, Y. & Cheng, H. (2019). Leaching of heavy metals from abandoned mine tailings brought by precipitation and the associated environmental impact. *Science of The Total Environment,* 695, 133893. doi:https://doi.org/10.1016/j.scitotenv.2019.133893

Wu, B., Peng, H., Sheng, M., Luo, H., Wang, X., Zhang, R.,... Xu, H. (2021). Evaluation of phytoremediation potential of native dominant plants and spatial distribution of heavy metals in abandoned mining area in Southwest China. *Ecotoxicol. Environ. Saf.*, 220, 112368.

Yan, D., Bai, Z. & Liu, X. (2020). Heavy-metal pollution characteristics and influencing factors in agricultural soils: Evidence from Shuozhou city, Shanxi province, China. *Sustainability*, 12(5), 1907.

Yang, Q., Li, Z., Lu, X., Duan, Q., Huang, L. & Bi, J. (2018). A review of soil heavy metal pollution from industrial and agricultural regions in China: Pollution and risk assessment. *Sci. Total Environ.*, 642, 690-700. doi:https://doi.org/10.1016/j.scitotenv.2018.06.068

Yang, Y., Yang, X., He, M. & Christakos, G. (2020). Beyond mere pollution source identification: Determination of land covers emitting soil heavy metals by combining PCA/APCS, GeoDetector and GIS analysis. *CATENA*, 185, 104297. doi:https://doi.org/10.1016/j.catena.2019.104297

Yu, R., He, L., Cai, R., Li, B., Li, Z. & Yang, K. (2017). Heavy metal pollution and health risk in China. *Global Health Journal*, 1(1), 47-55. doi:https://doi.org/10.1016/S2414-6447(19)30059-4

Zhang, Z., Lu, Y., Li, H., Tu, Y., Liu, B. & Yang, Z. (2018). Assessment of heavy metal contamination, distribution and source identification in the sediments from the Zijiang River, China. *Sci. Total Environ.*, 645, 235-243.

Zhao, X., Sun, Y., Huang, J., Wang, H. & Tang, D. (2020). Effects of soil heavy metal pollution on microbial activities and community diversity in different land use types in mining areas. *Environmental Science and Pollution Research*, 27(16), 20215-20226.

Zouhri, L., El Amari, K., Marier, D., Benkaddour, A. & Hibti, M. (2019). Bacteriological and geochemical features of the groundwater resources: Kettara abandoned mine (Morocco). *Environmental Pollution*, 252, 1698-1708. doi:https://doi.org/10.1016/j.envpol.2019.06.098

INSTRUCTIONS TO AUTHORS

The "Agriculture and Forestry" journal publishes original scientific papers, review papers, short communications on agriculture, veterinary medicine, forestry, biology and other natural sciences. It is the endeavour of the journal to give place to papers of high scientific quality and international interest, authored by all the scientists from the South Eastern European Region, as well as other international scientist in order to stimulate contacts and exchange of knowledge fostering scientific productivity.

Manuscripts, submitted via electronic journal web system should be prepared in Microsoft Word ***(Times New Roman font, 11 pt)*** and submitted in format 17 x 24 cm ***(File / Page setup / Paper / Width = 17 cm; Height = 24 cm)***, with single line spacing ***(Format / Paragraph / Line spacing = Single)***, 2 cm margins all around ***(File / Page setup / Margins / Top = 2 cm; Bottom = 2 cm; Left = 2 cm; Right = 2 cm)***, that is approximately 44 lines per page in this format. All technical details are available in section AUTHORS / Check-list for Authors.

Manuscripts are published in English. Papers that have been published elsewhere, in whole or extracts (excerpts) of their important findings, will not be accepted. A manuscript should not exceed 10 pages. Exceptions can be made if content and quality of the paper justify it (at the discretion of the Editor).

Full research papers should include the following sections:

- Author/s name/s, Title with **DOI number**

The author's name should be placed above the title and with the author's appellation and affiliation in a footnote at the bottom of the front page. Author(s) affiliation should indicate name and address of institution, including the e-mail address of the corresponding author. Title should provide a concise but also an informative synthesis of the study (recommended not more than 100 characters including spaces). Short title (not more than 70 characters) should also be provided in order to be included in the header of the Manuscript. Ensure that the title contains the most important words that relate to the topic.

- Abstract

The summary, in English language, should provide basic data on the problem that was treated and the results obtained. It should be brief, preferably one paragraph only, up to 250 words, but sufficient to inform the reader of the character of the work, its results and its conclusions. Include the keywords and phrases you repeated in your abstract.

- Key words

Keywords should provide 4-6 words or compound words, suitable for an information retrieval system. Choose the appropriate keywords and phrases for your article. Think of a phrase of 2-4 words that a researcher might search on to find your article. Repeat your keywords and phrases 3-4 times throughout the abstract in a natural, contextual way.

Main text of the manuscript includes the following sections:

- INTRODUCTION

The introduction should answer the questions what was studied, why was it an important question, what was known about it before and how the study will advance our knowledge.

- MATERIAL AND METHODS

Material and methods explain how the study was carried: the organism(s) studied; description of the study site, including the significant physical and biological features, and the precise location (latitude and longitude, map, etc); the experimental or sampling design; the protocol for collecting data; how the data were analyzed. In this section also should be provided a clear description of instruments and equipment, machines, devices, chemicals, diagnostic kits, plants/animals studied, technology of growing/housing, sampling sites, software used etc.

- RESULTS followed by **DISCUSSION**

Results and Discussion may be combined into a single section (if appropriate) or it can be a separate section.

The results objectively present key results, without interpretation, in an orderly and logical sequence using both text and illustrative materials (tables and figures).

The discussion interpret results in light of what was already known about the subject of the investigation, and explain new understanding of the problem after taking results into consideration.

The International System of Units (SI) should be used.

- CONCLUSIONS

The conclusion should present a clear and concise review of experiments and results obtained, with possible reference to the enclosures.

- ACKNOWLEDGMENTS

If received significant help in designing, or carrying out the work, or received materials from someone who did a favour by supplying them, their assistance must be acknowledged. Acknowledgments are always brief and never flowery.

- REFERENCES (LITERATURE)

References should cover all papers cited in the text. The in-text citation format should be as follows: for one author (Karaman, 2011), for two authors (Erjavec and Volk, 2011) and for more than two authors (Rednak *et al*., 2007). Use semicolon (Rednak *et al*., 2012; Erjavec and Volk, 2011) to separate multiple citations. Multiple citations should be ordered chronologically. The literature section gives an alphabetical listing (by first author's last name) of the references. More details you can find in the Annex to the INSTRUCTIONS TO AUTHORS / Bibliographic style on the web page of the Journal: www.agricultforest.ac.me.

Short communication should include the following sections: Title, Abstract, Key words, Main text, Acknowledgments, References, Tables and Figures with captions.

SUPPLY OF ARTWORK, PHOTOS: Diagrams and graphs should be provided as finished black and white line artwork or colour images. Electronic graphics included in your manuscript should be either inserted in the word document or as .gif or .jpg formats. Please check with the editor if you wish to submit any other type of graphic for conversion suitability. Photos should be supplied un-screened in original form or in electronic form. All illustration (diagrams, graphs, tables, photos) must be fully captioned. When there are a number of illustrations, the author should endeavour to reduce the amount of text to accommodate the illustrations in the limited space available for any article.

THE REVIEW PROCESS: Submitted manuscripts are reviewed anonymously by 2 (3) referees (duble blind review): one from the journal Editorial board, one must be an international reviewer, working out of the University of Montenegro. All tracking of manuscripts and reviewers is done by the Editor. All attempts will be made to ensure submissions will be reviewed within three months after the submission. Manuscripts will be returned to the coresponding authors when each review is completed.

Examples available on **www.agricultforest.ac.me**.